University of Southampton

Faculty of Environmental and Life Sciences

School of Ocean and Earth Science

Development of Automated Nucleic Acid Technologies for Marine Point of Sample Diagnostics

DOI [enter DOI]

by

Matthew William Wilson

Thesis for the degree of doctor of philosophy

JULY 2020

University of Southampton

Abstract

Unsafe water, poor hygiene and inadequate sanitation are responsible for about 90% of diarrheal associated deaths worldwide, which are the second leading cause of death in children under five, globally (1.2 million deaths in 2005). The economic cost associated with unsafe water is also significant, with the World Bank estimating that a lack of access to safe water and sanitation amount to equivalent global economic losses of US$260 billion, annually. Coastal communities also face challenges from harmful algal blooms, which deplete oxygen and essential nutrients, and produce toxins that threaten human health; this impacts on locally important industries such as aquaculture, mariculture, leisure and tourism. Current, widely used methods for the detection of biological hazards in water sources rely on culturing or visual inspection of water samples via light microscopy. These techniques are time consuming, require well stocked laboratories and expensive equipment, are dependent on highly trained technical staff, and are often unable to differentiate morphologically similar organisms. Molecular techniques, on the other hand can provide better discrimination between related taxonomical groups, and are suited for miniaturisation and automation, enabling the analysis to be undertaken outside of the laboratory, and by minimally trained personnel.

Recent advances in microfluidic technologies have demonstrated that molecular-biology techniques (e.g. genetic sequence amplification and detection) can be applied using lab-on-a-chip (LOC) systems for testing samples for the target organisms at the 'point of sample' or 'point of care'. Nucleic acid sequence-based amplification (NASBA) and recombinase polymerase amplification (RPA) are particularly attractive for LOC applications as, unlike the current gold standard Polymerase Chain Reaction (PCR), they require simple, isothermal heating and a generally lower reaction temperature. NASBA is also attractive for LOC-based methods targeting RNA (e.g. RNA viruses) as it directly amplifies RNA removing the need for an additional reverse transcription step.

This study indicates several, novel advances towards the provision of point of sample genetic testing for a range of harmful microorganisms and viruses. For the first time, the isothermal amplification of a fragment of the Hepatitis E virus using NASBA is reported with comparable sensitivity to a clinically relevant PCR-based assay. Further, amplification of a fragment of the *Alexandrium minutum* ITS1-5.8s-ITS2 rRNA gene region via RPA was achieved with a limit of detection of 10 cells exceeding the required sensitivity of 40 cells L^{-1} for statutory *A. minutum* surveillance in seawater. In addition to this, two methods for the long-term, dry storage of amplification reagents are presented. Trehalose and sucrose sugars combined with lyophilisation were sufficient to retain reagent activity after storage for four weeks at room temperature. Air drying in the presence of pullulan maintained reagent functionality for six weeks. Alongside these advances, a portable, handheld prototype concept for nucleic acid amplification was developed and tested, with the *A. minutum* ITS1-5.8s-ITS2 RPA assay being successfully performed on the handheld device achieving the same sensitivity as when performed on laboratory equipment. These advances demonstrate that nucleic acid amplification on a miniaturised device is possible, and that in future, rapid, specific and sensitive testing for harmful species may be able to be performed at the point of sample by non-technically trained operators.

Faculty of Environmental and Life Sciences

School of Ocean and Earth Sciences

Ocean Technology and Engineering

Thesis for the degree of Doctor of Philosophy

Development of automated nucleic acid Technologies for marine point of sample diagnostics

by

Matthew William Wilson

Table of Contents

Table of Tables

Table of Tables

Table of Figures

Research Thesis: Declaration of Authorship

Print name: Matthew William Wilson

Title of thesis: Development of automated nucleic acid Technologies for marine point of sample diagnostics

I declare that this thesis and the work presented in it are my own and has been generated by me as the result of my own original research.

I confirm that:

1. This work was done wholly or mainly while in candidature for a research degree at this University;
2. Where any part of this thesis has previously been submitted for a degree or any other qualification at this University or any other institution, this has been clearly stated;
3. Where I have consulted the published work of others, this is always clearly attributed;
4. Where I have quoted from the work of others, the source is always given. With the exception of such quotations, this thesis is entirely my own work;
5. I have acknowledged all main sources of help;
6. Where the thesis is based on work done by myself jointly with others, I have made clear exactly what was done by others and what I have contributed myself;
7. Parts of this work have been published as:-

McQuillan, J. S. & Wilson, M. W. (2019). 'Ready Mixed', improved nucleic acid amplification assays for the detection of *Escherichia coli* DNA and RNA. *Journal of Microbiological Methods*, 105721.

Wilson, M.W., Evans, S., Mcquillan, J.S. and Robidart J.C. (In prep). A novel, rapid recombinase polymerase amplification assay for the detection of *Alexandrium minutum* in environmental waters. To be submitted to *Environmental Science and Technology*.

Signature: Date:

Acknowledgements

I would like to express my thanks to my primary supervisor Dr Julie Robidart, and to my secondary supervisor's Dr Jonathan McQuillan, Dr Phyllis Lam and Professor Matthew Mowlem for their guidance, encouragement and support during my PhD. I would also like to thank Dr Annika Simpson for always providing words of encouragement and motivation. I would like to thank my parents who have always supported my education, and all my friends and the people I shared 251/28 with for all the support and fun times we had. I would like to thank Sam Monk for the insightful discussions on fluid dynamics. Finally, special thanks go to Amy for getting me through the darkest times and making sure I would never give up.

Definitions and Abbreviations

BLAST	Basic Local Alignment Search Tool
BSA	Bovine Serum Albumin
cDNA	Complimentary Deoxyribonucleic Acid
CRISPR	Clustered Regularly Interspaced Short Palindromic Repeats
cRNA	Complimentary Ribonucleic Acid
ddH_2O	Double Distilled Water
DNA	Deoxyribonucleic Acid
dNTPs	Deoxynucleotides
dsDNA	Double-Stranded Deoxyribonucleic Acid
DTT	Dithiothreitol
EDAB	Ecosystem Disruptive Algal Blooms
EDTA	Ethylenediaminetetraacetic acid
ESP	Environmental Sample Processor
FIB	Faecal Indicator Bacteria
FISH	Fluorescent *in situ* Hybridisation
gDNA	Genomic Deoxyribonucleic Acid
GOCI	Geostationary Ocean Colour Imager
HAB	Harmful Algal Bloom
HAV	Hepatitis A Virus
HDA	Helicase Dependant Amplification
HEV	Hepatitis E Virus
HIV	Human Immunodeficiency Virus

Definitions and Abbreviations

HPLC	High-performance Liquid Chromatography
HPV	Hydrogen Peroxide Vapour
IC	Internal Control
IDT	Integrated DNA Technologies
IMO	International Maritime Organisation
ITIS	Integrated Taxonomic Information System
ITS	Internal Transcribed Spacer
LAMP	Loop Mediated Isothermal Amplification
LC-MS	Liquid-chromatography – Mass Spectrometry
LED	Light Emitting Diode
LOC	Lab on a Chip
LOD	Limit of Detection
LOQ	Limit of Quantification
LRM	Laboratory Reference Material
MERIS	Medium Resolution Imaging Spectrometer
MGB	Minor Groove Binder
MODIS	Moderate Resolution Imaging Spectrometer
NA	Nucleic Acid
NAA	Nucleic Acid Amplification
NAAT	Nucleic Acid Amplification Technology
NASBA	Nucleic Acid Sequence Based Amplification
NFW	Nuclease Free Water
NTC	No Template Control
NTR	Non-Translated Region

NV	Norovirus
OMZ	Oxygen Minimum Zone
ORF	Open Reading Frame
PBS	Phosphate Buffered Saline
PCR	Polymerase Chain Reaction
PDMS	Polydimethylsiloxane
PHE	Public Health England
PID	Proportional-Integral-Derivative
PMT	Photomultiplier Tubes
POS	Point of Sample
PSP	Paralytic Shellfish Poisoning
PST	Paralytic Shellfish Toxins
PTE	Peltier Thermoelectric Elements
rDNA	Ribosomal Deoxyribonucleic Acid
RNA	Ribonucleic Acid
RPA	Recombinase Polymerase Amplification
rRNA	Ribosomal RNA
RT	Reverse Transcription
RT-qPCR	Reverse Transcription Quantitative Polymerase Chain Reaction
RT-RPA	Reverse Transcription Recombinase Polymerase Amplification
SDA	Strand Displacement Amplification
SISO	Single Input, Single Output
SSB	Single Stranded Binding Protein
STX	Saxitoxin

PTE	Thermo Electric Cooler
T_g	Glass Transition Temperature
THF	Tetrahydrofuran
T_m	Theoretical Melting Temperature
TTP	Time to Positive
UNCED	United Nations Conference on Environment and Development
UTR	Untranslated Region
UV	Ultraviolet
WoRMS	World Register of Marine Species

Chapter 1 Introduction

1.1 Aquatic Microbes and Human Health

The oceans cover approximately 72% of the earth's surface and more than 2.4 billion people (approximately 40%) of the world's population live within 100 km of the coast, with many coastal communities dependent on the oceans for their livelihoods (WHO, 2019). This dependence makes coastal communities vulnerable to negative natural occurrences in coastal waters such as flooding, erosion and natural biological hazards such as waterborne disease and toxins produced by harmful algal species. Furthermore, many inland communities suffer from a lack of clean drinking water with the World Health Organisation (WHO) estimating 785 million people lack a basic drinking-water service, with an estimated 2 billion people drinking water contaminated with faeces. This is responsible for 485,000 diarrhoeal deaths annually (WHO, 2019). Economically, global losses are also high with harmful algal outbreaks costing >US$17.6 billion annually (Sanseverino *et al.*, 2016).

The methods used for detecting harmful biological agents in water traditionally involve culture-based methods or visual identification by microscopy. These techniques are time consuming, require well equipped laboratories and extensive technical expertise – which are lacking in many areas where water quality is a serious issue. Molecular techniques, such as the polymerase chain reaction (PCR), nucleic acid sequence based amplification (NASBA), and recombinase polymerase amplification (RPA) offer benefits over these traditional techniques in that they are fast (results in a few hours, rather than days or weeks), sensitive, specific to the targeted DNA or RNA sequence (specific to a certain organism), and are amenable for miniaturisation and automation. These features form the scope of this thesis, which involves the development of molecular assays for the detection of Hepatitis E virus (a human enteric virus transmitted via the faecal-oral route) and *Alexandrium minutum* (a harmful algal species that produces the paralytic shellfish toxin saxitoxin), followed by the development of a prototype miniaturised handheld device for the assays to be performed on, alleviating the need for a well-stocked laboratory and trained technical staff. In addition to this, techniques for the long-term dry storage of reagents were also investigated, to simplify screening through the provision of chips with preserved reagents for the quantification of target genes, as in many regions where this technology will be of greatest benefit refrigeration is unavailable.

Faecal indicator bacteria (FIB) such as coliform bacteria, *Escherichia coli*, *Enterococcus* and *Streptococcus* spp. are frequently used to assess levels of faecal contamination in water. However, bacteria have been shown to be significantly less resistant to wastewater treatment and less persistent in the environment than enteric viruses (Fong *et al.*, 2005; Kim *et al.*, 2009; Lin and Ganesh, 2013; Prez *et al.*, 2015; Sidhu *et al.*, 2017; Staley *et al.*, 2012). FIB are therefore seen as

poor indicators of viral infection risk, and water quality monitoring based solely on FIB is inadequate (Farkas *et al.*, 2020).

1.2 Hepatitis E Virus

Human enteric viruses are viruses that reproduce in a human host, are transmitted via the faecal-oral route and include Hepatitis A Virus (HAV), Hepatitis E Virus (HEV) and Norovirus (NV). Many enteric viruses are resistant to environmental stresses, making effective wastewater management essential in preventing the discharge of potential pathogenic micro-organisms into receiving waters (Woods and Burkhardt lll, 2013). It is estimated that up to 25% of the global population is consuming water contaminated with faecal matter (WHO and UNICEF, 2014), with unsafe water, poor hygiene and inadequate sanitation being responsible for about 90% of diarrheal deaths worldwide (UNICEF, 2012), and the second leading cause of death in children under five globally (1.2 million deaths in 2005) (UNICEF, 2012). The economic cost associated with enteric viruses is also large with the World Bank estimating that a lack of access to safe water and sanitation results in a global economic loss of US$260 billion annually (WHO, 2012).

Hepatitis E virus (HEV) is responsible for Hepatitis E infection. Several outbreaks of Hepatitis in India were originally thought to be attributable to Hepatitis A virus (HAV) infection but retrospective studies confirmed the existence of a new form of enterically transmitted viral Hepatitis, later named Hepatitis E (Wong *et al.*, 1980). HEV itself was first identified in 1983 during an outbreak of Hepatitis amongst Soviet soldiers in occupied Afghanistan (Balayan *et al.*, 1983). There are four known genotypes of HEV: HEV1, HEV2, HEV3, and HEV4. HEV1 and HEV2 are predominant in developing countries due to poor sanitation and are transmitted via the faecal oral route primarily via contaminated water (Kamar *et al.*, 2014). In developed countries, however, HEV3 and HEV4 are predominant, and are transmitted zoonotically from animal reservoirs, specifically swine (Kamar *et al.*, 2014). Swine transmission of HEV3 to humans is the number one cause of HEV infection in the UK with Public Health England (PHE) reporting 100,000 HEV infections per year (Ijaz, 2018). It is currently thought that HEV is responsible for the majority of acute viral Hepatitis in the world (Hoofnagle *et al.*, 2012; Kamar *et al.*, 2012; Purcell and Emerson, 2008). In developing countries, HEV causes a self-limiting illness that lasts for a few weeks. Symptoms include fever and nausea followed by acute abdominal pain, vomiting, anorexia, malaise, and hepatomegaly (Kamar *et al.*, 2014), with jaundice occurring in 40% of patients (Labrique *et al.*, 2010). Although mortality rates are usually under 0.5%, in pregnant women genotype 1 can lead to rates as high as 25% (Van der Poel, 2014).

HEV is a positive sense single-stranded RNA virus with a 7.2kb genome, which is capped and polyadenylated at both the 5' and 3' termini and contains three Open Reading Frames (ORF). ORF1 encodes for a 1,693 amino acid protein, containing non-structural proteins, ORF2 encodes the 660 amino acid viral capsid proteins, whilst ORF 3 encodes for a small protein (113-114 amino acids) involved in virion morphogenesis and release (Kamar *et al.*, 2014).

Coupled with sea level rise associated with human induced climate change resulting in increased flooding events globally (Cai *et al.*, 2014) there is a high likelihood of increased incidences of outbreaks of waterborne illnesses including Hepatitis E in the future (Cann *et al.*, 2013).

1.3 Harmful Algal Blooms (HABs)

Growing global populations have led to a higher demand for resources from the sea. Harmful algal blooms (HABs) negatively impact the successful harvest of marine resources, constraining the sustainable development of coastal areas (Anderson, 2009; Zingone and Oksfeldt Enevoldsen, 2000). There are two characteristics that define HABs (i) is that they are caused by microalgae and (ii) is they all have a negative impact on human activities (Anderson, 2009; Zingone and Oksfeldt Enevoldsen, 2000).

HAB species exhibit different negative impacts on ecosystems. The diatoms *Chaetoceros sp* and *Skeletonema sp* are not directly toxic to humans but blooms have resulted in losses of farmed fish due to asphyxiation caused by gill damage by the diatoms siliceous spines (Bruno *et al.*, 1989). The diatom *Pseudo-nitzschia seriata* produces the toxin domoic acid that accumulates in filter feeding bivalves causing amnesic shellfish poisoning (ASP) in humans or domoic acid poisoning (DAP) in wildlife (Fernandes *et al.*, 2014; Trainer *et al.*, 2012). These toxins accumulate as they pass up the food chain, leading to increased toxin concentration at higher trophic levels. HABs thereby have negative impacts not just on human health but also on the economy and ecology of marine environments.

Dinoflagellates are another group of microalgae that form harmful blooms. The genus *Alexandrium* produces saxitoxins (STX) linked with paralytic shellfish poisoning (PSP) (Burson *et al.*, 2014). *Alexandrium* is usually present in the water column of marine and brackish areas throughout most of Europe but at low concentrations insufficient to cause harm. Certain environmental conditions initiate blooms however, caused by a rapid proliferation in algal cells. This in turn leads to an increase in STX present in the water, which can reach concentrations high enough to impact human and animal health. Some of the changing environmental conditions linked with HAB initiation include temperature, water column stability, turbidity, nutrient input, grazing pressure, ocean acidification and wind mediated transport (Bresnan *et al.*, 2020). It is currently unknown if

individual cells contain different levels of STX, however toxin content appears to be linked to nutritional status (Han *et al.*, 2016; Yang *et al.*, 2011). A study by Wiese *et al.* (2014) demonstrated that there is no significant difference in toxin gene expression, even though differences in the levels of toxin were observed during different growth stages of the closely related dinoflagellate *Alexandrium catanella*. This indicates that the production of PSP toxins is likely mediated by post transcriptional modification of the gene products, though this is yet to be determined.

As noted previously, there are a variety of issues that arise from the propagation of HABs. The toxins produced by some species can have a direct medical impact on people living close to the bloom. The human illnesses associated with HABs include paralytic shellfish poisoning (PSP), diarrhetic shellfish poisoning (DSP), neurotoxic shellfish poisoning (NSP), amnesic shellfish poisoning (ASP) and ciguatera fish poisoning (CFP), as well as respiratory problems and skin irritation (Zingone and Oksfeldt Enevoldsen, 2000). The symptoms of these illnesses vary from vomiting, nausea, diarrhoea and abdominal pain (PSP, DSP, CFP); paraesthesia of the mouth, lips and tongue, and dizziness (NSP); and hallucinations, memory loss, and coma (ASP) (Gingold *et al.*, 2014; Glibert *et al.*, 2005; Jeffery *et al.*, 2004; Taylor *et al.*, 2013; Watkins *et al.*, 2008). Humans come into contact with these toxins through a variety of means including consumption of marine organisms that have bioaccumulated the toxins through filter feeding (e.g. shellfish) or through the food chain (e.g. fish) as well as by direct water ingestion or contact and aerosolised transport (Davidson *et al.*, 2014). Illnesses caused by HAB events have an associated economic impact; an example being a red-tide event in Florida, USA caused by the dinoflagellate *Karenia brevis* that is estimated to have cost local health authorities US$60 000 to US$700 000 annually, with the potential to increase to over $1 million in the case of a prolonged bloom (Hoagland *et al.*, 2014).

HABs also have economic impacts via the loss of fisheries and farmed stocks via the production of toxins or causing mechanical damage to gills due to their hard-exterior structures. In the Arabian Seas in 2008 massive HAB outbreaks caused by the dinoflagellate *Cochlodinium polykrikoides* (Richlen *et al.*, 2010) resulted in large regional fish losses, with over 650 tons of dead fish washed ashore in Dibba Al-Hassan and more than 700 tons in Khor Fakkan reported (Pankrantz, 2008). The total quantities of fish (including demersal species in the south and west, and shrimp and pelagic species in the north (Al-Abdulrazzak *et al.*, 2015)) produced were reduced to 37% of the quantities in 2006 (Al Shehhi *et al.*, 2014). This has also led to a reduction in fisherman numbers that in turn led to a degradation of traditional fishing communities around the Arabian Seas (Al Shehhi *et al.*, 2014). The economic impacts of removing dead fish that wash up on beaches, and in canals and rivers can also be high. The removal of 2367 tonnes of dead fish in St. Petersburg, Florida, in 1971 is estimated to have cost US$155,763 (Kirkpatrick *et al.*, 2004). In the UK in 2018 toxins produced by harmful algal species resulted in the temporary closures of four shellfish farms in England and

Wales for varying lengths of time, with associated economic impacts due to stock loss (Parks *et al.*, 2020). Toxin levels in UK waters are tested for and reported annually by Cefas (https://cefaswebsitedev.cefastest.co.uk/data-and-publications/habs/).

HAB outbreaks have also caused economic losses to the tourism industry. In 2009, the whole of Jumeirah beach near the Burj Al Arab in Dubai had to be closed because of skin and eye irritation caused by the toxicity of a HAB (*C. polykrikoides*). During this time many beach hotel bookings were cancelled, resulting in significant economic losses to the region (Al Shehhi *et al.*, 2014). Some HAB species can also harm tourism indirectly such as through bad odours that deter people from visiting the areas and even lead to the temporary closing of some buildings (Al Shehhi *et al.*, 2014; Peralta *et al.*, 2006).

HABs also have negative impacts on the ecosystem by causing damage to species that are of no economic value to humans but play important roles in their ecosystems, categorized as EDABs (ecosystem disruptive algal blooms). EDABs are often caused by increased nutrient input into the marine environment from terrestrial sources. Blooms of unpalatable species reduce the grazing rate, which decreases nutrient cycling (Sunda and Shertzer, 2014). When the bloom has used up all the nutrients in the water it will start to decay. The breakdown of the algal material and any zooplankton feeding on it is carried out by aerobic bacteria that can remove the oxygen from the water resulting in an anoxic environment. This can lead to high mortalities in the surrounding ecosystem whether toxins are produced or not (Heisler *et al.*, 2008).These “oxygen minimum zones” (OMZs) are expanding globally (Bertagnolli and Stewart, 2018). Although algal blooms have been identified as a cause of OMZ formation they aren’t solely responsible, with physical factors such as nutrient upwelling driving intense primary production leading to a net drawdown of oxygen producing an oxygen minimum zone that is functionally anoxic (Bertagnolli and Stewart, 2018).

1.3.1 Increasing HAB Incidences

HAB events have been reported throughout history, with observations in 1528 – 1534 of shellfish harvests being suspended seasonally along Galveston Island off the coast of Texas, most likely due to a red tide (Walsh *et al.*, 2006). In the USA there are reports from Alaska in 1799 of more than 150 people suffering from paralytic shellfish poisoning, with 100 dying (Lewitus *et al.*, 2012). The first HAB recorded in the Arabian Sea was in 1908 and extended from the Malabar Coast to the Laccadive Islands along the Indian coastline (Al Shehhi *et al.*, 2014). Although HAB outbreaks have been recorded throughout history, they have only occurred sporadically. In recent times, however, they are becoming annual events and are occurring in areas where historically they have not

previously been detected (Glibert *et al.*, 2005). The increases are likely due to increased outbreaks due to human induced climate change and improvements in monitoring technologies, in addition to more widespread testing due to the expansion of aquaculture.

In order to try and quantify temporal trend of HAB incidences, Lewitus *et al.* (2012) collected data on occurrences of illnesses related to HABs reported in the western coastal states of the USA, Canada and Mexico and used this data as an indicator of a HAB occurring. Their results show that there is an increase in the number of cases reported, with two deaths reported in Alaska in 2010 due to PSP. These west coast outbreaks are primarily caused by dinoflagellates of the genera *Alexandrium*, *Gymnodinium*, and *Pyrodinium*, and the diatom genus *Pseudo-nitzschia*, all of which produce toxins. However coastal blooms do not seem to follow the global trend of forming in coastal regions due to eutrophication, but initiate offshore and are carried inshore where, fuelled by nutrient upwelling, they are able to propagate further (Lewitus *et al.*, 2012). The shellfish industry is particularly important in the Pacific Northwest, as is the salmon aquaculture industry. Continued outbreaks have already had a negative impact on these two industries (Lewitus *et al.*, 2012).

The domoic acid toxin producing diatom *Pseudo-nitzschia australis* was responsible for a major HAB event along the whole of the US Pacific coast in both 2015 and 2016, which had major socio-economic impact. Fishing communities that primarily rely upon Dungeness crab (*Metacarcinus magister* [WoRMS] or *Cancer magister* [ITIS]) in Washington State (WA), Oregon (OR) and California (CA) were all impacted when fisheries were closed completely for between one month (WA and OR) and five months (CA). The estimated economic loss to the industry, and the associated communities is estimated to be in the region of US$97.5 million, not just from fishing, but from recreational and hospitality industries too (Moore *et al.*, 2020).

In the Arabian Sea, Al Shehhi *et al.* (2014) also identified that the number of HAB events has gone from being a rare occurrence to an almost annual event. Increases have also been noted in Europe, with the first bloom in the Adriatic Sea recorded in 1989 and harmful species recorded with some frequency in the Venice Lagoon since the 1970's, with the number of recorded blooms showing a general increase year on year (Facca *et al.*, 2014).

Highlighting the global nature of HAB outbreaks, HAB occurrences have been increasing in Asia, for example off the coast of Korea in semi-enclosed bay areas in the East Sea (Choi *et al.*, 2014). Choi *et al.* (2014) used the Geostationary Ocean Colour Imager (GOCI) to monitor a red tide event near the Korean peninsula in 2013. The HAB was linked with a cold-water mass in the region, and the species that caused the bloom was identified as the dinoflagellate *C. polykrikoides*, which has also bloomed off the coast of California and Europe (Gárate-Lizárraga *et al.*, 2004; Kudela and Gobler,

2012). Potential problems associated with *C. polykrikoides* include massive fish kills (both wild and cultured) as well as rapid mortality in reef building coral, copepods, other phytoplankton, shellfish larvae, and bivalves due to the production and excretion of mucilagic polysaccharides that may be an indirect, important mechanism of mortality (Richlen *et al.*, 2010). The economic impact of these outbreaks has been significant with estimated Korean fishery losses of over US$100 million annually (Kudela and Gobler, 2012).

Several theories have been put forward and there is much debate about the primary cause of the increased HAB incidents. As many HAB species are known to thrive on nitrogen and phosphorous, the increased loading of these nutrients into the sea via agricultural, sewage and industrial discharge is considered a factor. However some HABs have occurred in areas where there is minimal pollution detected (Anderson, 2009). It is also believed that ballast water from commercial shipping has led to the observation of HABs in areas where they have not been observed previously. This is the case with many other alien invasive species that have been transported to locations outside their natural range and have caused considerable damage (Miehls *et al.*, 2009). It is understood that dinoflagellates can be transported through ballast water during their cyst life cycle stage. When they arrive in their new location they are able to hybridize with the organisms already present at the recipient sites, creating progeny with greater ecological fitness than the local strains, allowing them to outcompete and form blooms (Smayda, 2007). The issue of transport of non-indigenous species was recognized at the United Nations Conference on Environment and Development (UNCED) in Rio de Janeiro, 1992. Subsequently, the International Maritime Organization (IMO) began investigating viable methods of eliminating the transport of alien species via ballast. In 2004 the International Convention for the Control and Management of Ships' Ballast Water and Sediments was adopted (IMO, 2004). This required all ships to carry a ballast record book and carry out ballast management procedures, such as conducting ballast water exchange 200 miles from the nearest land in water at least 200 m deep, or treating with chemicals that must be approved by the IMO (IMO, 2004). Molecular tools allow for high throughput sequencing of species that may be present in ballast water, and could be powerful tools in monitoring the microbial composition of ballast water. These molecular tools eliminate some of the problems associated with tradition testing (morphological taxonomy). These limitations include the use of bulky sampling gear including sampling nets and are time consuming, with tight time constraints typical for commercial shipping. Additionally, many transported species may be transported in a juvenile life stage and be difficult to identify accurately. Molecular techniques can be used for the amplification and identification of potential transported species from traces of DNA within the environment, so called environmental DNA (eDNA). Due to the sensitivity of these molecular techniques large scale

sampling is not required, and their highly specific nature removes any chances for misidentification (Rey *et al.*, 2019).

The historic increased incidences in HAB outbreaks may simply be an artefact caused by improvement in monitoring. Historically, light microscopy has been used to identify algal species, however, in the last 20 years there has been a shift towards using molecular tools for identification, which increases the number of laboratories that can perform surveillance (Rhodes *et al.*, 2013). As aquaculture has expanded, water quality is being studied much more rigorously than in the past and this has led to detection of HAB species in locations where they have not been recorded previously. It is possible that they were simply not detected previously, rather than arriving into a new region (Anderson, 2009). The expanded use of satellites for ocean observing (Choi *et al.*, 2014) increases the spatial coverage of bloom detection. Problems can arise with the use of satellite data, however. Satellite imagers monitor the colour of the sea surface and then use algorithms to determine the amount of chlorophyll. It is not possible to determine the species or whether it is harmful with this methodology. In order to get around this problem Kurekin *et al.* (2014) developed HAB discrimination techniques that analyse differences in optical properties and backscatter to establish whether a bloom is composed of harmful or non-harmful algal species. This technique has correctly identified 89% of *Phaeocystis glabosa* and 88% of *Karenia mikimotoi* blooms in waters off the UK when used on MODIS (Moderate Resolution Imaging Spectrometer) and MERIS (Medium Resolution Imaging Spectrometer) data. This will lead to greater identification of HABs and these data will determine whether HABs are expanding globally, in the future.

Increasing aquaculture can also lead to the spread of HABs. A study by Rosa *et al.* (2013) shows that HAB species survive transport through the guts of biofouling species associated with aquaculture. Biofouling organisms are typically molluscs that cover man-made structures and overgrow and outcompete the endemic species. These organisms are physically removed accounting for ~15% of annual aquaculture running costs, transported a short distance away and dumped overboard. Many of these organisms will still be alive and will subsequently excrete harmful algae into the receiving waters.

Global climate change has been linked with an increase in harmful algal events, not only due to temperature rises but other, associated environmental changes such as ocean acidification and increased extreme weather events. Studies have shown that HABs appear to be progressing poleward with increased warming (Gobler *et al.*, 2017; Griffith *et al.*, 2019; Hallegraeff, 2010), additionally increased oceanographic levels of CO_2 caused by dissolution of increased atmospheric CO_2 has been shown to increase HAB occurrences. It has been suggested that the RuBisCO (the enzyme responsible for carbon fixation and the first step of photosynthesis) found in dinoflagellates

has a lower affinity for CO_2 than other phytoplankton, makes them more likely to benefit than other types of algae (Reinfelder, 2011). A recent study by Brandenburg *et al.* (2019) appears to confirm this as in a meta-analysis of 26 HAB species the authors demonstrated that growth rates increased consistently with rising CO_2 levels, whilst non-harmful algae did not. The ability of HABs to grow preferentially in extreme conditions has led to them being classed as a co-stressor on native organisms during these events (Gobler, 2020)

1.3.2 Alexandrium minutum

Several members of the dinoflagellate genus *Alexandrium* produce the potent neurotoxin saxitoxin (STX), responsible for paralytic shellfish poisoning (PSP) (Figure 3). The genus *Alexandrium* contains over 30 species. Only *A. tamarense*, *A. fundyense*, *A.catanella*, and *A. minutum* are responsible for most PSP producing blooms (Lilly *et al.*, 2005).

The first population of *A. minutum* (Figure 1) was identified in 1960 in the port of Alexandria in Northern Egypt, where the genus takes its name (Halim, 1960). Traditional methods of identification rely heavily on light microscopy. However, molecular techniques have been utilised more recently including PCR (Galluzzi *et al.*, 2004), FISH (Touzet *et al.*, 2009), and sequence ID of microsatellite markers (Casabianca *et al.*, 2012). These molecular techniques have resulted in the reclassification of related species *Alexandrium lusitanicum* and *Alexandrium angustibulatum* into *A. minutum* (Lewis *et al.*, 2018). *A. minutum* is distributed globally and molecular techniques readily identify them from field samples. Areas of identified *A. minutum* occurrence are shown in Figure 3.

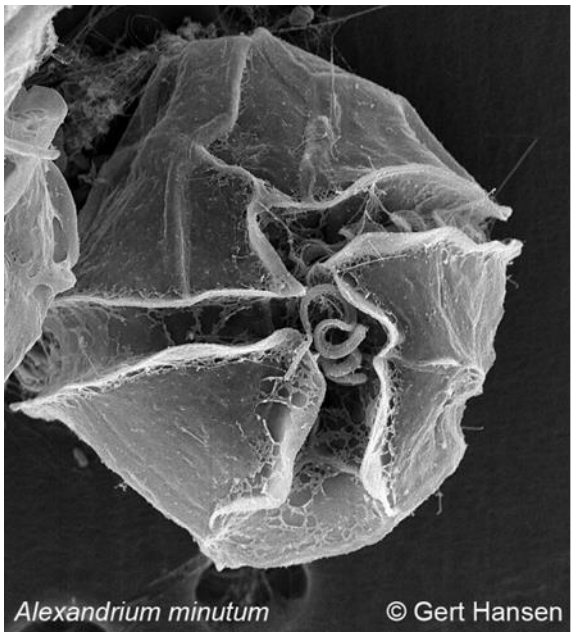

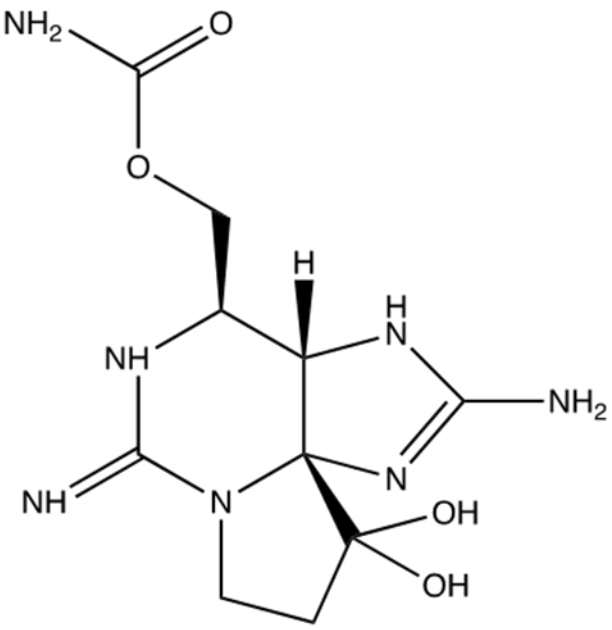

Figure 1 The armoured dinoflagellate *Alexandrium minutum* (Hansen, 2009), and the chemical structure of saxitoxin, a potent neurotoxin and the PST produced by *A. minutum*.

Traditionally *A. minutum* outbreaks were restricted to the warmer waters of the Mediterranean, however, since the 1980's and the proliferation of global rising sea temperatures, *A. minutum* PSP toxin producing blooms have been recorded in more temperate regions including the North Sea, in the coastal waters of Ireland (Ní Rathaille and Raine, 2011), and Scotland (Smayda, 2006). Ideas proposed for the increase in incidence of *A. minutum* outbreaks include nutrient loading from coastal eutrophication and aquaculture (Lilly *et al.*, 2005). There are very few records of non-toxic *A. minutum*, however different strains and isolates have been shown to demonstrate high toxin variability, ranging from 11.3 to 88.2 pg cell^{-1} (Martens *et al.*, 2017). Blooms of *A. minutum* are known to have impacted on humans and food security, impacts that are likely to continue with an ever increasing global human population (Lewis *et al.*, 2018).

Alexandrium species have complex lifecycles (Figure 2) that include several different stages. During the vegetative stage cells are haploid and motile. Under stress conditions some of these motile cells are able to transform into non-motile pellicle cysts which are able rapidly transform back to the motile stage when conditions improve. The sexual phase starts with the formation of gametes which conjugate and form a diploid planozygote. Depending on environmental conditions this planozygote can transform into a resting cyst (hypnozygote) which can spend variable amounts of time in the sediments until germination and release of a motile cell (Anderson *et al.*, 2012a). This ability to form cysts has led to localised outbreaks, whereby a previous bloom has left cysts in the sediment and then when local conditions become favourable vegetative cells are released back into the water column (Brosnahan *et al.*, 2020).

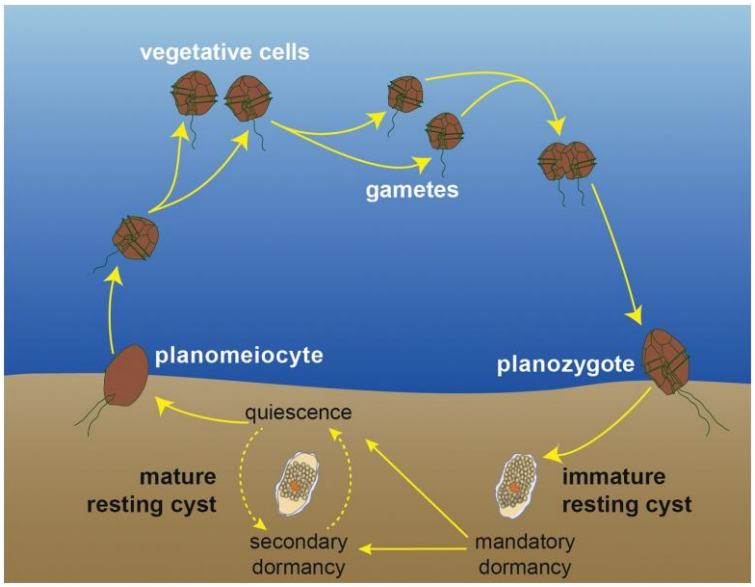

Figure 2 The *Alexandrium* life-cycle. The haploid vegetative cells form short lived gametes that fuse to form a diploid planozygote, which can then transform to become resting cysts which germinate in response to favourable oxygen and temperature conditions (taken from Brosnahan *et al.* (2020))

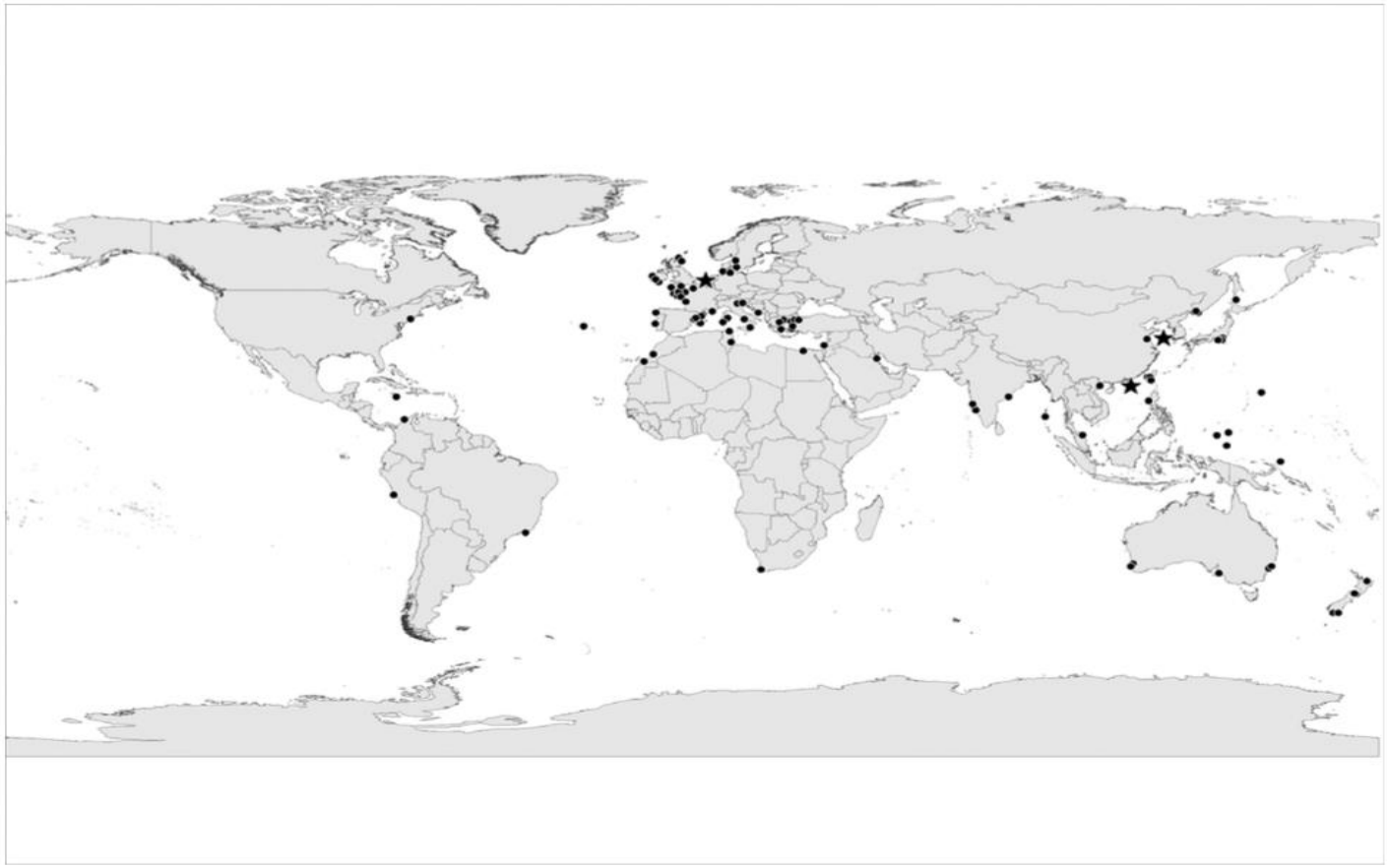

Figure 3 Map of the global distribution of *A. minutum*. Dots denote confirmed locations whilst stars denote regions of occurrence where the definitive location is unclear in the literature (Lewis *et al.*, 2018)

1.3.3 Molecular Detection of HABs

Traditional methods of identification of HABs have relied upon microscopy. Although they can be accurate, these techniques are time consuming and require trained microscopists. Molecular techniques on the other hand offer powerful and efficient alternatives. For example, they are high-throughput, allowing many samples to be examined simultaneously. Molecular assays can be highly sensitive, potentially allowing detection of up to a single gene copy from a particular organism. If RNA techniques are used (NASBA, RT-qPCR, RT-RPA) there is the potential to differentiate between live and dead cells, and to gain insight into potential factors that drive gene expression.

1.4 Cell Lysis and Nucleic Acid Extraction

Before any nucleic acid (NA) analysis can take place, genetic material must be extracted from the cell. This process includes cell lysis; removal of membrane lipids, proteins, and other NAs; NA purification; and NA concentration. Cell lysis is typically achieved via physical, chemical, or enzymatic disruption of the cell wall/membrane, with the method used dependant on the sample type. Physical disruption utilises mechanical processes to disrupt the cells such as grinding, shearing, bead-beating and shocking. Chemical methods utilise lytic enzymes, chaotropic agents and different types of detergents to achieve the same goals (Ali *et al.*, 2017). Enzymatic methods rely on a suite of enzymes to conduct cell disruption such as carbohydrases, beta-glucanases, xylanases, mannanases, xyloglucanases, pectinases, and glycosidases (Manen *et al.*, 2005), and have been integrated with microfluidic architecture (Thompson *et al.*, 2016).

Silica matrices have become a widespread tool in the purification and concentration of NA. Under alkaline conditions and high salt concentrations silica has a positive charge and a high binding affinity for DNA, which is negatively charged. Binding to the silica membrane allows the cellular material left over from the lysis phase to be washed out. Hypoosmotic solutions such as nuclease-free water, or buffers such as Tris-EDTA are then used to elute the NA from the silica matrix. This technique is fast and reproducible, with its main drawback being the requirement for centrifugation. There are many commercial kits available for purification and concentration of NAs from a variety of starting material including both solid-phase and liquid-phase extraction methods.

1.5 Nucleic Acid Amplification

1.5.1 Real-Time Polymerase Chain Reaction (RT-PCR)

The polymerase chain reaction (PCR) (Figure 4) was developed by Kary Mullis in the mid 1980's (Mullis *et al.*, 1986) and since then has become a 'gold-standard' tool for the analysis of nucleic acids. PCR utilises DNA polymerase to exponentially amplify a specific target region of a DNA sequence. Primers are designed to anneal to the flanks of the desired region of DNA to be amplified. The polymerase can then extend the strand of DNA by adding nucleotide bases downstream from the primer binding region. PCR is achieved through iterative cycles of three processes: template sequence **denaturation**, primer **annealing**, and strand **elongation**. Denaturation takes place at around 95°C which splits complementary strands of double stranded DNA (dsDNA). This is followed by the primer annealing stage, which typically involves temperatures between 50-65°C, where primers bind to the extreme termini of the target region of DNA. The final stage, elongation, takes place at temperatures between 70-80°C, allowing the extension of complimentary DNA (cDNA) to the target, resulting in a copy of the original DNA strand. The amplified products of the PCR, the amplicons, can then be analysed. This typically involves staining and separation through an agarose gel in tandem with a DNA ladder containing a range of DNA fragments of known size to determine their size (number of base pairs). The requirement for 'thermal cycling' has been cited as a limitation to miniaturization and subsequent *in situ* deployment of PCR capable devices (Lee *et al.*, 2019). This is due to the energy requirements of Peltier Thermoelectric Elements (PTE), which enable rapid temperature changes, and require bulky heatsinks to draw heat away during the cooling phases.

The standard PCR technique can be combined with a target-specific hydrolysis probe making the process quantitative and measurable in real-time (qPCR) (Glass *et al.*, 2009). Quantification is achieved as the cycle number that the reaction crosses a set threshold (C_t) and is related to the initial target gene concentration. High target concentration amplification begins earlier as target is located by the primers earlier, with the inverse being the case in low concentration reactions, this is coupled with an increased number of cycles lower concentrations require for the detected signal to cross the C_t, as each cycle increases the amount of amplicon produced exponentially. The hydrolysis probe is a short (20-30 bp) oligonucleotide, which sometimes adopts a hairpin structure, containing a fluorophore at the 5' end and a quencher at the 3' in close proximity: this is the 'lights off' conformation. In the presence of the complimentary target sequence the probe anneals to the target sequence. DNA polymerase then cleaves the quencher making the fluorophore no longer quenched, producing a fluorescent signal that can be detected: the 'lights on' conformation. The probe fluorescence is perpetual once it has been incorporated into each new strand of DNA. As the

polymerase used in PCR is a DNA-dependent DNA polymerase a modification to the process is required if the target of interest is RNA. This modification consists of an initial treatment of the sample with reverse transcriptase (RT; RT-qPCR), converting the RNA target into its cDNA counterpart, followed by standard PCR as described above.

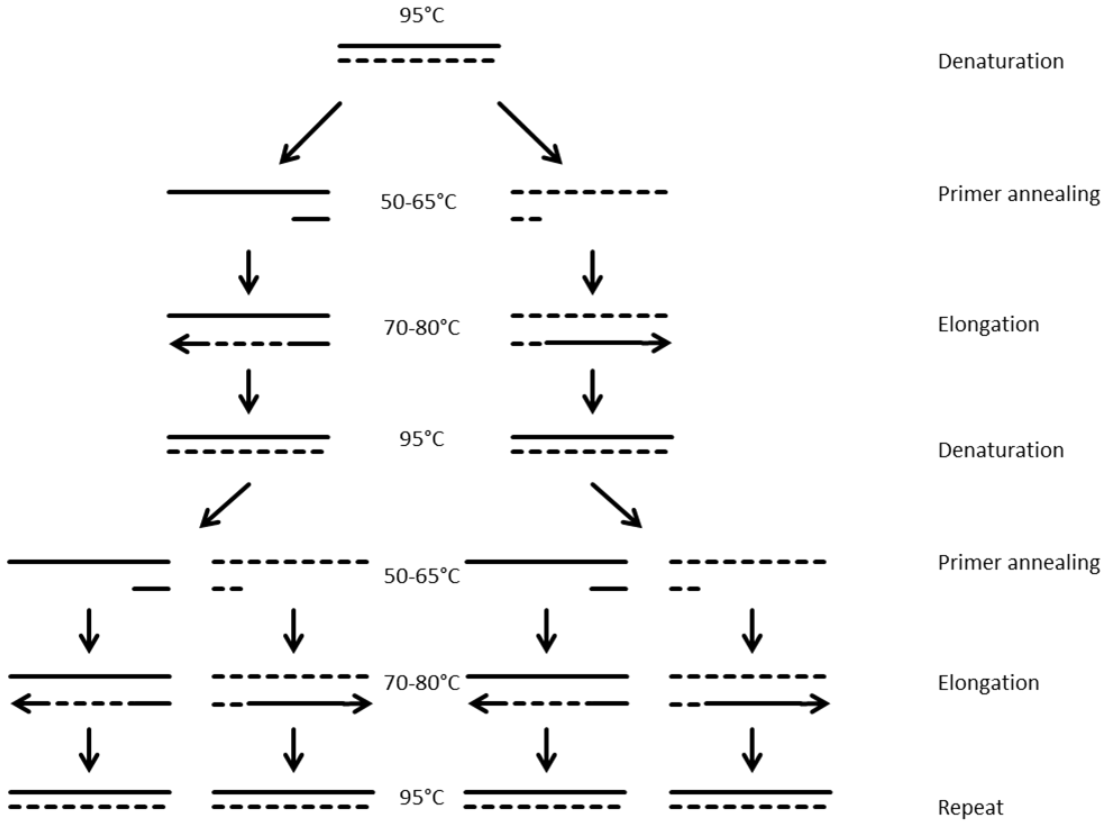

Figure 4 A diagrammatic representation of PCR

RT-qPCR assays have been used previously to identify Hepatitis A Virus (HAV) (Cromeans *et al.*, 1997), Hepatitis E Virus (HEV) (Mokhtari *et al.*, 2013), Norovirus (NV) (Atmar and Estes, 2001) and *A. minutum* (Galluzzi *et al.*, 2004; Orr *et al.*, 2013) from water samples.

1.5.2 Nucleic Acid Sequence Based Amplification (NASBA)

Unlike PCR, NASBA (Figure 5) utilises three enzymes to amplify an RNA target, as opposed to a DNA target. NASBA is an isothermal amplification reaction that mimics retroviral replication (Chang *et al.*, 2012). During NASBA, a 'forward primer', which includes a T7 RNA polymerase promoter sequence fused to its 5' terminus, hybridizes to the target RNA molecule. It is then reverse transcribed by reverse transcriptase, creating an RNA: DNA hybrid molecule. RNase H degrades the RNA strand and a complementary DNA strand is constructed by the DNA polymerase activity of the reverse transcriptase, using the reverse primer. The resulting double-stranded DNA (dsDNA) contains the T7 promoter sequence. T7 RNA polymerase then uses this dsDNA to produce anti-

sense RNA strands, which are complimentary to the original target RNA. This cycle is repeated starting with the newly synthesized anti-sense RNA for amplification (Asiello and Baeumner, 2011). Amplified targets are detected using a molecular beacon for real time measurement of the amplification reaction, enabling quantification of amplified targets, similar to qPCR. Apart from the initial denaturation step, the NASBA reaction occurs isothermally at a constant 41°C using a water-bath or hot block (Lauri and Mariani, 2009). Measuring specific messenger RNA (mRNA) sequences can be used to analyse gene regulation and therefore also provide a view as to what processes and biogeochemical cycles a cell population may be actively involved in (Poretsky *et al.*, 2005). The quantification of a specific target RNA sequence is achieved by comparing the time taken for the reaction to produce a defined quantity of product, known as the time to positive (TTP), which is inversely proportional to the abundance of the target sequence in the sample. Due to the reliance on three different enzymes however, NASBA amplification kinetics are more complex than qPCR, which may lead to a greater run-to-run variability. Therefore, a spiked internal control (IC) is advised for reliable quantification and inter-sample comparison. An internal control is a synthesised piece of RNA composed of the same sequence as the target amplicon, with the beacon site removed and replaced with a sequence from a separate assay. The ratio is then taken between the spiked IC-RNA and the target to give precise RNA quantification (Patterson *et al.*, 2005).

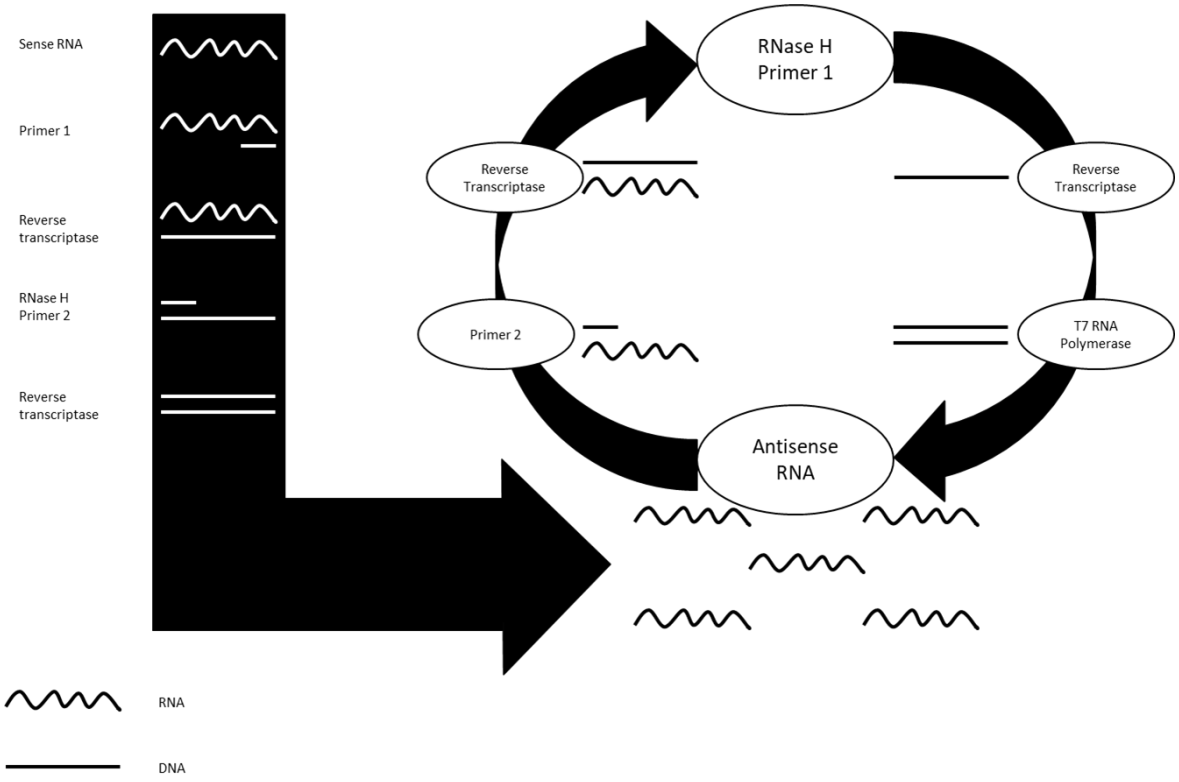

Figure 5 A diagrammatic representation of NASBA

1.5.3 Recombinase Polymerase Amplification (RPA)

Recombinase Polymerase Amplification (RPA) (Figure 6) is an isothermal NAAT that utilises recombinase enzymes to anneal primers to template DNA allowing extension and amplification by an isothermal polymerase (Armes and Stemple, 2002). During the RPA reaction recombinase proteins form complexes with the forward and reverse primer before hybridising to a homologous sequence on the target DNA. The primers are then inserted at the target site by the strand-displacement activity of the recombinase. Single stranded binding proteins (SSB)s then bind to the displaced DNA strand, stabilising it. The recombinase then detaches, leaving the 3' end of the primers accessible to a strand displacing DNA polymerase, elongating the primer. A near exponential amplification is achieved by cyclic repetition of this process. RPA demonstrates a greater deal of flexibility compared to other nucleic acid amplification technologies (NAATs) with amplification being possible at temperatures ranging from room temperature to 65°C in under an hour (Lobato and O'Sullivan, 2018).

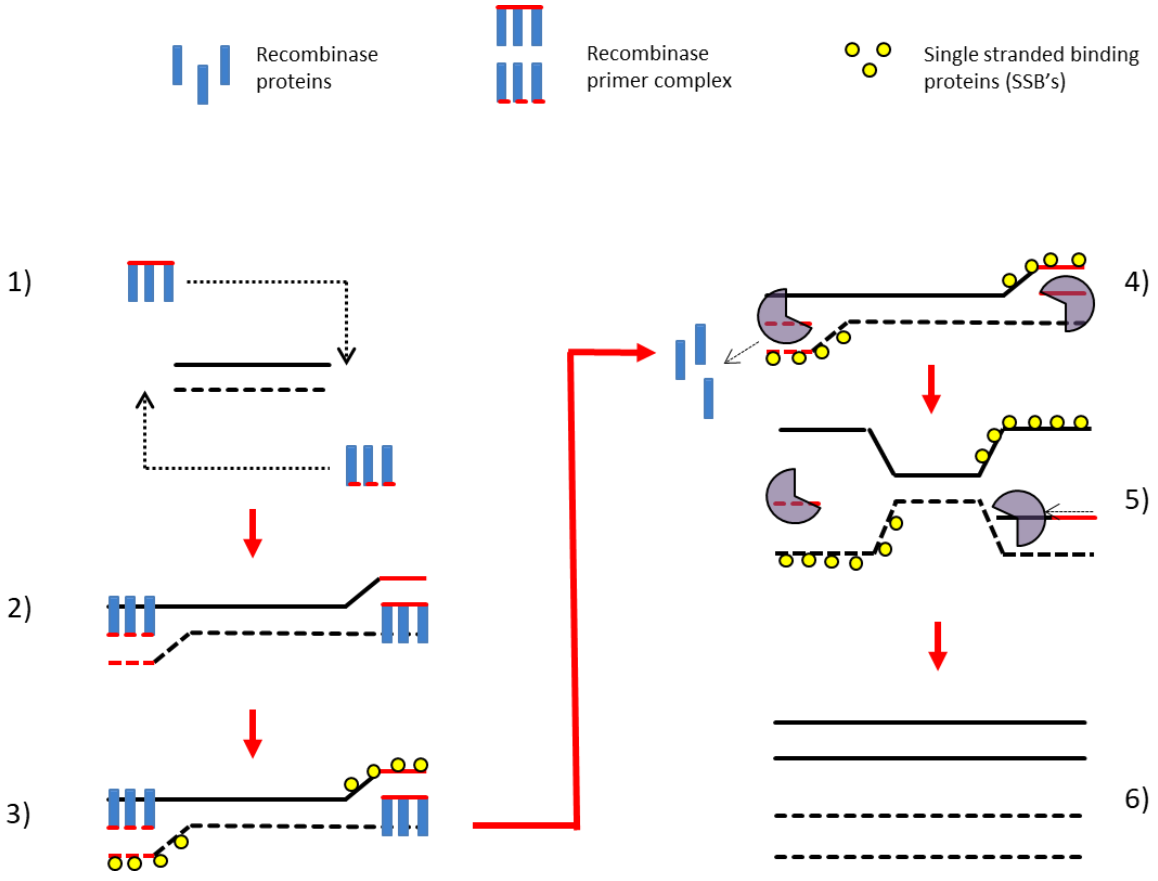

Figure 6 The RPA process. 1) Recombinase proteins form complexes with the primers, 2) the recombinase/primer complexes bind to the complimentary sites in the target DNA forming a D-loop, 3) single stranded binding proteins hold the two DNA strands apart, 4) DNA polymerase binds and 5) extends each strand in the 5' to 3' direction resulting in two new strands of target DNA 6).

1.5.4 Other Isothermal Techniques

NASBA and RPA are but two of several isothermal nucleic acid amplification techniques available. LAMP (Loop-Mediated isothermal amplification) (Notomi *et al.*, 2000), RCA (Rolling Circle Amplification) (Liu *et al.*, 1996), SDA (Strand Displacement Amplification) (Walker *et al.*, 1992b), EXPAR (Exponential Amplification Reaction) (Qian *et al.*, 2012), ICANS (Isothermal and Chimeric Primer-Initiated amplification of Nucleic Acids) (Asiello and Baeumner, 2011), and SMART (Signal Mediated Amplification of RNA Technology) (Hall *et al.*, 2002) have been used previously for viral detection and all have the potential for implementation on miniaturised analytical devices such as the novel 'lab-on-a-chip' (LOC) Instrument, which is described in the following sections of this thesis.

1.6 Current Technologies

1.6.1 Lab on a Chip

Traditionally, chemical and molecular analytics require bulky, power hungry and expensive bench-top equipment in order to obtain data. However, the volumes of reagents used per reaction are in the 10s of microlitres, and are therefore amenable to miniaturisation. LOCs are frequently used as a means for the miniaturisation of these often complicated, bulky and expensive pieces of equipment and to increase efficiency including reduced operating costs, lower power requirements, reduced equipment costs, and portability.

There are several novel PCR and isothermal DNA and RNA methods that have now been miniaturised. A device primarily designed for oceanographic applications is the IISA-gene, developed for microbiological studies in extreme environments. The IISA-gene uses several stationary heat blocks which the reaction fluid is moved over to produce thermal cycles, and a light emitting diode (LED) combined with a photomultiplier (PMT) to perform qPCR *in situ* (Fukuba *et al.*, 2011) Additionally, the Rotary Zone Thermal Cycler (RZTC) is a prototype miniaturised, low-powered thermal cycler that can currently perform up to seven replicate reactions and utilises rotating heat blocks to perform thermal cycling within small bore tubing (Bartsch *et al.*, 2015). Another example of an emerging technology in the field is Digital Droplet PCR (ddPCR), which requires minute reaction volumes and is intrinsically quantitative (i.e. without the use of standards), making it a simple and therefore robust option which is advantageous for integration with LOC (McQuillan and Robidart, 2017). Two recent studies (Hatch *et al.*, 2014; Larsen *et al.*, 2016) have demonstrated the capability of ddPCR to be miniaturised. Bian *et al.* (2015) designed a polydimethylsiloxane (PDMS) chip based ddPCR system that successfully detected pathogenic *E.*

coli and *Listeria monocytogenes*, whilst Schuler *et al.* (2016) implemented ddPCR on a disk, which uses centrifugal force in the creation of the droplets and then rotates the reaction chamber to different temperature zones to perform the thermal cycling. A limitation of ddPCR, however, is that the patent is owned by Bio-Rad (USA), and they have been unwilling in sharing the patent, an additional reason for the development of new, alternative technologies.

1.6.2 Microfluidics – chip design

Microfluidics is defined as the science and technology of systems that manipulate or process small amounts of fluids, typically between 10^{-9} to 10^{-18} litres, using channels with dimensions in the tens to hundreds of micrometres (Whitesides, 2006). Using fluids in such small volumes offers a number of benefits in capability over macro-fluidics, including the ability to use smaller quantities of samples and reagents and perform high resolution detection with high sensitivity, lower costs, shorter analysis times, and smaller footprints than standard instrumentation (Manz *et al.*, 1992).

There are several differences that occur with fluid dynamics that arrive from scaling from the macro- to micro- scale. The most important of these being turbulence – at larger scales fluids mix convectively as larger volumes are dominated by inertial forces. At smaller scales however, viscosity is the dominant force, causing two liquids coming together in a micro-channel to flow in parallel, the only mixing being diffusion of particles across the interface between the two liquids. The ratio of inertial to viscous forces is characterised by the Reynolds number (Re), a dimensionless parameter used in the study of fluids (Squires and Quake, 2005).

Microfluidics and lab on chip technologies (LOC) commonly utilise Polydimethylsiloxane (PDMS) for 'rapid prototyping' of the chips and micro-channels. PDMS is an organosilicon compound that has been used in applications ranging from contact lenses and breast implants to shampoo, foodstuffs and lubricants. PDMS is an ideal material to use in microfluidics as it is optically clear, non-toxic, chemically inert, thermally stable, gas permeable, easy to manipulate, cheaper than similar compounds, and conforms to submicron features to develop microstructures (McDonald and Whitesides, 2002). Glass is another material that has been utilised for microfluidic applications. Glass offers several benefits in that it is thermally insulating, allowing the generation of large temperature gradients (Iliescu *et al.*, 2012) and is mostly transparent from ultraviolet through to infrared making it an ideal substrate for optical detection assays. Its high melting temperature also makes it handy where thermocycling is required and it is non-toxic making it ideal for biological and environmental applications.

1.6.3 The Novel LOC Genetic Sensor

The National Oceanography Centre (NOC) Ocean Technology and Engineering (OTE) LOC Genetic Sensor (Figure 7) is a portable nucleic acid amplification and detection device. It consists of a series of LED's aligned with solid-state silicon photomultipliers that are positioned over reaction chambers on prototype chips manufactured from PDMS and glass. The LOC chips (Figure 41) contain six identical, but spatially separated microfluidic features, allowing synchronous amplification of six different DNA or RNA samples.

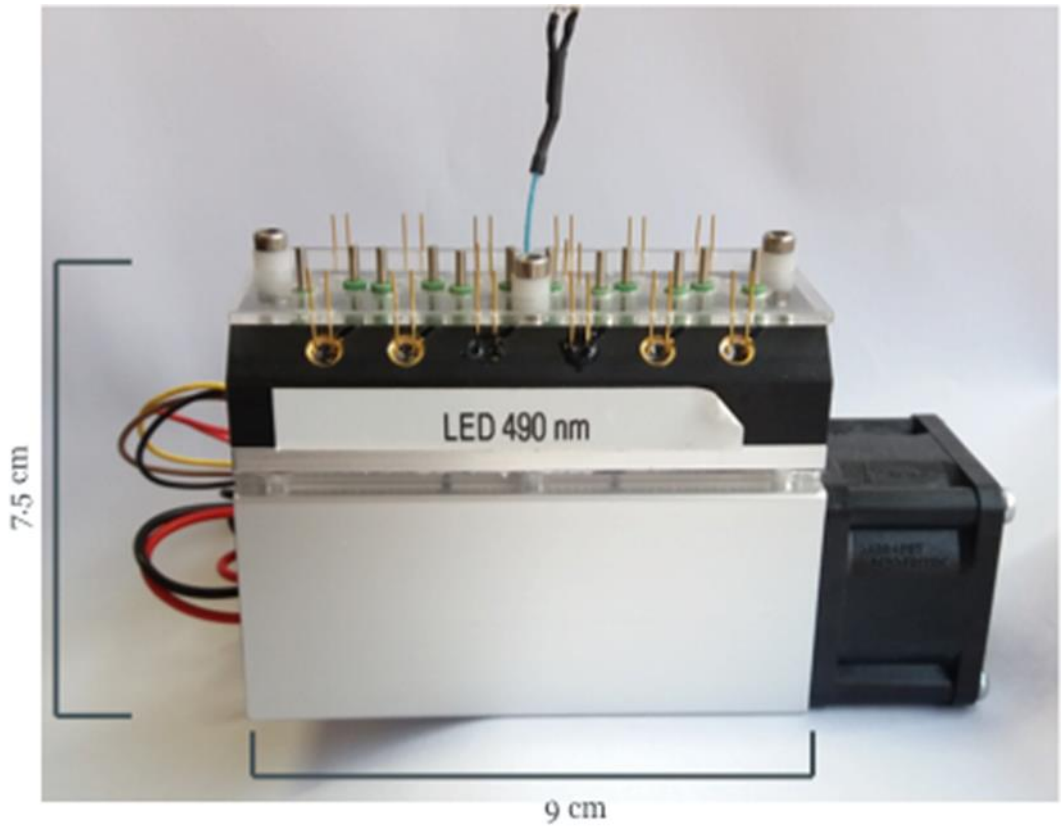

Figure 7 The prototype handheld genetic sensor.

The chips for the device can be assembled containing preserved reagents for the target of choice within the reagent chamber. Each reaction uses three chambers, a reagent chamber, the reaction chamber and an air chamber, which is displaced to allow movement between the chambers. The sample containing the target RNA is introduced to the sample chamber. Fluidics are actuated using a finger press to allow the mixing of the reagents with the sample nucleic acids, and to deposit the combined mixture into the reaction chamber. A PTE then heats the sample to the desired temperature required for the molecular assays to perform optimally. This temperature is then held for as long as the assays require. The use of a PTE allows thermal ramping when required (NASBA) but also allows temperatures to be held stable with little variation (±0.2°C).

1.7 Current limitations and possibilities

1.7.1 Elimination of optical noise

LEDs are semi-conductor light sources that emit light as a current is passed through. LED's can produce light at a range of different wavelengths and have low energy requirements. This makes them ideal in the optical excitation of amplified nucleic acids. For use in real time detection of amplicons LED's must be used in conjunction with a fluorescent chemical compound (such as a fluorophore or a nucleic acid stain such as SYBR Green, EvaGreen, Hoescht or YOYO-1), and a PMT to amplify and detect an optical signal.

In real-time PCR systems this relationship is the chosen method of detection. Whether using DNA stains such as SYBR or a fluorophore attached to a specific oligonucleotide (such as a hydrolysis probe or a molecular beacon). The fluorescent agents used have both excitation and emission wavelengths that differ. For example, a commonly used fluorophore is fluorescein amidite (FAM). FAM has an excitation wavelength of 495 nm and an emission wavelength of 520 nm. The increase in signal at 520 nm can be used to measure the amount of DNA being produced (Marras, 2006).

To receive a clean amplification signal it is essential to remove as much of the excitation wavelength from the PMT as possible. This can be achieved in several ways, including the use of optical filters and waveguides. Optical filters are membranes that selectively filter light of a particular wavelength. The positioning of a filter in front of the PMT that excludes all wavelengths bar 520 nm will result in only the light at 520 nm reaching the detector, meaning only the light emitted in the creation of new DNA strands is measured.

Alternatively, wave guides are structures that guide light waves with minimal loss in energy by restricting expansion to one or two dimensions. By using wave-guides it is possible to direct the light from the LED to a specific part of the reaction well without any backscattering towards the PMT. An example of an optical waveguide is an optical fibre. Any material that has a high optical permittivity and a high index of refraction can be used to make an optical waveguide (Adams, 1981).

1.7.2 Reagent storage

All nucleic acid amplification methodologies depend upon enzymes to function. Enzymes, like all proteins, are inherently sensitive to thermal fluctuations (Bischof and He, 2005). Proteins are also vulnerable to additional stresses, both physical and chemical, such as desiccation (Wang, 2000), photo-activation (Maity *et al.*, 2009), and changes in pH (Chi, 2003). Traditionally, enzymes are stored at low temperature (-20C) and kept on ice until they are to be added to reactions. For a

robust, stand-alone device, reagents should be integrated and therefore stable at room temperature. Methods of dry reagent storage include lyophilisation (O'Fagain, 2011), trehalose addition (Mancini *et al.*, 2012), and pullulan addition (Jahanshahi-Anbuhi *et al.*, 2014).

1.7.2.1 Lyophilisation

Lyophilisation, also known as freeze-drying, is a commonly used method for preparing solid protein-containing pharmaceuticals (Andersen *et al.*, 2008; Kadoya *et al.*, 2010; Kasper and Friess, 2011; Wang, 2000). Lyophilisation consists of two steps 1) freezing of a protein solution and 2) drying of the frozen protein solution under vacuum by sublimation. Drying the sample at low temperature (below -58°C) and under vacuum lowers the partial pressure of the water to below its triple point, which prevents the formation of a liquid phase as the ice crystals sublimate into water vapour (Matejtschuk, 2007). Drying takes place in two phases: primary and secondary drying. The primary drying removes the frozen water, whilst the secondary drying removes non-frozen 'bound' water, which forms a protein hydration shell (Arakawa *et al.*, 1991; Wang, 2000). This water must be substituted if the dehydration process is to leave the protein structure unchanged.

1.7.2.2 Trehalose

Trehalose (Figure 8) is an alpha-linked glucose disaccharide that imparts stability to organisms that can tolerate anhydrobiosis and cryobiosis (Kaushik and Bhat, 2003). It has also been shown that trehalose has an unusually high ability to prevent water crystallisation. The ability of trehalose to prevent water crystallisation combined with its high glass transition temperature (Tg) are suggested to be the main cause of its stabilising mechanism (Olsson *et al.*, 2016). It is also understood that trehalose stabilises proteins by replacing the water in the hydration shell during desiccation (Jain and Roy, 2009). Trehalose has been utilised previously, often in combination with sucrose (Figure 8), as a preservative for whole sheep ovaries (Du *et al.*, 2015), stem cells (Buchanan *et al.*, 2010), and enzymes (Ji *et al.*, 2014).

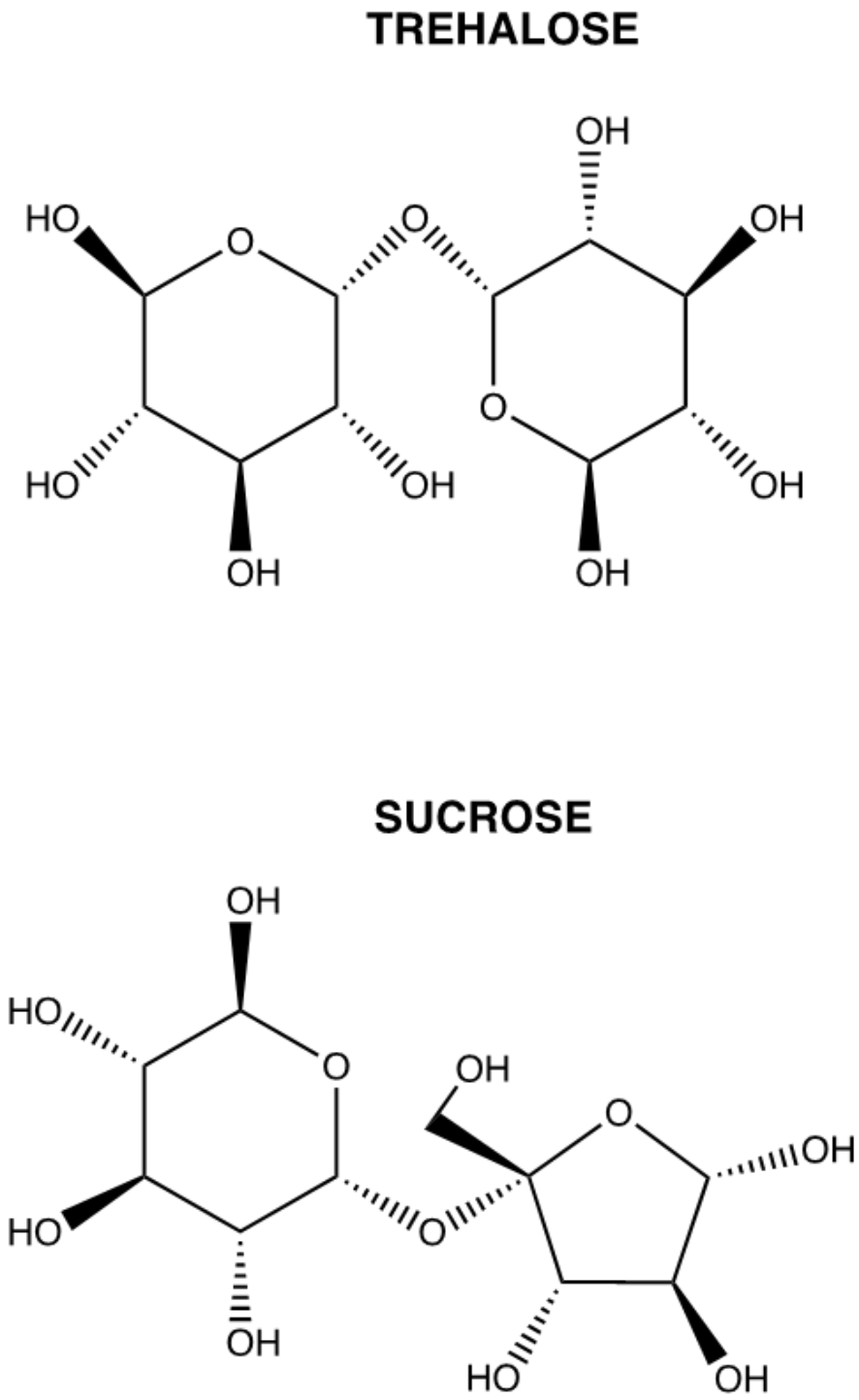

Figure 8 The structure of both trehalose and sucrose disaccharides.

1.7.2.3 Pullulan

Pullulan is a natural polysaccharide produced by the fungus *Aureobasidium pullulans* (Figure 9), that readily dissolves in hot or cold water and forms films upon drying, and is non-toxic, non-mutagenic, odourless, tasteless, and edible (Singh *et al.*, 2008). Although pullulan dissolves in water it is insoluble in organic solvents and is stable up to 250°C, at which point it begins to decompose (Singh *et al.*, 2008).

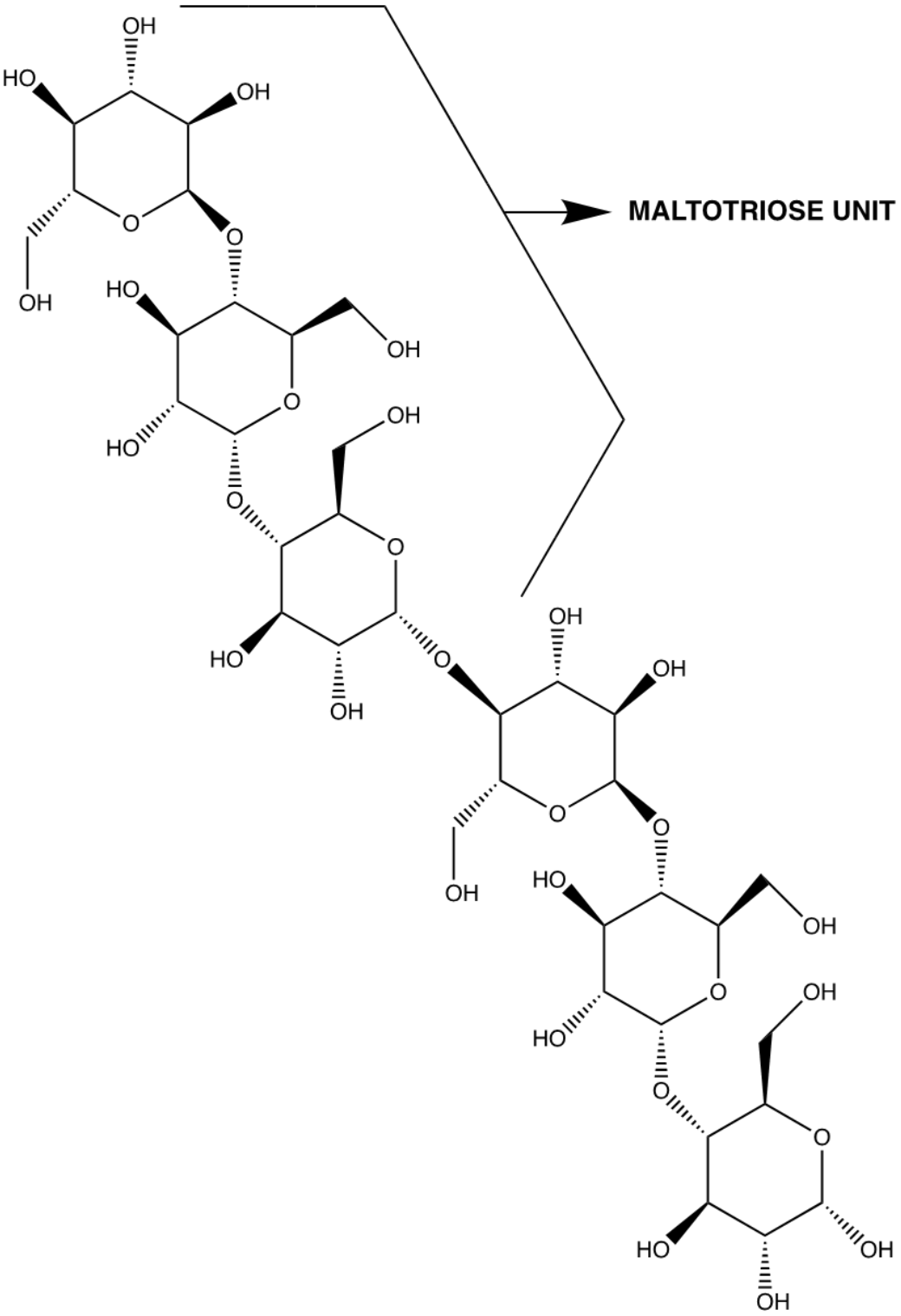

Figure 9 The structure of pullulan. Pullulan is made up of repeating maltotriose units which allows it to form films.

Jahanshahi-Anbuhi *et al.* (2014) utilised pullulan to store the Taq DNA polymerase (*TaqDP*) enzymes used in PCR, and acetylcholinesterase (*AChE*) and idoxyl acetate (*IDA*), used for pesticide detection. Pullulan has been shown to provide an oxygen barrier when applied to food packaging and also preserves the viability of bacteria under several storage conditions. Jahanshahi-Anbuhi *et al.* (2014) successfully created pullulan tablets containing *TaqDP* and performed positive PCR by dissolving

the tablets in water. Using this tablet method of reagent preservation, the *TaqDP* retained 90% of initial activity after 50 days of storage at room temperature.
As part of this thesis, lyophilisation, trehalose and pullulan were compared for dry reagent storage, as no comprehensive comparison for amplification enzymes has been performed to date.

1.8 Thesis Aims

This thesis approaches several aspects of chemistry, molecular science, and hardware development in order to develop a robust, miniaturised, LOC diagnostic device for water quality monitoring at the point of sample.

In Chapter 2 a novel isothermal HEV NASBA assay is developed and compared to a current RT-qPCR assay for the potential to detect HEV using LOC architecture.

In Chapter 3 the potential for RPA to provide rapid detection of the HAB species *Alexandrium minutum* is investigated and compared with a published and widely used PCR assay.

Chapter 4 investigates techniques for the long-term storage of nucleic acid amplification reagents at ambient temperatures, without the need for refrigeration.

Chapter 5 looks at the development of a miniaturised genetic sensor for point of sample diagnostics and the development of a Lab on a Chip for amplification and optical detection.

The knowledge gained through these studies will address the ultimate aim of creating a miniaturised genetic sensor for use by untrained staff in remote and resource limited environments.

Chapter 2 The development of a Hepatitis E NASBA assay for use with the miniaturised genetic sensor

2.1 Introduction

Human enteric viruses are transmitted via several means, with the faecal-oral route being a major transmission route, and they can be prevalent in sewage-contaminated water. Some notable examples, such as Hepatitis A Virus (HAV), Hepatitis E Virus (HEV) and Norovirus (NV) are able to remain viable for long periods outside a human host, making wastewater treatment and management essential for preventing the discharge of pathogenic viruses into water supplies (Woods and Burkhardt lll, 2013). Unsafe water, poor hygiene and inadequate sanitation are responsible for approximately 90% of diarrheal associated deaths worldwide (UNICEF, 2012).

HEV is responsible for Hepatitis E infection. There are four known genotypes of HEV: HEV1, HEV2, HEV3, and HEV4, with HEV1 and HEV2 predominant in developing countries in areas of poor sanitation, transmitted via the faecal oral route usually through contaminated water (Kamar *et al.*, 2014). In developed countries HEV3 and HEV4 are predominant and are transmitted zoonotically from animal reservoirs (Kamar *et al.*, 2014). In the UK HEV3 is the predominant genotype, and is transmitted to humans through contaminated swine. In 2018 it was estimated that there are 100,000 cases of HEV diagnosed in the UK annually (Ijaz, 2018). It is currently thought that HEV is responsible for the majority of acute viral Hepatitis in the world (Hoofnagle *et al.*, 2012; Kamar *et al.*, 2012; Purcell and Emerson, 2008). In developing countries HEV causes a self-limiting illness that lasts for a few weeks. Symptoms include fever and nausea followed by acute abdominal pain, vomiting, anorexia, malaise, and hepatomegaly (Kamar *et al.*, 2014), with jaundice occurring in 40% of patients (Labrique *et al.*, 2010). Although mortality rates are usually under 0.5%, in pregnant women genotype 1 can lead to rates as high as 25% (Van der Poel, 2014). The increased incidences of extreme weather events globally is predicted to increase the frequency of waterborne disease outbreaks, including Hepatitis E (Funari *et al.*, 2012). The ability to assess water sources at the point of sample and detect the presence of HEV virus will allow treatment or closure of water points reducing the risk to public health.

Typical viral detection techniques include viral plaque assays, immunofluorescence foci assays, immunoblotting and enzyme-linked immunosorbent assays (ELISA) amongst others, a summary of which is given in Table 1. The majority of these techniques require expensive, large instrumentation and trained technical staff. These techniques also typically take hours to days between sampling and test results.

Table 1 A list of viral detection techniques and associated factors (adapted from Kumar (2013)). *NASBA is the molecular assay chosen in this study.

Technique	Detection Principle	Reproducibility	Time	Labour	Cost
Viral plaque assay	Infectivity assay	Poor	Days	High	Inexpensive
$TCID_{50}$, LD_{50}, EID_{50}	Infectivity assay	Poor	Days	High	Inexpensive
Immunofluorescence foci assays	Infectivity assay	Poor	Days	High	Expensive
qPCR	Viral nucleic acid	Excellent	Hours	Moderate	Inexpensive
NASBA*	Viral nucleic acid	Good	Hours	Moderate	Expensive
Immunoblotting	Viral protein	Good	Days	Moderate	Inexpensive
Immunoprecipitation	Viral protein	Good	Days	Moderate	Inexpensive
ELISA	Viral protein	Good	Hours	Moderate	Inexpensive
Hemagglutination assay	Viral protein	Good	Hours	Moderate	Inexpensive
Viral flow cytometry	Viral particle	Excellent	Hours	High	Expensive
Transmission electron microscopy	Viral particle	Excellent	Days	High	Expensive

Viral detection is also complicated, as a majority of organisms and viruses are unculturable in the laboratory. Thus, nucleic acid amplification has become an essential tool in microbiological studies and pathogen detection as it does not require the viruses to be cultured, since nucleic acids can be amplified directly from viral contaminated samples. These molecular techniques also offer advantages over the alternatives in that they are highly specific and highly sensitive. Nucleic acid amplification also has the potential for being adapted for miniaturisation and lab-on-a-chip (LOC) devices, as they use low reagent volumes (µL), are suitable for automation, and are cheap RT-qPCR ~$0.82 per reaction (Technologies, 2015)). Areas where HEV is prevalent are generally poorer, and where resources and healthcare are limited, the benefits associated with nucleic acid amplification make them uniquely suited for use in resource limited environments (Banting *et al.*, 2016). ELISA is an attractive option for miniaturised viral detection and is cheap, with individual reactions costing as little as $1.20 (Tamashiro *et al.*, 1993). At the time of writing, however, no commercial ELISA test for HEV was available and therefore a comparison between the HAV NASBA and ELISA was unable to be investigated.

The “gold standard” nucleic acid amplification technique is the polymerase chain reaction (PCR) (Fykse *et al.*, 2012). PCR is performed using a single or double stranded DNA template and requires two oligonucleotide primers, a thermally stable DNA polymerase (typically *Taq* polymerase), metal ion co-factors, and deoxynucleotides (dNTPs). The introduction of fluorescence-based dyes or fluorophore containing oligonucleotides to PCR can make detection possible in real-time, a technique known as quantitative PCR (qPCR) However, qPCR suffers several drawbacks that limit its application in miniaturised LOC devices. These include the thermal cycling regime, which requires a large power source, and high temperatures of up to 95°C, which can result in sample evaporation and high pressure in the reaction chamber that can lead to structural damage.

Alternate to qPCR, several isothermal nucleic acid amplification techniques have been developed that address some of these issues, making them potentially more suited to miniaturisation for portable instruments. Isothermal methods often require lower reaction temperatures and do not require iterative temperature cycling. Some of the isothermal assays available include, but are not limited to; **L**oop mediated isothermal **AMP**lification (LAMP) (Notomi *et al.*, 2000), **N**ucleic **A**cid **S**equence **B**ased **A**mplification (NASBA) (Compton, 1991), **H**elicase **D**ependant **A**mplification (HDA) (Vincent *et al.*, 2004), **R**ecombinase **P**olymerase **A**mplification (RPA) (Piepenburg *et al.*, 2006), and **S**trand **D**isplacement **A**mplification (SDA) (Walker *et al.*, 1992a). Of these, NASBA shows potential for the detection of RNA viruses due to the simplicity in assay design and because it amplifies an RNA target directly, removing the need for an additional reverse transcription. This is a limitation for qPCR, which requires an additional reverse transcription (RT-qPCR) step to amplify RNA. This both increases the reaction time and reduces the sensitivity, due to inefficiency of the reverse transcriptase enzyme, making NASBA an ideal alternative for the detection of RNA viruses.

The HEV genome is positive sense single stranded RNA at 7.2kb long, is capped and polyadenylated at both the 5' and 3' termini, and contains 3 open reading frames (ORF). ORF1 encodes for a 1,693 amino acid residue protein, containing non-structural proteins; ORF2 encodes the 660 amino acid residue viral capsid proteins, whilst ORF 3 encodes for a small protein (113-114 amino acid residues) involved in virion morphogenesis and release (Kamar *et al.*, 2014) (Figure 10).

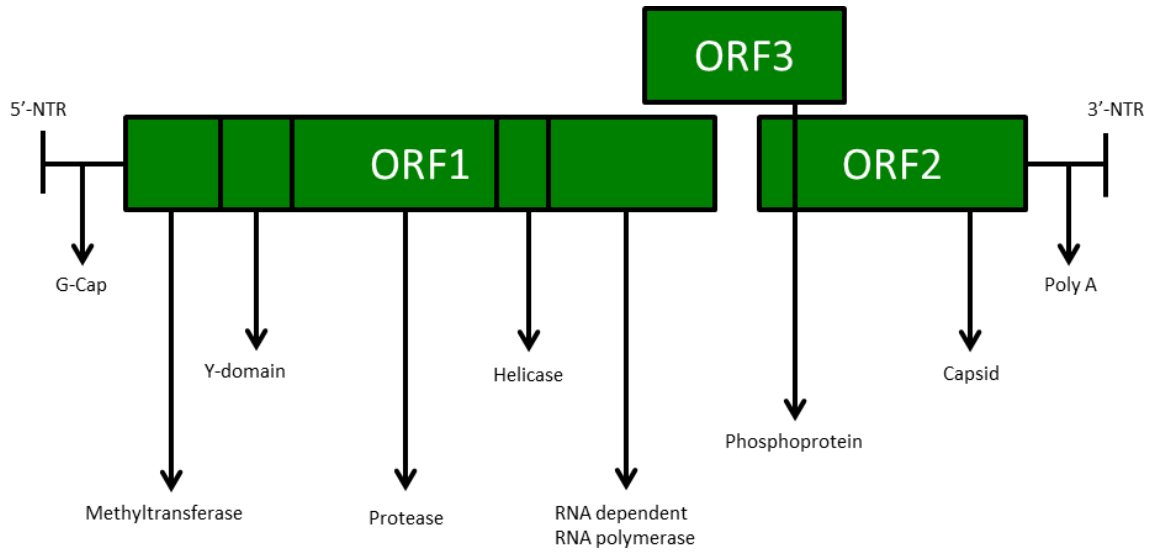

Figure 10 The HEV genome and its organisation. HEV is a positive sense single stranded RNA virus with three open reading frames encoding structural and non-structural proteins (adapted from Kumar et al. (2013)).

In this study a novel isothermal NASBA assay was developed to target the ORF 2/3 overlapping region of the HEV genome, as this region has been established as well conserved and an ideal

candidate for assay design (Mokhtari *et al.*, 2013). This NASBA assay was then compared to a published RT-qPCR assay (Jothikumar *et al.*, 2006) to understand its viability as a diagnostic tool. The simplified technological requirements for NASBA over qPCR enable it to be coupled with the LOC technology described in Chapter 5 of this thesis, potentially allowing for point of sample HEV detection on a miniaturised device.

The specific aims of this chapter are:

- The design and development of a novel isothermal NASBA assay for the detection and quantification of HEV in water samples.
- Comparing the above NASBA assay against a previously described RT-qPCR assay.
- Examining the feasibility of the HEV NASBA assay for incorporation with a miniaturised, handheld, microfluidic LOC, genetic sensor.

2.2 Methods

2.2.1 HEV template generation for assay development

To remove the dangers associated with working with live viruses (chiefly the threat of infection), initial assay design was done using a synthetic construct of a fragment of the HEV ORF 2/3 overlap region of the HEV genome which was designed by aligning 10 HEV genome sequences using ClustalW, and synthesised as follows. First, a 440 bp double stranded DNA construct was synthesised commercially (gBlocks, Integrated DNA Technologies or IDT, USA) containing a T7 RNA polymerase promoter sequence followed by a short (6 bp) purine spacer upstream of a 409 bp region corresponding to a fragment of the HEV ORF2/3 overlap region of the HEV genome (Appendix A). The dsDNA was cloned into the pCR4 TOPO plasmid using the TOPO TA Cloning Kit (Invitogen, USA) according to the manufacturer's recommendation, and used to transform competent *E. coli* (TOP10 cells, Invitrogen, USA). The plasmid DNA containing the inserted construct was purified from TOP10 cells using a DNA MiniPrep Kit (Qiagen, USA), also following the manufacturers recommendations. The presence of the insert was confirmed via white/blue screening and colony PCR. T7 RNA Polymerase (NEB, USA) was used to synthesize RNA as per the manufacturer's instructions and samples were purified using an RNA Clean and Concentrator kit (Zymo, CA, USA). Final RNA concentration was determined using a Qubit spectrophotometer (high sensitivity RNA) (Invitrogen, USA) and stored at -80°C until further use.

2.2.2 HEV reference material nucleic acid extraction

For validation of the NASBA assay HEV reference material (human serum containing infectious HEV virions) was provided by the World Health Organisation (WHO). A phenol-chloroform extraction followed by an ethyl alcohol precipitation was used to extract viral RNA via the following protocol. First, 0.5 mL of lyophilised serum was dissolved in a 0.5 mL of Lysis Buffer (0.5 % SDS, 5 mg/mL Proteinase K in 50 mM Tris-EDTA (pH 8.5)), mixed, and incubated at 55°C for 30 minutes. Following this, 250 µL of lysate was transferred into new 1.5 mL nuclease-free tubes and mixed with 750 µL Trizol LS reagent before incubation for five minutes at room temperature. Into each lysate tube 1 µg of carrier RNA extracted from *E. coli* was added, before addition of 200 µL of chloroform and the samples centrifuged for 15 minutes at 12,000 x g and 4°C. The aqueous phase was recovered and mixed with an equal volume of 70% ethanol. The samples were then loaded onto RNeasy spin columns and centrifuged at 8,000 x g for 60 seconds, repeating until all of the sample passed through the column. Collection tubes were cleared and the columns washed with 700 µL RW1 buffer (Qiagen, USA), before transferring to clean collection tubes. The columns were washed twice with 500 µL RPE buffer and centrifuged dry. Columns were transferred to clean 1.5 mL tubes, and 40 µL of nuclease free water was added to the column, then incubated for two minutes at room temperature and centrifuged at 8,000 x g. The eluate was stored at -80°C until future use.

2.2.3 Nucleic Acid Sequence Based Amplification (NASBA)

NASBA reactions were prepared using the Nuclisens EasyQ Basic Kit v2 following the manufacturers recommended protocol to a final reaction volume of 10 µL with final primer concentrations of 4 µM and a final molecular beacon concentration of 2 µM. Oligonucleotides (Table 2) were obtained from Integrated DNA Technologies (IDT, USA). Reactions were performed on a Stratagene MX3005P thermal cycler (Agilent, USA) and incubated at 65°C for 5 minutes before reducing the temperature to 41°C for two minutes. At this point enzymes were added and the reaction incubated for a further 90 minutes at 41°C. Readings for real-time detection were taken every 30 seconds.

Table 2 The oligonucleotides used in this study to amplify a part of the HEV ORF2/3 overlap region.

NAME	SEQUENCE 5'-3'	Reaction	REFERENCE
Custom Fwd A	TTCTGCCTATGCTGCCCGCGCCA	NASBA	This study
Custom Rev A	TATTCATCCAACCAACCCCTT		
Custom Fwd B	TTCCGGCGGTGGTTTCTGGGGTGA		
Custom Rev B	GTGGTTTCTGGGGTGACCGGGTT		
Custom Mol Beacon A	FAM-CGATCGGGGTTGATTCTCAGCCCTTCGCCGATCG-BHQ		
Custom Mol Beacon B	FAM-CGATGCTGGTTTCTGGGGTGACCGGGTTCGATGC-BHQ		
JVHEVF	GGTGGTTTCTGGGGTGAC	RT-qPCR	Jothikumar et al (2006)
JVHEVR	AGGGGTTGGTTGGATGAA		
JVHEVP	FAM-TGATTCTCAGCCCTTCGC-BHQ		

2.2.4 Reverse Transcription Quantitative Polymerase Chain Reaction (RT-qPCR)

RT-qPCR assays for HEV were prepared exactly as described by Jothikumar *et al.* (2006) for comparison with the NASBA assay developed in this study. cDNA was synthesised from the initial reference material RNA template using Quantitect Reverse Transcriptase (Qiagen, USA) following the manufacturer's recommendations.

For initial real-time detection, the DNA intercalating agent SYBR green was used and reactions prepared to 25 µL using iQ SYBR Green Supermix (Bio-Rad) following the manufacturers protocol. Thermocycling conditions were as follows: initial denaturation at 95°C for two minutes, followed by 40 cycles of 95°C for 10 seconds, 55°C for 20 seconds, and 72°C for 15 seconds. Any positive real time amplification was subsequently examined via 1.5% agarose gel electrophoresis to determine whether the correct size target was amplified. Subsequent HEV RT-qPCR reactions were performed using a target specific hydrolysis probe (Table 2) to remove any potential non-target detection from the SYBR binding to non-specific amplified DNA in the reaction, increasing the specificity of the RT-qPCR.

2.3 Results and Discussion

2.3.1 Primer design

Eight HEV total genome sequences were downloaded from GenBank and aligned using ClustalW. The complete genome sequences shared a 74.8% pairwise identity. The region from 5235 bp to 5434 bp was the most highly conserved with an 89.7% identity, this site corresponds to the ORF2/3 overlapping region (Figure 11). This 200 bp region was used as the template for designing two sets of novel NASBA primers used in this study, and a pair of molecular beacons for real-time detection (Table 2).

```
Consensus   CATGCGCCCTCGGGCTATTTTGCTGYTGCTCCTCATGCTTCTGCCTATGC   50
M73218.1    .............C........T..C...........T..T.........   50
NC_001434.1 .............C...........T...........T............   50
M74506.1    ..........A..C..C........T..T.....T..T...........T   50
KJ496143.1  ........................T........T.....T.........   50
KX387865.1  ....T..A........G.AC..T..C..T.....C...............   50
AB573435.2  ..........A..............C.....G..G..............T   50
AB602441.1  ......T...A.....G.A......C..T.....................   50
EF077630.1  .......T........C.....T.TT........C.....T.........   50

Consensus   TGCCCGCGCCACCGGCCGGTCAGCCGTCTGGCCGCCGTCGTGGGCGGCGC  100
M73218.1    ..............C.................................  100
NC_001434.1 ..............C.....................C............  100
M74506.1    ..............A.................................  100
KJ496143.1  ........................T..........T..C.........  100
KX387865.1  ................................................  100
AB573435.2  ...................C...T.................C........T  100
AB602441.1  ..........................................C........G  100
EF077630.1  ..................................T..............  100

Consensus   AGCGGCGGTTCCGGCGGTGGTTTCTGGGGTGACCGGGTTGATTCTCAGCC  150
M73218.1    ................................................  150
NC_001434.1 ....................................C............  150
M74506.1    .........A......................................  150
KJ496143.1  ................................A...............  150
KX387865.1  ................................................  150
AB573435.2  .........G....TA.........................C........  150
AB602441.1  ..............A.........................C........  150
EF077630.1  .........G.....A.....................................  150

Consensus   CTTCGCACTCCCCTATATTCATCCAACCAACCCCTTYGCCYCCGATGTCA  200
M73218.1    .......A.............................C...C.........  200
NC_001434.1 .......A.............................C...C.........  200
M74506.1    .......A.............................T...C.A..C..TG  200
KJ496143.1  ................................A..C...G.T......T  200
KX387865.1  ....................................T.T.G.A..CA...  200
AB573435.2  ......C..............C..............T..AT.....AC..  200
AB602441.1  ......C..............C..............T..AT.......TT  200
EF077630.1  ......C.............................C..AT.T..CA.TC  200
```

Figure 11 The sequence alignment for the most conserved region of the ORF 2/3 overlapping region of the HEV genomes extracted from the GenBank database and the consensus sequence returned. Primers were designed to target this region. Custom Fwd A binds at bp 39 – 61; Custom Fwd B binds at 109 – 132 bp; Custom Rev A binds at 166 – 186 bp; Custom Rev B binds at 117 – 139 bp; Custom Mol Beacon A binds at 135 – 156 bp; Custom Mol Beacon B binds at 118 – 139 bp.

2.3.2 Nucleic Acid Sequence Based Amplification (NASBA)

In this study HEV was successfully detected for the first time using a novel isothermal NASBA assay. Positive amplification was observed using the designed primers for NASBA reactions. Successful amplification was achieved using template material containing ORF 2/3 copy numbers ranging from 10^7 to 1 estimated copy (Figure 12). All dilutions show positive amplification however they nearly all reach a threshold fluorescence simultaneously, between 2520 seconds (42 minutes) and 2760 seconds (46 minutes). Similar amplification times may be due to the presence of salts and non-target RNA due to carry over from the initial human serum reference material and the RNA extraction process. These may inhibit the NASBA reaction as has been observed previously (Fykse *et al.*, 2012).

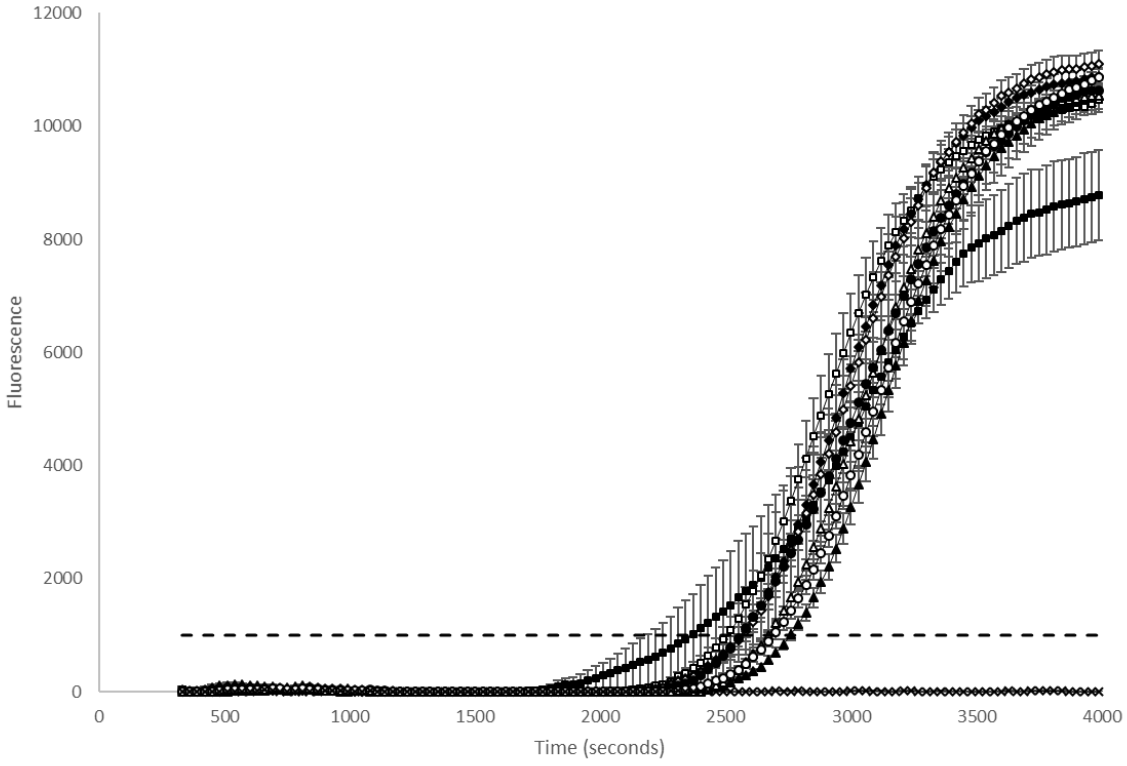

Figure 12 The HEV real-time NASBA using a custom designed molecular beacon (Table 2). ■ = 10^7 copies (TTP = 2580s), □ = 10^6 copies (TTP = 2520s); ◆ = 10^5 copies (TTP = 2580s); ◇ = 10^4 copies (TTP = 2580s), ▲ = 10^3 copies (TTP = 2760s), △ = 10^2 copies (TTP = 2700s), ● = 10^1 copies (TTP = 2580s), ○ = 1 copy (TTP = 2700s), × = NTC. The dashed line is the threshold set to 1000. Error bars, where visible are the standard error (*n*=3).

NASBA offers benefits in an environmental setting over the detection methods listed in Table 1 (with the exception of RT-qPCR) as it is highly specific, and an amplification technique and so can therefore detect very low numbers of the target analyte, down to 1 copy number (1 virion) as demonstrated in this assay. Additionally, there is no need for an initial culturing phase, reducing

time and complexity. The viral detection techniques presented in Table 1 are typically used in a clinical setting on blood samples. When a patient is infected with HEV the virus will be undergoing rapid replication, therefore there will be large amounts of virion within the blood stream. High limits of detection, while acceptable in a clinical setting, remain unproven in environmental settings, where virion numbers are several orders of magnitude lower.

2.3.3 Reverse Transcription Quantitative Polymerase Chain Reaction (RT-qPCR)

RT-qPCR using primers from Jothikumar *et al.* (2006) was able to successfully amplify a dilution series of HEV RNA ranging from 10^6 (after 10 cycles) to 1 (35 cycles) ORF2/3 overlap target copies (Figure 13). The R^2 value between the dilutions was 0.99 indicating a strong linear relationship between the copy number dilutions. The RT-qPCR reaction had a calculated efficiency of 244.62%. As there were five cycles between the more concentrated copy numbers pointing to potential inhibitors within the sample. The RNA template for the RT-qPCR was extracted from human serum containing infectious Hepatitis E virions, therefore there may be heparin or serum free haemoglobin present within the extracts, inhibiting the RT-qPCR. There may also be traces of Proteinase K or ethanol carried over from the extraction steps that also act as inhibitors to the RT-qPCR reaction. The high efficiency value may be solved by primer optimisation, as an alternate RT-qPCR master mix to that used by Jothikumar *et al.* (2006) was used in this study. As such this RT-qPCR assay is taken to be semi-quantitative, with the potential to be optimised to be fully quantitative. As the NASBA reaction was unable to be performed to a satisfactory level the need to optimise this assay was removed and alternate isothermal amplification methods and targets investigated. The efficiency of the RT-qPCR reaction cannot be used for comparison with the NASBA assay, as NASBA is not cyclical so efficiency cannot be calculated. The relationship between each template dilution should be used to compare the different techniques, however as the NASBA reactions didn't amplify as expected from most concentrated template to most dilute template comparison between the NASBA assay and RT-qPCR assay is not possible.

RT-qPCR, is also an amplification technique able to detect target copy numbers down to a single virion. As this was the lowest concentration of target copy number that was abled to be amplified via this method this is taken to be the sensitivity of the assay. This gives it potential to be used in an environmental setting where virion numbers will be low. Even if these amplification techniques lack some of the specificity of the other diagnostic methods, they hold value as an early indication system that can be combined with, for example; plaque assays, cell culture or ELISA to confirm the presence of HEV.

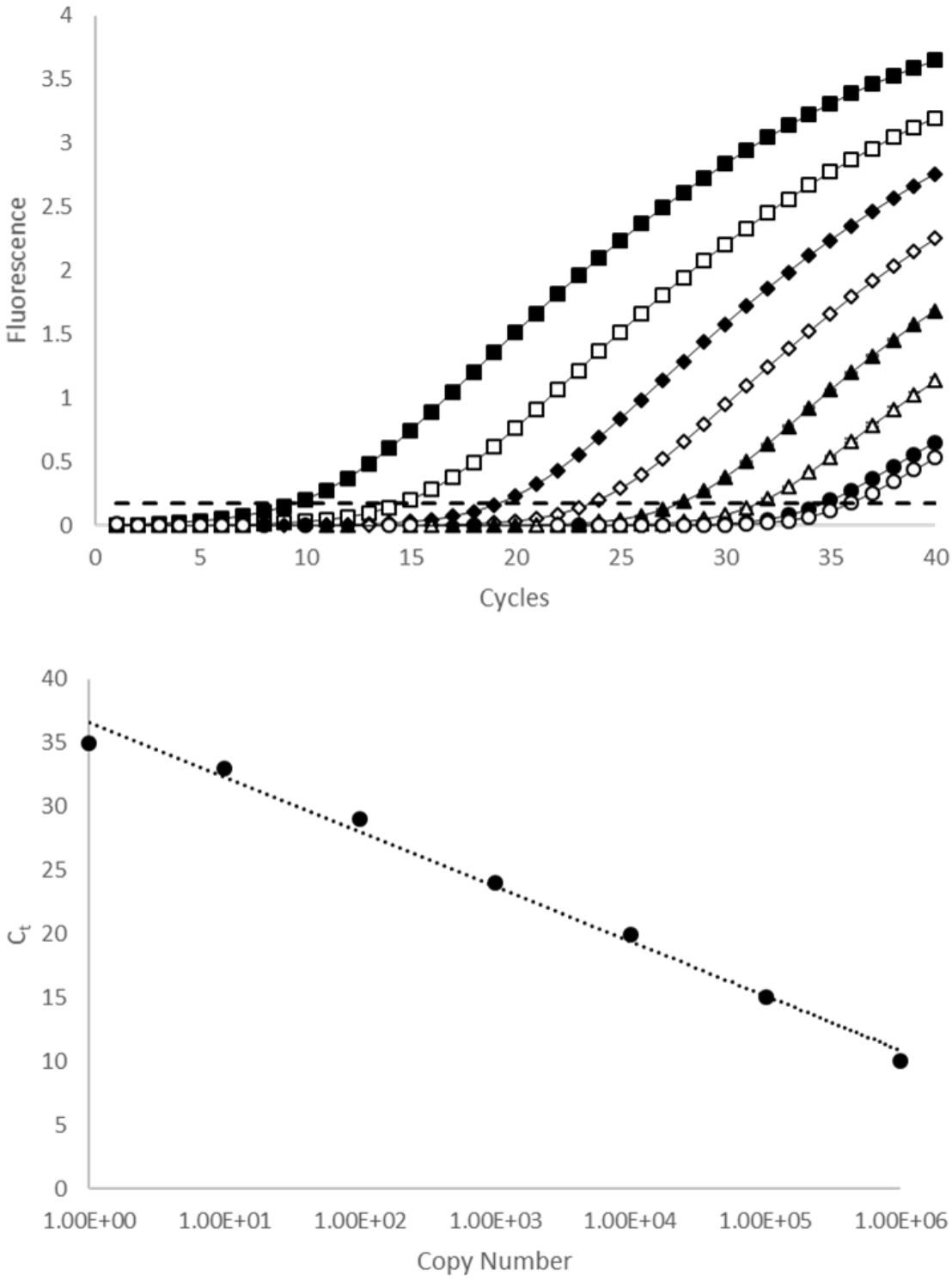

Figure 13 The HEV RT-qPCR using Jothikumar *et al.* (2006). ■ = 10^6 copies, □ = 10^5 copies, ◆ =10^4 copies, ◇ = 10^3 copies, ▲ = 10^2 copies, △ = 10^1 copies, ● = 1 copy, ○ = NTC's. The R^2 value is 0.99 indicating a strong linear relationship between the copy number dilutions. The calculated efficiency of the PCR is 244.62%. Error bars, where visible are the standard error (*n* = 3).

2.4 Conclusions

This chapter describes the first successful NASBA assay for the detection of HEV. Amplification of HEV RNA extracted from human serum containing HEV virions using NASBA was achieved with the same sensitivity as the Jothikumar *et al.* (2006) RT-qPCR assay. As these techniques are able to detect very low virion copies they have potential to be used in an environmental setting (requiring a low LOD, i.e. 1 virion as reported in this study) as opposed to clinical settings where concentrations in blood will be much higher. Unfortunately, due to issues involved in working with human pathogenic viral samples this study was unable to establish the specificity of the HEV assays, and this would be the desired next step in the study. Ideal candidates for specificity testing would be other members of the *Hepeviridae* family of viruses, as well as other waterborne viruses likely to be present in areas of poor sanitation, such as hepatitis A virus, norovirus, adenovirus, astrovirus, rotavirus and other caliciviruses, and enteroviruses, including coxsackieviruses and polioviruses (Gall *et al.*, 2015).

The NASBA assay lacked the quantitative nature of the RT-qPCR assay. However, despite this it may still have promise as a yes/no warning system. Other issues were also encountered when using NASBA in combination with the miniaturised genetic sensor. These include the increased number of steps in the reaction set-up and the 65°C denaturation step causing the sample to evaporate within the LOC reaction chamber, as well as the high costs associated with the NASBA reagents. In combination with these issues there are also problems specific to viruses that make environmental detection difficult, particularly difficulties associated with extracting and concentrating viral nucleic acids, as virions contain small quantities of genetic material and are present in low numbers in the environment, as opposed to in clinical samples where, in infected patients, virions will be present in much higher concentrations. Because of these issues encountered with NASBA, alternate isothermal techniques and targets were selected going forward.

Chapter 3 The Development of an Isothermal Nucleic Acid Amplification Assay for the Rapid Detection of the Harmful Algal Species *Alexandrium minutum*

3.1 Introduction

Harmful Algal Blooms (HABs) are naturally occurring events whereby large outbreaks of algae grow out of control. This growth is stimulated by changes within the environment, such as temperature increases (Gobler *et al.*, 2017), salinity changes (Xu *et al.*, 2017), or nutrient input (Glibert and Burford, 2017). HABs occur globally and impact mariculture and wild fisheries, as many HAB species are responsible for the production of toxins that are responsible for human illnesses via consumption. These illnesses include amnesic shellfish poisoning (ASP), diarrhetic shellfish poisoning (DSP), neurotoxic shellfish poisoning (NSP), and paralytic shellfish poisoning (PSP). The European Commission estimates that in 2016 HABs were responsible for estimated fisheries losses of up to $100 million per HAB event (Sanseverino *et al.*, 2016). Other coastal activities also suffer losses during HAB events, including tourism and recreation, with total global loses attributed to HABs in the marine environment estimated to be >US$2 billion annually (Kudela *et al.*, 2015). In the UK during recent years when higher temperatures have been recorded, a coinciding increase in HAB species is expected (Bresnan *et al.*, 2020). As aquaculture is a major industry in the UK (US$807 million in 2015) (FAO, 2017) with all sectors including fin-fish, demersal fish, molluscs and crustaceans susceptible to negative impacts from HAB proliferation. The production of a cheap and fast method of testing for *Alexandrium* will be of great benefit to fisheries managers in mitigating HAB induced losses. In the Uk in 2019 PSP toxins were detected above maximum permissible levels at one test site (Fowey – Point Hill), however there has been a noted increase in detected PSP levels overall between 2018 and 2019, however levels are below that of a PSP peak that occurred in 2011 when it was detected at 44 sites around the UK (Parks *et al.*, 2020).

Recent studies into time series data in the Belgian sector of the North Sea have shown that incidences of dinoflagellate blooms have changed between the 1970's and 2000's. Dinoflagellate cell numbers have been found to have significantly increased since the 1970's with a corresponding increase in observed genera. Additionally, the temporal distribution has altered between the 1970's and 2000's with blooms in the 1970's occurring as two short events in spring and autumn. By the 2000's however the bloom temporal dynamics and changed and more prevalent was large, prolonged growing season from spring to autumn, with the highest values in the summer months. These changes have been linked to anthropogenic factors such as sea surface temperature, light, and nutrient input (nitrogen, phosphorous and silica). Additionally, it has been observed that a transition from succession of different species to a homogenised mix of species has occurred (Nohe *et al.*, 2020). In addition, increased windspeeds shown to influence increases in diatom *Pseudo-nitszchia* and the dinoflagellate *Tripos* (Bresnan *et al.*, 2020). Global extreme HAB outbreaks at been reported in recent years that have had major impacts on local ecology and aquaculture industries.

In the eastern Pacific a warm water anomaly which has persisted since 2014 has resulted in significant *Pseudo-nitzschia* blooms and resulted in several shellfish closures as well as additional ecosystem impacts. Additionally, a strong El Niño in 2015 Resulted in catastrophic fish kills in Chile from blooms of *Pseudochattonella* and *A. catenella* (Bresnan *et al.*, 2020; Du *et al.*, 2016). Although such extreme events have not occurred in the UK yet, the potential exists due to the proliferation of extreme weather events.

Alexandrium minutum is a globally distributed armoured marine dinoflagellate. Many *A minutum* strains are known producers of paralytic shellfish toxins (PSTs), causative agents of the condition in humans known as paralytic shellfish poisoning (PSP) (Lewis *et al.*, 2018). PSTs are neurotoxic alkaloids, the parent toxin of which is saxitoxin (STX) (Lewis *et al.*, 2018). Several genes have been identified in the production of STX, two of which were chosen as the targets for molecular assays– *sxtA* and *sxtG*. These two targets were chosen as they are responsible for the production of pre-proteins in the earliest phase of STX production (Figure 14) (Kellmann *et al.*, 2008).

PSTs have been a cause of public health and economic loss to communities worldwide (Hallegraeff, 1993), problems that have increased with the reported global rise in PSP observations (Figure 15) (Anderson *et al.*, 2012b). Currently there are few records of nontoxic *A. minutum. A. minutum* is recognised as one of many harmful algal species that occur naturally globally, known to have impacts on human health, food security and other marine organisms (Costas and Lopez-Rodas, 1996; Erdner *et al.*, 2010; Ranston *et al.*, 2007; Santos *et al.*, 2014; Usup *et al.*, 2002).

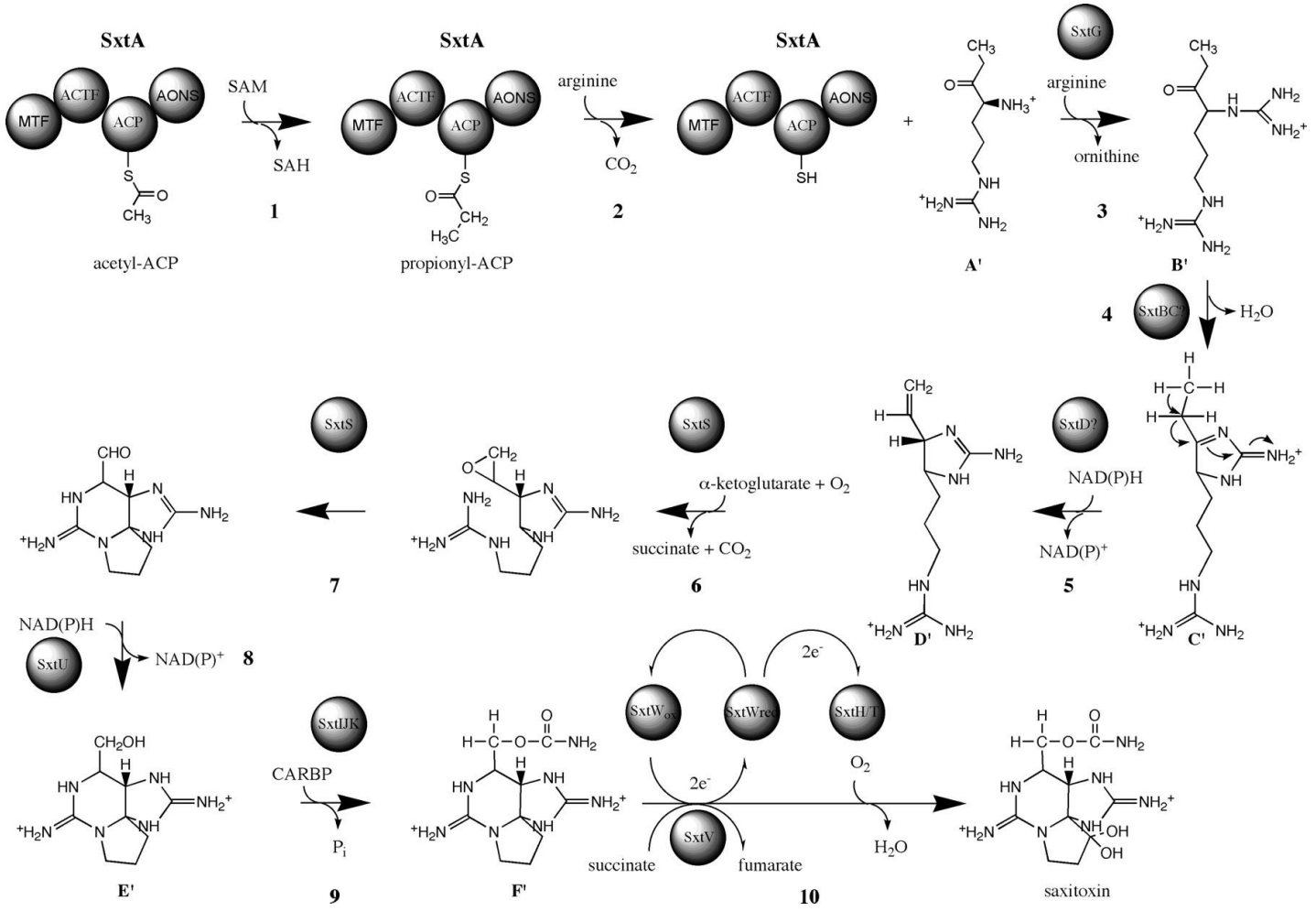

Figure 14 The saxitoxin production pathway (Kellmann *et al.*, 2008) This shows that the initial pre-protein in STX production is SxtA, coded for by the *sxtA* gene, followed by interaction with the SxtG protein, coded for by the *sxtG* gene, leading ultimately to the production of saxitoxin.

A phytoplankton bloom is defined as cell concentrations rise above 10^3 cells L^{-1} seawater (Lewis *et al.*, 2018) and in the UK the regulatory trigger for *Alexandrium* is 40 cells L^{-1} (FSA, 2018). Regulatory triggers can change over time as more insight is gained into toxin levels that could cause widespread illness due to more data becoming available to feed in to better models for understanding risk. Current methods of HAB monitoring rely on light microscopy, which is time consuming, requires trained taxonomists and is unable to differentiate between morphologically similar individuals, such as toxic or non-toxic strains of the same species, which is why monitoring of the toxin is currently taken as paramount in aquaculture management. Monitoring via light microscopy alone lacks reliability to identify beyond the genus level for *Alexandrium.* However molecular methods have the potential to act as an early indicator, with positives from using these techniques highlighted for further analysis or toxin detection. Species level detection is possible using alternative techniques such as electron microscopy, Fluorescent *in situ* Hybridisation (FISH), or Polymerase Chain Reaction (PCR) (Hatfield *et al.*, 2019).

PCR assays for *A. minutum* have been developed for multiple gene targets, including 5.8S rRNA (Galluzzi *et al.*, 2004), the D1/D2 region of the small subunit RNA (Lilly, 2003) *sxtA* toxin producing gene (Murray *et al.*, 2011) and *sxtG* toxin producing gene (Orr *et al.*, 2013). Additionally, isothermal Loop Mediated Isothermal Amplification (LAMP) assays have also been developed targeting the internal transcribed spacer (ITS) of rRNA (Zhang *et al.*, 2012) and the 5.8S rRNA region (Wang *et al.*, 2008). Whilst the Galluzzi *et al.* (2004) method has been widely used to quantify cell numbers, it has been shown that rRNA gene copy number varies widely between *Alexandrium* species, as well as during different growth phases, a critical consideration when applying molecular methods for cell enumeration (Anderson *et al.*, 2012a; Brosnahan *et al.*, 2010; Galluzzi *et al.*, 2009).

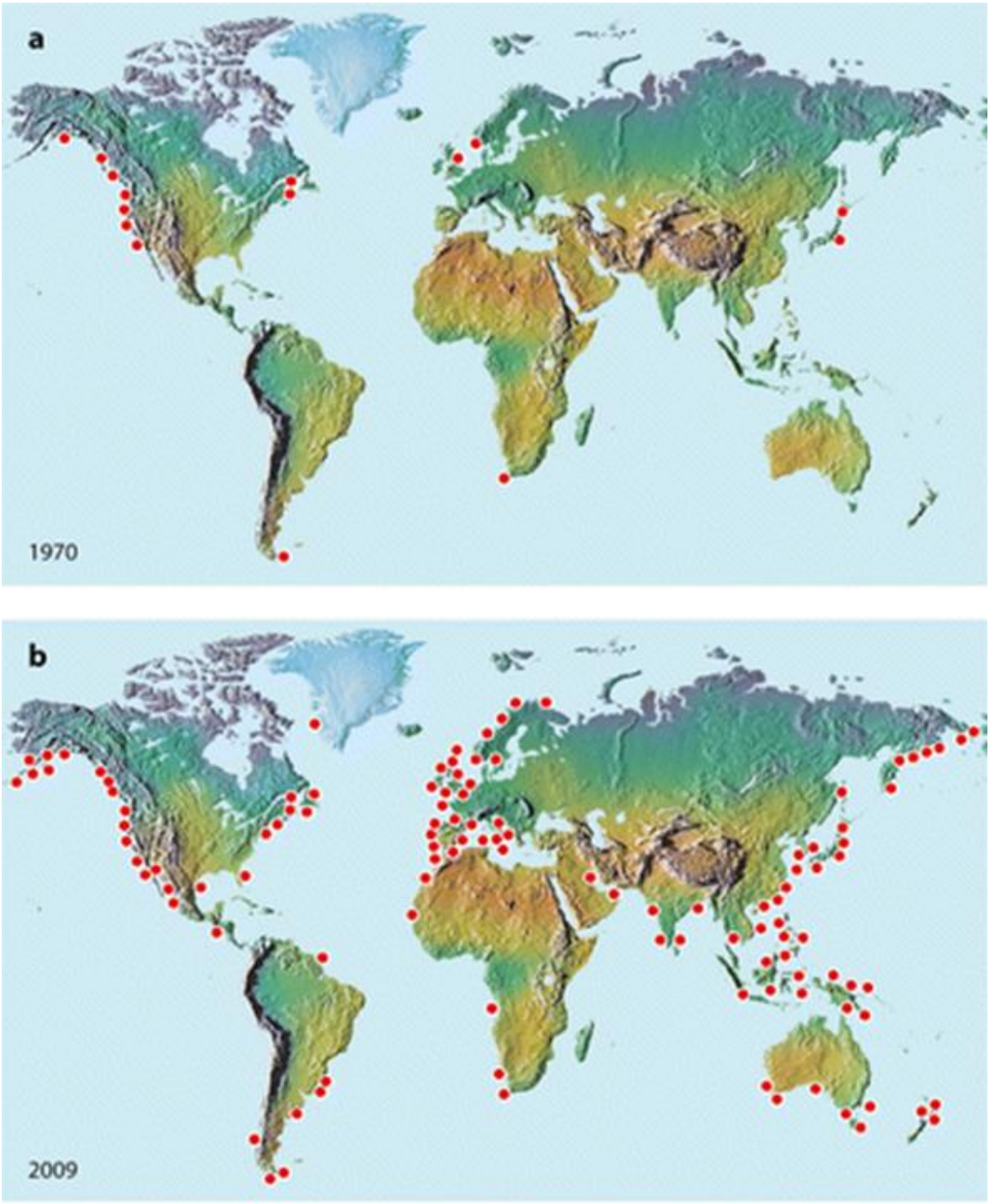

Figure 15 The distribution of observed detection of PSP toxins detected in shellfish or fish up to a) 1970 and b) 2009 (Anderson *et al.*, 2012b). This shows a noticeable increase in observed HAB incidences over the time period. The increases are likely due to increased outbreaks due to human induced climate change and improvements in monitoring technologies.

Recombinase Polymerase Amplification (RPA) is an isothermal nucleic acid amplification methodology that utilises recombinase enzymes that form complexes with gene-specific oligonucleotide primers to bind specifically to the homologous sequence within the target DNA. A single stranded binding protein (SSB) binds to the displaced DNA strand, stabilising the D loop.

Amplification by the polymerase is initiated from the primer in the presence of the target sequence and, once initiated, progresses rapidly. The recommended technique for real-time RPA is via the use of Exo probes (Figure 16). An exo probe is an oligonucleotide containing a tetrahydrofuran (THF) residue flanked on each side by thymine residues bound to a fluorophore on one side and a quencher on the other. The addition of the DNA repair enzyme Exonuclease III to the reaction cleaves the probe at the THF position, separating the fluorophore and quencher resulting in a detectable signal when excited via a light source. The use of a gene-specific probe also provides an additional layer of specificity not afforded by the use of intercalating agents.

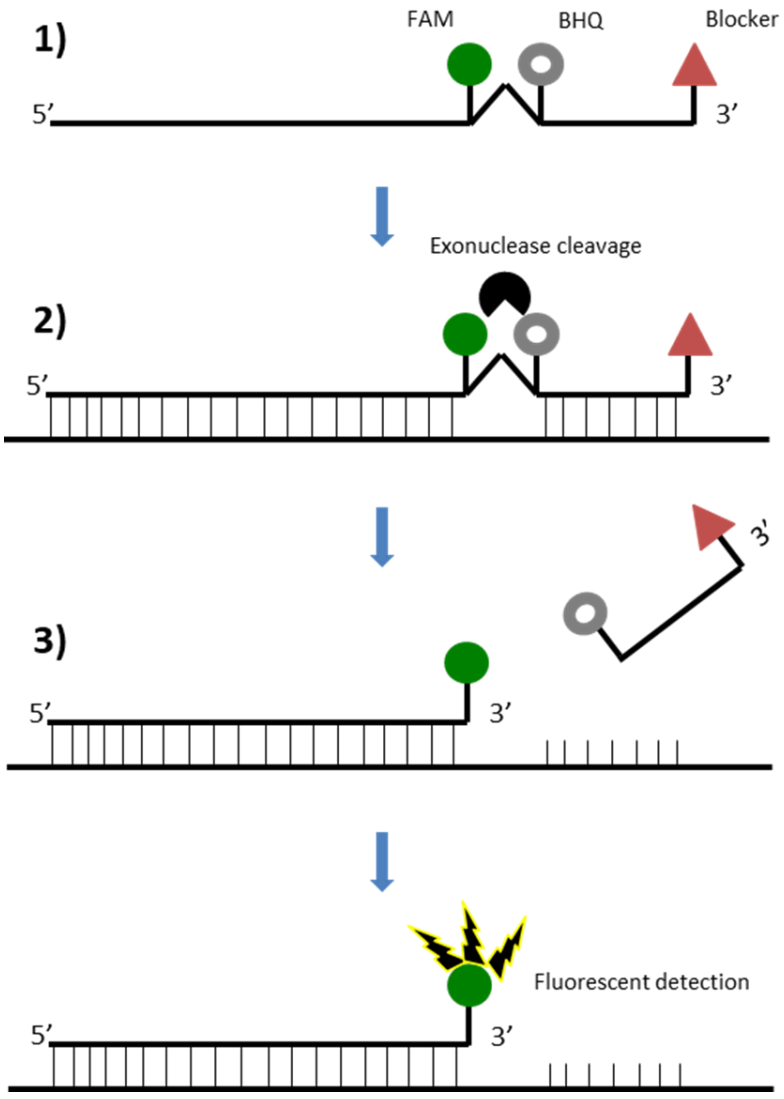

Figure 16 A schematic representation of the functioning of Exo probe detection. FAM is the fluorophore, BHQ refers to the black hole quencher and the triangle is a 3' blocker. 1) The Exo probe is not bound to target DNA therefore FAM is quenched by the BHQ. 2) The Exo probe binds to the complimentary sequence in the target DNA and the tetrahydrofuran residue (THF) (/\) is cleaved and 3) The oligo downstream of the THF is degraded by Exonuclease III. 4) The FAM is now separated from the BHQ so its emission signal at 520 nm is detectable.

RPA is a fairly recent technique that has been widely used in studies including bacteria (Boyle *et al.*, 2014; Euler *et al.*, 2013; Euler *et al.*, 2012b; Tsaloglou *et al.*, 2015), viruses (Abd El Wahed *et al.*, 2013; Amer *et al.*, 2013; Euler *et al.*, 2012a; Teoh *et al.*, 2015), fungi (Sakai *et al.*, 2014), parasites (Crannell *et al.*, 2014a; Kersting *et al.*, 2014b), genetically modified organisms (Xu *et al.*, 2014), and HIV diagnosis in low-resource settings (Boyle *et al.*, 2013; Crannell *et al.*, 2014b). RPA offers several benefits over PCR including being isothermal, requiring a single temperature of 37°C, having a simple reaction set-up and producing positive results in under 20 minutes. Traditional methods for phytoplankton detection and identification are relatively costly and time consuming, requiring specialist personnel. Molecular methods, including RPA, offer improved accuracy, quicker results and are amenable to automation; removing the need for highly trained technical staff.

Because of these factors RPA is an attractive prospect for miniaturisation and incorporation with a point of sample device, such as the genetic sensor described later in this thesis (Chapter 5). An easy to use, point of sample device, with the ability to provide a rapid, positive signal when *Alexandrium* cells rise above 40 cells L^{-1} would allow proactive management of fisheries by owners, and potentially go a long way towards minimising economic losses and reducing incidences of human illness. In addition, the ability to detect the expression of functional genes, such as *sxtA* and *sxtG* will allow even tighter management, allowing steps to be taken when toxin production is initiated. Proactive measures that could be employed include harvesting stocks early, or closing fisheries until the bloom passes and shellfish can be cleared for consumption.

The aims of this study were:

- To develop a rapid, sensitive real-time RPA assay for the detection of *Alexandrium minutum*, and compare it to a widely used existing qPCR assay (Galluzzi *et al.*, 2004).
- To investigate the similarities in toxin producing gene sequences across *Alexandrium* species and develop novel qPCR and isothermal RPA assays for their amplification and detection.
- To extract nucleic acids from shellfish flesh contaminated with STX to detect the presence of *Alexandrium*, and if there is a correlation between *Alexandrium* 5.8S copy numbers and STX concentration.

3.2 Methods

3.2.1 Culture conditions

Alexandrium minutum (CCAP 1119/48) used in this study was isolated from the east coast of Scotland. Strains were grown at 18 ± 0.1°C in 150 ml volumes of artificial seawater enriched with

L1 nutrients (Guillard and Hargraves, 1993), under a 12:12 light:dark (L:D) photoperiod at an irradiance of ~ 40.5 µmol photons m^{-2} s^{-1} from cool fluorescent lighting. Cultures were not axenic but were handled aseptically to prevent cross-contamination. Between 7 and 14 days after inoculation, algal cell density in 1 ml of culture was determined using a Sedgwick-Rafter counting chamber (Pyser Optics-S51). Cell counts were repeated in triplicate until the total number of cells was greater than 100. The average number of cells/mL was used to estimate the number of cells in the culture. In addition to *A. minutum* cultures of several other HABs (Table 3) were prepared as described above for use in assay specificity tests.

Table 3 The HAB strains used for testing the specificity of the *A. minutum* assay developed in this study.

Species designation	Strain		Isolation location	Culture source	Culture media
Alexandrium minutum	1119/48	dinoflagelate	East coast of Scotland	CCAP	L1
Alexandrium tamarense	1119/27	dinoflagelate	Loch Ainort, W coast of Scotland	CCAP	L1
Karenia brevis	CCMP2229	dinoflagelate	Gulf of Mexico	Roscoff Culture Collection	L1
Karenia mikimotoi	1513 (SFC1)	dinoflagelate	English channel, Rance Estuary	Roscoff Culture Collection	K/2
Lingulodinium polyedra	1121/2	dinoflagelate	Loch Creran, W coast of Scotland	CCAP	L1
Prorocentrum cordatum	1112/1	dinoflagelate	Knapp Buoy, Plymouth	CCAP	L1
Prorocentrum lima	1136/9	dinoflagelate	Gibralter Point Visitor Centre, Lincolnshire, UK	CCAP	f/2
Pseudo-nitzschia pungens	1061/44	diatom	LY1, W coast of Scotland	CCAP	f/2 + Si
Synechococcus sp.	1479/9	cyanobacteria	South basin, Windermere	CCAP	BG11

3.2.2 Nucleic Acid Extraction

Initially, 5 mL of *A. minutum* culture containing ~500,000 cells were placed into 50 mL conical centrifuge tubes and centrifuged at 4,000 x g for 10 minutes at 4°C. The supernatant was removed and 20 mL of phosphate buffered saline (PBS) was added before another round of centrifugation at 4,000 x g for a further 10 minutes. The supernatant was removed and the pellet frozen at -80°C until further processing.

DNA extraction was performed using a PowerPlant Pro DNA Isolation Kit (Qiagen, Germany) as per the manufacturer's instructions. The extracted DNA was quantified using a Qubit fluorometer (ThermoFisher, USA). The number of 5.8S rRNA gene copies was estimated (Galluzzi *et al.*, 2004) from the extracted DNA, which was used to assemble a dilution series ranging from 10^8 to 1 ITS1-5.8S-ITS2 gene copies. This dilution series was subsequently used to establish the limit of detection (LOD) of the ITS1-5.8S-ITS2 RPA assay. In addition, the number of *sxtA* and *sxtG* gene copies were also estimated using the data of Stüken *et al.* (2015) and Orr *et al.* (2013) respectively, and the assembled dilution series was used to examine the LOD of the *sxtA* and *sxtG* assays developed here. The dilution series assembled for *sxtA* and *sxtG* ranged from 10^5 to 1 copy of each gene.

For testing the specificity of the primers, DNA was also extracted from the additional HAB species *Lingulodinium polyedrum*, *Prorocentrum lima*, *Prorocentrum cordatum*, and *Karenia brevis* using the methodology described above.

3.2.3 Primer Design

Primers for RPA were designed to target the ITS1 – 5.8S – ITS2 region, *sxtA* and *sxtG* saxitoxin genes (Table 4). 5.8S primers were designed to anneal with the consensus sequence, derived after aligning 10 *A. minutum* 5.8S sequences (Table S 1) downloaded from GenBank National Centre for Biotechnology Information (NCBI) database (December 2018) and aligned using a ClustalW. The most conserved regions were selected and primers designed meeting the criteria for RPA as described in Armes and Stemple (2002) and prepared to 10 μM stocks in nuclease free water (NFW). All primers were supplied by Integrated DNA technologies (IDT, USA).

For the design of RPA primers for *sxtA* and *sxtG* firstly, 67 *sxtA* and eight *sxtG A. minutum* sequences (Table S 1) were downloaded from Genbank and aligned using ClustalW. This was repeated for *Alexandrium affine* (one *sxtA* sequence, six *sxtG* sequences), *Alexandrium fundyense* (eight *sxtA* sequences, eight *sxtG* sequences), *Alexandrium pacificum* (six *sxtA* sequences), *Alexandrium tamarense* (nine *sxtA* sequences, five *sxtG* sequences), *Alexandrium andersonii* (one *sxtG* sequence) and *Alexandrium catenella* (24 *sxtA* sequences) (Table S 1). Once the target sequences for all of these species were aligned the consensus sequences were compiled. Consensus sequences were aligned for all *Alexandrium* species to design degenerate primers with species-specific coverage for *sxtA* and genus specific coverage for *sxtG*. The *sxtA* primers were designed to target *A. minutum* only, whereas the *sxtG* primers covered all *Alexandrium* species aligned with the exception of *A. andersonii*.

Exo probes were designed using the criteria recommended by TwistDX (TwistDX, 2018) and provided by Eurogentec (Eurogentec LTD, Belgium).

Table 4 The RPA oligonucleotides used in this study to amplify part of the 5.8S rRNA region of the *A. minutum* genome and the *sxtA* and *sxtG* toxin producing genes. The bases in **bold** in the exo probe sequence relate to the FAM, THF residue and BHQ respectively.

Primer Name	Primer Sequence (5' - 3')	Target Region	Amplicon Size (bp)	Reference
AMRPA 1.1	TATATTATTGAGACTGATAGCAAACAAGTACC	5.8s rRNA	152	This study
AMRPA 1.2	TATAAATGATAGAGTAAGCACAACAATCTCAC			
AMRPA 2.1	GGTAAATATATTATTGAGACTGATAGCAAACA		92	
AMRPA 2.2	CAAATGCAGACTCTTTTAATTCTCTTTTCAAA			
AMRPA 3.1	GTGAGATTGTTGTGCTTACTCTATCATTTATA		199	
AMRPA 3.2	AAAAGAGCATATACAAATTTCACCAAACACAT			
AMRPA 4.1	TTGAATTGTAATTTTGAAATGTATTGCCAATG		200	
AMRPA 4.2	AGTCTCAATAATATATTTACCTTTACATGGAA			
AMRPA 5.1	AAATATATTATTGAGACTGATAGCAAACAAGT		134	
AMRPA 5.2	AACAATCTCACCAAGTAAAATCAATTCTGTTT			
AM Exo Probe	ACCTTGAATGTCAGCTTCTATTTCTGCAAA**T**C**A**T**T**ACCCTTGCACATGAA			
sxtA RPA 1.1	GTGCGCYTGAAGCACAACGACACGGAGCWG	*sxtA*	123	This study
sxtA RPA 1.2	CARGTCGGCGAGCTCTCCGYCCGTGGRGTA			
sxtA RPA 2.1	CYTGAAGCACAACGACACGGAGCWGCTCGA		217	
sxtA RPA 2.2	TTGCTCCGAGTCGGRGTYGCGGCCAAGAACGCCGCA			
sxtG RPA 1.1	GGAGGACCCCGACGAGATGCACAGRTACAT	*sxtG*	162	
sxtG RPA 1.2	TTGCTCACCATCGACTCCATGCAGAAGACG			
sxtG RPA 2.1	AGGCGGTAYTTYTACTCCGAGGTGGACGTGCCGAT		150	
sxtG RPA 2.2	ATCCGCTTCTCGTCCAGCGAGAGCGTGTTCA			

3.2.4 Recombinase Polymerase Amplification (RPA) and real-time RPA (RT-RPA)

RPA reactions were performed using the RPA Basic kit (TwistDX, Cambridge UK). RPA reactions consisted of: 1 μL of template added to 12.2 μL of NFW and mixed. Each primer (final concentration 0.48 μM) was added to the template/NFW (nuclease free water) and 29.5 μL of rehydration buffer added to the mix, vortexed and spun down. 47.5 μL of the reaction mixture was added to the lyophilised RPA pellet and mixed via pipetting. MgOAc at a final concentration of 13.44 mM was added to the tube lid strips and centrifuged. When the MgOAc is mixed into the reaction the RPA process is initiated. After incubation for 20 minutes at 37°C using a Lightcycler 96 qPCR instrument (Roche, Switzerland) the reaction product was purified using the MinElute PCR Purification Kit (Qiagen, Germany), DNA stained using SYBR safe dye (Invitrogen, US) and visualised on a 2% TAE agarose gel, run for 45 minutes at 90 V. For real-time detection EvaGreen® (Biotium, US) was applied and, separately, a gene specific exo probe (Figure 16). Exo probes were designed to target the conserved regions of the sequenced amplicons and used in conjunction with an RPA Exo Kit (TwistDX, UK) at a final concentration of 120 nM. This kit contains the same components as the TwistDX basic kit but with the inclusion of exonuclease III to cleave the exo probe at the THF region; an abasic site identified by the exonuclease III as a cleavage point in DNA repair systems.

Amplified ITS1 – 5.8S – ITS2 RPA products using primer AMRPA 3.1 and AMRPA 3.2 were ligated to a pGEM®-T vector (Promega, USA) and cloned using One Shot TOP10 Chemically competent *Escherichia coli* cells (Invitrogen, USA). Cells were grown overnight on LB medium containing ampicillin at 37°C and transformants were screened by colony PCR using M13 primers. Colonies

identified as containing the insert were re-plated onto new antibiotic free LB plates, grown overnight and used in another colony PCR reaction. The PCR product was purified using a GenEluteTM PCR Clean-Up kit (Qiagen, USA) as per the manufacturer's instructions and Sanger sequenced (Eurofins, Germany) using M13 primers (M13 (-21) F: TGTAAAACGACGGCCAGT; M13R: CAGGAAACAGCTATGAC) (Eurofins, Germany). In total, 25 colonies were sequenced and aligned using a ClustalW and there was a 93.6% pairwise identity between the 25 colonies picked (Figure 19). The regions of highest conservation were used to design the Exo probe for real-time RPA.

The concentrations of the AMRPA 3.1/3.2 primers were optimised to increase the rate of the RPA reaction. RPA reactions were prepared as described above but with the concentration of each primer altered. Equivalent forward and reverse primer concentrations tested were 0.1, 0.2, 0.3, 0.4, 0.5 and 0.6 µM. In addition to optimising primer concentration, reaction temperature was also investigated by trialling the RPA reactions at 40, 45, 50 and 55°C.

Specificity testing of the *A. minutum* 5.8S rRNA RPA assay were performed by setting up RPA reactions as described above but with the substitution of the *A. minutum* template DNA for the DNA extracted from *Lingulodinium polyedrum*, *Prorocentrum lima*, *Prorocentrum cordatum*, or *Karenia brevis.*

3.2.5 Polymerase Chain Reaction (PCR) and quantitative Polymerase Chain Reaction (qPCR)

To compare the newly developed assays to published protocols, *A. minutum* PCR primers from Galluzzi *et al.* (2004), and Orr *et al.* (2013) were used to target the 5.8S region of the rRNA and *sxtG* saxitoxin producing genes respectively. For the 5.8S assay the following qPCR amplification protocol was used: one cycle of 95°C for 10 minutes followed by 40 cycles of 95°C for 15 seconds and 60°C for one minute (Galluzzi *et al.*, 2004). To modify the Galluzzi *et al.* (2004) assay for real-time quantitative detection SYBR chemistry was used, followed by a high-resolution melting curve and gel electrophoresis to confirm primer specificity. The *sxtG* qPCR protocol used consisted of: 1 cycle of 95°C for 10 minutes, followed by 45 cycles of 94°C for 10 seconds, 64°C for 20 seconds, and 72°C for 10 seconds. All primers were from IDT (USA) and all reactions were performed using a Lightcycler 96 qPCR instrument (Roche, Switzerland).

Table 5 The PCR primer sequences used in this study to amplify a part of the ITS1-5.8s-ITS2 gene and the *sxtG* gene of *A.minutum*.

Primer Name	Primer Sequence (5' - 3')	Target Region	Amplicon Size (bp)	Reference
5.8S-b5'	YGATGAAGAATGCAGCAAMATG	5.8s rRNA	111	Galluzzi et al., 2004
5.8S-b3'	CAAGCAHACCTTCAAGMATATCC			
sxtG PCR 1.1	ACGTGCGGGACCCCTTCATCATGCT	*sxtG*	250	This study
sxtG PCR 1.2	ACGGGAACGGCTACAACGGGAGGAT			
sxtG PCR 2.1	AGGACCCCGACGAGATGCACAGGTA		150	
sxtG PCR 2.2	AGGCGCGTCTTCTGCATGGAGTCGA			
sxtG Taqman 1	6FAM-CGGACGGGAACGGCTACAACGGGA-BHQ1			
sxtGq559F	GACGGGAACGGCTACAA		64	Orr et al., 2013
sxtGq605R	GCTCGAAGATCGGGTCCT			

Optimal annealing temperature for the *sxtA* and *sxtG* qPCR assay was determined via gradient PCR with annealing temperatures ranging from 50°C to 70°C. Readings were taken in real-time using SYBR chemistry and amplification product analysed via a high-resolution melting curve, from 65°C to 97°C.

3.2.6 Contaminated Bivalve Screening

To test the RPA assays on environmental samples, PSP contaminated mollusc samples were provided by Cefas (Andrew Turner) and were a mix of razor clam (*Ensis* spp.), mussel (*Mytilus edulus*), cockle (*Cerastoderma edule*) and oyster (*Ostrea edulis*) (Table 6). Nucleic acids were extracted from 250 mg of mollusc flesh using a Soil DNA kit (Omega Bio-Tek, USA) following the manufacturer's instructions and DNA quantified using a Nanodrop spectrophotometer (Thermo Scientific, USA). RPA reactions were prepared as previously described and PCR reactions performed in parallel.

3.2.7 Inhibition qPCR

Inhibitor testing of DNA extracted from PSP contaminated mollusc samples was done by adding an internal positive control to samples before reactions commenced. *E. coli* DNA was selected for the internal positive control as it is readily available, is distinct from the *A. minutum* 5.8S target sequence, and a well characterised assay already exists (Walker *et al.*, 2017). *E. coli ybbW* qPCRs were prepared as per Walker *et al.* (2017). Into these reactions 5 ng of mollusc extracted DNA and 5 ng of *E. coli* DNA was added. qPCR's were done using the Galluzzi *et al.* (2004) thermal protocol as described above and fluorescence readings taken in real-time using SYBR chemistry in a LightCycler 96 instrument (Roche, Switzerland). Alongside *E. coli ybbW* positive controls, *A. minutum* 5.8S rRNA positive controls using *A. minutum* culture extracted DNA, and negatives for *E. coli*, *A. minutum*, and the combined mollusc/*E.coli* samples were included.

Table 6 The mollusc samples provided by Cefas for this study. nd refers to samples that are known to be contaminated with SXT but the toxin concentration is unknown.

Sample Number	Species	PST toxicity (µg STX eq/kg flesh)
Samples with known toxicity		
BTX19/ 2926	Razor clams	nd
BTX19/ 2925	Mussel	nd
BTX19/ 2919	Oyster	nd
PO CRM	Oyster	668
LRM	Mussel	2800
Blind samples		
BTX19/ 0871	Mussel	?
BTX19/ 0990	Mussel	?
BTX19/ 2895	Mussel	?
BTX19/ 1032	Mussel	?
BTX18/ 1058	Cockle	?
BTX19/ 2887	Mussel	?
BTX18/ 0776	Oyster	?
BTX19/ 2901	Mussel	?

3.3 Results and Discussion

3.3.1 Primer design

A total of 10 *A. minutum* ITS1-5.8S-ITS2 sequences were downloaded from the NCBI GenBank database and aligned using a ClustalW. There was found to be excellent similarity of 99.8% between the 10 *A. minutum* sequences (Figure 17). This high degree of conservancy makes this region an ideal candidate for an *A. minutum* assay as all potential strains of the species will be covered by a primer set that targets this region. Five sets of RPA primers were designed spanning this ITS1-5.8S-ITS2 region and to produce amplicons of differing lengths (152 bp, 92 bp, 199 bp, 200 bp, and 134 bp) (Table 4), three of which successfully amplified their desired target region (Figure 18).

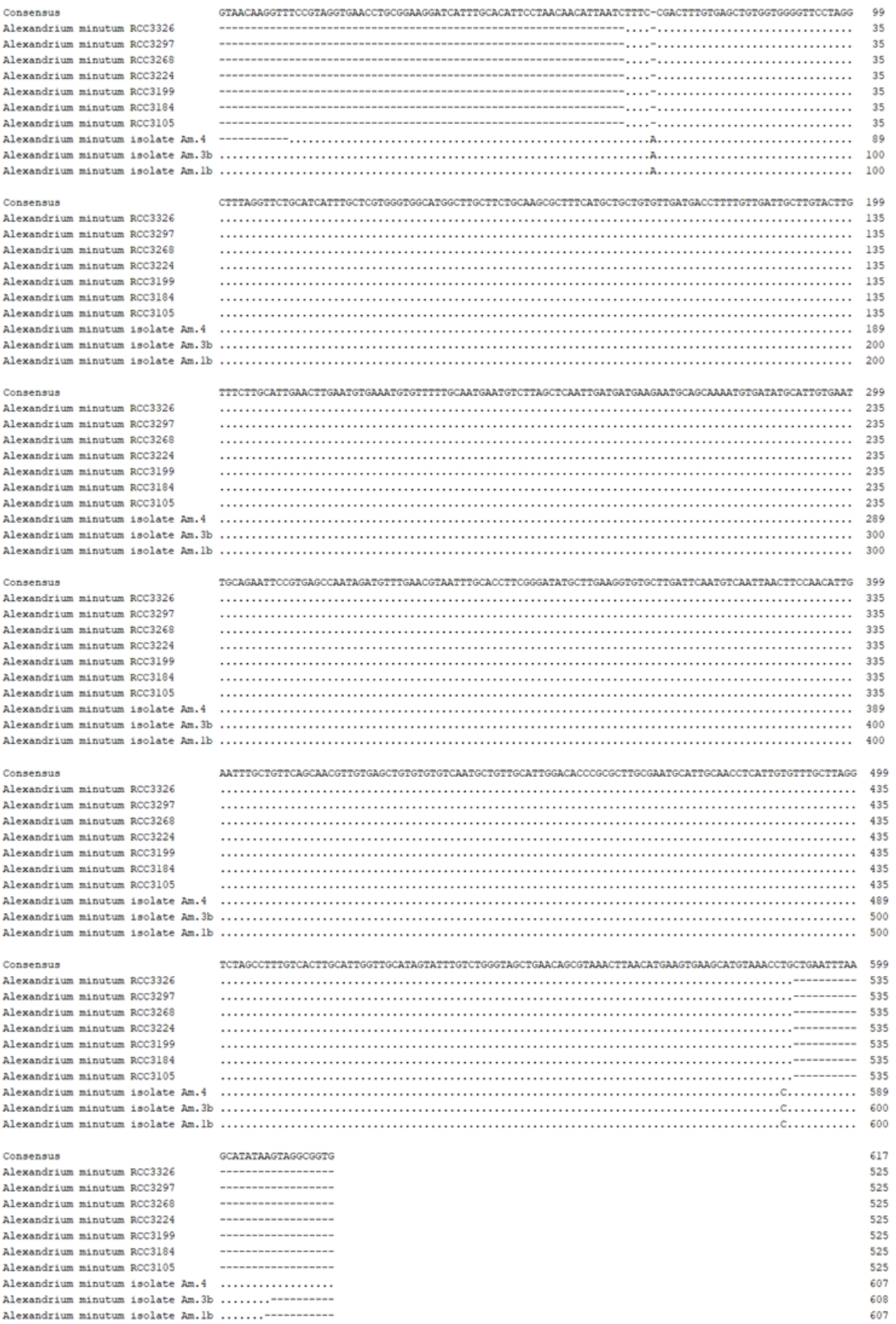

Figure 17 The ClustalW alignment of 10 *A. minutum* ITS1-5.8S-ITS2 genome region downloaded from the NCBI GenBank database in December 2018. There is a pairwise identity of 99.8%. Due to the high degree of conservancy of this region it is ideal as a target site for primer design. Letters in the sequences below the consensus sequence represent bases that vary from the consensus sequence.

3.3.2 ITS1-5.8S-ITS2 Recombinase Polymerase Amplification (RPA)

Of the five sets of RPA primers (Table 4) designed to target the ITS1-5.8S-ITS2 region of the *A. minutum* genome primer sets AMRPA 1.1/1.2, AMRPA 2.1/2.2 and AMRPA 3.1/3.2 all produced amplification. Primer sets AMRPA 4.1/4.2 and AMRPA 5.1/5.2 did not, however (Figure 18). Primer set AMRPA 3.1/3.2 was chosen for further analysis as they produced the brightest bands at the correct target size (199 bp) when separated via gel electrophoresis. This indicates that this primer pair were the most efficient at amplifying the desired target. Upon closer inspection of primer set AMRPA 3.1/3.2 product a faint band was observed at the wrong size, indicating potential non-specific amplification of a product approximately 400 bp in length. Raising the reaction temperature to 45°C removed this non-specific amplification whilst still amplifying the desired target. Additionally, the incorporation of 0.8 M betaine to the RPA reaction as described by Luo *et al.* (2019) also removed the presence of the non-specific band by enhancing the specificity of the RPA assay (Kersting *et al.*, 2014a; Luo *et al.*, 2019; Mok *et al.*, 2016), believed to be attributable to the molecular barrier effect of betaine (Luo *et al.*, 2019).

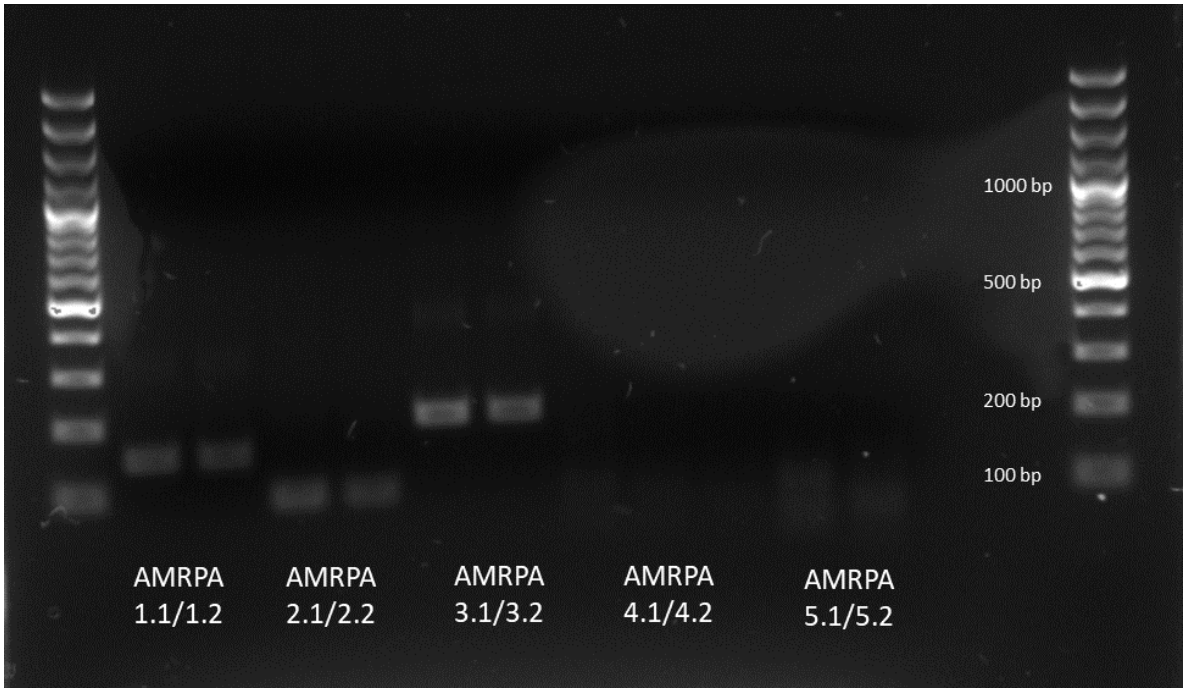

Figure 18 *A. minutum* ITS1-5.8S-ITS2 rRNA RPA using the primers designed in this study. Primer set 3.1 and 3.2 produced the brightest band indicative of a more efficient amplification. The ladder used is a 100 bp ladder (NEB, UK).

A noted drawback associated with RPA is its incompatibility with hydrolysis probes and molecular beacons, commonly used, target-specific, real-time detection format in PCR assays (Busi, 2020). This is due to the strand displacing property of the polymerase used in the RPA reaction, which results in the 5'-3' exonuclease activity inherent in *Taq* DNA polymerase used in qPCR (required for

hydrolysis probes to function) to degrade the displaced DNA strand as it is being synthesized. Historically, RPA has been reported as being compatible with SYBR chemistry (Cao *et al.*, 2018) but this is not the best method for real-time detection. This is because SYBR, as an intercalating agent, binds to all dsDNA that may be present in the sample, including interference from primer dimers, potentially leading to false-positives in targeted assays. Additionally, in this study, it was found that the use of SYBR chemistry is not compatible with the RPA reaction, as there were found to be false positive samples when using this real-time detection technique when examined using downstream analyses (melting curve, 2% agarose gel electrophoresis), therefore designing a gene-specific exo probe was essential for real-time RPA reactions.

The RPA amplicon was sequenced using Sanger sequencing (Eurofins, Germany) and the presence of the desired amplicon confirmed. There was a degree of variability in the amplicon sequences between *A. minutum* individuals (Figure 19), with 99.5% base identity between the 25 sequences examined. This amplicon sequence data was used to design a gene specific exo probe for subsequent real-time RPA detection targeting a highly conserved region flanked by the AMRPA 3.1/3.2 primers. The exo probe, once cleaved, acts as an additional forward primer, adding an additional level of specificity to the assay.

The number of 5.8S gene copies was estimated by using the published data of Galluzzi *et al.* (2004), who determined that each *A. minutum* cell contains 1084 $\pm$ 120.3 copies. Using this information, it was estimated that an extraction from ~600,000 cells would yield $7.5x10^7$ copies of the ITS1-5.8S-ITS2 region. A-dilution series was subsequently prepared containing $7.5x10^7$ to 7.5 ITS1-5.8S-ITS2 copies and used as template for amplification reactions. This dilution series was used to determine the limit of detection (LOD) of the RPA assay developed in this study. The 5.8S rRNA dilution series showed a strong linear relationship ($R^2 = 0.99$) when amplified using AMRPA 3.1/3.2 primers (Figure 20), with positive amplification of the 5.8S rRNA region down to 10^4 copies (Figure 20) and no amplification at copy numbers lower than 10^4. The 10^4 gene copies detected in this study equates to 10 *A. minutum* cells, well below the 10^3 cells L^{-1} seawater used to define the presence of a bloom (Lewis *et al.*, 2018), and is within the 40 cells L^{-1} warning level for UK aquaculture.

```
Consensus               AGATTGTTGTGCTTACTCTATCATTTATATGGTTGATGTGGGTGCGATGGTTCTTACCTTGAATGTCAGCTTCTATTTCTGCAAA   85
SingleResultFileDownload ..........................................................................................  85
SingleResultFileDownload ..........................................................................................  85
SingleResultFileDownload ..........................................................................................  85
SingleResultFileDownload ..........................................................................................  85
SingleResultFileDownload ..........................................................................................  85
SingleResultFileDownload ..........................................................................................  85
SingleResultFileDownload ..........................................................................................  85
SingleResultFileDownload ..........................................................................................  85
SingleResultFileDownload ..........................................................................................  85
SingleResultFileDownload ..........................................................................................  85
SingleResultFileDownload ..........................................................................................  85
SingleResultFileDownload ..........................................................................................  85
SingleResultFileDownload ..........................................................................................  85
SingleResultFileDownload ..........................................................................................  85
SingleResultFileDownload ..........................................................................................  85
SingleResultFileDownload ..........................................................................................  85
SingleResultFileDownload ..........................................................................................  85
SingleResultFileDownload ..........................................................................................  85
SingleResultFileDownload ..........................................................................................  85
SingleResultFileDownload ..........................................................C.............................  85
SingleResultFileDownload ..........................................................................................  85
SingleResultFileDownload ..........................................................................................  85
SingleResultFileDownload ..........................................................................................  85
SingleResultFileDownload ..........................................................................................  85
SingleResultFileDownload ..........................................................C.............................  85
SingleResultFileDownload ..........................................................................................  85

Consensus               TCATTACCCTTGCACATGAATGGTAATTTGCCTGCGGGTATTGGAATGCATGTGTTTGCAATGATTTGTGATTTGACGCATGTGT  170
SingleResultFileDownload ....................................C.....................................................  170
SingleResultFileDownload ..........................................................................................  170
SingleResultFileDownload ..........................................................................................  170
SingleResultFileDownload ......................C...................................................................  170
SingleResultFileDownload ......................C...................................................................  170
SingleResultFileDownload ......................C...................................................................  170
SingleResultFileDownload ......................C...................................................................  170
SingleResultFileDownload ...C..................C...................................................................  170
SingleResultFileDownload ......................C...................................................................  170
SingleResultFileDownload ......................C...................................................................  170
SingleResultFileDownload ......................C...................................................................  170
SingleResultFileDownload ..........................................................................................  170
SingleResultFileDownload ..........................................................................................  170
SingleResultFileDownload ......................C...................................................................  170
SingleResultFileDownload ..........................................................................................  170
SingleResultFileDownload ..........................................................................................  170
SingleResultFileDownload ..........................................................................................  170
SingleResultFileDownload ......................C...................................................................  170
SingleResultFileDownload ..........................................................................................  170
SingleResultFileDownload ..........................................................................................  170
SingleResultFileDownload ..........................................................................................  170
SingleResultFileDownload ..........................................................................................  170
SingleResultFileDownload ..........................................................................................  170
SingleResultFileDownload ..........................................................................................  170
```

Figure 19 ClustalW alignment of sequenced ITS1-5.8S-ITS2 RPA product from 25 *E. coli* colonies after TOPO cloning and amplified by PCR using M13 universal primers. The consensus identity was 99.5% showing few polymorphisms between sequences.

The failure to detect amplification at copy numbers lower than 10^4 could be due to the Exonuclease III degrading newly synthesized template DNA at a faster rate than it was being produced from these initial low DNA concentrations. To test this, RPA reactions were prepared using DNA from 10^3 to 1 gene copy as template and analysed using gel electrophoresis. There were no products present in the gel supporting a LOD of 10^4 5.8S rRNA copies for this assay. The failure of RPA to amplify low copy numbers may also be a result of the lower reaction temperature imparting less thermal energy (and by proxy, kinetic energy) on the reaction sample, so particles within the mix have less kinetic

energy and will not move around as fast, reducing potential interactions that may occur between the reaction components.

The ITS1-5.8S-ITS2 RPA assay developed in this study produced rapid results, with detectible amplification after 3.5 minutes for the 10^7 copy number reactions. The most dilute copy number sample to amplify (10^4 estimated gene copies) did so at 8.1 minutes. This is much quicker than PCR assays, which usually take between one and three hours to reach completion.

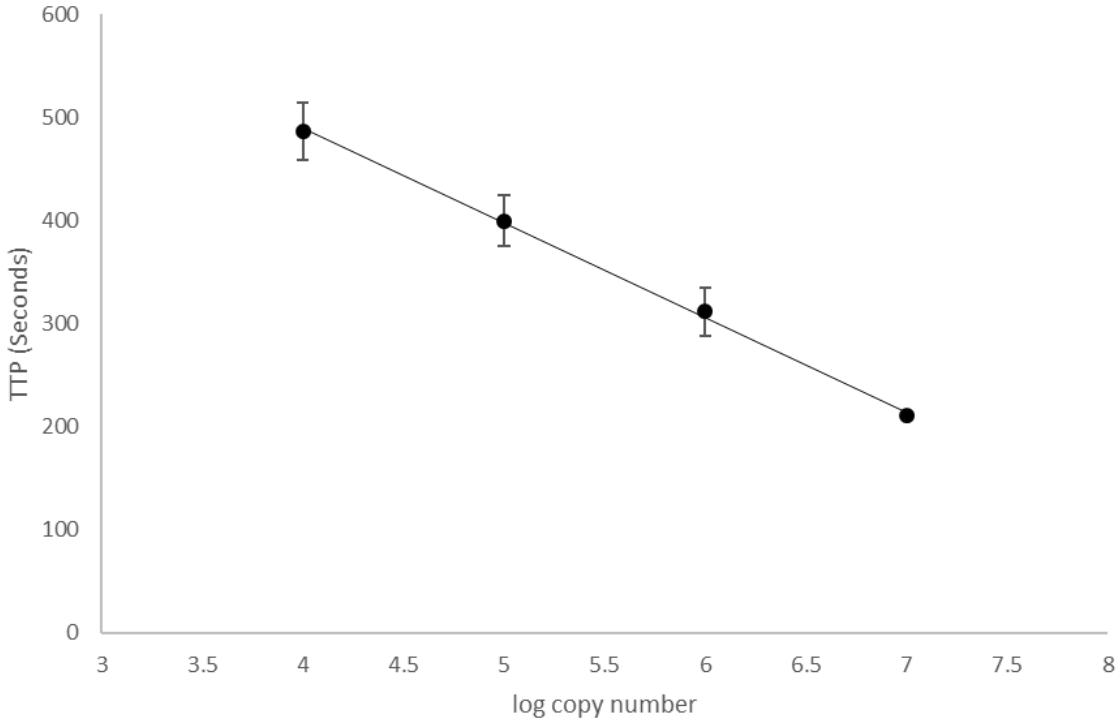

Figure 20 Amplification of a dilution series using RPA 5.8S rRNA AMRPA 3.1/3.2 primers. A Linear Regression analysis of the data indicated a linear trend, with an R^2 of >0.99. Error bars, where visible, are the standard error of the mean (*n* = 2). This strong relationship between dilutes allows the RPA to be used in a semi-quantitatively to estimate *A. minutum* cell concentration in unknown samples.

The specificity of the 5.8S rRNA AMRPA 3.1/3.2 primers was investigated using other dinoflagellate species available in culture in the lab (Table 7) and show that the primer set is specific to *A. minutum.* RPA products were analysed via gel electrophoresis, with the only product being visible for *A. minutum* (Figure S 2). This specificity makes the 5.8S rRNA RPA assay an attractive option for *Alexandrium* monitoring due to the rapid reaction speed and the highly specific nature of the reaction.

Table 7 The specificity testing for the 5.8S rRNA PCR and RPA assays, and *sxtG* PCR and RPA assays.

Organism	Strain	5.8s rRNA PCR (Galluzzi et al., 2004)	5.8s Rrna RPA (this study)	*sxtG* PCR (this study)	*sxtG* PCR (Orr et al., 2013)	*sxtG* RPA (this study)
Alexandrium minutum	1119/48	+	+	+	+	+
Prorocentrum lima	1136/9	-	-	+	-	-
Prorocentrum cordatum	1112/1	-	-	+	-	-
Lingulodinium polyedrum	1121/2	-	-	+	-	-
Karenia brevis	CCMP2229	-	-	+	-	-

The manufacturer of the RPA reaction kits (TwistDX™, Cambridge, UK) recommend using 0.42 µM of each primer per reaction. In this study, RPA reactions were trialed containing 0.1 µM, 0.2 µM, 0.3 µM, 0.4 µM, 0.5 µM, and 0.6 µM primer concentrations in an attempt to optimize the 5.8S rRNA RPA, a standard procedure in the design and development of qPCR assays. This is because primer concentration can influence the specificity of the primers, and as RPA is isothermal it's one of the few parameters that can be used to tune the assay specificity (i.e. It can't be done by modulating annealing temp, as it can with PCR). As the concentration of the primers in the RPA reaction were decreased below the recommended 0.4 µM, the TTP increased in a linear fashion down to a primer concentration of 0.2 µM (R^2 = 0.99). However, the 0.1 µM primer set showed a marked increase in the TTP (from 344.6 seconds for the 0.2 µM concentration to 576.6 seconds for the 0.1 µM concentration) (Figure 21). This is likely due to RPA, unlike PCR, being non-cyclical and therefore the initial concentrations of the reagents that are present in the reaction will govern the rate at which the reaction happens. Whereas in PCR the primer concentrations are always in excess, in RPA the primer concentration appears to be reaction-limiting. At the higher primer concentrations (0.4 µM, 0.5 µM and 0.6 µM), the primers are present in excess, and therefore are not reaction limiting, hence amplification occurs at a similar time at these primer concentrations.

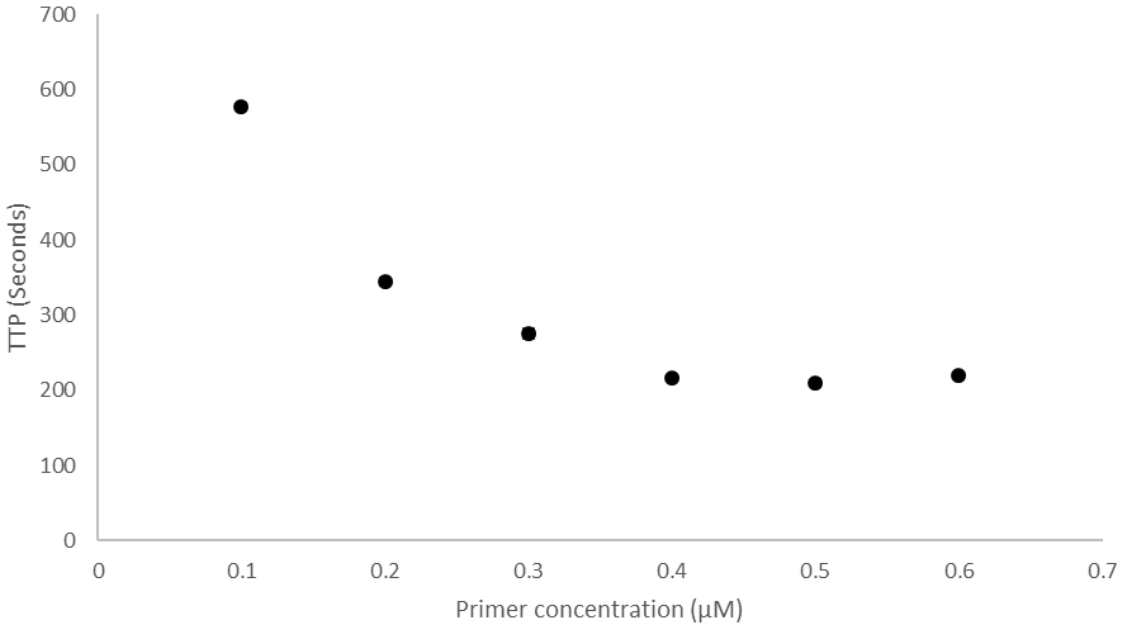

Figure 21 *A. minutum* 5.8SrRNA RPA performed with different primer concentrations. Concentrations above 0.4 µM all resulted in similar TTP, whilst there was a strong linear relationship between the 0.4 µM 0.3 µM and 0.2 µM concentrations (R^2 = 0.99). The lowest concentration tested 0.1 µM produced a high TTP not in line with the higher concentrations tested. Standard error (*n* = 2) among replicates was low.

3.3.3 *sxtA* and *sxtG* Recombinase Polymerase Amplification (RPA)

In addition to RPA assays for the 5.8 rRNA region, RPA assays were also designed to target the *sxtA* and *sxtG* saxitoxin key functional genes (Figure 24). Several *sxtA* and *sxtG* sequences for *A. minutum* and several other *Alexandrium* species, including *A. affine*, *A. fundyense*, *A. pacificum*, *A. tamarense*, and *A. andersonii* were downloaded from Genbank and their sequence similarity investigated. Alignment of consensus sequences demonstrated that the *sxtG* gene is more conserved between *Alexandrium* species than the *sxtA* gene (pairwise % identity: 97.2% for *sxtG*; 79.3% for *sxtA*) (Figure 22 and Figure 23).

Primers were therefore designed to differentiate species using *sxtA* and across all *Alexandrium* species for *sxtG*. (Table 7). After RPA using the *sxtA* and *sxtG* primers and 10^5 estimated *sxtA* and *sxtG* gene copies followed by product analysis via gel electrophoresis demonstrates that neither of the *sxtA* primers produced any detectible amplification (Figure 24). However, *sxtG* RPA 1.1/1.2 primers designed to target a 162 bp region of the *sxtG* gene amplified a product of the expected size (Figure 24). When combined with a dilution series containing 10^1 to 10^5 *sxtG* copies and analysed via gel electrophoresis the *sxtG* RPA assay appears to amplify all reactions. However, the

lower concentrations (10^1 and 10^2 *sxtG* copies) produce a very faint band, likely indicating inefficient RPA at these low concentrations (Figure 24).

The *sxtG* RPA product was subsequently cloned and Sanger sequenced. The pairwise identity of 11 recovered *sxtG* sequences was 95.2%, confirming the relatively conserved nature of the *sxtG* gene amplicon, and additionally that the primers were amplifying the desired target region (Figure 25). The primers were also tested for specificity using DNA from four different dinoflagellate species with no cross reactivity of primers (Table 7). This demonstrates that RPA has the potential to amplify low copy number functional gene targets and could be used in harmful algae screening assays. The design and incorporation of a *sxtG* specific exo probe will allow for the real-time detection of the *sxtG* gene using RPA and may also improve amplification of lower gene copy number reactions as, once cleaved, the exo probe oligonucleotide sequence upstream of the THF residue acts as an additional forward primer, potentially increasing the amount of amplification.

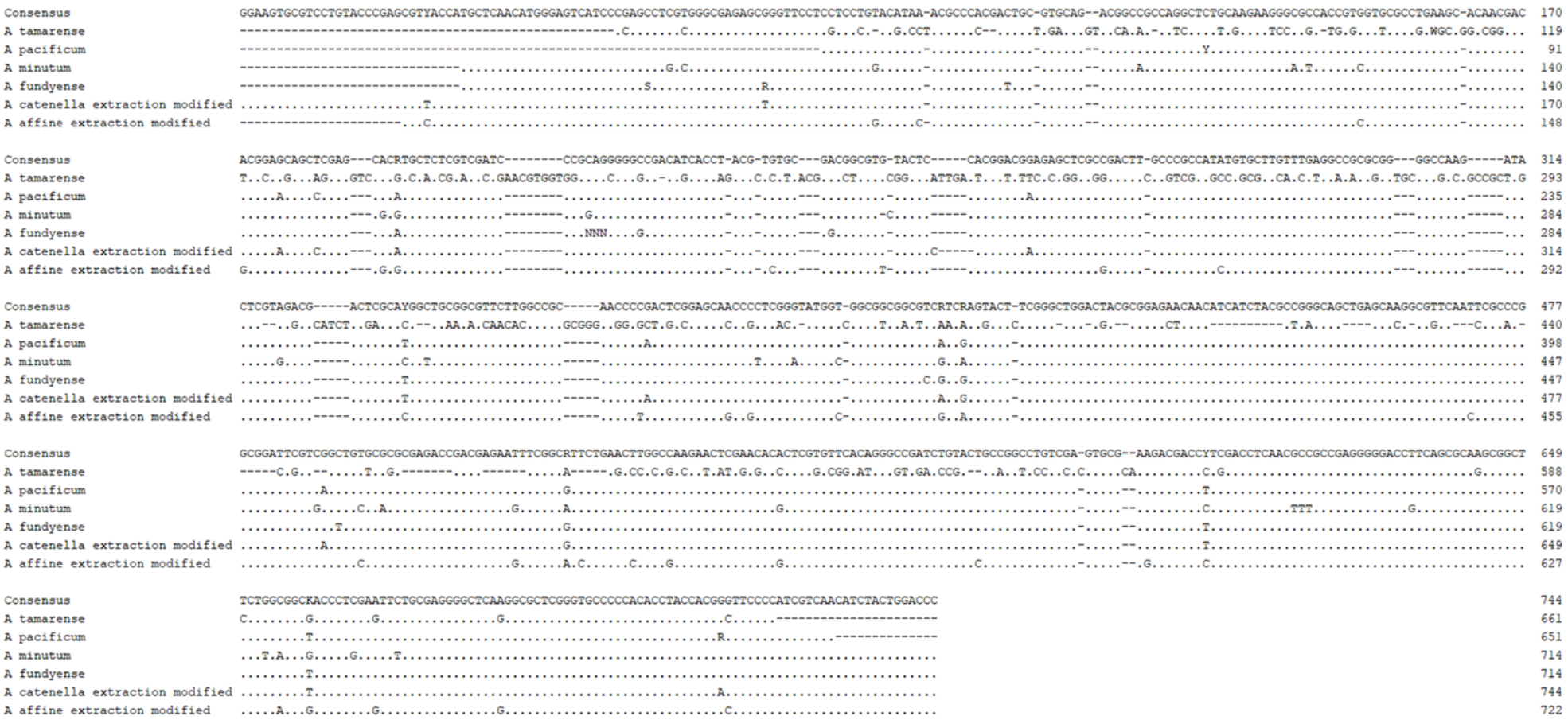

Figure 22 The ClustalW sequence alignment of consensus *sxtA* gene sequences from six different *Alexandrium* species. The pairwise identity was 79.3% indicating a degree of divergence in the *sxtA* gene sequence between different species of *Alexandrium*. This makes designing a primer set to cover the genus difficult, however it may be possible to use this gene to identify the presence of individual *Alexandrium* species

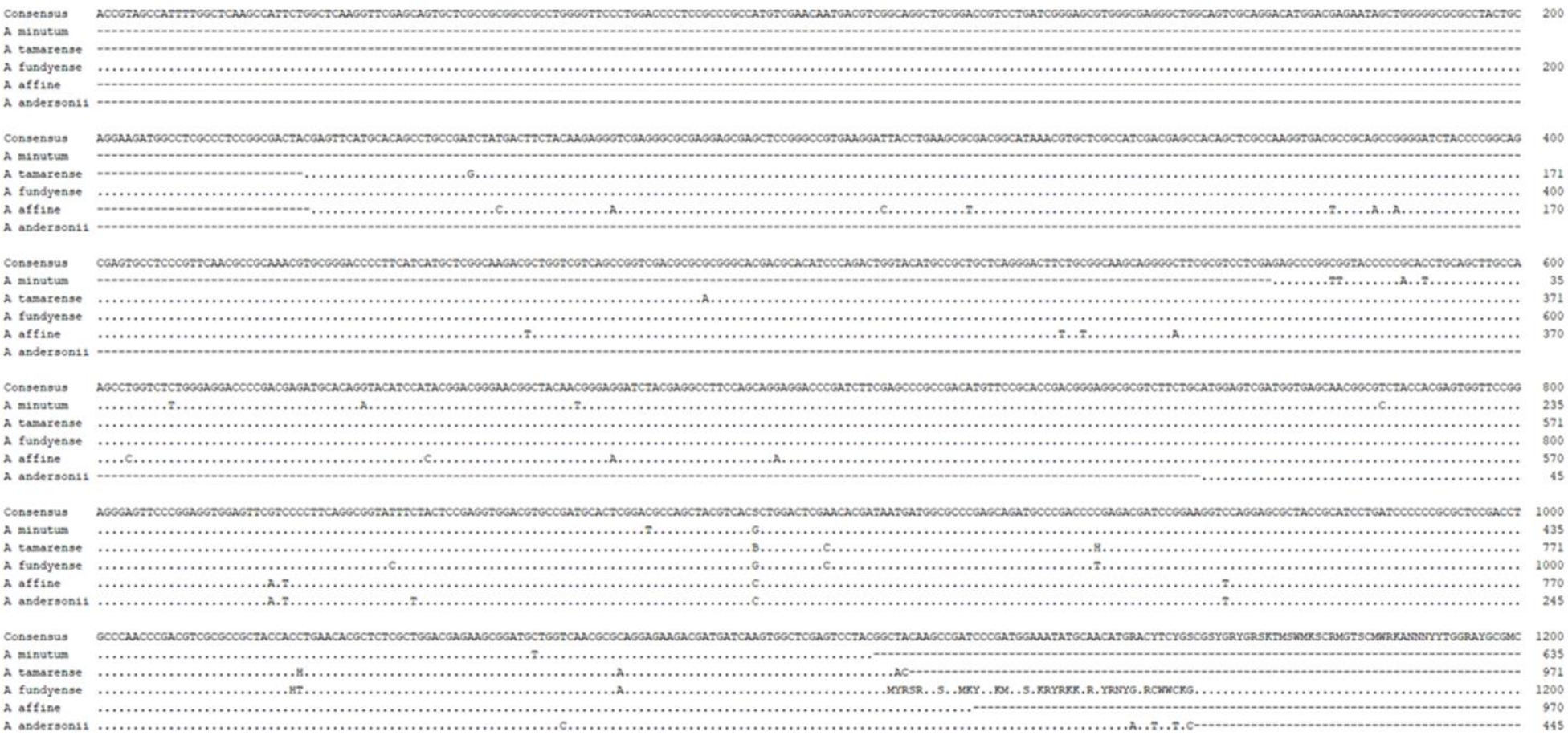

Figure 23 The ClustalW sequence alignment of consensus *sxtG* gene sequences from five different *Alexandrium* species. The pairwise identity was 97.2% indicating a higher degree of conservancy between *Alexandrium* species than demonstrated by the *sxtA* gene.

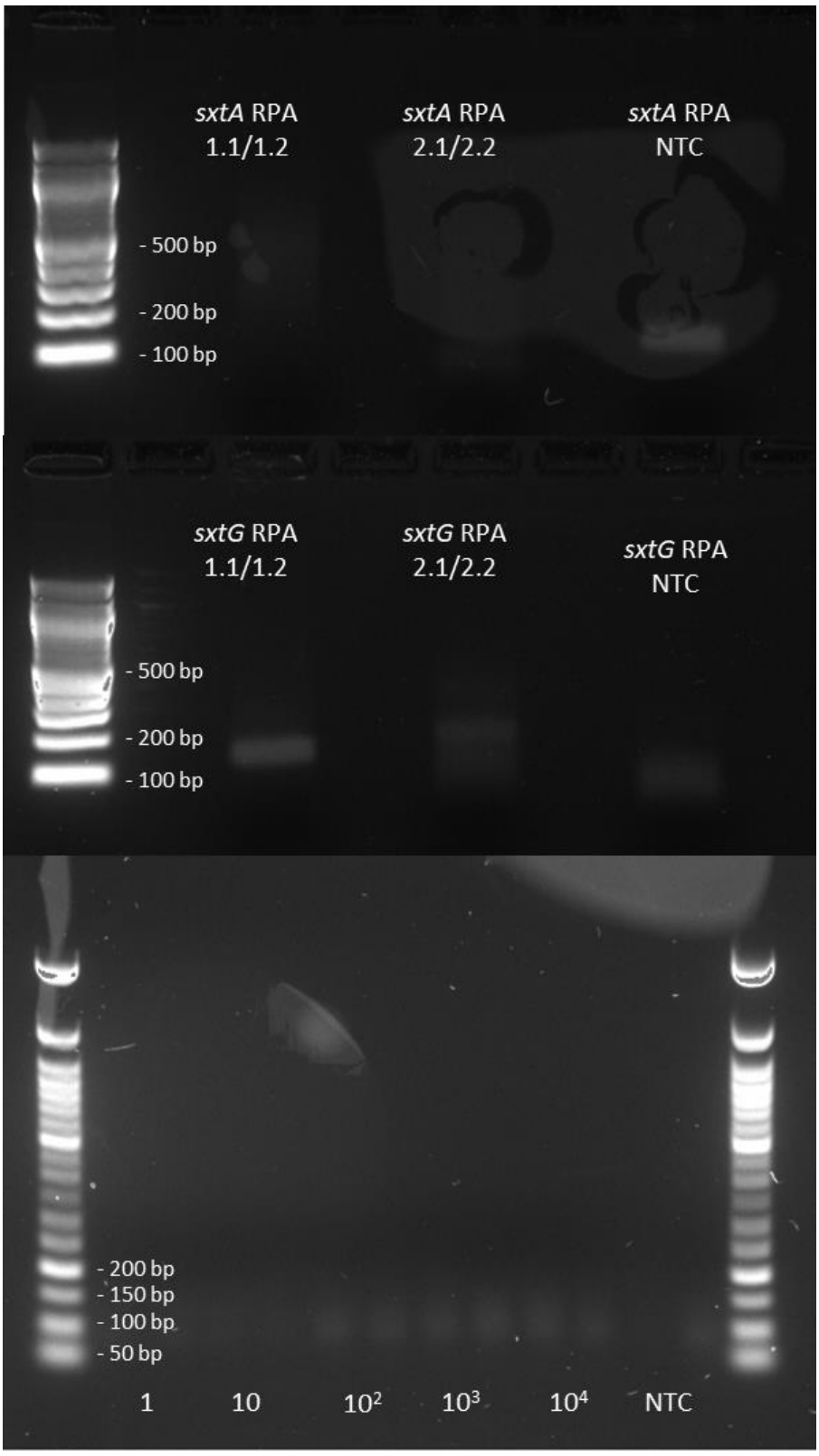

Figure 24 RPA amplification of the *sxtA* gene and the *sxtG* gene (top panel) of *A. minutum*. The expected amplicon sizes can be seen in Table 4 The ladder used is a 100 bp ladder. The bottom panel is the RPA amplification the *sxtG* gene using *sxtG* RPA 1.1/1.2 primers from a dilution series ranging from 1 to 10^4 gene copies. The expected amplicon size is 162 bp, the third band in the ladder is 150 bp. There is a signal between 100 and 150 bp in length, likely the intended target.

Figure 25 ClustalW alignment of 11 sequenced *sxtG* RPA products. The similarity between the sequences was 95%. This level of similarity between the sequenced individuals highlight this region as a suitable target for amplification.

3.3.4 5.8S rRNA qPCR

PCR primers were taken from Galluzzi *et al.* (2004) and used to provide a benchmark for the RPA assay developed in this study. For real-time detection, SYBR green was added to the reaction mix. Using the Galluzzi *et al.* (2004) qPCR assay with SYBR green added for real-time detection a standard curve was created on the assembled ITS1 – 5.8S – ITS2 dilution series ranging from 10^8 to 10^2 copies with an efficiency of 103.4 % (R^2 = 0.99) (Figure 26). The limit of detection of this qPCR assay of 10^2 ITS1 – 5.8S – ITS2 gene copies is equivalent to 0.1 *Alexandrium* cell. This is possible as each *Alexandrium* cell contains multiple copies of the ITS1 – 5.8S – ITS2 rRNA. This LOD is two orders of magnitude more sensitive than the RPA assay developed in this study, which had a LOD of 10 *Alexandrium* cells. Both of these LODs however, are lower than the detection limits of microscopy-based detection and enumeration (20 – 100 cells L^{-1}), and roughly equivalent to flow-cytometry (10 cells L^{-1}) using a FACScanTM flow cytometer (Becton-Dickenson, San Jose, CA.) (Hawkins, 2010). In comparison with the 5.8S qPCR assay, the 5.8S RPA assay produced positive results much quicker, with the last reaction to amplify (10^4 gene copies) amplifying in 8.1 minutes. The equivalent sample within the 5.8S qPCR took 52.5 minutes. The rapid detection of the 5.8S RPA assay alongside the simplified technological requirements make it an attractive option for miniaturisation and point of sample testing, even though the LOD is not as high as the qPCR assay as it still falls below current statutory testing requirements, being able to detect as little as 10 cells, with current alert level for *Alexandrium* being 40 cells L^{-1}.

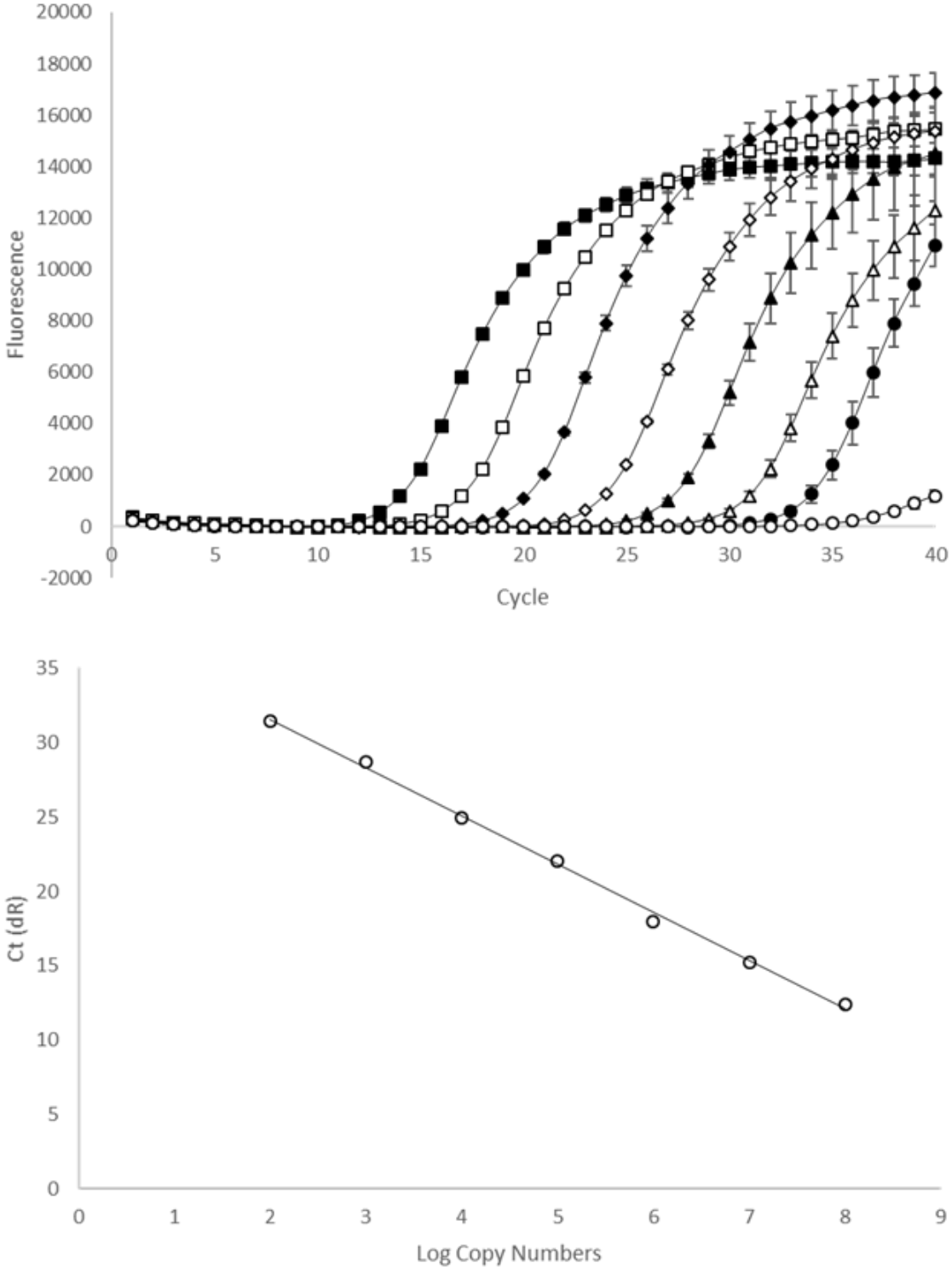

Figure 26 A standard curve of qPCR using Galluzzi *et al*., (2004) 5.8S rRNA primers. The R^2 is 0.99 and the PCR efficiency is 103.4%. The amplification plots (top) show the amplification of 10^8 (■), 10^7 (□), 10^6 (◆), 10^5 (◇), 10^4 (▲), 10^3 (△), 10^2 (●) ITS1 – 5.8S – ITS2 copies. (○) are NTC's, which show a slight increase in the latter cycles likely due to the formation of primer dimers binding with the EvaGreen present in the reaction. Error bars, where visible are the standard error of the mean (*n* = 3).

3.3.5 Saxitoxin Gene PCR

Two qPCR assays using SYBR Green for real-time detection were developed to amplify and detect a 161 and 127 bp region of the *A. minutum sxtA* gene. *sxtA* gene copy numbers were estimated using the data of Stüken *et al.* (2015), who determined that there are between 1.5±1 – 10.8±3.3 *sxtA* copies per *A. minutum* genome. For this study this was assumed to be the number of *sxtA* gene copies per cell. Several studies show that in dinoflagellates the genome size is dependent on cell size (Dapena *et al.*, 2015; LaJeunesse *et al.*, 2005; Stüken *et al.*, 2015), a feature that is in agreement with other eukaryotic lineages, including jawless fishes, cartilaginous fishes, uradele amphibians, anuran amphibians, reptiles and birds (Cavalier-Smith, 2005; Gregory, 2001) therefore the median value of 6.15 *sxtA* copies cell^{-1} was taken (assuming a normal Gaussian distribution in cell size).

An additional two qPCR assays were also developed to amplify a 250 bp and 150 bp region of the *sxtG* gene. According to Orr *et al.* (2013) the *sxtG* gene is present in considerably lower copies than the 5.8S rRNA gene, being present at around three orders of magnitude less in *A. minutum*. Orr *et al.* (2013) also suggest that the *sxtG* gene is present in differing amounts between various *Alexandrium* species. In this study we used the study of Orr *et al.* (2013) to assume each *A. minutum* cell contained one copy of the *sxtG* gene.

The optimal annealing temperature for the STX primers was determined via a gradient PCR performed in real-time and using a high-resolution melt curve analysis to identify PCR products. The temperatures tested ranged from 52.9°C to 69.3°C. Figure 27 shows that for *sxtA* at the lower annealing temperatures (52.9°C) there was positive amplification after 25 cycles. The resulting high-resolution melting curve has a high level of non-specific amplification. For annealing temperatures >52.9°C the amount of non-specific amplification decreases with increasing annealing temperatures as expected, and the amplification occurs later (Figure 27). This is a demonstration of the non-specific amplification that can occur at lower annealing temperatures. The use of EvaGreen for real time detection in this assay explains why the amplification appears to occur earlier in the lower temperature reactions, as it is binding to the non-specific product, and producing a detectible signal. The single peaks of the melt curves using annealing temperatures above 67.9°C supports the use of annealing temperatures at or above this temperature for reliable specificity using a SYBR real-time PCR assay. The *sxtG* qPCR produced less non-specific amplification at the lower annealing temperatures (Figure 28), demonstrating a higher level of specificity with the primers. Positive amplification was achieved consistently after 24 cycles and any non-specific amplification disappears at annealing temperatures above 57.7°C. Using these melting curve data, identical qPCR protocols for both the *sxtA* and *sxtG* gene targets were subsequently used for future

reactions: 95°C for 2 minutes, followed by 35 cycles of 95°C for 10 seconds, 68°C for 15 seconds and 72°C for 10 seconds.

Using this qPCR protocol and a custom designed hydrolysis probe (*sxtG* Taqman 1; Table 4) with the *sxtG* qPCR primers and an *A. minutum* DNA dilution series (1 – 10^5 estimated *sxtG* gene copy numers), C_t's were achieved ranging from 27.56 for the 10^5 copies to 38.82 for the 10 copies reactions respectively (Figure 29). The presence of a single product was confirmed via gel electrophoresis. The standard curve generated can also be seen in Figure 29. This shows an R^2 value of 0.98, which is adequate to determine the order of magnitude of abundances (Figure 29). The PCR efficiency of 73.02% indicates low efficiency amplification, which is common in qPCR at low copy numbers (Vaerman *et al.*, 2004).

Although the *sxtG* PCR assay amplified *A. minutum* DNA as expected, it failed specificity tests using *Prorocentrum lima*, *Prorocentrum cordatum*, *Lingulodinium polyedrum* and *Karenia brevis* (Table 7). When analysed via gel electrophoresis there was product present for each of the tested organisms (Figure S 1). Using the primers developed by Orr *et al.* (2013) qPCR amplification was achieved and there was no amplification detected when using the dinoflagellate species listed above. When used in this study however, the Orr *et al.* (2013) assay lacked the reproducibility that the *sxtG* qPCR primers designed here were able to achieve. The subsequent incorporation of a target specific hydrolysis probe may remove the non-specific real-time detection observed by the *sxtG* primer set when using EvaGreen as it adds an additional layer of specificity, being complimentary to the desired assay target. The lack of specificity produced when using the *sxtG* qPCR primers developed in this study may not be an issue when using the assay on environmental samples as the primers should bind more efficiently to *Alexandrium* DNA than that from other dinoflagellates. This will produce amplification from reactions set up containing a lower initial template concentration, allowing differentiation between amplification of different dinoflagellate species.

Although the efficiency of qPCR was low (73.02%; Figure 29), the detection limit achieved for the *sxtG* qPCR assay developed here of approximately 100 cells L^{-1} is comparable with a previously published *sxtA* qPCR assay (~110 cells) (Murray *et al.*, 2011), with *sxtA* and *sxtG* genes present in similar numbers per cell the assays are comparable (Orr *et al.*, 2013; Stüken *et al.*, 2015). Currently, flow cytometry offers a higher LOD (10 cells L^{-1}) (Hawkins, 2010), but suffers the disadvantage of requiring technically competent staff, whilst the hardware required is problematic for miniaturisation and does not lend itself easily to automation. As the concentration of PSP toxins within the shellfish flesh is unknown (with the exception of the CRM and LRM) no correlation could be examined between STX gene C_t and toxin concentration, an area that needs to be investigated further if molecular methods are to become more widely accepted for shellfish screening. The

maximum permitted levels of STX in shellfish flesh is 800 µg Kg^{-1} of flesh (FSA, 2018). As the concentration of STX in the samples provided by Cefas is unknown, no parallels could be drawn between STX concentration and how, or if, it relates to STX gene amplification in this study.

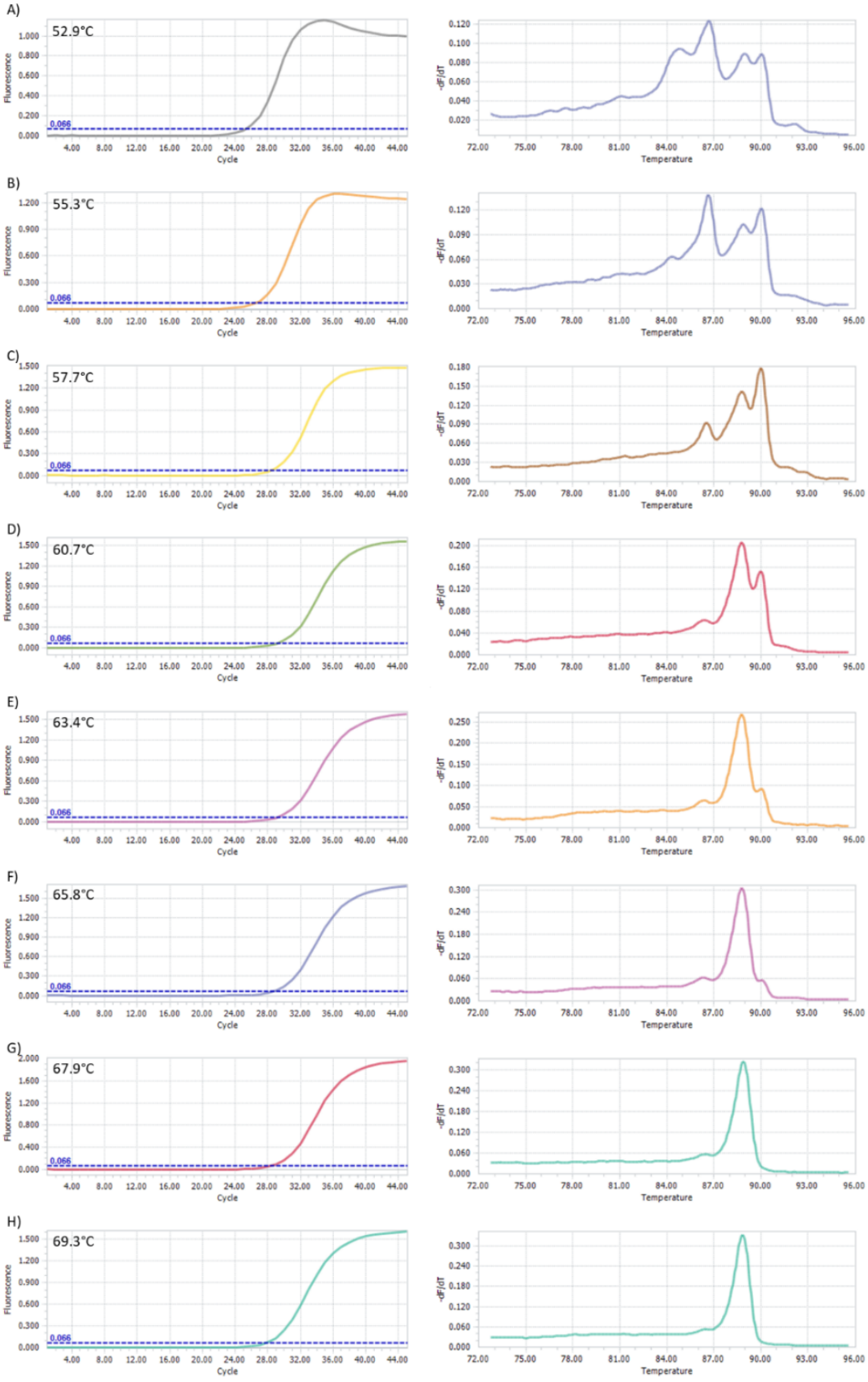

Figure 27 The annealing temperature analysis for the *sxtA* PCR assay. The images on the left show the amplification curve and the images on the right show the melt curve for the different annealing temperatures trialled. The annealing temperatures trialled were: A) 52.9°C; B) 55.3°C; C) 57.7°C; D) 60.7°C; E) 63.4°C; F) 65.8°C; G) 67.9°C; H) 69.3°C.

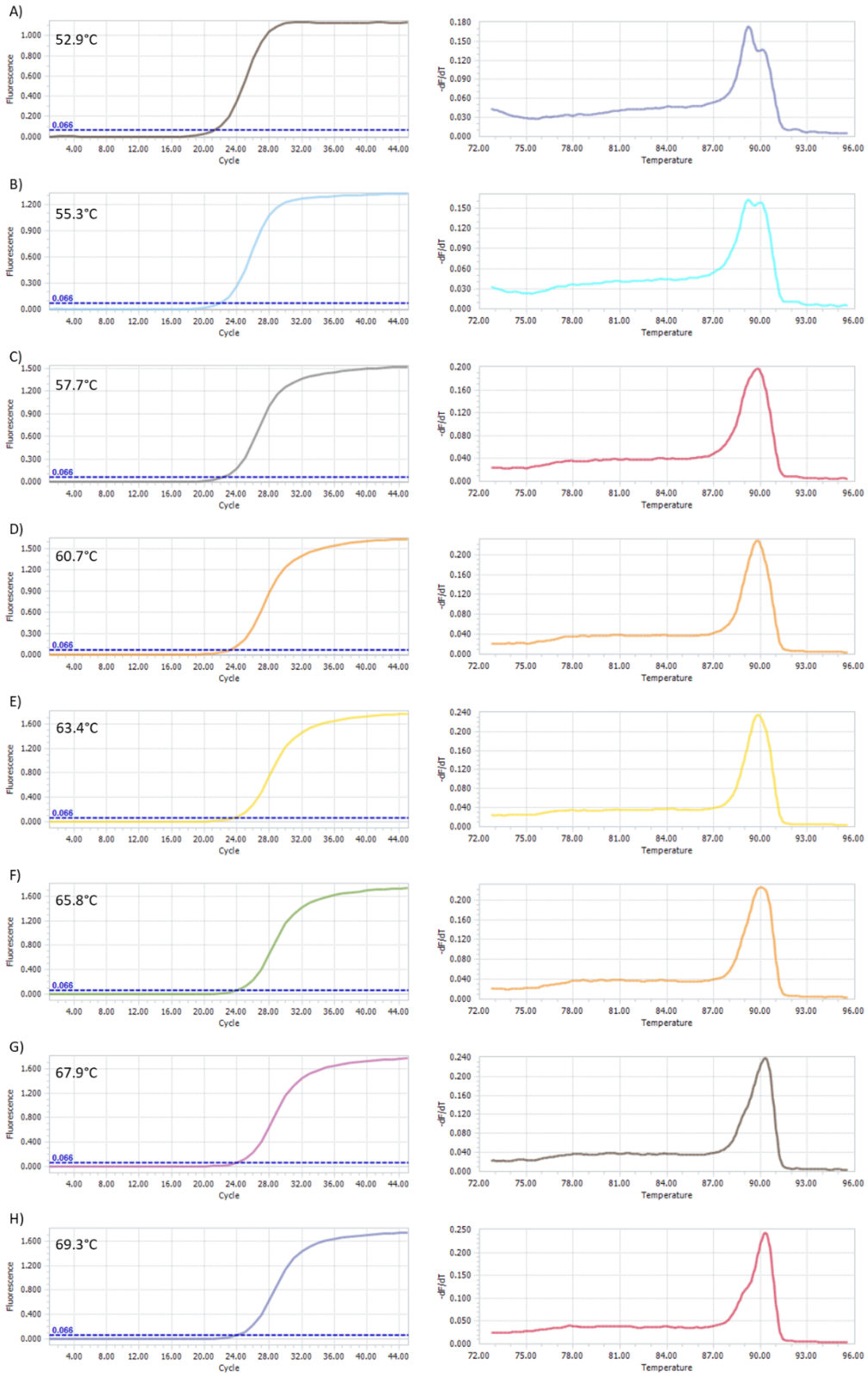

Figure 28 The annealing temperature analysis for the *sxtG* PCR assay. The images on the left show the amplification curve and the images on the right show the melt curve for the different annealing temperatures trialled. The annealing temperatures characterised were: A) 52.9°C; B) 55.3°C; C) 57.7°C; D) 60.7°C; E) 63.4°C; F) 65.8°C; G) 67.9 °C; H) 69.3 °C. The single peaks of the melt curves between 57.7°C and 67.6°C demonstrate a higher primer specificity than the *sxtA* gene at these annealing temperatures.

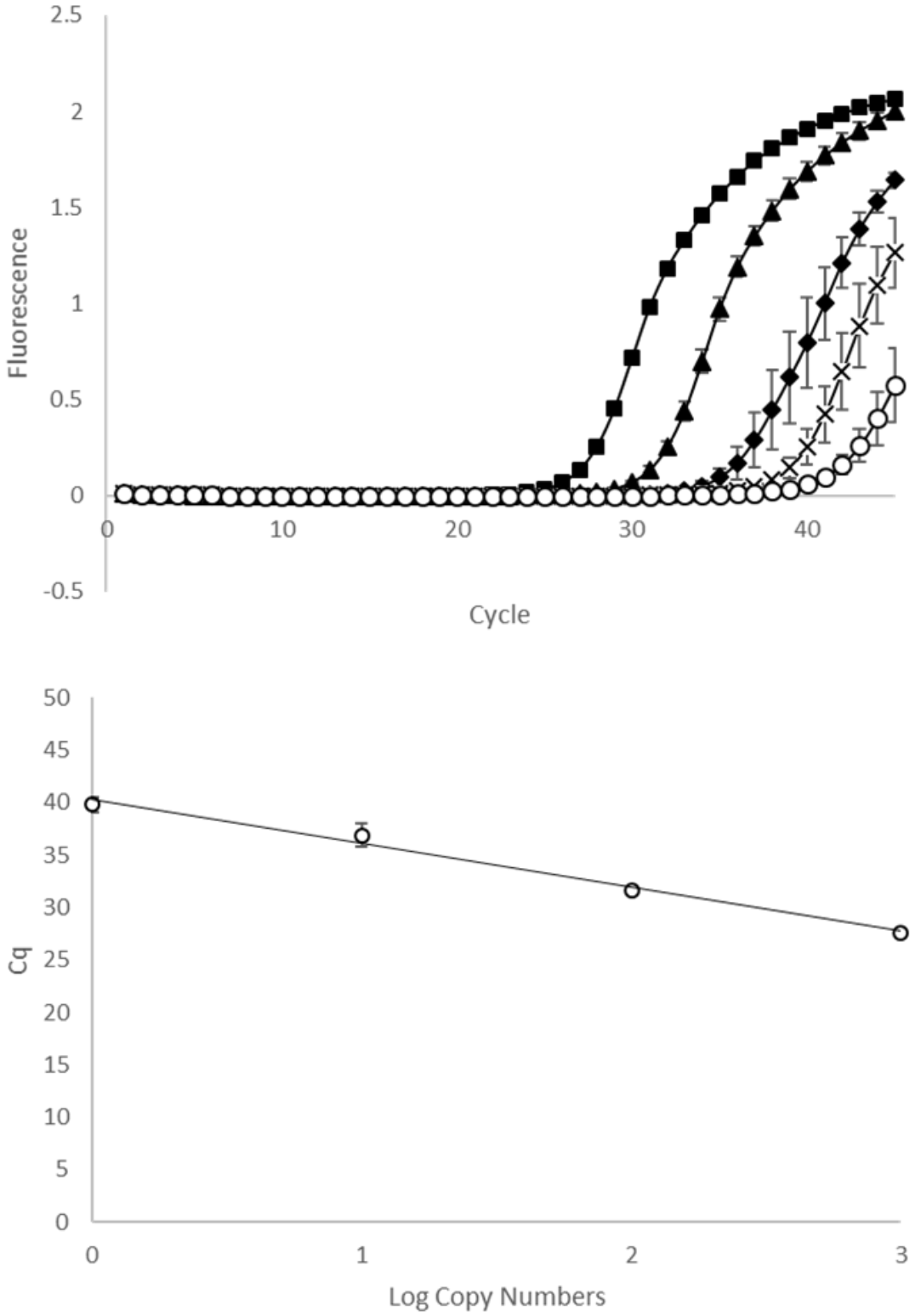

Figure 29 The *sxtG* qPCR assay using a hydrolysis probe for real-time detection developed in this study. The top panel shows amplification reactions and bottom panel shows the standard curve assembled from these data (bottom). ■ = 10^5 *sxtG* copies, ▲ = 10^4 *sxtG* copies, ◆ = 10^3 *sxtG* copies, × = 10^2 *sxtG* copy, ○ = NTC. The R^2 value for the standard curve is 0.98 and the slope is -4.2, corresponding to a PCR efficiency of 73.02%. The error bars, where visible show the standard error (*n* = 3).

3.3.6 Contaminated bivalve screening and Inhibition PCR

DNA was successfully extracted from mollusc laboratory reference material (LRM) provided by Cefas containing 2800 µg STX eq/kg flesh and used to see if the RPA assay designed in this study can detect the presence of *A. minutum* in STX contaminated flesh. The LRM was analysed using the ITS1-5.8S-ITS2 RPA assay and an RPA Basic kit with end point analysis via gel electrophoresis. There was no amplification product of the correct size (199 bp) detected. There was however a product of approximately 50 bp in each reaction well (Figure 30). As this was also present in the NTC wells it is likely to be indicating dimerization between the primers used in the reaction.

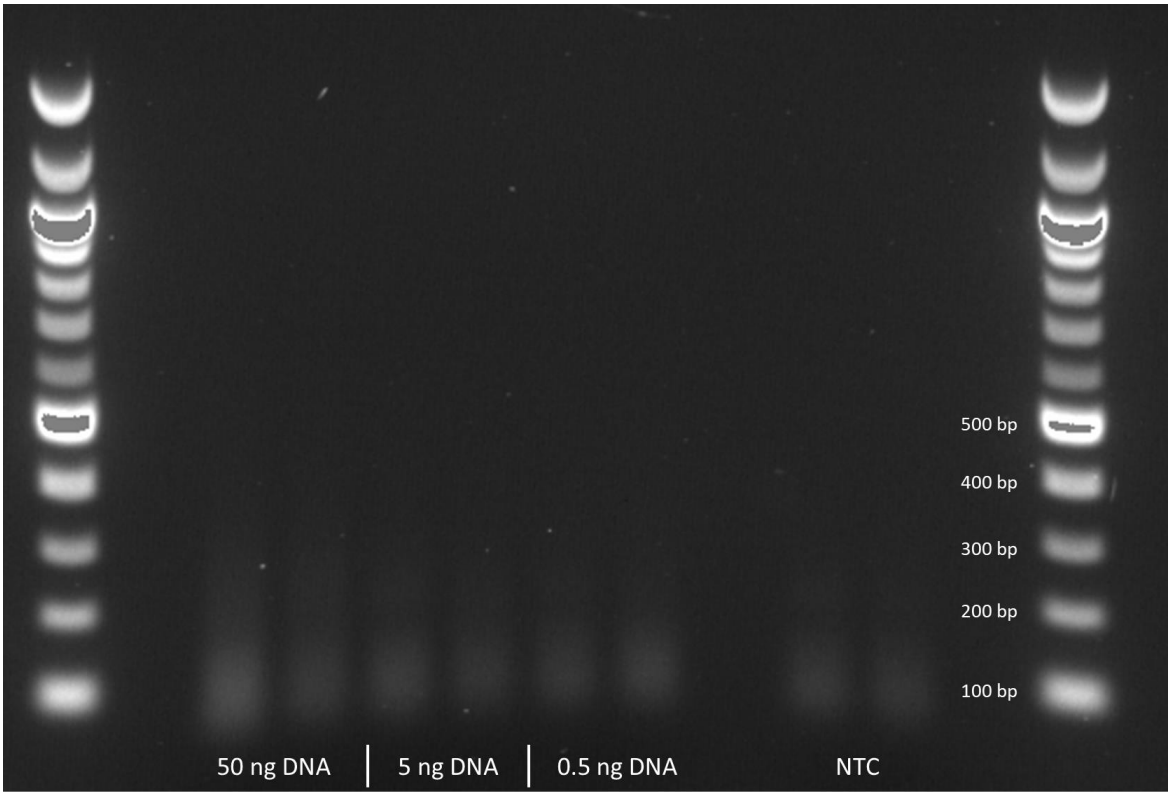

Figure 30 End point gel electrophoresis of the *A. minutum* 5.8S rRNA RPA assay performed using DNA extracted from STX contaminated LRM mollusc tissue. The 5.8S rRNA amplicon is 199 bp in length. The product seen here is approximately 100 bp in length, and as it is also present in the NTC columns, it is assumed to be primer dimers.

Extracting DNA for NAA purposes from molluscs has been previously reported as being problematic, as the mollusc flesh is rich in mucopolysaccharides, which affect the yield and quality of DNA and additionally act as PCR inhibitors if not fully removed (Jaksch *et al.*, 2016). To test if there was any inhibition from carry over artefacts present in the mollusc LRM DNA extract a qPCR using established *E. coli ybbW* primers (Walker *et al.*, 2017) was conducted using *E. coli* DNA spiked into the extracted mollusc DNA as template (Figure 30). These *E. coli* spiked samples (Walker *et al.*, 2017) amplified after 13 cycles, whilst the *ybbW* qPCRs performed with "pure" *E. coli* DNA crossed

the threshold after 12 cycles (Figure 31). As an equal amount of *E. coli* DNA was added to each reaction this difference of one cycle is likely due to PCR inhibitors present within the DNA extracted from the mollusc flesh.

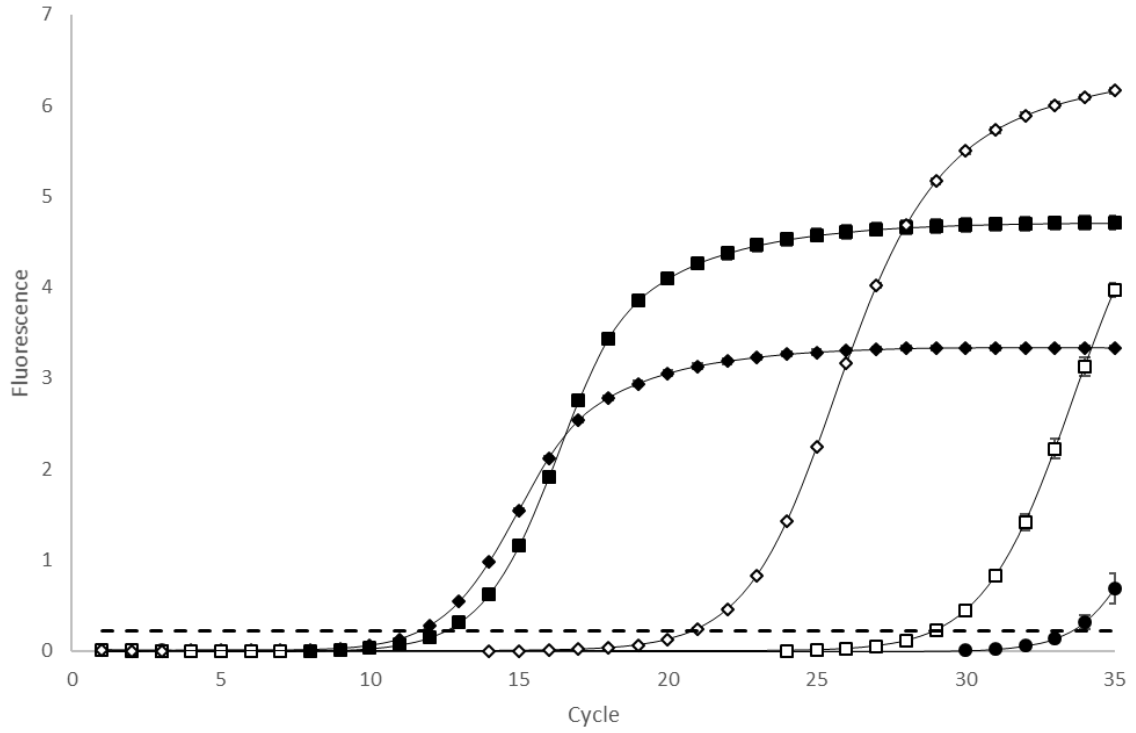

Figure 31 Inhibition testing on DNA extracted from mollusc LRM. ■ = *ybbW* assay using extracted mollusc DNA spiked with E. coli DNA, ◆ = *ybbW* assay using only *E. coli* DNA, ● = NTC. □ = *A. minutum* 5.8S rRNA using DNA extracted from mollusc LRM, ◇ = *A. minutum* 5.8S rRNA using DNA extracted from cultured cells, ○ = NTC. Error bars where visible are the standard error of the mean (*n* = 3).

To determine whether *A. minutum* 5.8S rRNA amplification could be indicative of saxitoxin-contaminated shellfish, the Galluzzi *et al.* (2004) qPCR assay was used to amplify from DNA extracted from 5ng of SXT-positive LRM mollusc tissue. This material amplified with a C_t of 29 cycles, which is >1000 gene copies or >1 cell based on the amplification kinetics of the qPCR assay (Figure 26). This equates to four *A. minutum* cells per gram tissue. A high-resolution melt curve (Figure 32) of this LRM-produced amplification product was identical to the melt curve produced from the 5.8S rRNA amplification product from an *A. minutum* culture extract, confirming specific amplification of the target *A. minutum* 5.8S rRNA gene in the mollusc tissue.

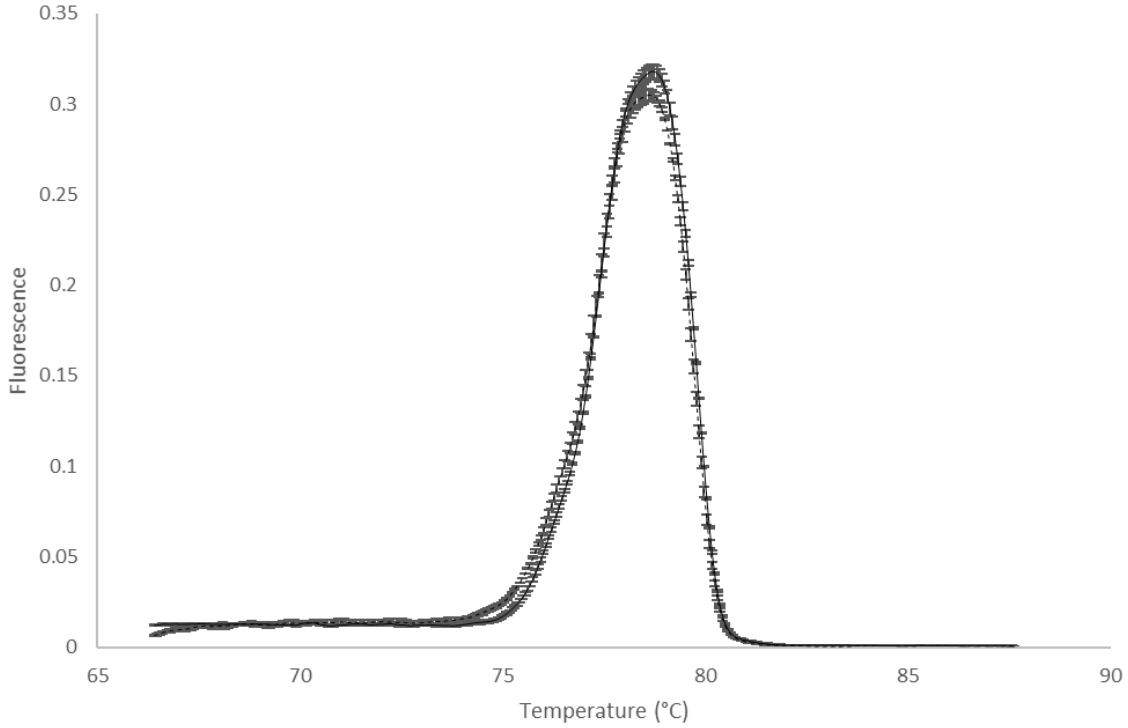

Figure 32 The high-resolution melt curve analysis for the Galluzzi *et al.* (2004) PCR assay for both the culture extracted DNA template (solid line) and mollusc extracted DNA. The peaks at the same temperature indicate the dissociation of a dsDNA target at the same temperature, indicating a similar GC content and, by proxy, the same sequence. Error bars, where visible, show the standard error of the mean (n = 3).

The difference of one cycle between the mollusc extract spiked with *E. coli* DNA and "pure" *E. coli* DNA suggests there is some inhibition of PCR, but it decreases calculated quantities of target genes by less than half an order of magnitude. These results demonstrate that *A. minutum* 5.8S rRNA NA amplification has the potential to be used as an indicator for STX shellfish contamination. Whether there is any correlation between the toxin concentration and the C_t remains to be determined. A correlation between STX and 5.8S rRNA genes would require accurate gene quantification. In order to increase the accuracy of the qPCR, additional template preparation steps may be required such as addition of BSA or gp32, selection of resistant polymerases, chloroform extraction, PEG precipitation or active carbon treatment (Schrader et al., 2012). Amplicons should be sequenced to confirm they are the correct target, and efforts taken to minimise contamination in the negative controls.

3.3.7 Comparison of Molecular and Non-Molecular HAB Monitoring

Reliable monitoring of low concentrations of *Alexandrium* is essential, because concentrations as low as 200 cells L^{-1} have been associated with STX uptake in shellfish (Todd, 2001). The general

method for enumeration of HAB forming phytoplankton is microscope-based counting of cells, whilst direct detection of toxins is conducted either via mouse bioassays (Suzuki and Machii, 2014), HPLC (Yang *et al.*, 2017), liquid-chromatography-mass spectrometry (LC-MS) (Harju *et al.*, 2015), or antibody-based immunoassays, such as ELISA (Sato *et al.*, 2014). These methods suffer many drawbacks that make them unsuitable for miniaturisation and automation. For example HPLC requires a well-equipped analytical laboratory, pure standards of STX and its many analogues (Todd, 2001), is time consuming and expensive. The more recent ELISA methods, although eliminating some of these drawbacks, are not available for several common STX derivatives, and experience cross-reactivity as toxin profiles are quite complex.

The molecular methods described in this thesis (RPA and qPCR) have many advantages when compared to microscopy counts and direct toxin detection, which include being simple to set up, having a lower requirement for extensive training, are cheap (qPCR reagents <US$1 per sample), quick, and highly suited to automation. In addition to this qPCR-based assays for the detection of *Alexandrium* may be more sensitive than microscopy-based methods at low cell abundances, and where the species of interest may comprise a small portion of the phytoplankton. Previous *Alexandrium* qPCR assays have achieved detection limits of 0.1 cell L^{-1} for ITS1-5.8S-ITS2 rRNA gene (Galluzzi *et al.*, 2004) and ~110 cells L^{-1} for *sxtA* (Murray *et al.*, 2011). In this study an isothermal RPA assay was developed with reliable limits of detection of 10 cells L^{-1} for the ITS1-5.8S-ITS2 rRNA gene. Although this is two orders of magnitude less sensitive than the PCR assay described in Galluzzi *et al.* (2004) it is much faster, with results in minutes rather than hours. Although not as sensitive as the Galluzzi *et al.* (2004) qPCR assay the RPA assay developed here is more sensitive than the current microscopy-based methods of detection and enumeration, and is also more specific, as morphologically many dinoflagellate species are indistinguishable, and removes the possibility of mistakes due to human error.

The *sxtG* qPCR assay developed in this study had a reliable detection limit of 100 cells L^{-1}, comparable to a *sxtA* qPCR assay reported by Murray *et al.* (2011), with each gene present in similar quantities per cell (Orr *et al.*, 2013; Stüken *et al.*, 2015) making the LODs comparable. Future studies involving quantification of *sxtA* and *sxtG* gene transcripts and any potential correlation with measured toxin concentrations could make toxin gene molecular assays a viable method for detecting the presence of STX in water samples, replacing the current methods of toxin measurement, which are all labour intensive and expensive, with the exception of ELISA (Table 8).

A comparison of detection methods is listed in Table 8. It is clear that molecular techniques in general provide more sensitive detection at lower costs, with reduced technical expertise required, and in less time. This, combined with their adaptability to automation and miniaturisation makes

molecular detection techniques desirable for implementation using miniaturised, lab-on-a-chip devices – a topic explored in detail in the subsequent chapters of this thesis.

Table 8 A comparison of methods used in the detection and enumeration of *Alexandrium* and Saxitoxin concentrations.

Method	Time	Labour	Cost	LOD	Reference
Algae					
Microscopy	Days	Intensive	Expensive	20 - 100 cells L^{-1}	Murray *et al*, 2011
Flow cytometry + FISH	Hours	High	Expensive	10 cells L^{-1}	Hawkins, 2010
rRNA PCR	Hours	Moderate	Cheap	10 cells L^{-1}	Galluzzi *et al*, 2004
rRNA RPA	< 1 hour	Moderate	Cheap	10 cells L^{-1}	This study
sxtA PCR	Hours	Moderate	Cheap	110 cells L^{-1}	Murray *et al*, 2011
sxtG PCR	Hours	Moderate	Cheap	100 cells L^{-1}	This study
Toxin					
Mouse Bioassay	Days	Intensive	Expensive	0.3 µg STX equivalent	Suzuki and Machii, 2014
HPLC	Hours	Intensive	Expensive	0.33 µg kg-1 mollusc flesh	Yang *et al*, 2017
LC-MS	Hours	Intensive	Expensive	6.0 ±0.7 ng mL^{-1}	Harju *et al*, 2015
ELISA	Hours	Moderate	Cheap	0.02 ng mL^{-1}	Sato *et al*, 2014

3.4 Conclusions

In this chapter a novel isothermal RPA assay for real-time isothermal detection of *Alexandrium minutum* is described for the first time. The RPA is rapid (<10 minutes) and has the ability to detect in real-time down to 10 *A. minutum* cells from culture. Although this is not as sensitive as established PCR assays (Galluzzi *et al.*, 2004) it is much quicker and has a lower technological requirement making it an attractive prospect for a miniaturised point of sample device. The RPA assay was able to detect *A. minutum* 5.8S rRNA from culture samples down to 10^4 gene copy numbers, equivalent to 10 *A. minutum* cells. Inhibitor testing using PCR showed that potential inhibitors present within the mollusc extracted DNA did not greatly inhibit the PCR reaction. It was also demonstrated that *A. minutum* nucleic acids can be detected in STX contaminated mollusc flesh. This gives nucleic acid amplification technologies potential to be used for point of sample screening of contaminated shellfish.

Future work will involve trialling the 5.8S rRNA RPA assay on mollusc extracted DNA treated to remove anything that may potentially be inhibiting the RPA reaction. Additionally, qPCR and RPA assays that detect the STX genes *sxtA* and *sxtG* should be investigated using mollusc extracted DNA. Investigating reverse transcription RPA to detect *A. minutum* RNA rather than DNA would also be useful in cultured samples to allow investigation of toxin gene regulation when subjected to different environmental stresses. In situ nutrient sensors for nitrate, phosphate and iron are in various levels of development by the Ocean Technology and Engineering group and are ideal

candidates for pairing with SXT RNA analysis. Additionally, sea surface temperature, *p*CO2, and pH could also be examined with relation to toxin gene expression. This will also be of value as RNA is much more transient than DNA in environmental water samples (Wood *et al.*, 2020) and could potentially indicate the recent presence of live *A. minutum* as opposed to dead cells with intact DNA. Subsequently the design of a *sxtG* specific exo probe for use with the *sxtG* RPA primer set designed in this study could be used in a miniaturised device in combination with environmental data to provide insights into the environmental drivers of toxin production.

Chapter 4 Dry-Preserved, Complete Nucleic acid Amplification Reaction Mixtures for use on Portable Instrumentation

Note: The contents of this section have been published in The Journal of Microbiological Methods (165, 2019) under the title - 'Ready Mixed', improved nucleic acid amplification assays for the detection of Escherichia coli DNA and RNA.

4.1 Introduction

Nucleic acid amplification chemistries usually depend upon cold-chain for shipping and storage of heat-sensitive reagents. These include enzymes and dNTPs; the shelf-life of which, at ambient temperatures, is limited to a few days (Garcia *et al.*, 2004). The need for refrigeration means that, in the context of a portable or deployable nucleic acid amplification-based sensor, either some cooling mechanism must be implemented or the reagents should be preserved somehow such that cooling isn't required. The latter is by far the more reasonable option considering the complexity (e.g. compressed gases) and power-requirement of most cooling solutions

Most biological molecules are inherently unstable when stored in their hydrated form, however they can be stabilised by drying in the presence of additives, which reduce or eliminate the effects of dehydration on their molecular structures. In particular, enzymes have an activity that is dependent upon their structure, particularly at the 'active site' where catalysis occurs. The binding of a cognate ligand and the association of heavy metal ion cofactors for structural support or redox catalysis all depend fully on the tertiary structure of the enzyme polypeptide chain and the positioning of amino acid residue sidechains (Cowan, 1998). Other factors affecting enzyme structure include the presence or absence of contaminating heavy metals, and their concentration (Hagmann *et al.*, 2015), as well as the reducing strength of the surrounding solution which can disrupt crucial thiol-thiol bonds (disulphide bridges) (Matsumura and Matthews, 1989). In an aqueous solution the hydrogen bonds that form between water molecules and the amino acids that compose the enzyme contribute to the enzyme tertiary structure. When the surrounding liquid is removed, these hydrogen bonds are lost, leading to structural changes.

Trehalose is a non-reducing disaccharide sugar that is accumulated in some animals during environmental stresses, particularly dehydration and desiccation (Westh and Ramløv, 1991). The mechanism of action remains unclear; however, it is widely accepted that trehalose is the fundamental to the mechanism by which some animals can survive in dehydrated form. One hypothesis for the activity of trehalose in this scenario is that trehalose protects protein structure through direct interactions (e.g., hydrogen bonds) that substitute surrounding water molecules during the drying process, stabilising structure and reducing chemical degradation (Kadoya *et al.*, 2010).

Lyophilisation (freeze-drying) has been demonstrated in combination with trehalose for the dry storage of biological samples (McGinnis *et al.*, 2005), DNA (Zhu *et al.*, 2007) and RNA (Jones *et al.*, 2007). Lyophilisation is a process during which a liquid sample is frozen, and under vacuum water is removed via sublimation. The water vapour is condensed on a cold surface and extracted.

Lyophilisation only occurs when the temperature is reduced to or below the triple point (the temperature and pressure at which the three phases of solid, liquid and gas coexist in thermodynamic equilibrium) of the solvent, which is typically water. With the substance held at its triple point the direct conversion from the solid phase into the gas phase under vacuum can be achieved whilst preventing sample melt (Adams, 2007). Protein stability can be protected further with the incorporation of non-reducing sugars, such as the aforementioned trehalose, which is sometimes used in combination with sucrose (McGinnis *et al.*, 2005).

In addition to trehalose, the sugar pullulan, has been employed for the preparation of dried biological agents for storage, specifically for the long-term (up to two months) dry storage of PCR reagents (Jahanshahi-Anbuhi *et al.*, 2014). Pullulan is a polysaccharide produced by the fungus *Aureobasidium pullulans,* and it is water soluble, mechanically strong, and transparent in its solid form, with low permeability to oil and oxygen (Singh *et al.*, 2008). Pullulan forms a 3D structure encasing the reagents and a barrier to extrinsic factors that may speed the decaying process (e.g. temperature, moisture). More recently, efforts have been made to combine both trehalose and pullulan into a single preservation matrix which has demonstrated the ability to maintain the stability of the model protein β-galactosidase for up to four weeks at 30°C and high humidity's (54%) (Teekamp *et al.*, 2017). This is of benefit, as combining a small disaccharide and a large polysaccharide will provide tight molecular packing and a high T_g (glass transition temperature), essential in preventing the damaging Maillard, or browning, reaction (Bell *et al.*, 1998).

An additional, sugar-free method is gelification. This proprietary technique, developed by BioTools Ltd (Spain), incorporates a gellification component (a gelator) to a solution of the substance to be preserved, followed by partial dehydration. After this, the substance is contained within a viscous gel-like matrix and is resistant to deterioration when stored without refrigeration. Gellification has been demonstrated for the preparation of NASBA reagents that were stable for more than 6 weeks, even after long-distance shipping and fieldwork (Loukas, 2016). However, gellification has several limitations including (i) a relatively high cost per sample to be preserved, (ii) the influence of the gelator with downstream reaction chemistry and (iii) the reagents are not readily available. For this reason, it was not considered.

In this study, two techniques were developed for the dry-preservation of complete nucleic acid amplification reactions, excluding template DNA. The objective was to then, after a period of storage, rehydrate the reactions with a solution of template DNA, and evaluate their performance against reactions that were freshly prepared from refrigerated reagent stocks. The techniques were a lyophilisation-based method utilising trehalose, and a dehydration-based method using pullulan.

Existing and well characterised *E. coli* PCR and NASBA assays (Walker *et al.*, 2017) were used to develop and test these methods. The specific objectives were:

- To determine the stability of both iQ SYBR Supermix® and a standard Taq DNA polymerase after several weeks' storage at room temperature.
- To assess whether the addition of trehalose or pullulan inhibits the PCR reaction.
- To investigate the performance of PCR reagent mixes after lyophilisation in the presence of trehalose, after storage for up to five weeks.
- To investigate the performance of PCR reagent mixes after the dehydration in the presence of pullulan after storage for up to six weeks.

4.2 Methods

4.2.1 DNA and RNA Template Preparation

Genomic DNA standards were prepared from an *E. coli* type strain (NCTC 9001), following the method of Walker *et al.* (2017). The *E. coli* were revived from storage at -80°C and cultured in Luria Broth at 37°C. An exponentially dividing culture was harvested by centrifugation (5,000 x g for five minutes) and resuspended in Maximum Recovery Diluent (Millipore, USA) for one hour. The cells were centrifuged again, and the cell pellet used to prepare a genomic DNA extract using the GeneElute Bacterial Genomic DNA Isolation Kit (Sigma, UK). The DNA was eluted and stored in Tris-EDTA buffer (pH 8.0) at -20°C. The mass of the extracted DNA was estimated by Qubit Fluorometer (Qubit dsDNA high-sensitivity assay kit (ThermoFisher, UK)), and used to estimate the number of genome copies. The extracted DNA was subsequently used to prepare a dilution series of genome copy number standards by diluting the extract in RT-PCR grade water (Promega, UK) to between 10 and 10^5 copies per microlitre. Standards were prepared from a DNA stock immediately prior to use.

RNA standards were prepared as follows. First, a fragment of the *clpB* gene sequence was amplified by PCR using the primers shown in Table 9 (*clpB* gene standard forward and reverse primers). These primers produced a dsDNA PCR product which was used for the synthesis of template RNA using T7 RNA polymerase (NEB, USA). The PCR product was purified using the GeneElute PCR Purification Kit (Sigma, UK) and used directly for RNA synthesis using the Hi Scribe T7 RNA Synthesis Kit (NEB, USA) following the manufacturers recommended protocol. The synthesised RNA was purified using the RNeasy Mini Kit (Qiagen, UK), and contaminating dsDNA removed using RQ1 RNase-Free DNase (Promega, UK), following the manufacturer's instructions. DNA elimination was confirmed by a *Taq*-based PCR, the results of which were negative. The DNA-free RNA was subsequently purified a second time using the RNA Clean and Concentrator (Zymo, USA) following the manufacturers

recommended procedure. The mass of RNA was estimated using a BioAnalyser Instrument, and the RNA 6000 Nano Kit (Agilent, UK). The molecular weight of the RNA was calculated from its sequence, and in combination with the concentration, was used to estimate the number of target copies. A series of RNA copy number standards were prepared by diluting the RNA sample in RT-PCR grade water to between 10 and 10^5 copies per microlitre. Standards were prepared from stock RNA solution immediately prior to use.

4.2.2 qPCR Mix Life

To establish how long qPCR mixes could last with no preservation. Two types of qPCR mix were assembled, one using iQ™ SYBR® Green Supermix (Bio-Rad, California, US) and one using standard Taq DNA polymerase (New England Biolabs, Massachusetts, US). Each iQ™ SYBR Supermix® reaction was set up to a volume of 25 µL with the following composition: 12.5 µL iQ SYBR Supermix®, 0.2 µM of each primer (Table 9), and 11 µL of RT-PCR grade water. The standard Taq reactions were also set up to a final volume of 25 µL containing 2.5 µL of 10X Standard Taq (Mg-free) Reaction buffer, 2 nM of $MgCl_2$, 0.2 µM of dNTPs, 0.2 µM of each primer, 0.5 µL of 20x EvaGreen dye (Biotium, California, US) and 625 U of Taq DNA polymerase, and 18.875 µL of RT-PCR grade water. Mixtures were stored in the dark at room temperature (20°C) and tested weekly, by using them in qPCR reactions. This was done for five weeks. Each test was done by adding 0.5 µL of template DNA at a concentration of 18 ng μL^{-1} to each reaction mix. The qPCR reactions were carried out using a LightCycler® 96 instrument (Roche, Basel, Switzerland) with the following thermal-cycling program: 95°C for 15 seconds, 68°C for 20 seconds, and 72°C for 45 seconds, for 40 cycles, followed by a high-resolution melt curve to confirm if any visible qPCR amplification was the desired amplicon.

The following protocol was followed to determine whether the presence of trahalose, sucrose or pullulan, changed the efficiency of qPCR reactions. A trehalose/sucrose mixture or pullulan were separately added to qPCR mixes assembled as above to test if either of the sugars interfere with the qPCR amplification reaction. Each sugar was added to a 0.2% (w/v) final concentration. qPCR was then performed as described above and the potential effect of each sugar on qPCR amplification examined.

4.2.3 Preparation of Trehalose Containing qPCR Mixes and Dehydration by Lyophilisation

Reaction mixtures were prepared in sterile, nuclease-free PCR tube strips (LightCycler 8-tube strips, Roche Molecular Systems Inc.). The qPCR reactions were prepared to contain 20mM of Tris-HCl (pH 8.3), 100mM of KCl, 1.5mM of $MgCl_2$, 2mM each of dNTPs (dATP, dTTP,dCTP, dGTP), 80 nM of each

primer, 40 nM of the hydrolysis probe, 0.2% (w/v) of Sucrose, 0.2% (w/v) of trehalose and 2 U of GoTaq G2 DNA polymerase (Promega, UK); with water added to a final volume of 100 µL. RT-qPCR reactions were prepared using the GoTaq Probe 1- Step RT-qPCR System (Promega, UK) following the manufacturers recommended protocol with the exception that the final 20 µL reactions were mixed with 80 µL of RT-PCR grade water to a final volume of 100 µL. The mixtures were frozen at −80°C for 30 minutes, before transfer to a vacuum chamber sterilised with both DNAaway (Sigma, UK) and RNaseZap (Thermofisher, UK) according to the manufacturers recommended method. Lyophilisation was initiated using a ZL (8 L) Lyophilisation Instrument (SPScientific, UK). Lyophilisation continued for precisely 16 h at <200 µBar, at which point the mixtures had formed a crystalline, white powder. Air for re-pressurisation was passed through a 0.2 µm Sterivex filtration cartridge (Millipore, USA). Decontamination was confirmed by no template control reactions showing negative amplification. After varying periods of time in storage at room temperature, the lyophilised reaction mixtures were activated by adding a 20 µL solution of *E. coli* DNA or RNA containing a known quantity of the target sequence, prepared as described in 4.2.1. Each qPCR reaction was done using a LightCycler 96 qPCR instrument (Roche, Switzerland) with an initial denaturation of 95°C for 2 min, followed by 40 cycles of 95°C for 20 seconds and 60°C for 60 seconds. The RT-qPCR reactions were carried out as described above, but with the addition of an initial reverse transcription step of 42°C for 15 min prior to thermal cycling.

Table 9 The oligonucleotides used in this study to amplify the *ybbW* and *clpB E. coli* genes. FAM is the specific fluorophore used, ZEN is an additional internal quencher, and IABkFQ is an Iowa Black® quencher. *clpB* standard forward primer contained a T7 RNA Polymerase promoter sequence at the 5' terminus (shown in **bold**), followed by a short 'spacer' (shown <u>underlined</u>), upstream of the target-binding sequence.

Primer Name	Primer Sequence (5' - 3')	Reference
ybbW forward primer	TGATTGGCAAAATCTGGCCG	Walker et al., 2017
ybbW reverse primer	GAAATCGCCCAAATCGCCAT	
ybbW hydrolysis probe	FAM-CCGCCG[ZEN]AAAACGATATAGATGCACGG-IABkFQ	This study
clpB forward primer	GCGACAATCCGGTCTTCA	This study
clpB reverse primer	AAATCCACATTTCTGACGAGG	Heijnen and Medema, 2009
clpB hydrolysis probe	FAM-CTTCCA[ZEN]GGCGAATCACTTTACCCGG-IABkFQ	This study

4.2.4 Preparation of Pullulan Containing PCR Reaction Mixtures and Evaluation of Stability

Pullulan (Sigma, UK) was prepared as an aqueous solution in RT-PCR grade water (Sigma, UK) at concentrations of 10% (w/v), 15% or 20% (100, 150 and 200 mg/mL respectively). The solutions were stored at 4°C and were warmed in a water bath set to 60°C, immediately prior to use, in order to maintain a low working viscosity. Pullulan-containing qPCR master mixes where prepared to 25

µL using the IQ SYBR Supermix®, as described above, with the addition of 25 µL pullulan solution per reaction, to a final volume of 50 µL. The mixtures were transferred into sterile, nuclease-free PCR tube 8-cap strips (Roche Molecular Systems Inc) and left to dry overnight in the dark, at room temperature (20°C) and pressure, in a sterile container. The pullulan-containing qPCR mixtures were stored at either room temperature or 12°C for a period of up to eight weeks. The 12°C storage was used to emulate average UK sea temperature; conditions in which the preserved mixtures would ultimately be used in an *in situ* scenario during deployment at sea. Untreated PCR mixes (i.e. containing no pullulan) were prepared simultaneously, and stored at room temperature in the dark for comparative analysis.

The activity of the pullulan-encapsulated qPCR reagents was evaluated over a time course. At weekly intervals, preserved mixtures were activated by rehydrating them with 24.5 µL of RT-PCR grade water and 0.5 µL of an aqueous solution of *E. coli* genomic DNA at a concentration of 18 ng μL^{-1}. The solutions were added to the tube cap containing the air-dried reagents and left to rehydrate for five minutes. A sterile PCR 8-tube strip was added to the caps to seal the reaction vessel, the tubes inverted, followed by centrifugation for 10 seconds at 6900 x g to transfer the rehydrated qPCR reagents to the tube bottoms. Subsequent qPCRs were performed using the conditions described above.

To investigate the film forming properties of pullulan on the individual components of the iQ SYBR Supermix® the individual components were identified from a search of the literature. Each component was individually combined with a 20% w/v pullulan solution. A 25 µL solution of each component at reaction concentrations was combined with pullulan and aliquoted onto the hydrophobic side of a sheet of parafilm M (Bemis, USA) and left to dry overnight at room temperature and pressure. The ability of each component to form a film with the addition of pullulan was determined through visual and mechanical inspection.

4.3 Results and Discussion

4.3.1 Untreated qPCR mixes

The lifespan of untreated qPCR reaction mixtures (i.e. no trehalose or pullulan added) when stored in the dark at room temperature was determined over a time course of five weeks. Two qPCR reaction mixtures, the iQ SYBR Supermix® from BioRad, containing proprietary enhancers and stabilisers (
Table 10), and a standard Taq-polymerase based mix (no stabilisers) could be used to amplify an *E. coli* target DNA sequence after room temperature storage for up to three weeks (Figure 25). The deviation between standard Taq mastermix amplification over the time course was markedly more

pronounced than that of the iQ SYBR Supermix®. At week one the iQ SYBR Supermix® based amplification generated a C_t of 16.21 ±0.08 from duplicate reactions whereas the standard Taq mix had a C_t of 15.85 ±0.09. At week two, the iQ SYBR Supermix® C_t's had decreased to 12.91 ±0.15, indicating an increased rate of amplification. This reduction in C_t is likely due to dehydration – the concentration of reaction components increases as the reaction volumes decrease over time, leading to a concurrent increase in the amplification rate (i.e. reduced C_t). Crucially, other performance indicators of the qPCR were not established, and therefore whilst the improvement in amplification performance is contrary to expectation, it does not necessarily imply that room temperature storage had improved the overall integrity of the qPCR method.

The standard Taq mix was also stable for two weeks at room temperature (C_t of 16.38 ±0), however by the third week both mixes showed signs of degradation, with only single replicates for each mix amplifying (standard Taq C_t = 12.4; iQ SYBR Supermix® C_t = 16.73). As the reagent mixes are kept at room temperature external factors may be influencing the chemistry within the mixes. For example, the ambient external temperature may be causing the aqueous component of the reagent mixes to evaporate, altering the component concentrations and changing the pH of the reagent mixture. pH is an important factor in the stability of enzymes therefore changes to the pH will cause the formation, or breakage, of intra- and intermolecular bonds altering the shape of the enzyme. Any potential pH changes will also cause degradation of the oligonucleotide qPCR primers in the reaction mixture, as decreasing pH will cause DNA to hydrolyse – breaking the phosphodiester bonds between the bases. Alternatively, if the pH of the qPCR reaction mix were to increase, the DNA structure can denature (Ageno *et al.*, 1969).

Potential contaminants that may be introduced during the qPCR reaction mix preparation, for example DNases, may also be degrading the primers within the reaction mixture, disrupting the initiation of DNA replication.

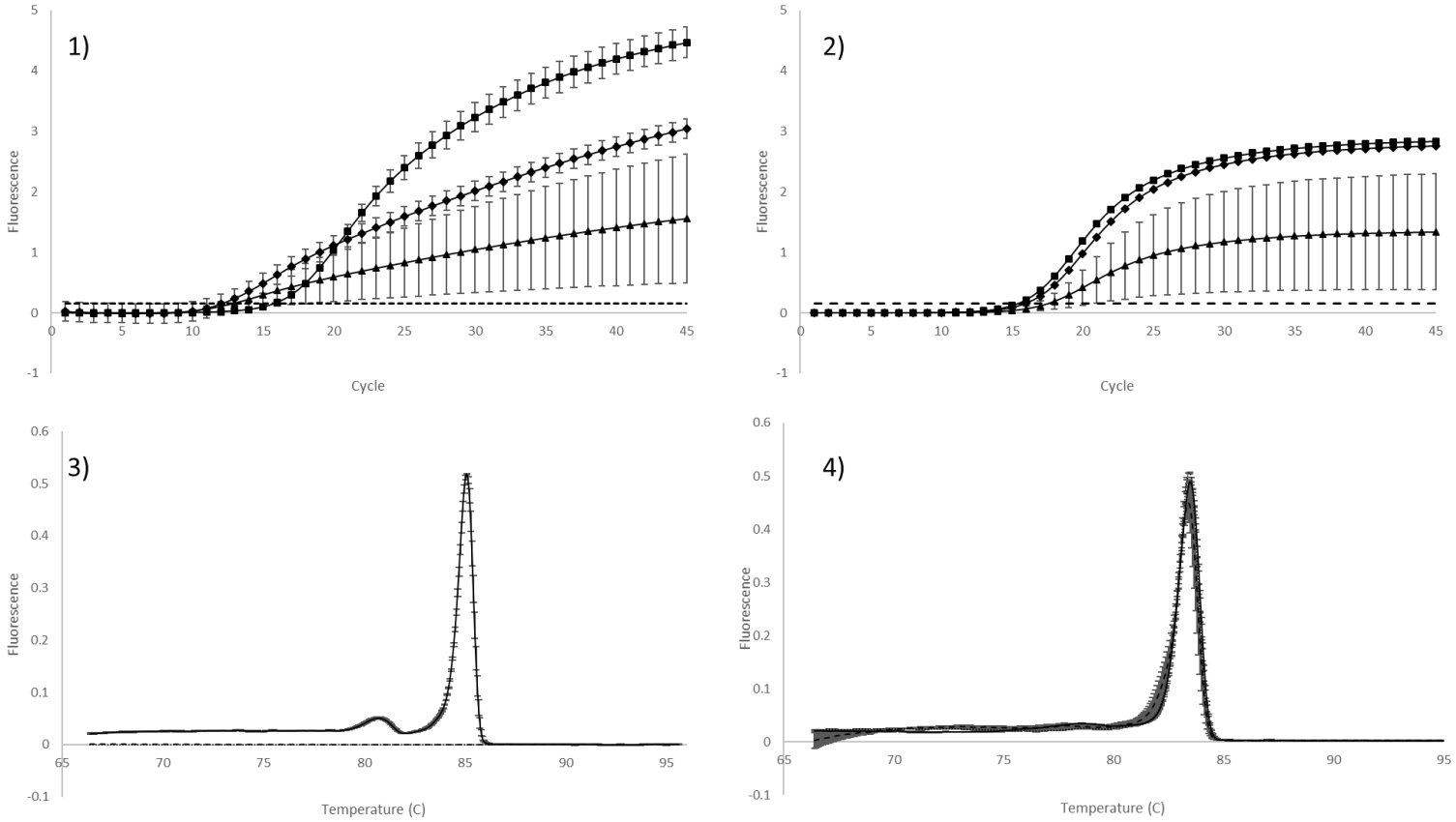

Figure 33 Two different qPCR mixes trialled after storage in the dark for three weeks and their associated melt curve analysis. 1) standard Taq PCR mix; 2) iQ SYBR Supermix®. ■ = week 1, ◆ = week 2, ▲ = week 3. The black dashed line is the threshold. 3) is the melt curve for the standard Taq mix and 4) is the melt curve for the iQ SYBR Supermix®. Solid line = week 1, dotted line = week 2, dashed line = week 3. The shoulder peak in 3) may be due to inefficient dissociation during the melting curve analysis or misalignment of amplicons in AT rich regions. Error bars are standard error (*n* = 2).

4.3.2 qPCR in the Presence of Preservatives

qPCR mixes were prepared with and without the addition of a preservative in order to assess if the addition of either a trehalose/sucrose mixture or pullulan has any effect on qPCR efficiency. Figure 34 shows that the addition of pullulan to the qPCR mixes had no impact on the time to positive amplification. In contrast, the addition of the trehalose/sucrose mix resulted in an increase of the C_t by an average of 3.5 cycles (Figure 34). Assuming 100% efficiency of the qPCR reaction, there is a 3.33 cycle difference between each order of magnitude of copy numbers present in the initial sample. This difference of 3.5 cycles when trehalose/sucrose is added indicates that in the presence of trehalose/sucrose the initial template concentration would be underestimated by an order of magnitude. This may be considered a worthy trade-off if trehalose offers enhanced long-term preservation of samples at room temperature, but pullulan is substantially less inhibitory to qPCR.

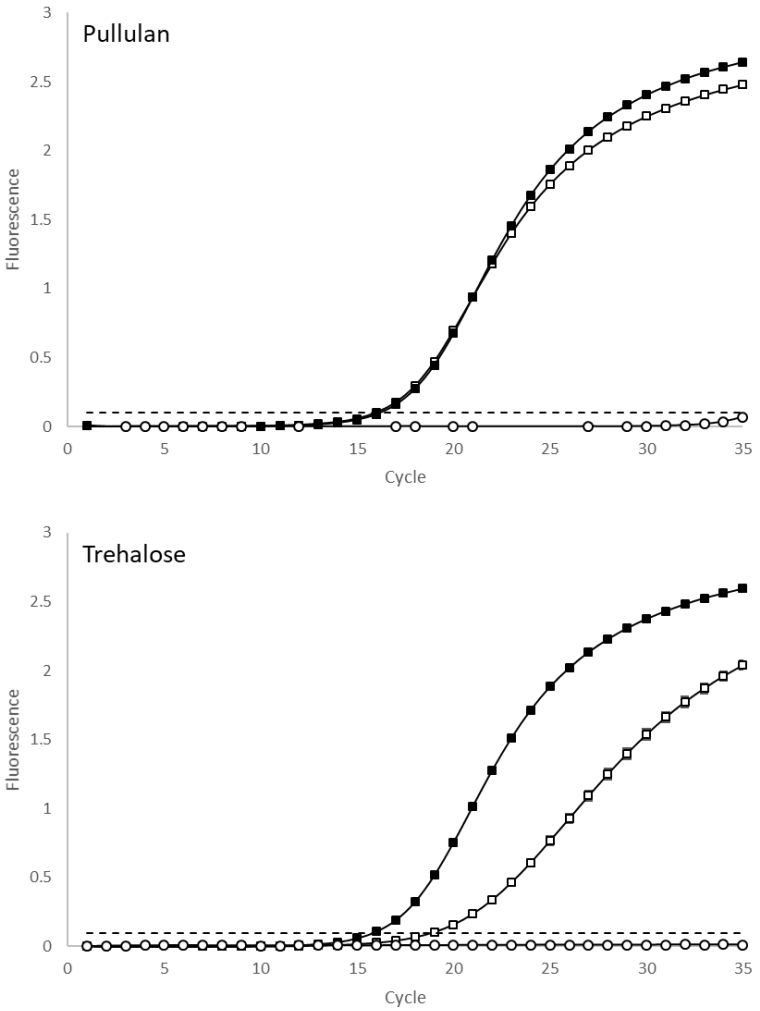

Figure 34 qPCR mixes with and without pullulan and with and without trehalose. (□) are preservative positive reactions, (■) are preservative negative reactions, and (○) are NTC's. The dashed line is the threshold. Where visible, the error bars represent the standard error (*n* = 3).

4.3.3 Lyophilisation

The optimal storage conditions described above were applied to previously developed assays for *E. coli ybbW* and *clpB* based upon a highly selective primer set (Walker *et al.*, 2017) (Table 9) and adapted to work using reverse transcription qPCR (RT-qPCR) for indirect mRNA with hydrolysis probe based real time fluorescent detection. The preserved mixtures could amplify between 10 and 10^5 estimated target sequence copies (Figure 35).

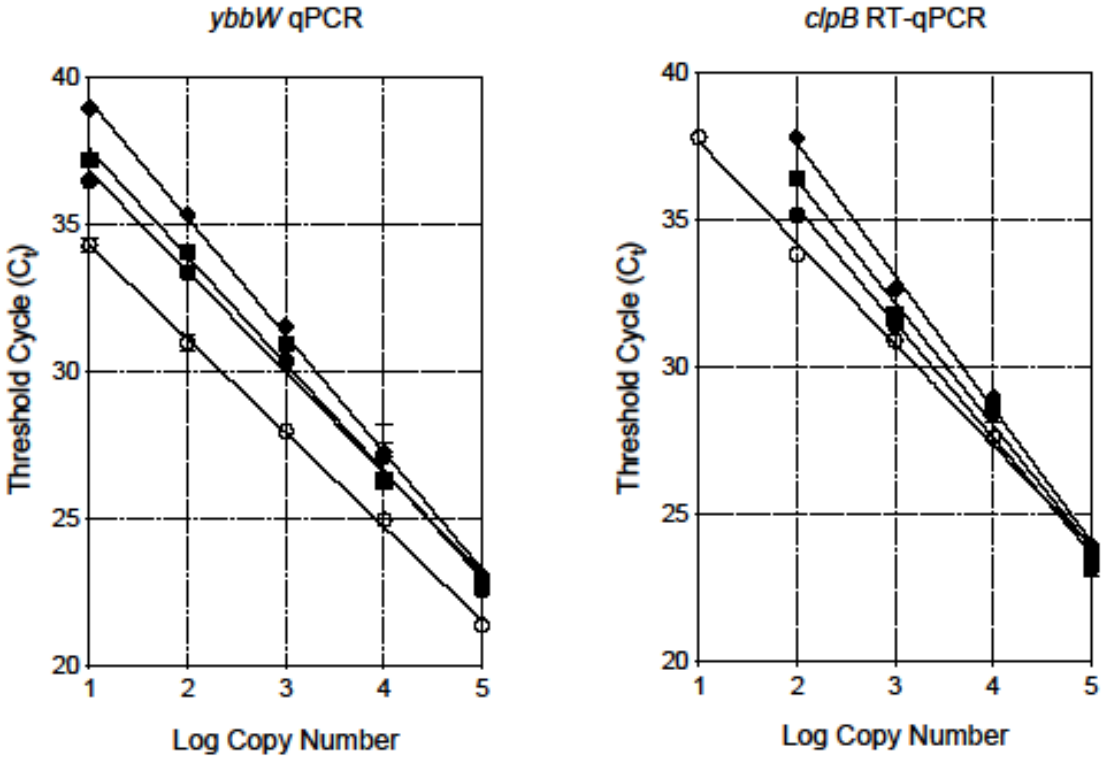

Figure 35 The amplification of the *ybbW* and *clpB* RNA sequences using the oligonucleotides in Table 9 using lyophilised reaction mixes which had been stored for up to 4 weeks without refrigeration. After 1 week (●), 2 weeks (■), or 4 weeks (◆) the mixtures were rehydrated with water containing DNA or RNA template at an estimated concentration of between 10 and 100,000 copies. For comparison the open circles (○) indicate reactions prepared using fresh reagents with no preservation, but containing an equivalent amount of trehalose and sucrose sugars. The results show the mean threshold cycle (C_t) versus template copy number from quadruplicate reactions. The error bars, where visible, show the standard error of the mean (n = 4). No symbol represents a null amplification.

Each of the modified assays consistently detected at least 10 copies of the target sequence, but when diluted further to one copy only a portion of the replicate reactions produced amplification curves and so the limit of quantification (LOQ) was taken to be ≥10 estimated copies per assay. The

relationship between template sequence copy number and C_t was linear over five orders of magnitude, with a linear fit (R^2) of 0.9934 (*clpB* RT-qPCR) and 0.9991 (*ybbW* qPCR). Primer efficiency was found to be 97.2% (*ybbW*) and 91% (*clpB*) when using freshly prepared mixtures. Storage for up to four weeks did not impact the LOQ of the qPCR, however the amplification rate was reduced (C_t increased). Preservation did however increase the LOQ of the RT-qPCR to 100 copies. After four weeks the amplification efficiency of the primer sets was 89% (*ybbW*) and 83% (*clpB*); the linear relationship ($R^2 \geq 0.99$) was unaffected by storage. After six weeks storage there was a significant loss in reagent activity, and only samples containing the highest copy number (10^5 per reaction) could be amplified. Therefore the 'shelf-life' of the preserved reagents is taken as four weeks.

4.3.4 Pullulan

At the lowest concentration of pullulan (10% w/v pullulan – final concentration 15.82 µM) the iQ SYBR Supermix® failed to form tablets as expected and instead formed films, which were able to be completely dissolved within four minutes after the addition of 25 µL of RT-qPCR grade water containing DNA template. Successful qPCRs were performed using these pullulan encapsulated reagents, stored at room temperature for up to six weeks, after which none of the prepared mixtures amplified (Figure 34). This was, therefore, considered to be the 'shelf life' of the pullulan preserved reagents.

There was a slight delay (~2 cycles) in the detectible amplification observed between the pullulan and non-pullulan reagent mixes. This may be due to pullulan being an acid polysaccharide (Leal-Serrano *et al.*, 1980), previously observed to be an inhibitor in qPCR reactions (Demeke and Adams, 1992; Rezadoost *et al.*, 2016).

The pullulan preserved reagents that were stored at 12°C, however, failed to amplify after storage for two weeks. A potential reason for the failure of the reagents stored at 12°C to yield positive amplification may be that the reduced temperature increases the density of the pullulan matrix, resulting in incomplete dissolution of the reagent film with the re-addition of the DNA template containing RT-PCR grade water. Following the success of the 10% pullulan films at preserving the qPCR reagent mixes reagent tablets were attempted by increasing the amount of pullulan used. When 20% pullulan was added to the qPCR master mix it failed to form a tablet - still producing a film. When 20% pullulan solution was added to 25 µL Milli-Q water however, after overnight drying a hard tablet was formed. After identifying qPCR master mix components (

Table 10) and adding 20% pullulan solution to each separately it was found that the Taq DNA polymerase enzyme (which is preserved in a high viscosity solution to prevent freezing) was preventing the pullulan from setting into a solid tablet.

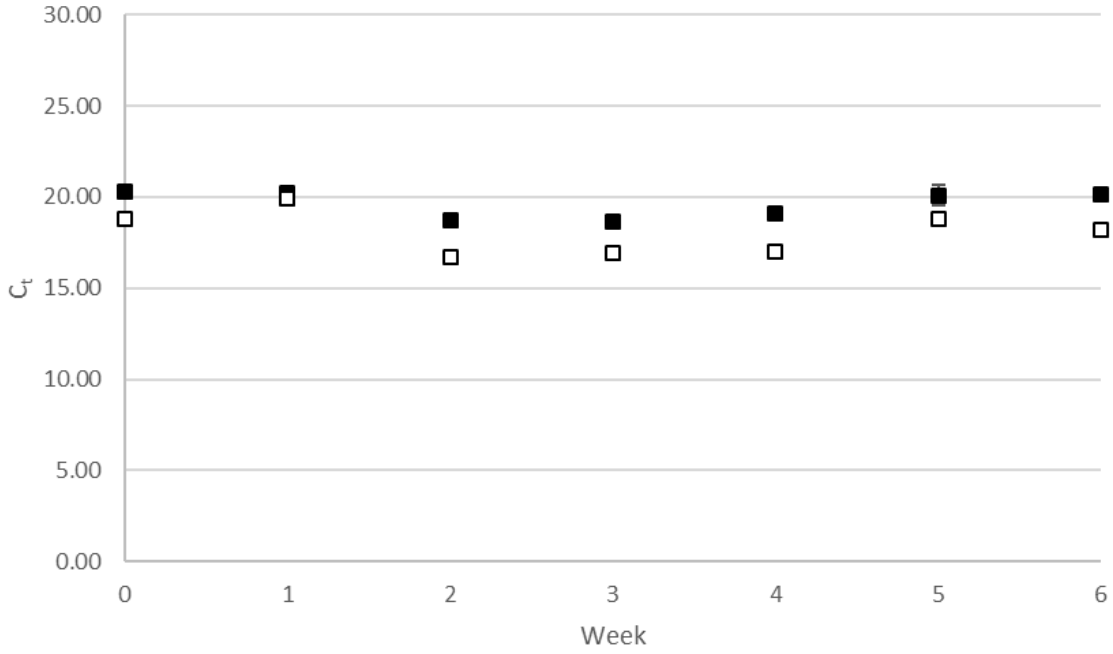

Figure 36 qPCR reactions using reagents set in a pullulan film (■) and freshly assembled reagents (□) over 6 weeks storage at room temperature. The pullulan leads to a slightly later reaction (approximately 2 cycles). Error bars, where visible, are the standard error of the mean (*n* = 3).

Table 10 The components that make up the iQ SYBR Supermix® used in the study and their concentrations. Whether they solidify or not after being left overnight at room temperature is indicated in the right column. When combined with 20% pullulan all of the components solidify into a tablet with the exception of the Hot-start Taq Polymerase. The Set column indicates whether the component solidified after dehydration in the presence of pullulan.

iQ SYBR Mix Component	Concentration	Set (✔/✖)
Hot-start Taq Polymerase	50 U/ml	✖
dNTP's	10 µM	✔
MgCl2	25 µM	✔
SYBR green dye		✔
Enhancers and stabilisers		✔
- Tested BSA, DMSO, Betaine, Formamide, TMAC, Tween		
Fluorescein	20 nM	✔
Primers	10 µM	✔
KCl	100 mM	✔
Tris-HCL pH 8.4	40 mM	✔

Pullulan was also added to NASBA reaction mixes to investigate if it inhibits the NASBA reaction in any way. Figure 37 shows that the addition of pullulan into the NASBA reaction slows the reaction down and reduces the reproducibility of the replicates, suggesting pullulan may be inhibitory to the NASBA reaction. The TTP was increased in the pullulan positive reactions by an average of 13.33 minutes (std deviation = 5.03), suggesting that the enzymes, or the high viscosity solution they are stored in, interfere with the setting action of the pullulan in some way, as was noted with Taq polymerase in the qPCR master mix. As NASBA contains three enzymes (AMV-RT, RNase H, T7 DNA dependant RNA polymerase) as opposed to the single enzyme in qPCR (DNA polymerase), each or any of the three may be being impeded in some way by the presence of the pullulan, leading to reduced efficiency of the NASBA reaction.

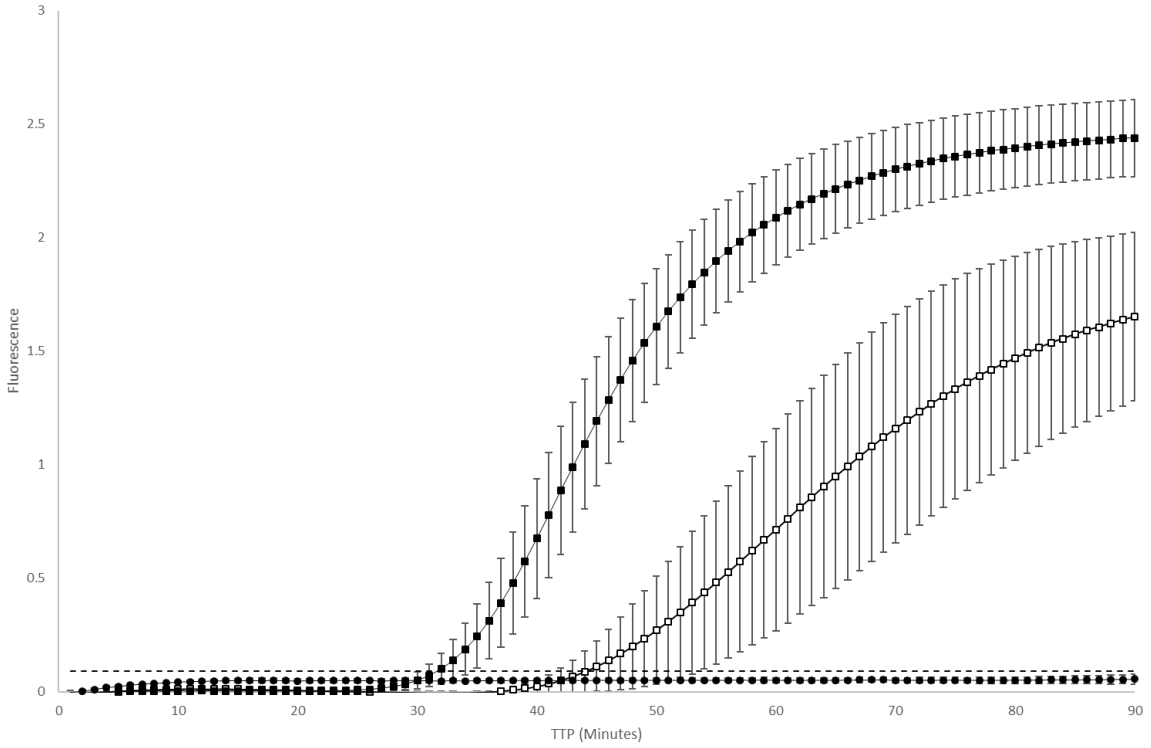

Figure 37 NASBA reactions in the presence (□) and absence (■) of pullulan. The average TTP for the non-pullulan samples is 30.08 minutes whilst the average TTP of the pullulan mixes is 42.46 minutes. Error bars show the standard error (*n* = 3). The introduction to the reaction of pullulan reduces the efficiency (TTP is increased) and also reproducibility (wider error bars) compared to pullulan free reaction mixes.

4.4 Conclusions

Here the stabilities of two PCR reagent mixes (iQ SYBR Supermix® and Standard Taq DNA polymerase mix) were investigated under two methods of preservation to increase the storage time of these reagent mixes (trehalose with lyophilisation, and pullulan encapsulation) when stored at

20°C. Although pullulan appears to have no inhibitory effect on PCR here it was observed that trehalose does. Each method successfully maintained PCR mix activity for several weeks. Trehalose and lyophilisation have been widely used for the preservation of biological substances including stem cells (Buchanan *et al.*, 2010), functional proteins (Garcia *et al.*, 2004), DNA (Ivanova and Kuzmina, 2013), RNA (Jones *et al.*, 2007), mouse sperm (McGinnis *et al.*, 2005), and enzymes (Colaço *et al.*, 1992). This study agrees with previous studies in finding that trehalose is an effective preservative when combined with lyophilisation.

Pullulan, though not as widely used, has also been demonstrated to have excellent biological reagent preservation properties (Jahanshahi-Anbuhi *et al.*, 2014; Singh *et al.*, 2008; Teekamp *et al.*, 2017; Xiao *et al.*, 2014). The results of this study are in alignment with previous studies and demonstrate pullulan has the potential to preserve reagents on-chip, simplifying reaction preparation at the point of sample. The preserved reagents if applied in conjunction with the microfluidic chips described next (Chapter 5) will allow the creation of pre-made cartridges for water quality testing, reducing the requirement for trained technical staff.

Although both sugars effectively preserved reagent mixtures for varying lengths of time trehalose offers several advantages over pullulan for integration with the LOC device described next: chiefly it is cheap and readily available, whereas pullulan is less so.

Chapter 5 A Novel 'Lab-on-a-Chip' and Instrument for Isothermal Nucleic Acid Amplification

5.1 Introduction

The surveillance of harmful microorganisms including, for example, enteric pathogens and toxin producing algae, is fundamental in protecting the biosecurity of the aquaculture, mariculture and water services industries, and for mitigating economic losses associated with contamination. Conventional techniques for microbial detection and identification typically require the cultivation and enumeration of target microorganisms in the laboratory using selective and differential growth medium, or the direct observation of microbial cells by microscopy. These approaches are laborious, with complex multi-step sample processing, and require a highly resourced laboratory with specialist personnel. In addition, many microorganisms are difficult or impossible to cultivate using current methods and apparatus, and microscopy is only useful for broad classification of cell morphologies (shape, size, surface features) and cannot discriminate harmful and non-harmful cells based on morphology alone. An alternative and more rapid approach is to identify species specific DNA or RNA sequences using molecular biological methods, specifically those for nucleic acid sequence amplification and detection. These are culture-independent and not limited by microbial growth rates; thus, results are available within in a few hours. In addition, **molecular methods are also relatively simple to automate, which could increase the throughput and accuracy of laboratory-based testing or enable testing at the point of sample using portable or deployable instrumentation.** Accordingly, nucleic acid amplification (NAA) could complement existing culture or microscopy-based laboratory analysis as an automated, advanced early warning system of microbial hazards.

The gold standard in nucleic acid amplification is the Polymerase Chain Reaction, or PCR. Soon after it's invention, the PCR was adapted for miniaturisation and use at the point of sample (Chandler, 1986) either in the clinical setting at the point of care, or in the environment as so-called "Ecogenomic Sensors" (Scholin, 2010). The latter has enabled several advances in the study of microbial ecology using 'molecular ecology' techniques (McQuillan and Robidart, 2017). Perhaps the most famous example of an Ecogenomic Sensor is the Environmental Sample Processor (ESP) featuring the Microfluidic Block (MFB) (Preston *et al.*, 2011) developed at the Monterey Bay Aquarium Research Institute (MBARI) (Scholin *et al.*, 2009). The ESP, often referred to as a lab-in-a-can is capable of filtering seawater, processing the samples and performing rRNA sandwich hybridisation assays, ELISA for toxin concentrations and qPCR. Since its first use the MFB and ESP has shed light on several microbial oceanic processes including crenarchaeal distribution using the 16s rRNA gene (Preston *et al.*, 2011), methane metabolism (Ussler *et al.*, 2013), nitrogen fixation (Robidart *et al.*, 2014), Dimethylsulfoniopropionate (DMSP) metabolism (Varaljay *et al.*, 2015), *Pseudo-nitzschia* presence and toxin concentration (Bowers *et al.*, 2016), and the influence of

nutrients on a *Pseudo-nitzschia* harmful algal bloom (HAB) in Monterey Bay, California (Ryan *et al.*, 2017). Despite the obvious application of the ESP for environmental analysis there are limitations. For example, the system is prohibitively expensive for widespread use, requires complex deployment logistics and a specialist team of operators, it is large, cumbersome and economically impractical for purposes other than scientific study. Environmental nucleic acid amplification techniques will benefit from the provision of inexpensive, miniaturised alternatives, which can be operated by minimally trained personnel and could be adopted for use by industries requiring solutions to biosecurity.

A NAA system has two principle requirements: (i) a stable temperature control system and (ii) a sensitive detection system. Precise thermal controls allow for a rapid and specific amplification reaction, and sensitive detection of the reaction products enables the detection of small quantities of target and the discrimination of amplification reactions containing different quantities of target sequence; this is necessary for quantification. Stable and interchangeable temperatures can be achieved using Peltier thermoelectric elements (PTEs) (**Error! Reference source not found.**). PTEs h ave been widely used to provide the temperature regulation required for nucleic acid amplification. This is due to the uniform temperature distribution across their surface, active cooling and precise temperature control that can be achieved when used in tandem with a proportional integrated derivative (PID) control algorithm (Ahrberg *et al.*, 2016). Uniform temperature distribution is vital in NAA systems as reactions are typically run in large numbers, distributed over a surface, or plate. Subtle changes in cycle temperature, over many cycles will lead to a big difference in the amount of nucleic acid amplified.

PID controllers offer a single input, single output (SISO) control loop feedback mechanism, and are widely used in industrial control systems. PID controllers use the three terms of proportional, integral, and derivative to influence the controller output. These terms enable the controller to adjust the current applied to the PTE, and modulate the rate of temperature change as the component reaches the 'set-point'. Equation (1) is the overall control function of PID:

$$u(t) = K_p e(t) + K_i \int_0^t e(t')\,dt' + K_d \frac{de(t)}{dt} \quad (1)$$

Where K_p, K_i, and K_d denote the coefficients for the proportional, integral, and derivative terms respectively. In the second, standard form of the equation (2) K_i and K_d are replaced respectively by K_p/T_i and K_pT_d, the advantage of this being that T_i and T_d have a physical meaning, representing the integration time and the derivative time respectively.

$$u(t) = K_p \left(e(t) + \frac{1}{T_i} \int_0^t e(t') + T_d \frac{de(t)}{dt} \right) \quad (2)$$

Alternative controllers are compatible with PTEs, including simple voltage controllers such as 'Boost and Buck' controllers. However, these controllers simply adjust the voltage entering the PTE and do not stop it completely, making accurate temperature control difficult. Electrical current based controllers, including PIDs, work by constantly turning the current on and off to achieve the desired set temperature with minimal under or overshoot during transitions. Whilst this enables precise thermal control, it increases the power requirement. Additionally, frequent and rapid large temperature changes cause the component to expand and contract, which could result in mechanical damage to the PTE over repeated use.

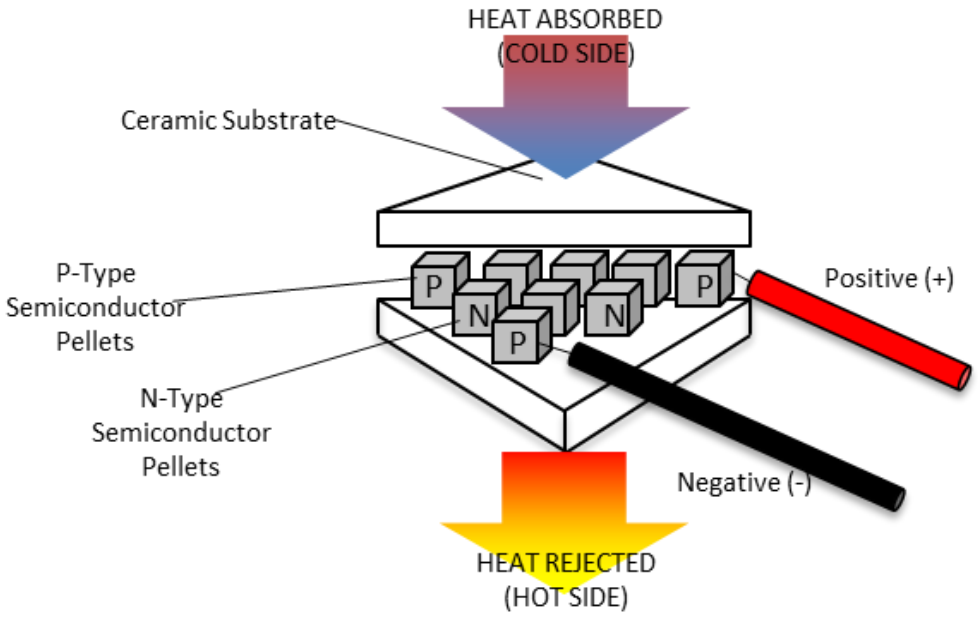

Figure 38 The internal structure of a Peltier element. Heat is transferred from the cold side to the hot side by passing a current through the junction of thermoelectric materials (bismuth and telluride). By reversing the direction of the current the hot and cold sides are reversed allowing the rapid cycling up and down of the temperature on the surface.

Different NAA chemistries have different temperature requirements, with PCR being the most complex in this regard and requiring iterative cycling between two or three different temperatures, ranging from as low as 45°C to as high as 95°C. These temperature fluxes have been noted as a complication in the adaptation of PCR in microfluidic devices (e.g. high power consumption, sample evaporation, high pressure resulting in structural damage to microchannels), and why isothermal techniques operating at lower overall temperatures, such as NASBA and RPA (as described in Chapter 2 and Chapter 3), are more attractive for automation. NASBA and RPA feature simplified thermal regimes, with NASBA requiring a two minute 65°C denaturing step followed by 30 minutes to one hour at 41°C, and RPA requiring a constant single temperature of between 37°C and 45°C.

Detection of nucleic acid amplification in real-time broadly can be achieved via colourimetric (Zhong and Kain, 1999), electrochemical (Drummond *et al.*, 2003; Jha *et al.*, 2012) or fluorometric (Schiavo *et al.*, 2005) methods. Fluorescent based detection is by far the most widely used technique enabling the real-time measurement of sequence replication using a target-specific fluorometric 'probe' (e.g. hydrolysis probes, molecular beacons, scorpion probes, exo probes). In these, a fluorophore and quencher pair are separated during the amplification reaction leading to the liberation of an optical signal. Other commonly used methods include the use of DNA binding dyes (e.g. SYBR, EVA, YOYO, PMA, Hoechst) (Foldesi, 2018), which display differential fluorescence in DNA bound and unbound states. Although these dyes are inexpensive they do not offer the additional layer of specificity provided by the use of a target specific hydrolysis probe, and have often been said to lead to the detection of the 'haystack' rather than the 'needle'.

An additional requirement, necessary when using dry preserved NAA reagents such as those discussed in Chapter 4, is the incorporation of a reaction mixing process to ensure rehydrated reagents are homogenously dispersed within the reaction vessel. In the lab mixing would be achieved manually, often using bulky equipment, however in automated systems consideration must be given as to how mixing can be achieved using simple, uncomplicated parts and procedures. Passive mixing via diffusion is inefficient at the small volumes used in microfluidic systems due to the viscosity of the mixtures, especially after the addition of stabilising sugars, leading to very slow diffusion rates. Although passive mixing using features such as 'wishbone' mixers, embedded barriers, and zigzag channels is possible they increase the technical complexity in chip design and manufacture, which ideally, in this application, was to be kept to a minimum. Alternatively, active mixing can be achieved in microfluidic systems using mechanical means such as acoustic/ultrasonic, dielectrophoretic, or electrokinetic time-pulsed mixing have been demonstrated, that typically require additional components but are effective (Lee *et al.*, 2011).

In this chapter, the key requirements for nucleic acid amplification, as outlined above, were considered for the development of a prototype miniaturised nucleic acid amplification instrument to feature PTE based temperature control, fluorescence based real-time detection and, in addition, a novel, single step "finger press" actuation of a mixing process for the rehydration of reagents that have been dry preserved on the microfluidic reaction chips.

The key objectives were:

- To develop a disposable microfluidic chip to contain dry preserved stabilised reagents for real-time nucleic acid amplification.
- To develop a simple, low-cost real-time detection system based upon dual wavelength fluorescence.

- To develop a temperature control system using PTE components for accurate, stable and adjustable thermal regulation controlled using PID.
- To develop a simple mixing mechanism enabling the rehydration of preserved reagents using an aqueous sample containing target nucleic acids.
- To evaluate the instrumentation using the RPA assays developed in Chapter 3.

5.2 Methods

5.2.1 Chip Fabrication

Chips were designed using standard microfluidic fabrication techniques, specifically replica moulding using an elastomeric material, in this case polydimethylsiloxane (PDMS). The chip was designed using CAD, using the Inventor 2015 software package (Autodesk, CA, USA). A mould was fabricated using a DATRON NEO micro milling machine. A 'negative' was cast from the mould using PDMS (Farnell, UK). This was prepared from a two-part kit containing a pre-polymer base and a cross-linker curing agent, which were mixed in a 10:1 ratio and de-gassed by negative pressure (25 mBar) using a custom-made vacuum chamber and an Edwards 6iC oil-free vacuum pump (Wolf Labs, UK). The PDMS was poured over the mould, de-gassed a second time, and placed in an oven at 130°C for 90 minutes until cured. This PDMS 'negative' was removed from the mould by hand, and exposed to a mixture of 70% (v/v) ethanol in Milli-Q and 0.1 g mL^{-1} non-ionic detergent (Teepol Multipurpose Detergent, Kent, UK) to act as a release agent in subsequent steps, as described by Arundell *et al.* (2011).

The PDMS negative was used to manufacture individual microfluidic chip prototypes. To do this, 20 g of de-gassed PDMS solution was added to the negative mould and de-gassed a second time before transferring the assembly to a hot-plate at 130°C for 90 minutes until the PDMS had cured. The cured chips were carefully peeled from the negative mould and any excess material was trimmed using a scalpel. Guiding holes to aid in the alignment of the chip reaction chamber to the optical detection system were punched using a 16-gauge laboratory dispensing syringe.

5.2.2 Chip Assembly

The moulded PDMS chips contained microfluidic features, which were prone to distortion in the flexible PDMS material. To alleviate this issue the PDMS chips were bonded to a rigid borosilicate glass substrate, which also served as a thermally conductive base for efficient transfer of heat from the PTE heating assembly to the reaction compartments of the chip. The use of a glass substrate was chosen as it is optically clear, facilitating the use of fluorescence-based real-time detection of

the NAA reactions occurring within the chip compartments. Two methods for bonding the PDMS chip component to the glass substrate were trialled: (i) by use of a spin coater and an additional PDMS layer, and (ii) using an Excimer UV laser to produce O_3 that reacts with the functional groups on the surface of the PDMS and glass facilitating the formation of covalent bonds.

5.2.2.1 Spin Coater Chip Assembly

A spin coater (EMS Photo Resist Spinner Model 4000) was used via the following protocol: glass microscope slides were added to the spin coater and washed with 100% isopropanol followed by 100% acetone (Sigma-Aldrich, UK). A new mixture of de-gassed PDMS was prepared as described previously and left at room temperature for one hour to initiate the curing process. The de-gassed, partially set PDMS was added to the centre of the microscope slide and spun at 200 x g for 30 seconds. The glass-liquid PDMS constructs were transferred to a hot-plate over varying temperatures and time regimes (Table 11) to further initiate the PDMS setting process, before being removed from the hot-plate and left to cool for two minutes at room temperature. After this cooling period, the aforementioned moulded PDMS (Section 5.2.1) reaction chambers were placed on top of the spin coated glass-liquid PDMS complex and returned to the hotplate with pressure applied until fully set.

5.2.2.2 Excimer UV Laser Chip Assembly

The second bonding method trialled involved the use of a Flat Excimer EX-mini (L12530-01; Hamamatsu, JP) vacuum UV laser. The EX-mini emits radiation in the short wavelength vacuum UV range (172 nm) which reacts with the oxygen within the air in the chamber producing ozone (O_3) and active oxygen whilst simultaneously breaking up the bonds in the surface of the PDMS and glass (Figure 42). This imparts hydrophilicity allowing the two surfaces to form covalent bonds. To initiate bonding pre-moulded PDMS reaction chamber containing chip and a glass slide were placed within the Flat Excimer EX-mini and positioned so that the vacuum UV laser was approximately 5 mm away from the surfaces to be bonded together. The pre-moulded PDMS and glass microscope slide were irradiated for 30 seconds and the two pieces placed on top of each other and placed in an oven at 40°C for one hour with uniform pressure applied using an aluminium block.

5.2.3 Chip Sterilisation

After bonding all chips were treated with hydrogen peroxide vapour (HPV). This treatment both sterilises the chips by killing microorganisms, and decontaminates the chips by denaturing organic compounds including nucleic acids. The technique was demonstrated by (Magiopoulos *et al.*, 2016) and is a highly effective surface sterilant and decontaminant. Vapour was produced from a 30%

solution of hydrogen peroxide using a Clarus L2 HPV generator (BioQuell, UK). Constructed chips were placed inside a negative pressure isolator cabinet (ESCO, UK) featuring dedicated ports for HPV based cleaning. The cabinet was filled with HPV at an injection rate of 2.0 g min^{-1} for 5 minutes resulting in a maximum HPV concentration of 374 ppm within the chamber. The HPV was allowed to dwell in the chamber for 30 minutes before the whole system was evacuated and aerated. Chips were then stored in sealed containers with desiccant until further use. HPV-cleaned chips were treated with ultraviolet radiation for 30 minutes using a CL-1000 ultraviolet crosslinker (UVP, USA), immediately prior to use in experiments.

5.2.4 On-Chip Reagent Mixing

PCR reagents were assembled containing a trehalose/sucrose preservation mixture as described in Chapter 4 with the addition of a blue gel loading dye (NEB, USA) to make the mixtures visible. Into the chip reaction chambers were added 10 µL reagent mixtures before lyophilisation using the process described in section 4.2.3. After lyophilisation, 10 µL of milli-Q was introduced to the reagent chamber containing the dry-stored reagents and the empty 'mixing' chamber pumped by finger actuation. The efficacy of this mixing method was assessed via visual inspection of the dyed reagent mixes.

5.2.5 Thermal regulation

PTEs were powered using an EL302RT DAC powerpack (Aim TTI, UK) and controlled via a custom built PID control box based on a commercially available PID controller board (TEC-1090-HV, Meerstetter Engineering, Switzerland). The PID controller was programmed via a USB connection to a laptop running PTE Service software (Version 3.0 Meerstetter Engineering, Switzerland). Voltage and current limits were set based on the PTE datasheet: 15 V and 2.2 A respectively, set to avoid thermally damaging the component during operation. The temperature was set to 41°C and when stability was achieved the PID autotuning function was used to tune the PID control of the specific PTE type used in the system (RS Components ET-190-1010-1212-RS). This uses the equations given in section 5.1 to determine the optimum K_p, T_i and T_d values for the fastest temperature ramping available. Post tuning the optimal K_p was 20.99, optimal T_i was 2.68, and optimal T_d was 0.64. This was done once and the same parameters were entered into the software manually for further uses. After tuning, thermal profiles were tested for PCR (95°C for 10 seconds, 65°C for 10 seconds and 72°C for 30 seconds), NASBA (65°C for two minutes, 41°C for 30 minutes), and RPA (37°C for 30 minutes) to determine whether the hardware had the capability to perform these NAA techniques.

5.2.6 Fluorescence Detection

A rudimentary fluorescence measurement system was generated for the purposes of testing the novel lab-on-a-chip design (Figure 39). Real-time PCR amplification using a fluorometric dye (SYBR Green) was used as the NAA chemistry for testing the system.

To understand the change in fluorescence signal observed during qPCR amplification, qPCR reagent mixtures were prepared as follows. First, 50 µL qPCR master mixes (iQ™ SYBR Supermix®, Bio-Rad) were prepared as per the manufacturer's instruction using primers 401F and 611R as shown in Table 9 (Chapter 4). The primers were specific for the *E. coli ybbW* gene, and *E. coli* genomic DNA was used as a template. This was because this particular assay was well characterised (McQuillan and Wilson, 2019; Walker *et al.*, 2017) and therefore a suitable 'test' for the system. Half of the prepared samples were subjected to qPCR via the following conditions: 45 cycles of 95°C for 15 seconds, 68°C for 20 seconds, and 72°C for 45 seconds. The other half of the prepared reactions were kept refrigerated and not subjected to PCR. After thermocycling (or refrigeration) reactions were diluted in 1.5 mL of Milli-Q and mixed before being transferred to a 1 mL cuvette. The final fluorescence of the mixes was measured using a Fluorolog FL3-222 fluorometer (Horiba, JP). The observed difference in fluorescent signal between the thermo-cycled and refrigerated samples was used as a benchmark for the requirements of the miniaturised genetic sensor optical detection hardware.

Fluorescent signal was measured during real-time RPA reactions within the microfluidic chips. To do this a 495 nm LED featuring a custom waveguide was used for fluorophore excitation. The emission was measured at 520 nm using a 'Powermeter' silicone photodiode (Newport 1919-R, Oxford, UK). The excitation LED was activated only every 30 seconds for approximately two seconds to avoid photobleaching. The optical detection set-up for RPA reaction testing can be seen in Figure 39.

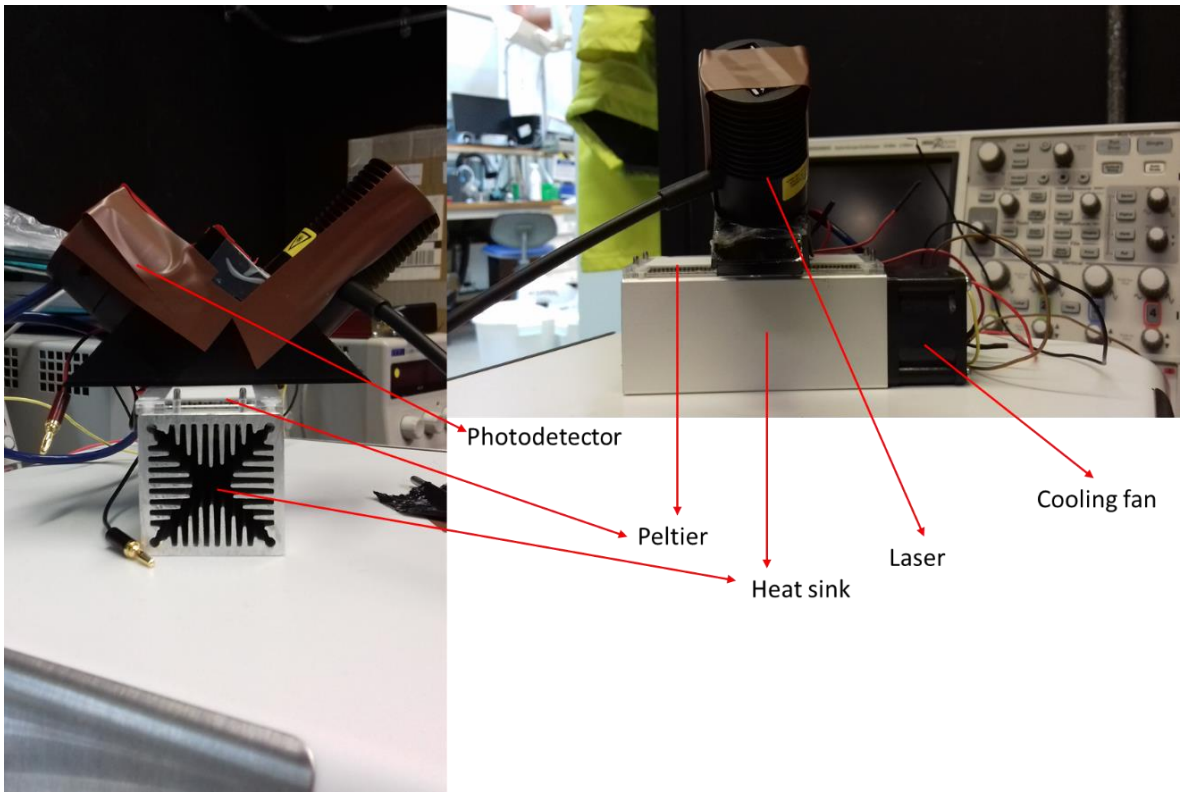

Figure 39 The set-up used to test the real-time on-chip RPA using fluorescent detection. The laser excited the fluorophore (FAM) at 495 nm wavelength whilst the 'Powermeter' measured the emission wavelength at 520 nm. The Peltier PTEs were used to hold the temperature stable at 37°C.

5.2.7 On-chip RPA

To test if NAA could be performed using the microfluidic chips the RPA assay as described in Chapter 3, was chosen due to issues encountered when attempting on-chip PCR in the laboratory. RPA reactions minus DNA template and co-factor MgOAc were assembled to 25 µL final volumes following the manufacturers recommended protocol, and stored on ice until the miniaturised NAA device had reached the required temperature and the optical system had been initialised. MgOAc (to a final reaction concentration of 14 mM) was injected into the chip reaction chamber followed by the addition of the DNA template, initiating the reaction. The pre-prepared RPA master mix was added immediately and the chips containing the RPA mixes were placed on to the PTE element, and held at a stable 39°C. The optics module was visually aligned above the chip reaction chamber and readings were taken manually every 30 seconds.

5.3 Results and Discussion

5.3.1 Chip design and manufacture

Mixing in NAA reaction mixtures is essential in order to ensure that the reaction components are homogeneously distributed within the reaction vessel. Failure to mix the reaction can lead to localised 'hot spots' of amplification followed by depletion of critical components; the reaction operates inefficiently as a result. In a laboratory setting, mixing would be achieved via the use of equipment such as a vortexer, or micropipette. These, however, are not readily available in the field and therefore the prototype was designed to emulate these mixing processes, removing the requirement for additional equipment. Mixing is essential for the NAA reagents due to their high viscosity: passive mixing by diffusion happens at an incredibly slow rate. Enhanced mixing can be achieved by both active and passive means. Active mixing requires additional components for mechanical, acoustic/ultrasonic, dielectrophoretic, or electrokinetic time-pulsed mixing (Lee *et al.*, 2011). Although these methods are effective, the additional components add to the cost and complexity of the device. Alternatively, passive mixing in microfluidic systems can be achieved via the incorporation of structural features such as 'wishbone' mixers, embedded barriers, and zigzag channels (Lee *et al.*, 2011). These features produce an additional degree of complexity and were deemed unnecessary for the application presented here, in keeping with the objective of producing a simple and robust, low-cost piece of hardware.

In the prototype chip presented in this chapter, an active mixing process was designed and tested based upon a 'finger press' to actuate fluid movement between adjacent chambers, thus creating the turbulent flow characteristics necessary to form a homogeneous mixture of NAA reaction mixtures. The incorporation of an air chamber into the microfluidic chips allowed finger actuated mixing of the aqueous target NA solution with integrated, dry stored reagents as described in Chapter 4. Successful mixing was observed by the addition of preserved reagents containing a blue dye and subsequent addition of an aqueous solution followed by finger actuated mixing, which produced a homogenous colour throughout the reaction chamber when inspected visually. This was taken as validation of this mixing method for this application.

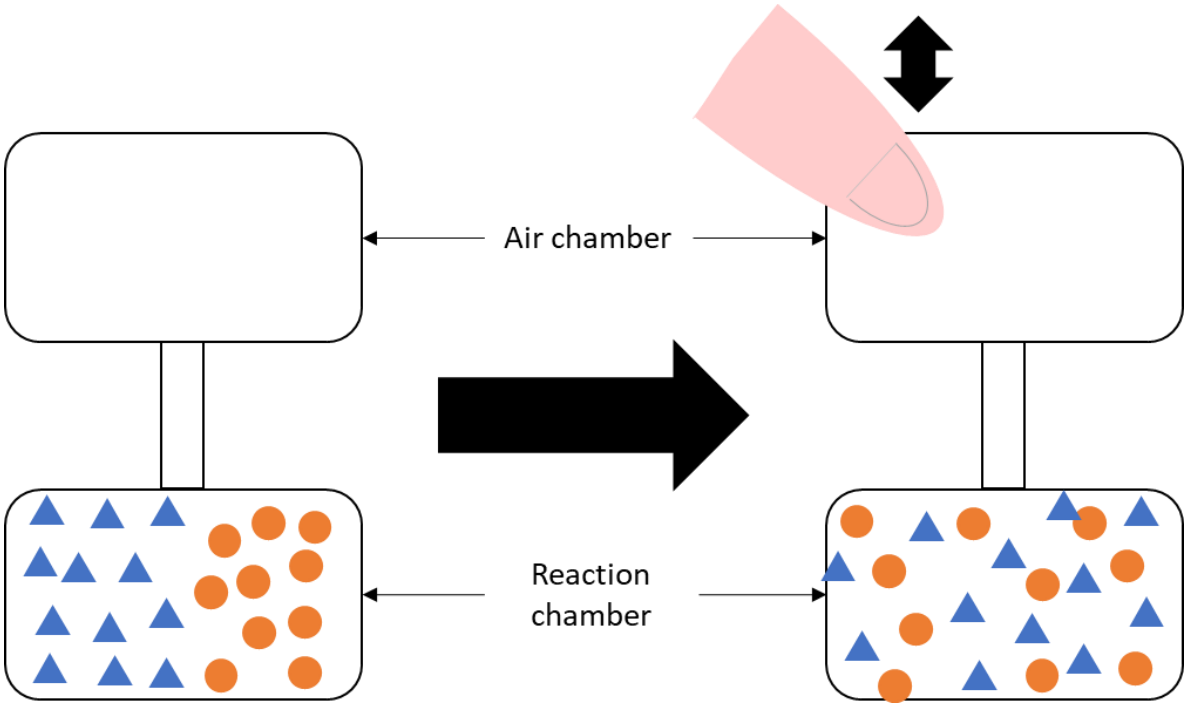

Figure 40 A schematic representation of mechanical mixing of the NAA reagents via finger actuation.

5.3.1.1 Spin Coater Chip Assembly

For the manufacture of the microfluidic chips via the spin coater method, a range of temperatures and times were used for binding the PDMS and glass components, the findings of which can be seen in Table 11. Temperatures of both 80°C and 90°C were used to bind the PDMS moulded chip half to the glass microscope slides. The length of time that the chips were held at these temperatures was varied from 60 seconds to 140 seconds and the setting time after joining ranged from 120 seconds to overnight. The optimal bonding parameters were found to be an initial temperature of 90°C for 60 seconds after addition of an even layer of unset PDMS and spin-coating, followed by 120 seconds at room temperature before the PDMS and glass components were wedded and placed back on the heat block at 90°C for between 120 and 140 seconds. This assembly protocol was able to produce chips with clear micro-channels to allow the movement of amplification reagents and samples between the reaction chambers. The final chips from the spin-coater manufacturing batches can be seen in Figure 41.

Table 11 The range of temperatures and holding times used to manufacture the completed chips for the genetic sensor (O/N = overnight).

No	Label	Temperature (°C)	Time on heat plate (secs)	Set temperature (°C)	Set time (secs)	PDMS/Glass bound	Chanels clear	
				Batch 1				
1	A1	80	60	80	120	Yes	No	
2	A2	80	60	RT	O/N	Yes	No	
3	A3	80	80	80	120	Yes	No	
4	A4	80	80	RT	O/N	Yes	No	
5	A5	80	100	80	120	Yes	No	
6	A6	80	100	RT	O/N	Yes	No	
7	A7	80	120	80	120	Yes	No	
8	A8	80	120	RT	O/N	Yes	No	
9	A9	80	140	80	120	Yes	No	
10	A10	80	140	RT	O/N	Yes	No	
				Batch 2				
11	B1	90	60	90	300	Yes	No	
12	B2	90	60	90	300	Yes	No	
13	B3	90	70	90	300	Yes	No	
14	B4	90	70	90	300	Yes	No	
15	B5	90	80	90	300	Yes	No	
16	B6	90	80	90	300	Yes	No	
17	B7	90	120	90	300	Yes	No	
18	B8	90	120	90	300	Yes	No	
				Batch 3				
19	C1	90	60	90	120	Yes	Yes	Batch 3 was also left to cool to room temperature for 120 seconds before the PDMS was layed on top and returned to the heatplate
20	C2	90	60	90	130	Yes	Yes	
21	C3	90	60	90	140	Yes	Yes	
22	C4	90	60	90	150	Yes	No	
23	C5	90	60	90	160	Yes	No	

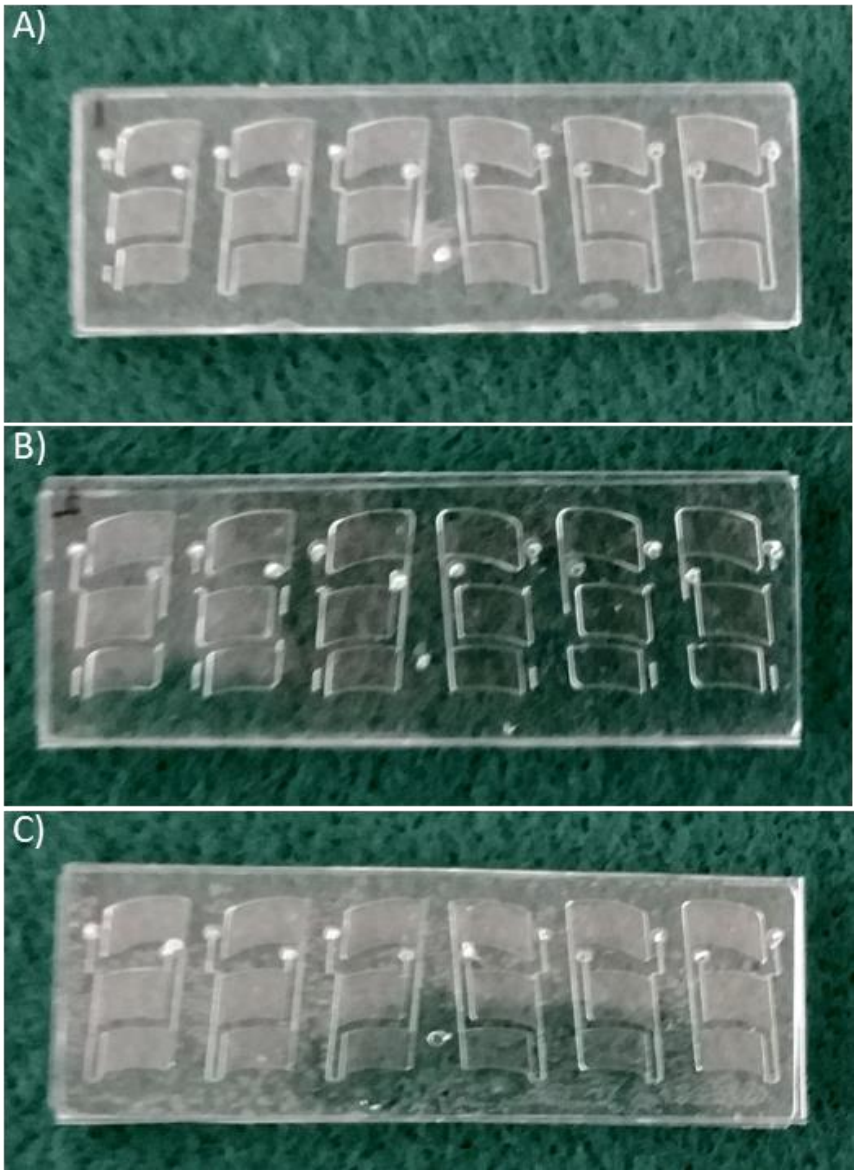

Figure 41 Chips produced using the three different spin coater bonding regimes described in Table 11 (batches A, B and C). After visual inspection both chip batches A and B have blocked micro-channels whilst chip batch C has clear channels.

5.3.1.2 Excimer UV Laser Chip Assembly

Alternatively, the use of a Flat Excimer EX-mini (L12530-01; Hamamatsu, JP) produced stronger bonding than the spin coater method with all channels clear. When mechanical force was applied the PDMS tore before it came away from the glass substrate. Bonding via this method had the additional benefit of being much quicker to produce assembled chips, taking approximately one hour to bind the PDMS microchannel containing chip half to the glass slide rather than the approximate four hours for the spin coating technique. This is due to the ozone generated by the vacuum UV laser activating the methyl group of PDMS and the oxygen molecule on the surface of the molecular structure of the glass forming 'activated' hydroxyl groups. These groups, when

subsequently exposed to heat and pressure form covalent bonds around a shared oxygen molecule (Figure 42), resulting in the structural integrity of the PDMS failing before the PDMS-glass covalent bonds does.

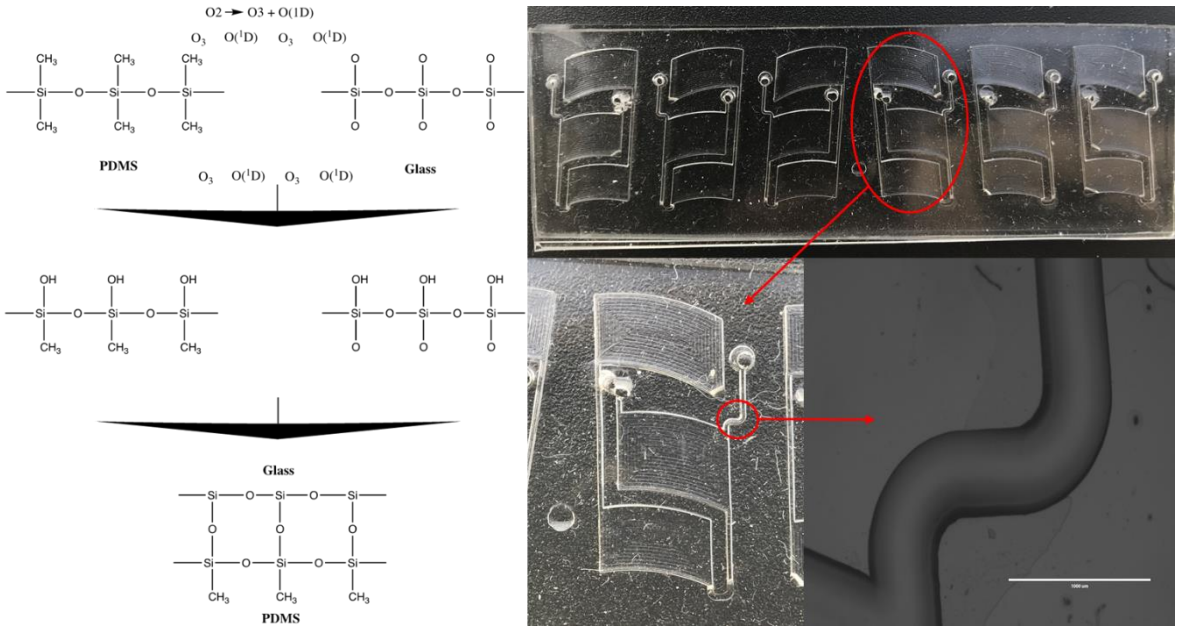

Figure 42 The chemistry that was used to promote the formation of covalent bonds between PDMS and the glass surfaces (left) and images of the chips manufactured using this process (right). The close-up images were taken using bright-field microscopy and show the microfluidic channels to be clear of debris. The scale in the bottom right image is 1 mm.

5.3.2 Thermal Regulation

Using PID regulated PTEs, temperature 'ramping' after calibration was achieved at a rate of 0.2°C sec^{-1}, for both heating and cooling. This is a much lower ramping rate than benchtop laboratory equipment which typically ramp at rates of 4.4°C per second heating and 2.2°C per second cooling (LightCycler 96, Roche, Switzerland), taking 88.7 seconds to reach the NASBA denaturation temperature of 65°C. Nonetheless, this was sufficient for the purposes of testing the overall system design. The reduction of the temperature from 65 to 41°C took 56.8 seconds (Figure 43). Although the slow decrease in temperature may not have an adverse effect on the NASBA reaction, as it will only prolong the reaction, an issue arose whereby the reaction volume (10 µL) evaporated from the reaction chamber when held at 65°C due to PDMS being gas permeable (Lamberti *et al.*, 2014). This issue together with the slow ramping rates meant that PCR or NASBA was not possible using the microfluidic chips on the handheld device. PID control was selected as the control system for this study because it works within a feedback loop system, where the current is constantly adjusted to maintain the programmed temperature in response to changes in the PTE surface temperature,

which was measured by a K-type thermocouple. Additionally, PID control systems are well established and widely available, keeping the cost and complexity of the system to a minimum. This system used proven technology to ensure that the novel aspects of the work (i.e. the microfluidic LOC design) could be developed and evaluated efficiently.

The slow ramping rate is not an issue with the use of amplification techniques that require a single temperature, such as RPA, HDA, RCA and LAMP, as the required temperature can be set and reached before the reaction components are added, and in this regard PID controlled PTCs were successful for this application. There is potential for the PTEs to be re-tuned to provide faster ramping rates however the thermal mass involved of the PTE, including the housing and heatsink, and reaction containing microfluidic LOC will result in a trade off in temperature stability. As the observed stability of ±0.01°C is far lower than the reported stability of the laboratory benchtop equipment (±0.2°C, Roche Lightcycler 96) there is room available to re-tune to speed up the temperature ramping.

PTEs were chosen for this application because of their ability to ramp between different temperatures as well as their stability and uniform heat distribution. However, in this utilisation the temperature ramping was unable to be achieved at a rate comparable to benchtop apparatus. This may potentially be a power issue, as PTEs 'move' heat from one side to the other, and increasing the power could increase the speed at which the heat is transferred. This leads to an additional drawback associated with the use of PTEs: the requirement for a large heatsink to remove heat transferred to the 'hot' side, and an additional cooling fan to aid in heat removal during cooling. Here a LAM 4 100 5 V (Fischer Elektronik, DE) heatsink with an incorporated 5 V cooling fan was used to remove the heat during the cooling phase. It was also noted that PTEs have a relatively high-power requirement, with each ramping step when performing at maximum capacity having a power requirement of 33 W (a 40 cycle, three step PCR would have a power requirement of approximately 2.6 kW) requiring six 9-volt batteries for each application.

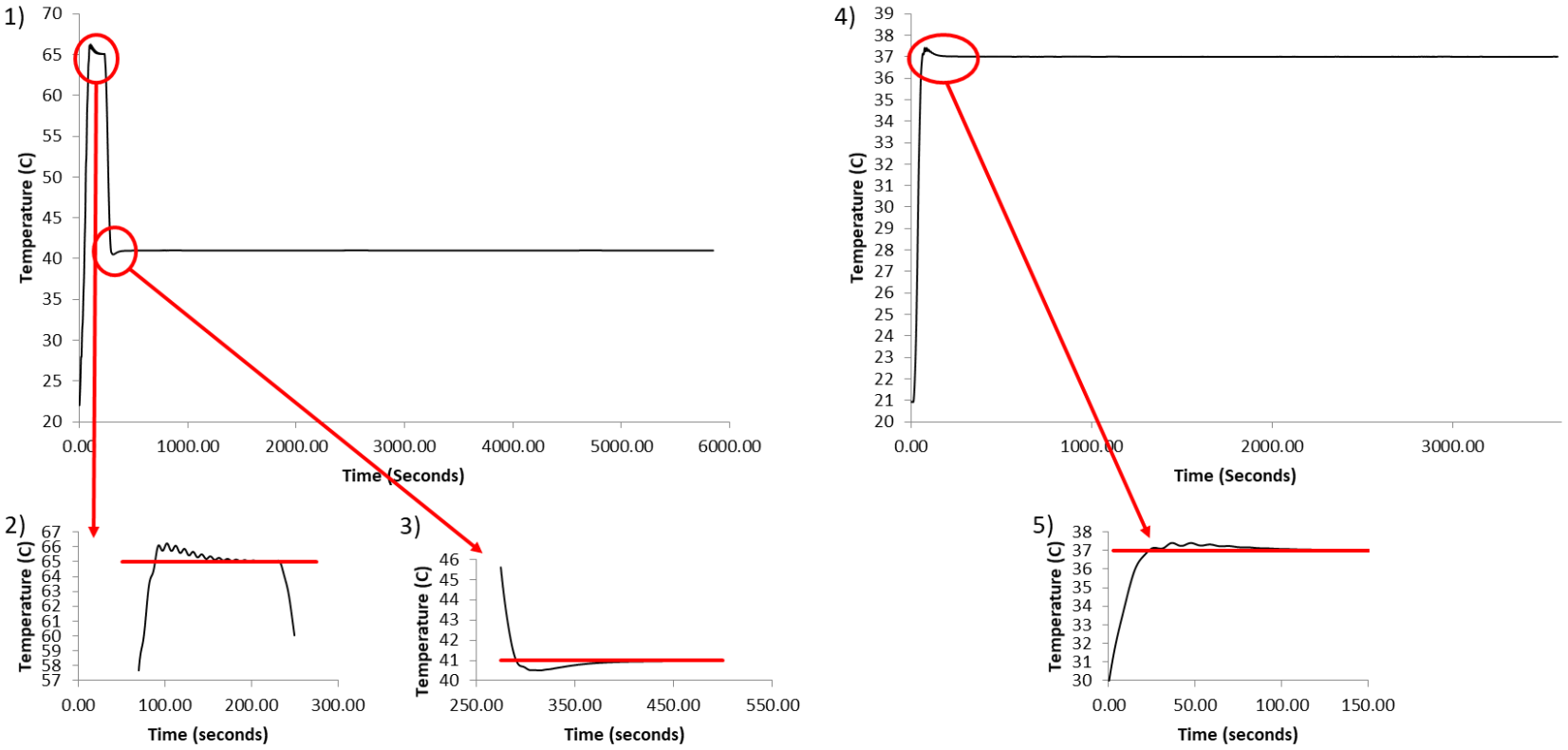

Figure 43 The temperature profiles for the Peltier units after PID tuning for 1) NASBA; 2) is a close up of the NASBA 65°C step and 3) is a close up of the NASBA 41°C step. Both 2) and 3) highlight a temperature overshoot and subsequent correction that occurs showing how the PID control works to stabilise the temperature. 4) shows the RPA temperature profile after PID tuning and 5) shows a closeup of the highlighted region. The programmed temperature is indicated by the red line. When the programmed temperature was reached it was held stable (±0.01°C).

Although the PTEs worked as required in this application there are alternative heating and cooling technologies that may alleviate some of the previously described limitations associated with PTEs that could be considered. For example, recent studies have utilised infrared radiation (IR) to rapidly heat and cool PCR reactions on a microfluidic scale. IR is selectively absorbed by the aqueous reaction solution, whilst the reaction housing is not heated to the same extent. Using this method ramping speeds of up to 10°C sec^{-1} for heating and 20°C sec^{-1} for cooling have been observed (Yu *et al.*, 2012). IR heating has been developed further via the addition of the photothermal effects associated with metal nanostructures, for example gold nanoparticles (AuNPs) or thin Au film. When combined with IR LEDs AuNPs act as a plasmonic heat converter, absorbing photonic energy and converting it to heat, increasing the temperature of the surrounding fluid. Using this plasmonic thermocycling ramping rates have been observed of up to 16.6°C sec^{-1} and 9.4°C sec^{-1} for heating and cooling respectively (Webb and Bardhan, 2014). Although these IR based methods show great potential for use for thermal regulation there are drawbacks associated that may limit their use in miniaturised point of sample devices, chiefly the additional, generally bulky, optical components required to focus the IR energy onto the reaction fluid. Additionally, focusing the IR beam on to the reaction volume reliably requires a tight range of tolerance in the mechanical design, adding an additional layer of complexity (Lee *et al.*, 2019).

Another potential ultrafast heating method is the use of microwave assisted dielectric heating, the benefit of which is that microwaves in the region of 300 MHz to 300 GHz can be delivered directly to the aqueous solution with little or no absorption from the substrate materials (Lee *et al.*, 2019). Shaw *et al.* (2010) utilised microwave heating to achieve heating ramp rates of 65°C sec^{-1} with an average power consumption of 500 mW, equating to approximately 10 hours of use using a standard 9-volt battery. Microwave heaters display similar disadvantages to IR and plasmonic heating, however, as they are dependent on a complex hardware system, posing challenges to miniaturisation. These difficulties associated with the technological requirements of both IR and microwave heating are counter to the initial goal of the handheld genetic sensor – that it is crude, and therefore robust and cheap, allowing for the potential of mass production and widespread use.

5.3.3 Real-time detection system

PCR reactions were prepared using *ybbW* primers 401F and 611R and SYBR green as a reporter dye. SYBR green was selected as it has excitation and emission wavelengths similar to those of FAM (FAM excitation = 495 nm, emission = 516 nm; SYBR excitation = 497 nm, emission = 520 nm), the fluorophore label most commonly used throughout this study and also being more affordable than a specific oligonucleotide-based probe. SYBR green functions by binding to the minor groove of dsDNA and extending its arm-like propyl groups along the groove (Dragan *et al.*, 2012). As SYBR

binds to any DNA present in the sample, the samples that have been through PCR will contain more dsDNA than those that haven't and so produce a higher signal at 520 nm than for the samples that had not been through PCR cycles (Figure 44). This was found to be the case, as when analysed via fluorometry (Fluorolog FL3-222 fluorometer, Horiba, JP) the thermal cycled PCR mixes had a 0.6 A higher fluorescence than those left at room temperature. This was used as a specification in the design of the genetic sensor optical module.

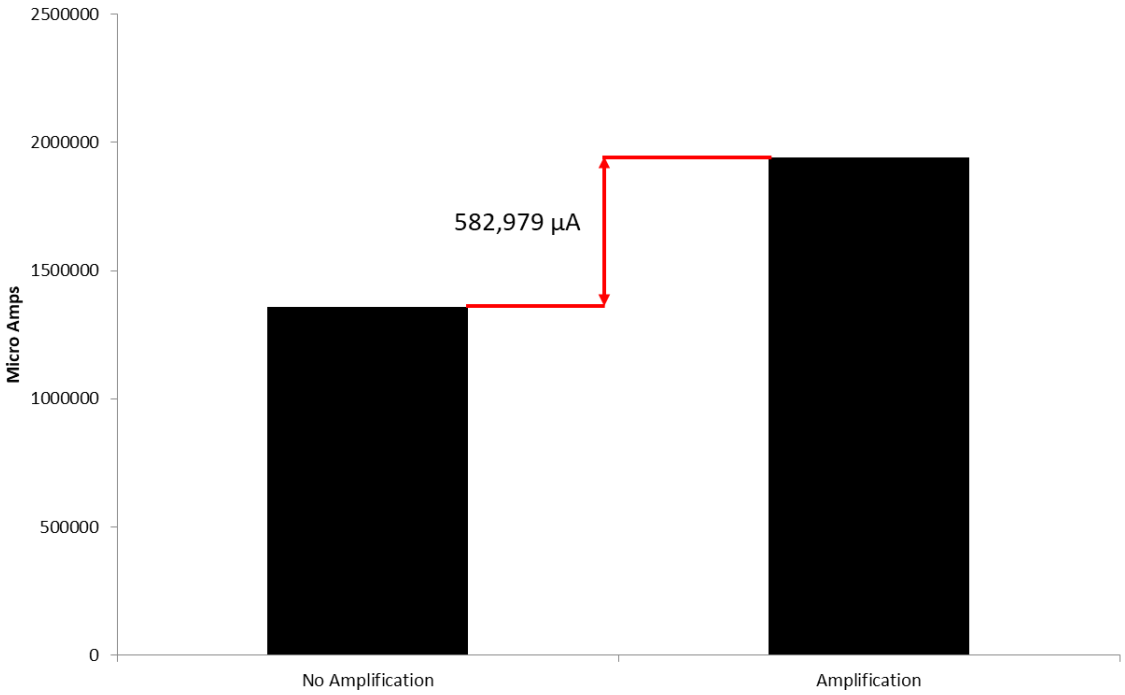

Figure 44 The fluorometry readings for assembled PCR mixes that had been through PCR thermal cycles and mixes that hadn't showing a clear difference in the signal returned.

The genetic sensor was initially designed featuring a dual channel system for simultaneous multiplex detection of several targets within each individual reaction chamber. In practice, this system proved ineffective, as the 45° angle between the LEDs and PMT, and the large aperture where the LEDs were positioned generated a large amount of light scattering that masked the signal from the DNA bound fluorophore. Due to the inability to differentiate a signal from the background fluorescence with the 45° angle between LED and PMT, the optical detection system was subsequently redesigned and simplified via the removal of one of the LEDs and moving the PMT so that it was positioned at a 90° angle from the remaining single LED (Figure 45). A waveguide was also incorporated into the design to direct the light from the LED directly onto the reaction chamber. These modifications removed the ability to perform multiplex reactions, reducing the system to a single target detection device.

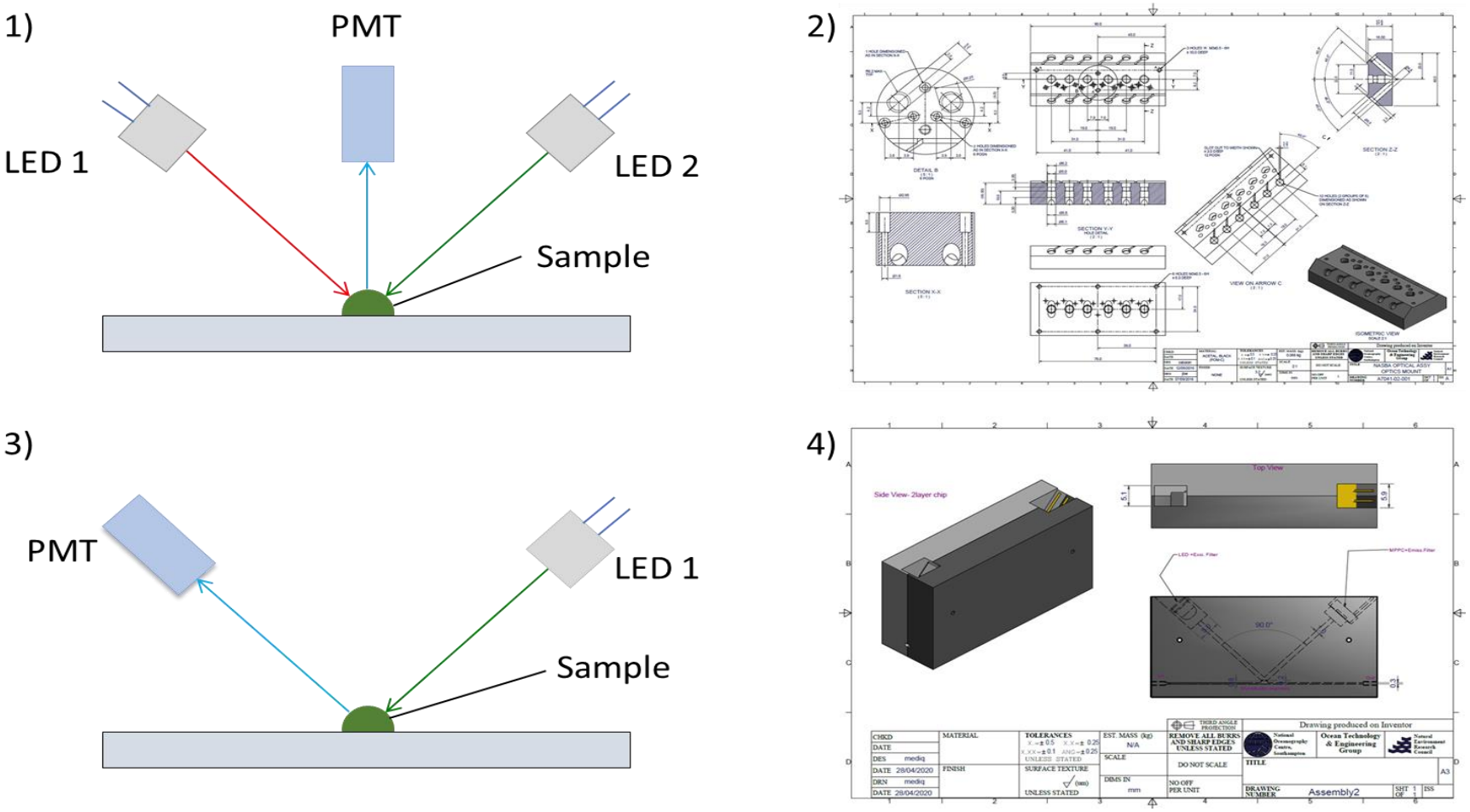

Figure 45 The design configurations for the genetic sensor optics unit. 1) A simplified representation of the initial configuration and 2) the CAD drawing of the configuration that produced too much noise to detect a clear signal. 3) is the simplified set-up designed to reduce "noise" as much as possible and 4) is the associated CAD drawing.

5.3.4 On chip isothermal amplification

The 90° LED/PMT real-time detection configuration was trialled using the *A. minutum* 5.8S rRNA assay developed earlier in this study (Chapter 3). The RPA assay containing an exo probe for real time detection using a Newport 1919-R Power Meter silicone photomultiplier was assembled. 10^8 target sequence copies were used for initial testing. A baseline signal was recorded at 0.17 nW with no sample present in the reaction chamber. With the RPA reaction mix present the signal increased to 0.19 nW. As the RPA reaction proceeded, additional increase in the detected signal was observed (Figure 46).

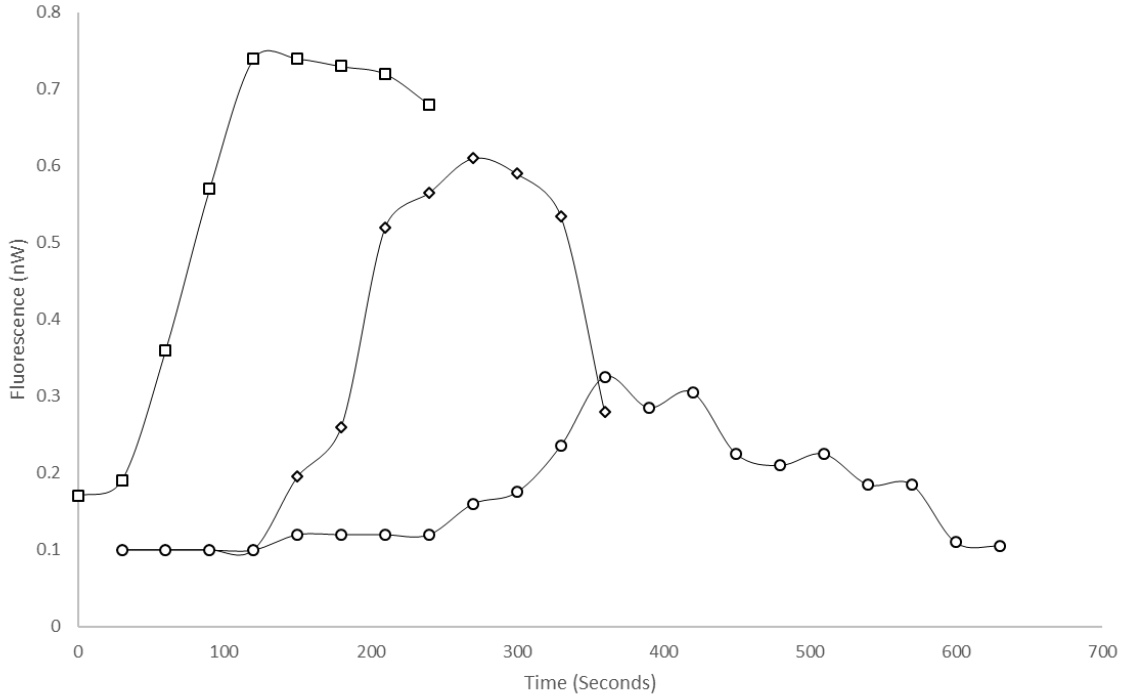

Figure 46 The *A. minutum* 5.8s rRNA assay performed on a microfluidic chip with 10^8 (□), 10^6 (◇) and 10^4 (○) copy numbers. This demonstrated the reactions can be performed on chip with real-time detection. The drop in the detected signal towards the end of the reactions is likely due to the bleaching of the fluorophore by the LED and the degradation of the DNA product by the exonuclease III enzyme.

Once it was established that real-time reactions could be amplified and detected on chip subsequent reactions were assembled containing 10^6 and 10^4 copies of the target sequence. The limit of detection (LOD) obtained when using the state of the art LightCycler 96 qPCR instrument was 10^4 copies, and therefore this experiment was able to determine if the novel system had an equivalent sensitivity (Figure 20). When running the reactions on the microfluidic chips all dilutions were detected in real-time suggesting the LOD for the *A. minutum* assay on the chips is equivalent

to the benchtop apparatus. An R^2 value of 0.97 indicates a fair linear relationship between the differing template concentrations (Figure 47); the linearity is necessary for a quantitative NAA assay. As there were two orders of magnitude between the 5.8S rRNA copy number dilutions this strong relationship likely indicates the amplification is successful. The lower TTP's between the LightCycler and genetic sensor (150.5 seconds for 10^8, 174 seconds for 10^6, and 201.2 seconds for 10^4 copies) indicate the reaction was faster on the genetic sensor than on the LightCycler 96 qPCR instrument. This may be because the genetic sensor preparation had several manual steps, with time lost between adding the RPA reaction mixtures to the chip and the loading of the chip onto the genetic sensor and the subsequent alignment of the optical detector over the chip reaction chamber. The MgOAc is an essential co-factor for the enzymes involved in RPA, and the reaction is initiated as soon as the MgOAc is added. This potentially leads to the RPA reaction being underway before the chip is integrated with the PTE and optical detection system. This may explain the perceived lower TTP of the miniaturised nucleic acid amplification device. This does not happen with the benchtop RPA reactions – master mixes are assembled and placed in PCR tubes before the addition of the MgOAc at the final step prior to placement in the thermocycler to initiate detection immediately. The longer amount of time that the LED was held on during detection may also lead to the perceived shorter TTP, as the LED may have a bleaching effect on free fluorophores, leading to a perceived higher signal being detected. Alternatively, the lower TTP's may be due to the difficulties encountered in setting the genetic sensor heater to 37°C, with it typically holding steady at 39°C. The difference of 2°C may cause faster kinetics of the reaction. Both the LightCycler and genetic sensor displayed a greater variability in TTP between replicates at lower template concentrations due to reduced incidences of interactions between the recombinase complexes and target DNA.

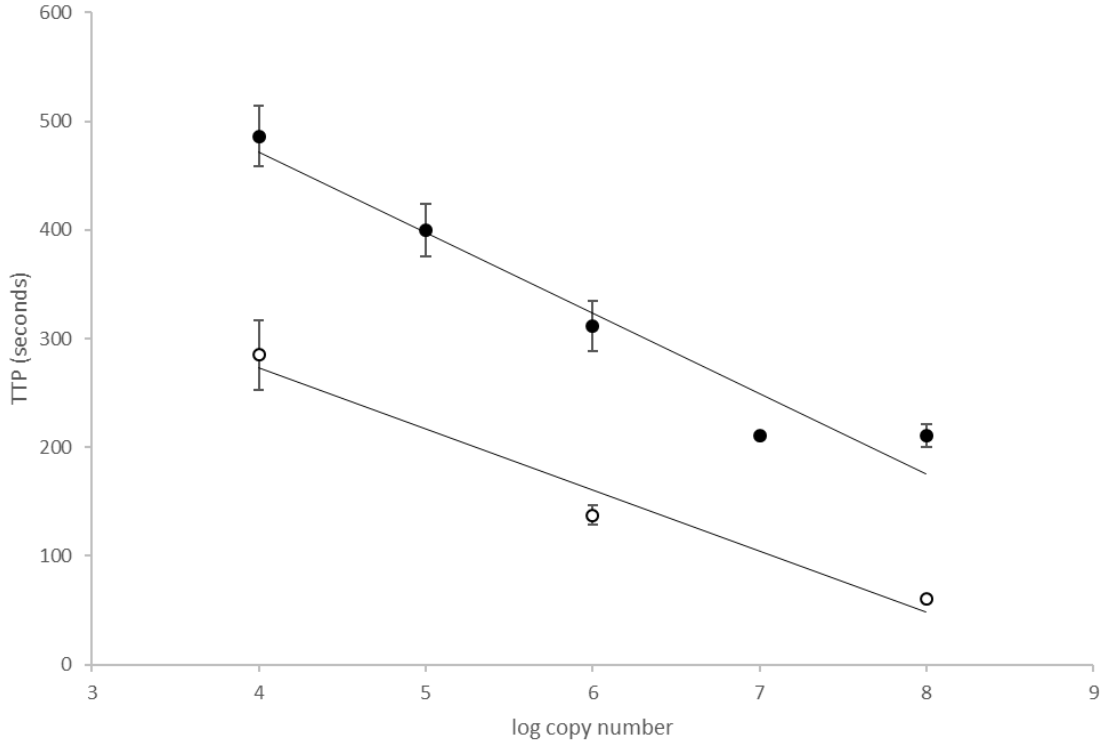

Figure 47 The 5.8S RPA dilution series using the benchtop LightCycler 96 instrument (●) and the Lab-on-a-Chip designed for the genetic sensor (○). The R^2 for the LightCycler series was 0.946 and 0.9687 for the genetic sensor series. The error bars, where visible are the standard error (*n* = 2).

It was noted with the RPA reactions on the chip that after the detected signal reached its peak there was a noticeable, rapid, drop in the signal detected in subsequent readings (Figure 46). This is likely due to enhanced photobleaching of the fluorophore whilst the LED was activated manually and held on for several seconds, whereas the benchtop equipment activates the LED for timeframes in the order of milliseconds. Additionally, the detected signal may be being decreased further by the Exonuclease III in the RT-RPA reaction degrading the dsDNA product.

5.4 Conclusions

The miniaturisation of NAA technologies offers the potential for point of sample detection of harmful organisms. This capacity will be of great interest to water quality monitoring organisations, such as Cefas and Marine Scotland, as well as aquaculture and mariculture, and potentially recreational water users. Microfluidics have several benefits including reduced reagent costs and simplified reaction configuration removing the need for trained technical staff.

Here, microfluidic chips were able to be successfully manufactured by covalently bonding PDMS to a glass substrate via two different methods. Firstly, use of a spin coater was successfully able to

bind the PDMS moulded microchannels to a glass microscope slide substrate, however this method was time consuming and difficult. In contrast, a Hamamatsu Flat Excimer Ex mini produced bonded chips with clear microfluidic channels in a quarter of the time.

The constructed microfluidic chips were used in combination with the previously described *A. minutum* RPA assay (Chapter 3) and successfully amplified *A. minutum* DNA with real-time detection using miniaturised and simplified real-time optical detection. Using PTEs a stable temperature of 39°C (±0.01°C) was achieved and used to successfully perform RPA reactions on the reaction chips, which was observable in real-time using a fluorescent detection system based on LED excitation and emission readings via silicone photomultiplier detection. Using this miniaturised system, the same LOD was achieved as when using the benchtop laboratory equipment, whilst also demonstrating a faster reaction time. This indicates that with future optimisation of the hardware there is the potential for a miniaturised NAA device for HAB detection at point of sample. Going forward, a bespoke, contained, optical housing would be beneficial, potentially including the incorporation of optical filter sets to allow for single well multiplex detection. Additionally, the PTE can be re-tuned to provide a faster ramping rate to allow for the use of thermocycling NAA techniques, such as PCR and NASBA, as there is room for a trade-off in thermal stability.

Chapter 6 Conclusions and future work

6.1 Conclusions

The aim of this study was to develop a miniaturised lab-on-a-chip system that uses molecular techniques to amplify and detect targets of importance in water quality monitoring, specifically the human enteric Hepatitis E virus and the harmful algal bloom forming marine dinoflagellate *Alexandrium minutum*. Novel isothermal assays for both of these targets were developed through the course of this thesis in addition to the development of a hand-held device with potential for point-of-sample testing. This thesis reports on (1) the development of a novel NASBA assay for the amplification and detection of Hepatitis E virus, and it's comparison with an established RT-qPCR assay (Jothikumar *et al.*, 2006); (2) the development of a novel RPA assay for the amplification and detection of *A. minutum* in real-time using a target specific exo probe; (3) the long-term preservation and storage of amplification reaction components; (4) the design and manufacture of microfluidic chips and a prototype handheld device that the novel isothermal assays can be performed on to provide point of sample testing.

6.1.1 Isothermal amplification as a monitoring tool

In Chapter 2 and Chapter 3 of this thesis novel isothermal assays were developed for the detection of targets of interest in water quality monitoring. HEV RNA was successfully amplified for the first time using NASBA down to as low as one target copy number. The NASBA assay was successfully used to amplify and detect HEV RNA extracted from human serum containing HEV virions. This is comparable to the Jothikumar *et al.* (2006) RT-qPCR assay, however the NASBA assay lacks the quantitative nature that the RT-qPCR assay possesses but technological requirements are much lower, making it an attractive option as an early warning yes/no monitoring tool for Hepatitis E virus. Although the HEV NASBA assay was successful there were problems encountered that may limit its use for application with the LOC device, such as a required temperature step from 65°C to 42°C, sample evaporation during the 65°C step, high reagent costs, and the inability for the assay to perform quantitative analysis of HEV. Because of these issues the alternate isothermal amplification technique of RPA and eukaryotic targets were selected going forward.

A novel RPA assay was developed that successfully amplified a region of the *Alexandrium minutum* ITS1-5.8S-ITS2 region for the first time. When compared with a published PCR assay (Galluzzi *et al.*, 2004) the RPA assay lacked the same level of sensitivity, amplifying an equivalent of 10 cells rather than the one cell of the PCR. The RPA reaction occurs 7.3 times faster than the PCR, delivering

positive results in <5 minutes. In addition to the aforementioned ITS1-5.8S-ITS2 RPA a successful RPA assay for detection of the *sxtG* gene involved in the production of STX pre-proteins was achieved after investigating gene sequence similarity *in silico*. However real-time amplification was not achieved during the time of this study. As with NASBA, RPA benefits from a reduced technological requirement making it ideally suited to miniaturisation for point of sample testing. The successful application of both NASBA and RPA in the amplification and detection of these two targets to acceptable levels make them a viable option as a water quality monitoring tool.

DNA was successfully extracted from STX contaminated mollusc flesh. As mollusc flesh is reported to contain high levels of PCR inhibitors a qPCR was prepared to test the amount of inhibition, which proved to be minimal. *A. minutum* DNA was also successfully amplified from STX contaminated mollusc flesh. This demonstrates that nucleic acid amplification has the potential to be used as a tool for monitoring SXT contamination in shellfish flesh.

6.1.2 Isothermal amplification integration with the genetic sensor

A prevailing issue with molecular amplification techniques is their dependence upon molecular reagents that require refrigeration to maintain their viability. In Chapter 4 of this thesis different methods for the long-term storage and preservation of these reagents at ambient temperatures were investigated. Firstly, the stability of two different PCR mixes at room temperature over a period of time was examined. Next two preservatives, trehalose and pullulan, were investigated to determine if they have any inhibitory effect on PCR, and it was found that trehalose does have an inhibitory effect on PCR whereas pullulan does not. Subsequently, trehalose was used in combination with lyophilisation to successfully store PCR reagents for up to four weeks without the need for refrigeration with acceptable losses in efficiency. This agrees with many previous studies where lyophilisation has been successfully used for the preservation of nucleic acids, enzymes, and proteins (Andersen *et al.*, 2008; Kadoya *et al.*, 2010; Kasper and Friess, 2011; Wang, 2000).

Alternatively, the polysaccharide pullulan was investigated for its preservation properties and found to be an excellent preservative, allowing reagents to be stored in readily-dissolvable tablet or film form. This method of preservation, produced positive PCR results six weeks after initial preservation. This offers benefits over the trehalose/freeze-drying technique as it removes the requirement for expensive machinery, is simple to prepare and appears to provide longer-term storage. Although pullulan produced positive results it failed to set completely when combined with the DNA polymerase enzyme potentially reducing the storage time of this component of the PCR master mix.

A microfluidic handheld device was developed that could utilise the aforementioned novel isothermal assays allowing for point of sample detection. Heating was provided by Peltier thermoelectric elements, whilst real-time detection was done using fluorophore excitation via LED and emission measured using a micro silicon photomultiplier. Reaction chips were designed featuring a three-chamber system: a reagent chamber where preserved reagents were to be stored; a reaction chamber where the amplification reaction occurs; and a third 'air' chamber used to allow finger actuated pumping to mix the reagents, removing the requirement for centrifuges or vortexes. Chips comprised two components: a moulded PDMS half containing the microfluidic architecture and a glass microscope slide used as a solid substrate due to its optical clarity and thermal conductivity. Two techniques were trialled for bonding of the two chip components: (i) using a spin coater and PDMS to form a bond between the PDMS and glass components; and (ii) using an excimer ultraviolet laser to generate ozone substituting the material surface with a hydroxyl group allowing the formation of covalent bonds between the two surfaces. Both of these techniques were successful however the excimer method was much faster and cleaner and consequently was adopted for chip production going forward.

The aforementioned *A. minutum* RPA assay was trialled using the handheld genomic sensor and it was found to have the same limit of detection of *A. minutum* cells as the benchtop laboratory equipment, and to be semi-quantitative. The handheld genetic sensor also appeared to produce positive results sooner than when using laboratory equipment. This demonstrates a huge potential for its utilisation as an in situ monitor of HAB outbreaks, as the LOC system developed in this thesis combines portability, ease of use, and the possibility for *in situ* environmental monitoring when used in combination with the long-term storage of reagents on the chips.

6.2 Further work

This section suggests further research that could further extend and improve the research performed in this thesis. These suggestions are listed as follows:

6.2.1 Isothermal amplification as a monitoring tool

- Methods for extraction and concentration of nucleic acids that can be incorporated onto a LOC system could be identified. As this system is intended for portability and ease of use any extraction method should limit user contact with harmful chemicals e.g. Guanidine thiocyanate and other potent lysis detergents. Enzymatic, thermal and mechanical lysis may provide safer alternatives.

- RPA primers targeting the *sxtG* gene were designed during this thesis and show potential using end-point analysis of the amplified DNA. To further increase the specificity of this assay and to provide real-time detection, an exo probe can be designed. As the exo probe also acts as an additional primer this could potentially increase the sensitivity of the *sxtG* RPA assay.
- Sequence analysis of both the *sxtA* and *sxtG* saxitoxin producing genes demonstrate *sxtG* to be highly conserved across *Alexandrium* species whereas *sxtA* displays a degree of variability between species. This could be used to design primer sets for *sxtA* that are able to identify down to species level whereas the *sxtG* assay can quantify members of the genus.
- The ability to amplify and detect an RNA rather than DNA target will provide insight into metabolically active organisms. To do this the pairing of a reverse transcriptase with the ITS1-5.8S-ITS2 RPA assay could be trialled, potentially as a single reaction.
- If reverse transcription RPA is successful it could be combined with the *sxtG* RPA assay and used to investigate factors affecting toxin production. *A minutum* cultures could be stressed under different conditions (e.g. temperature, salinity, nutrient concentration) to determine if there a single, or a combination, of factors that stimulate toxin production. This could then be paired with HPLC to investigate whether there is a relationship between *sxt* gene transcription and toxin concentration.
- A limitation when attempting RPA using contaminated shellfish flesh is the potential presence of mucopolysaccharides which may inhibit the amplification reactions. Additional treatment steps on extracted nucleic acids could be investigated for their potential at removing inhibitors from the reaction, such as addition of BSA or gp32, selection of resistant polymerases, chloroform extraction, PEG precipitation or active carbon treatment (Schrader *et al.*, 2012). This would be essential if the RPA assays are to be at the point of sample in aquaculture and mariculture facilities.
- The miniaturised genetic sensor has the potential to be paired with additional sensors developed by OTE to gain an understanding into the environmental factors that may stimulate toxin gene expression. For example, combination with nitrate or phosphate sensors will provide insights as to whether nutrient input is a driver of toxin production, likewise combination with a temperature sensor will show any potential links between SST and PSP toxin production.
- In addition to environmental testing the miniaturised genetic sensor has potential for use in a medical setting – as a screening tool for pathogens. The small size and simple operation, combined with dry storage of reagents at ambient temperatures allow for widespread use

in areas were access to laboratories is at a premium, for example in field hospitals in warzones or in regions where natural disasters occur.

6.2.2 Isothermal amplification integration with the genetic sensor

- Although each method of reagent preservation worked for several weeks further study may increase this further. Using a combination of both trehalose and pullulan, if subject to lyophilisation may produce better storage conditions than when used separately. The combination of a small disaccharide and large polysaccharide has been reported before (Teekamp *et al.*, 2017) and combining pullulan with lyophilisation my solve the problem of the DNA polymerase not forming a film or tablet.
- Previous studies have shown that for RNA analysis to take place microfluidic chips require further treatment due to the presence of RNases causing RNA degradation. For NASBA LOC analyses success was achieved using several wash steps including RNaseZAP®, molecular grade ethanol, bovine serum albumin (BSA), and RNase free water (Loukas, 2016). This washing protocol should be trialled on the LOC system described in this thesis if RNA amplification is to be attempted.
- Further development of the miniaturised genetic sensor should include the ability to perform multiplex reactions. This would be of value as novel RPA assays could be developed for a range of geographically important HAB species and detection of each could be achieved in a single reaction, drastically lowering costs. This could potentially be done by the use of optical filters or by redesigning the architecture to include more than a single LED/PMT pair.
- This would also allow the genetic sensor to be deployed with additional physical-chemical sensors to try and provide insights into environmental factors that may drive toxin production by *Alexandrium minutum*, for example nutrient input such as nitrate and phosphate, or changes to sea surface temperature or salinity.

Appendix A HEV gBlock sequence

Below is the sequence of the HEV gBlock used to generate cRNA to test the NASBA primers developed in this study

This sequence is complimentary to the HEV +ve sense RNA so when treated with T7 RNA polymerase produces RNA identical to that of HEV.

The sequence in red at the 5' end is the T7 promoter so T7 RNA polymerase can bind and synthesise a copy of the wild type RNA.

TAATACGACTCACTATAGGCGGAGCGACAATCACTAAAGGAGGCGTTCGAGTGCTTACATCGAGTCTACAC
ACACCTACAACAAAGGGCACAAATACCCCAAAGGGGACCTGAGCAAGTATTGGACTAACCGTACGATGTC
CGACAACGACTACCGTTCCGTGTAAAGTGACTCAGTCATTTTGGTCACGAGCTGAACTGTTTAAGTTAGAAC
ACAGCCCACCTTACTTATTGTACAGAAAACGACGCGGGTACCCAAGCGCTGGTACGCGGGAGCCGGATAA
AACAACGACGAGGAGTACAAAAACGGATACGACGGGCGCGGTGGCGGGCCAGTCGGCAGACCGGCGGC
AGCACCCGCCGCGTCGCCGCCAAGGCCGCCACCAAAGACCCCACTGGCCCAACTAAGAGTCGGGAAGCGT
TAGGGGATATAAGTAGGTTGGTTGGGGAAGCGGGGGCTACAGTGGCGACGCCGGCCCCGACCTGGAGCA
CAAGCGGTTGGGCGGGCTGGTGAGCCGAGGCGAACCGCACTGGTCCGGGTCGCGGGGCGGCAACGGAG
TGCAGCATCTGGATGGTGTCGACCCCGGCGCGGCGATTGGCGCCAGCGAGGCCGGGTACTGTGGGGCGG
TCACGGACTACAGCTGAGGGCGCCGCGGTAGAACGCGGCCGTCATATTGGATAGTTGTAGAGGGGAATG
GAGAAGGCACCGGTGGCCGTGATTGGACCAAGAAATACGGCGGGGAGAATCAGGCGAAAATGGGGAAG
TCCTGCCGTGGTTATGGGTATATTACCGGTGCCTTCGAAGATTAATACGGGTCATGGCCCAACGGGCACGG
TGTTAGGCAATGGCGGGCGACCAGGGGTTACGACAGCCGCCAATGCGGTAGAGGTAGAGTAAGACCGGT
GTCTGGTGGTGGTGGGGCTGCAGGCAACTATACTTAAGTTATTGGAGCTGCCTACAAGCATAAAATCAGG
TCGGGCCGTATCGGAGACTCGAACACTAGGGTTCACTCGCGGATGTGATAGCATTGGTTCCGACCGCGAG
GCAGCTCTGGAGACCCCACCGACTCCTCCTCCGATGGAGACCAGAACAATACGAAACGTATGTACCGAGTG
AGCATTTAAGGATATGATTATGTGGGATATGGCCACGGGAGCCCGACAACCTGAAACGGGAACTCGAACT
CAAAGCGTTGGAATGGGGGCCATTGTGGTTATGCGCCCAGAGGGCAATAAGGTCGTGACGAGCGGTGGC
GGAAGCAGCGCCACGCCTGCCCTGACGGCTCGAGTGGTGGTGCCGACGATGGGCGAAATACTTCCTGGA
GATAAAATGATCATGATTACCACAGCCACTCTAGCCGGCGCCCTATCGGGAGTGGGACAAGTTGGAACGA
CTGTGAGACGAACCGCCGGACGGCTGTCTTAACTAAAGCAGCCGACCACCGGTCGACAAGATGAGGGCAG
GGCAACAGAGTCGGTTACCGCTCGGCTGACAATTCAACATATGTAGACATCTCTTACGAGTCGTCCTATTCC
CATAACGTTAGGGCGTACTGTAACTGGAGCCTCTTAGAGCACACCAATAAGTCCTAATACTATTGGTTGTAC
TTGTTCTAGCCGGCTGCGGAAGAGGTCGGGGTAGCGCGGGAAAGAGACAGGAAGCTCGATTACTACACG
AAACCGAGAGAGAGTGGCGACGGCTCATACTGGTCAGGTGAATACCGAGAAGCTGACCGGGTCAAATAC

Appendix A

AAAGACTGAGACACTGGAACCAATTACAACGCTGGCCGCGCGTCCGGCAACGGGCCAGCGAGCTAACCTG

GTTCCAGTGTGAACTGCCAGCGGGGGGAGAGGTGGTAGGTCGTCATGAGCTTCTGGAAGAAACAGGACGG

CGAGGCGCCATTCGAGAGAAAGACCCTCCGTCCGTGTTGATTTCGGCCCATGGGAATATTAATATTGTGGT

GACGATCGCTGGTTGACGAACAGCTCTTACGGCGGCCCGTGGCCCAGCGATAAAGGTGAATGTGGTGATC

GGACCCACGACCAGGGCAGAGGTAAAGACGCCAACGGCAAAATCGGGGGGGTGAGACGCGATCGTAACG

AACTCCTATGGAACCTGATGGGACGGGCGCGGGTATGAAAACTACTAAAGACGGGTCTCACGGCGGGGG

AACCGGAAGTCCCGACGCGAAAGGTCAGATGACAGCGACTCGAAGTCGCGGAATTCTACTTCCACCCATTT

TGAGCCCTCAACATCAAATAAACGAACACGGGGGGGAAGAAAGACAA

Appendix B *A. minutum* RPA assay design

Table S 1 The accession numbers for the *Alexandrium* sequences used to design the 5.8S rRNA RPA assay and the *sxtA* and *sxtG* qPCR and RPA assays developed in this study.

	A. minutum	
5.8S rRNA	***sxtA***	***sxtG***
KJ781424.2	JF343313	JX995124.1
KJ781425.1	JF343314	JX995123.1
KF889359.1	JF343348	JX995122.1
KF889358.1	JF343315	JX995121.1
KF889357.1	JF343311	JX995133.1
KF889356.1	JF343265	
KF889355.1	JF343312	
KF889354.1	JF343324	
KF889353.1	JF343325	
KF889352.1	JF343327	
	JF343326	
	JF343349	
	JF343351	
	JF343317	
	JF343310	
	JF343316	
	JF343347	
	JF343350	
	JF343328	
	JF343318	
	JF343321	
	JF343320	
	JF343322	
	JF343319	
	JF343323	

	A. catenella	
5.8S rRNA	***sxtA***	***sxtG***
	KM100455.1	
	KM100453.1	
	KM100454.1	
	KJ886938.1	
	KM100452.1	
	JF343261.1	
	JF343260.1	
	JF343259.1	
	JF343246.1	
	JF343245.1	
	JF343244.1	
	JF343243.1	
	JF343242.1	
	JF343241.1	
	JF343240.1	
	JF343329.1	
	JF343283.1	
	JF343282.1	
	JF343281.1	
	JF343280.1	
	JF343279.1	
	KJ879213.1	
	KM104281.1	

	A. affine	
5.8S rRNA	***sxtA***	***sxtG***
	KM100454.1	JX995129.1
		JX995112.1
		JX995111.1

	A. fundyense	
5.8S rRNA	***sxtA***	***sxtG***
	KF985180.1	JX995130.1
	JF343239.1	JX995118.1
	JF343238.1	JX995117.1
	KJ999788.1	JX995134.1
	KJ999787.1	

	A. pacificum	
5.8S rRNA	***sxtA***	***sxtG***
	KF985182.1	
	KF985179.1	
	KF985178.1	
	KF985177.1	

	A. tamarense	
5.8S rRNA	***sxtA***	***sxtG***
	KF985177.1	JX995127.1
	JF343264.1	JX995126.1
	JF343263.1	JX995125.1
	JF343251.1	
	JF343249.1	
	JF343248.1	
	JF343332.1	

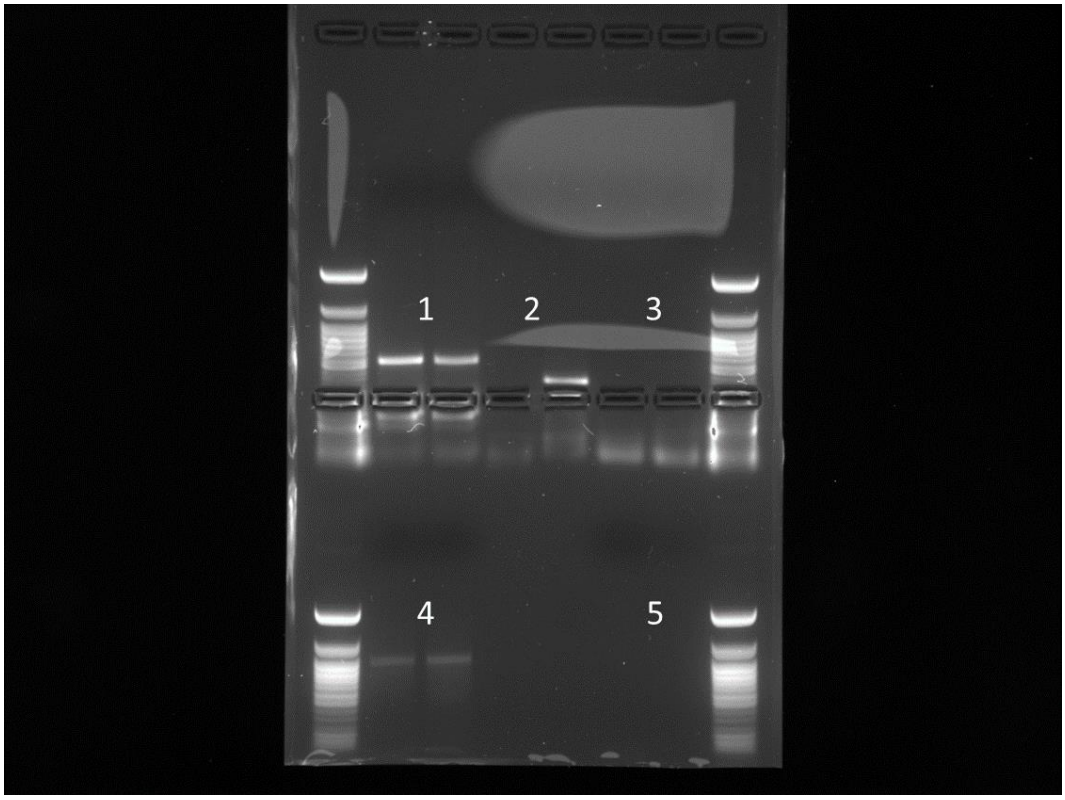

Figure S 1 *sxtG* PCR specificity test. 1 = *K. brevis*, 2 = *P lima*, 3 = *P cordatum* 4 = *L polyedrum*, 5 = NTC. The ladder used is a 50 bp ladder. This Shows that the *sxtG* PCR primers are not specific, amplifying DNA from all species tested.

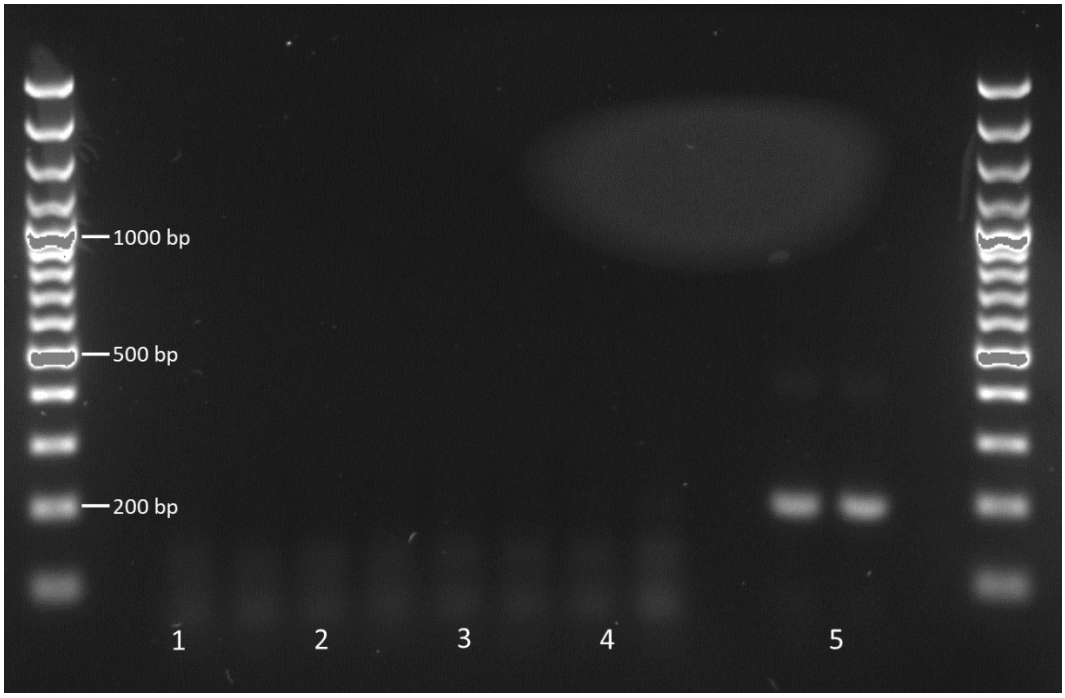

Figure S 2 *A. minutum* 5.8S rRPA specificity testing using primers AMRPA 3.1/3.2. 1: *P. lima*, 2: *P. cordatum*, 3: *L. polyedrum*, 4: *K. brevis*, 5: *A. minutum*. The ladder used is a 100 bp ladder. This shows the primers amplify *A. minutum* specifically.

Appendix C Additional Viral Work

In addition to HEV NASBA assays for Hepatitis A (HAV) virus and Norovirus (NV) were also considered, as like HEV, these are both waterborne RNA viruses. After investigation it was decided not to pursue these viral targets further. A summary of the work and findings is presented below.

C.1 HAV

- HAV genome sequences were aligned, and primer regions identified, via the same methodology described for HEV in section 2.2.1 of this thesis
- gBlock synthetic gene analogues (IDT, USA) were used synthesis cRNA to test the designed primers and demonstrated positive amplification of the desired target sequence using the NASBA protocol described in section 2.2.3
- For verification, lenticule discs containing inactivated Hepatitis A virions were provided by Public Health England (PHE)
- Lenticule discs were rehydrated in 1 mL of PBS as per the provided instructions, and an RNA extraction was performed using an RNA virus extraction kit (Macherey-Nagel, Germany) following the manufacturers recommended protocol
- Following extraction from six lenticule discs, RNA was quantified using a Qubit spectrophotometer and concentrations of RNA ranged from undetectable to 3.36 ng/µL
- NASBA reactions were prepared as described in section 2.2.3 and the extracted lenticule disc RNA used as template material
- Using this methodology, it was found that one of the primer sets appeared to produce positive amplification, however it occurred very late with a TTP of approximately 45 minutes and lacked reproducibility. In addition, negative controls prepared to contain everything for the NASBA reaction but with water added in place of template material always produced an amplification product. After measures taken to ensure sterility of the reaction preparation and reduce cross-contamination the problem persisted, leading to the conclusion that it may be the result of interaction between the primers and molecular beacon, rather than specific product
- In addition to the HAV NASBA an assay for HAV Helicase Dependant Amplification (HDA) was also developed and tested using cDNA synthesized from the HAV lenticule disc extracted RNA.
- Although this assay initially showed promise, with all prepared reactions showing positive amplification (and negative controls all showed no amplification)

- The optimal primer set, however, when tested using NV cDNA produced strong amplification, suggesting this primer set lacked specificity
- This was confirmed when a melt curve analysis was performed on the HAV HDA assay and it was found that there was a large degree of non-specific amplification

C.2 NV

- A previously developed NASBA assay for NV was found during a literature search (Lamhoujeb *et al.*, 2009) and chosen for testing for the presence of NV using the miniaturised genetic sensor described in this thesis
- NASBA reactions were prepared as described by Lamhoujeb *et al.* (2009) and template material was provided by The University of Southampton (Dr Chris McCormick) in the form of Laboratory Reference RNA. No positive amplification was observed
- Despite modifications to the NASBA assay in attempt to produce positive amplification, none was observed and so the decision was taken to focus time and effort on the HAV and HEV assays as they showed greater promise

Appendix D List of Conferences Attended

- AMBIO VIII (2017) – SAMS, Scotland poster title: Development of custom assays for the autonomous detection and quantification of targeted marine microorganisms using Lab on a Chip
- RSC Microfluidics for Analytical Chemistry (2018) – NOC, Southampton poster title: The development of a “lab on a chip” for the detection of pathogens in the marine environment
- IMMR ’18 (2018) – ESTM, Portugal poster title: Development of custom assays for the autonomous detection and quantification of human enteric viruses in seawater using Lab on a Chip
- Ocean Sciences Meeting 2020, San Diego, California poster title: The development of Recombinase Polymerse Amplification Assays for the Detection of *Alexandium minutum* with Lab-on-a-Chip Application

List of References

Abd El Wahed, A., El-Deeb, A., El-Tholoth, M., Abd El Kader, H., Ahmed, A., Hassan, S., Hoffmann, B., Haas, B., Shalaby, M. A., Hufert, F. T. & Weidmann, M. (2013). A Portable Reverse Transcription Recombinase Polymerase Amplification Assay for Rapid Detection of Foot-and-Mouth Disease Virus. *PLOS ONE,* 8**,** e71642.

Adams, G. (2007). The Principles of Freeze-Drying. *In:* DAY, J. G. & STACEY, G. N. (eds.) *Cryopreservation and Freeze-Drying Protocols.* Totowa, NJ: Humana Press.

Adams, M. J. (1981). *An Introduction to Optical Waveguides*, John Wiley & Sons.

Ageno, M., Dore, E. & Frontali, C. (1969). The alkaline denaturation of DNA. *Biophysical journal,* 9**,** 1281-1311.

Ahrberg, C. D., Manz, A. & Chung, B. G. (2016). Polymerase chain reaction in microfluidic devices. *Lab on a Chip,* 16**,** 3866-3884.

Al-Abdulrazzak, D., Zeller, D., Belhabib, D., Tesfamichael, D. & Pauly, D. (2015). Total marine fisheries catches in the Persian/Arabian Gulf from 1950 to 2010. *Regional Studies in Marine Science,* 2**,** 28-34.

Al Shehhi, M. R., Gherboudj, I. & Ghedira, H. (2014). An overview of historical harmful algae blooms outbreaks in the Arabian Seas. *Marine Pollution Bulletin,* 86**,** 314-324.

Ali, N., Rampazzo, R. C. P., Costa, A. D. T. & Krieger, M. A. (2017). Current Nucleic Acid Extraction Methods and Their Implications to Point-of-Care Diagnostics. *Biomed Res Int,* 2017**,** 9306564.

Amer, H. M., Abd El Wahed, A., Shalaby, M. A., Almajhdi, F. N., Hufert, F. T. & Weidmann, M. (2013). A new approach for diagnosis of bovine coronavirus using a reverse transcription recombinase polymerase amplification assay. *Journal of Virological Methods,* 193**,** 337-340.

Andersen, M. Ø., Howard, K. A., Paludan, S. R., Besenbacher, F. & Kjems, J. (2008). Delivery of siRNA from lyophilized polymeric surfaces. *Biomaterials,* 29**,** 506-512.

Anderson, D. M. (2009). Approaches to monitoring, control and management of harmful algal blooms (HABs). *Ocean & Coastal Management,* 52**,** 342.

Anderson, D. M., Alpermann, T. J., Cembella, A. D., Collos, Y., Masseret, E. & Montresor, M. (2012a). The globally distributed genus Alexandrium: multifaceted roles in marine ecosystems and impacts on human health. *Harmful algae,* 14**,** 10-35.

Anderson, D. M., Cembella, A. D. & Hallegraeff, G. M. (2012b). Progress in Understanding Harmful Algal Blooms: Paradigm Shifts and New Technologies for Research, Monitoring, and Management. *Annual Review of Marine Science,* 4**,** 143-176.

Arakawa, T., Kita, Y. & Carpenter, J. F. (1991). Protein–Solvent Interactions in Pharmaceutical Formulations. *Pharmaceutical Research,* 8**,** 285-291.

Armes, N. A. & Stemple, D. L. (2002). *Recombinase Polymerase Amplification*. US patent application 10/371,641.

Arundell, M., Perry, V. H. & Newman, T. A. (2011). Integration of a macro/micro architectured compartmentalised neuronal culture device using a rapid prototyping moulding process. *Lab Chip,* 11**,** 3001-5.

Asiello, P. J. & Baeumner, A. J. (2011). Miniaturized isothermal nucleic acid amplification, a review. *Lab on a Chip,* 11**,** 1420-30.

Atmar, R. L. & Estes, M. K. (2001). Diagnosis of Noncultivatable Gastroenteritis Viruses, the Human Caliciviruses. *Clinical Microbiology Reviews,* 14**,** 15-37.

Balayan, M. S., Andjaparidze, A. G., Savinskaya, S. S., Ketiladze, E. S., Braginsky, D. M., Savinov, A. P. & Poleschuk, V. F. (1983). Evidence for a Virus in Non-A, Non-B Hepatitis Transmitted via the Fecal-Oral Route. *Intervirology,* 20**,** 23-31.

Banting, G. S., Braithwaite, S., Scott, C., Kim, J., Jeon, B., Ashbolt, N., Ruecker, N., Tymensen, L., Charest, J., Pintar, K., Checkley, S. & Neumann, N. F. (2016). Evaluation of Various *Campylobacter*-Specific Quantitative PCR (qPCR) Assays for Detection and Enumeration of *Campylobacteraceae* in Irrigation Water and Wastewater via a Miniaturized Most-Probable-Number–qPCR Assay. *Applied and Environmental Microbiology,* 82**,** 4743-4756.

Bartsch, M. S., Edwards, H. S., Lee, D., Moseley, C. E., Tew, K. E., Renzi, R. F., Van De Vreugde, J. L., Kim, H., Knight, D. L., Sinha, A., Branda, S. S. & Patel, K. D. (2015). The Rotary Zone Thermal Cycler: A Low-Power System Enabling Automated Rapid PCR. *PLOS ONE,* 10**,** e0118182.

Bell, L. N., Touma, D. E., White, K. L. & Chen, Y.-H. (1998). Glycine Loss and Maillard Browning as Related to the Glass Transition in a Model Food System. *Journal of Food Science,* 63**,** 625-628.

Bertagnolli, A. D. & Stewart, F. J. (2018). Microbial niches in marine oxygen minimum zones. *Nature Reviews Microbiology,* 16**,** 723-729.

Bian, X., Jing, F., Li, G., Fan, X., Jia, C., Zhou, H., Jin, Q. & Zhao, J. (2015). A microfluidic droplet digital PCR for simultaneous detection of pathogenic Escherichia coli O157 and Listeria monocytogenes. *Biosensors and Bioelectronics,* 74**,** 770-777.

Bischof, J. C. & He, X. (2005). Thermal stability of proteins. *Annals of the New York Academy of Sciences,* 1066**,** 12-33.

Bowers, H. A., Marin, R., Birch, J. M., Scholin, C. A. & Doucette, G. J. (2016). Recovery and identification of Pseudo-nitzschia (Bacillariophyceae) frustules from natural samples acquired using the environmental sample processor. *Journal of Phycology,* 52**,** 135-140.

Boyle, D. S., Lehman, D. A., Lillis, L., Peterson, D., Singhal, M., Armes, N., Parker, M., Piepenburg, O. & Overbaugh, J. (2013). Rapid Detection of HIV-1 Proviral DNA for Early Infant Diagnosis Using Recombinase Polymerase Amplification. *mBio,* 4**,** e00135-13.

Boyle, D. S., Mcnerney, R., Teng Low, H., Leader, B. T., Pérez-Osorio, A. C., Meyer, J. C., O'sullivan, D. M., Brooks, D. G., Piepenburg, O. & Forrest, M. S. (2014). Rapid Detection of Mycobacterium tuberculosis by Recombinase Polymerase Amplification. *PLOS ONE,* 9**,** e103091.

Brandenburg, K. M., Velthuis, M. & Van De Waal, D. B. (2019). Meta-analysis reveals enhanced growth of marine harmful algae from temperate regions with warming and elevated CO2 levels. *Global Change Biology,* 25**,** 2607-2618.

Bresnan, E., Baker-Austin, C., Campos, C. J. A., Davidson, K., Edwards, M., Hall, A., Mckinney, A. & Turner, A. D. (2020). Impacts of climate change on human health, HABs and bathing waters, relevant to the coastal and marine environment around the UK. *MCCIP Science Review 2020***,** 521-545.

Brosnahan, M. L., Fischer, A. D., Lopez, C. B., Moore, S. K. & Anderson, D. M. (2020). Cyst-forming dinoflagellates in a warming climate. *Harmful Algae,* 91**,** 101728.

Brosnahan, M. L., Kulis, D. M., Solow, A. R., Erdner, D. L., Percy, L., Lewis, J. & Anderson, D. M. (2010). Outbreeding lethality between toxic Group I and nontoxic Group III Alexandrium tamarense spp. isolates: Predominance of heterotypic encystment and implications for mating interactions and biogeography. *Deep-sea research. Part II, Topical studies in oceanography,* 57**,** 175-189.

Bruno, D. W., Dear, G. & Seaton, D. D. (1989). Mortality associated with phytoplankton blooms among farmed Atlantic salmon, Salmo salar L., in Scotland. *Aquaculture,* 78**,** 217-222.

Buchanan, S. S., Pyatt, D. W. & Carpenter, J. F. (2010). Preservation of differentiation and clonogenic potential of human hematopoietic stem and progenitor cells during lyophilization and ambient storage. *PLoS One,* 5.

Burson, A., Matthijs, H. C. P., De Bruijne, W., Talens, R., Hoogenboom, R., Gerssen, A., Visser, P. M., Stomp, M., Steur, K., Van Scheppingen, Y. & Huisman, J. (2014). Termination of a toxic Alexandrium bloom with hydrogen peroxide. *Harmful Algae,* 31**,** 125-135.

Busi, F. (2020). Fluorescent Oligonucleotide Probes for the Quantification of RNA by Real-Time qPCR. *In:* V., A. & F., W. (eds.) *RNA Spectroscopy. Methods in Molecular Biology.* New York: Humana.

Cai, W., Borlace, S., Lengaigne, M., Van Rensch, P., Collins, M., Vecchi, G., Timmermann, A., Santoso, A., Mcphaden, M. J., Wu, L., England, M. H., Wang, G., Guilyardi, E. & Jin, F.-F. (2014). Increasing frequency of extreme El Nino events due to greenhouse warming. *Nature Climate Change,* 4**,** 111-116.

Cann, K. F., Thomas, D. R., Salmon, R. L., Wyn-Jones, A. P. & Kay, D. (2013). Extreme water-related weather events and waterborne disease. *Epidemiology and Infection,* 141**,** 671-86.

Cao, Y., Zheng, K., Jiang, J., Wu, J., Shi, F., Song, X. & Jiang, Y. (2018). A novel method to detect meat adulteration by recombinase polymerase amplification and SYBR green I. *Food Chemistry,* 266**,** 73-78.

Casabianca, S., Penna, A., Pecchioli, E., Jordi, A., Basterretxea, G. & Vernesi, C. (2012). Population genetic structure and connectivity of the harmful dinoflagellate Alexandrium minutum in the Mediterranean Sea. *Proceedings of the Royal Society B: Biological Sciences,* 279**,** 129-138.

Cavalier-Smith, T. (2005). Economy, speed and size matter: evolutionary forces driving nuclear genome miniaturization and expansion. *Ann Bot,* 95**,** 147-75.

Chandler, H. M. (1986). *Device for performing quantitative chemical and immunochemical assays*. USA patent application.

Chang, C.-C., Chen, C.-C., Wei, S.-C., Lu, H.-H., Liang, Y.-H. & Lin, C.-W. (2012). Diagnostic devices for isothermal nucleic acid amplification. *Sensors,* 12**,** 8319-8337.

Chi, E. Y., Krishnan, S., Randolph, T.W., and Carpenter, J.F. (2003). Physical stability of proteins in aqueous solution: mechanism and driving forces in nonnative protein aggregation. *Pharmaceutical Research,* 20**,** 1325-1336.

Choi, J.-K., Min, J.-E., Noh, J. H., Han, T.-H., Yoon, S., Park, Y. J., Moon, J.-E., Ahn, J.-H., Ahn, S. M. & Park, J.-H. (2014). Harmful algal bloom (HAB) in the East Sea identified by the Geostationary Ocean Color Imager (GOCI). *Harmful Algae,* 39**,** 295-302.

Colaço, C., Sen, S., Thangavelu, M., Pinder, S. & Roser, B. (1992). Extraordinary stability of enzymes dried in trehalose: simplified molecular biology. *Bio/technology,* 10**,** 1007-1011.

Compton, J. (1991). Nucleic acid sequence-based amplification. *Nature,* 350**,** 91-92.

Costas, E. & Lopez-Rodas, V. (1996). Enumeration and separation of the toxic dinoflagellate Alexandrium minutum from natural samples using immunological procedures with blocking antibodies. *Journal of Experimental Marine Biology and Ecology,* 198**,** 81-87.

Cowan, J. A. (1998). Metal Activation of Enzymes in Nucleic Acid Biochemistry. *Chemical Reviews,* 98**,** 1067-1088.

Crannell, Z. A., Castellanos-Gonzalez, A., Irani, A., Rohrman, B., White, A. C. & Richards-Kortum, R. (2014a). Nucleic Acid Test to Diagnose Cryptosporidiosis: Lab Assessment in Animal and Patient Specimens. *Analytical Chemistry,* 86**,** 2565-2571.

Crannell, Z. A., Rohrman, B. & Richards-Kortum, R. (2014b). Quantification of HIV-1 DNA Using Real-Time Recombinase Polymerase Amplification. *Analytical Chemistry,* 86**,** 5615-5619.

Cromeans, T. L., Naninan, O. V. & Margolis, H. S. (1997). Detection of Hepatitis A virus RNA in oyster meat. *Applied and Environmental Microbiology,* 63**,** 2460-2463.

Dapena, C., Bravo, I., Cuadrado, A. & Figueroa, R. I. (2015). Nuclear and Cell Morphological Changes during the Cell Cycle and Growth of the Toxic Dinoflagellate Alexandrium minutum. *Protist,* 166**,** 146-160.

Davidson, K., Gowen, R. J., Harrison, P. J., Fleming, L. E., Hoagland, P. & Moschonas, G. (2014). Anthropogenic nutrients and harmful algae in coastal waters. *Journal of Environmental Management,* 146**,** 206-216.

Demeke, T. & Adams, R. P. (1992). The effects of plant polysaccharides and buffer additives on PCR. *BioTechniques,* 12**,** 332-334.

Dragan, A. I., Pavlovic, R., Mcgivney, J. B., Casas-Finet, J. R., Bishop, E. S., Strouse, R. J., Schenerman, M. A. & Geddes, C. D. (2012). SYBR Green I: Fluorescence Properties and Interaction with DNA. *Journal of Fluorescence,* 22**,** 1189-1199.

Drummond, T. G., Hill, M. G. & Barton, J. K. (2003). Electrochemical DNA sensors. *Nature Biotechnology,* 21**,** 1192-1199.

Du, T., Chao, L., Zhao, S., Chi, L., Li, D., Shen, Y., Shi, Q. & Deng, X. (2015). Successful cryopreservation of whole sheep ovary by using DMSO-free cryoprotectant. *Journal of Assisted Reproduction and Genetics,* 32**,** 1267-1275.

Du, X., Peterson, W., Fisher, J., Hunter, M. & Peterson, J. (2016). Initiation and Development of a Toxic and Persistent Pseudo-nitzschia Bloom off the Oregon Coast in Spring/Summer 2015. *PLOS ONE,* 11**,** e0163977.

Erdner, D. L., Percy, L., Keafer, B., Lewis, J. & Anderson, D. M. (2010). A quantitative real-time PCR assay for the identification and enumeration of Alexandrium cysts in marine sediments. *Deep-sea research. Part II, Topical studies in oceanography,* 57**,** 279-287.

Euler, M., Wang, Y., Heidenreich, D., Patel, P., Strohmeier, O., Hakenberg, S., Niedrig, M., Hufert, F. T. & Weidmann, M. (2013). Development of a Panel of Recombinase Polymerase Amplification Assays for Detection of Biothreat Agents. *Journal of Clinical Microbiology,* 51**,** 1110-1117.

Euler, M., Wang, Y., Nentwich, O., Piepenburg, O., Hufert, F. T. & Weidmann, M. (2012a). Recombinase polymerase amplification assay for rapid detection of Rift Valley fever virus. *Journal of Clinical Virology,* 54**,** 308-312.

Euler, M., Wang, Y., Otto, P., Tomaso, H., Escudero, R., Anda, P., Hufert, F. T. & Weidmann, M. (2012b). Recombinase Polymerase Amplification Assay for Rapid Detection of Francisella tularensis. *Journal of Clinical Microbiology,* 50**,** 2234-2238.

Facca, C., Bilaničovà, D., Pojana, G., Sfriso, A. & Marcomini, A. (2014). Harmful Algae Records in Venice Lagoon and in Po River Delta (Northern Adriatic Sea, Italy). *The Scientific World Journal,* 2014**,** 11.

Fao. (2017). *Fishery and Aquaculture Country Profiles: The United Kingdom of Great Britain and Northern Ireland* [Online]. Rome: Food and Agriculture Organization of the United Nations. Available: http://www.fao.org/fishery/facp/GBR/en [Accessed 2020].

Farkas, K., Walker, D. I., Adriaenssens, E. M., Mcdonald, J. E., Hillary, L. S., Malham, S. K. & Jones, D. L. (2020). Viral indicators for tracking domestic wastewater contamination in the aquatic environment. *Water Research***,** 115926.

Fernandes, L. F., Hubbard, K. A., Richlen, M. L., Smith, J., Bates, S. S., Ehrman, J., Léger, C., Mafra, L. L., Kulis, D., Quilliam, M., Libera, K., Mccauley, L. & Anderson, D. M. (2014). Diversity and toxicity of the diatom Pseudo-nitzschia Peragallo in the Gulf of Maine, Northwestern Atlantic Ocean. *Deep Sea Research Part II: Topical Studies in Oceanography,* 103**,** 139-162.

Foldesi, B. (2018). *The 10 Best DNA Dyes and Probes* [Online]. biomol: biomol. Available: https://www.biomol.com/resources/biomol-blog/the-10-best-dna-dyes-and-probes [Accessed 15/5/2020 2020].

Fong, T.-T., Griffin, D. W. & Lipp, E. K. (2005). Molecular Assays for Targeting Human and Bovine Enteric Viruses in Coastal Waters and Their Application for Library-Independent Source Tracking. *Applied and Environmental Microbiology,* 71**,** 2070-2078.

Fsa. (2018). *Biotoxin and phytoplankton monitoring* [Online]. Available: https://www.food.gov.uk/business-guidance/biotoxin-and-phytoplankton-monitoring [Accessed 09/11/2020].

Fukuba, T., Miyaji, A., Okamoto, T., Yamamoto, T., Kaneda, S. & Fujii, T. (2011). Integrated in situ genetic analyzer for microbiology in extreme environments. *RSC Advances,* 1**,** 1567-1573.

Funari, E., Manganelli, M. & Sinisi, L. (2012). Impact of climate change on waterborne diseases. *Annali dell'Istituto Superiore di Sanità,* 48**,** 473-487.

Fykse, E. M., Nilsen, T., Nielsen, A. D., Tryland, I., Delacroix, S. & Blatny, J. M. (2012). Real-time PCR and NASBA for rapid and sensitive detection of Vibrio cholerae in ballast water. *Marine Pollution Bulletin,* 64**,** 200-6.

Gall, A. M., Mariñas, B. J., Lu, Y. & Shisler, J. L. (2015). Waterborne Viruses: A Barrier to Safe Drinking Water. *PLoS pathogens,* 11**,** e1004867-e1004867.

Galluzzi, L., Bertozzini, E., Penna, A., Perini, F., Garcés, E. & Magnani, M. (2009). Analysis of rRNA gene content in the Mediterranean dinoflagellate Alexandrium catenella and Alexandrium taylori: implications for the quantitative real-time PCR-based monitoring methods. *Journal of Applied Phycology,* 22**,** 1-9.

Galluzzi, L., Penna, A., Bertozzini, E., Vila, M., Garcés, E. & Magnani, M. (2004). Development of a Real-Time PCR Assay for Rapid Detection and Quantification of Alexandrium minutum (a Dinoflagellate). *Applied and Environmental Microbiology,* 70**,** 1199-1206.

Gárate-Lizárraga, I., López-Cortes, D. J., Bustillos-Guzmán, J. J. & Hernández-Sandoval, F. (2004). Blooms of Cochlodinium polykrikoides (Gymnodiniaceae) in the Gulf of California, Mexico. *Revista de Biología Tropical,* 52**,** 51-58.

Garcia, E., Kirkham, J. R., Hatch, A. V., Hawkins, K. R. & Yager, P. (2004). Controlled microfluidic reconstitution of functional protein from an anhydrous storage depot. *Lab on a Chip,* 4**,** 78-82.

Gingold, D. B., Strickland, M. J. & Hess, J. J. (2014). Ciguatera fish poisoning and climate change: analysis of National Poison Center Data in the United States, 2001-2011. *Environmental Health Perspectives,* 122**,** 580-6.

Glass, R. I., Parashar, U. D. & Estes, M. K. (2009). Norovirus Gastroenteritis. *The New England Journal of Medicine,* 361**,** 1776-1785.

Glibert, P. M., Anderson, D. M., Gentien, P., Granéli, E. & Sellner, K. G. (2005). The Global, Complex Phenomena of Harmful Algal Blooms. *Oceanography,* 18**,** 136-147.

Glibert, P. M. & Burford, M. A. (2017). Globally Changing Nutrient Loads and Harmful Algal Blooms: Recent Advances, New Paradigms, and Continuing Challenges. *Oceanography,* 30**,** 58-69.

Gobler, C. J. (2020). Climate Change and Harmful Algal Blooms: Insights and perspective. *Harmful Algae,* 91**,** 101731.

Gobler, C. J., Doherty, O. M., Hattenrath-Lehmann, T. K., Griffith, A. W., Kang, Y. & Litaker, R. W. (2017). Ocean warming since 1982 has expanded the niche of toxic algal blooms in the North Atlantic and North Pacific oceans. *Proceedings of the National Academy of Sciences,* 114**,** 4975-4980.

Gregory, T. R. (2001). Coincidence, coevolution, or causation? DNA content, cell size, and the C-value enigma. *Biol Rev Camb Philos Soc,* 76**,** 65-101.

Griffith, A. W., Doherty, O. M. & Gobler, C. J. (2019). Ocean warming along temperate western boundaries of the Northern Hemisphere promotes an expansion of Cochlodinium polykrikoides blooms. *Proceedings of the Royal Society B: Biological Sciences,* 286**,** 20190340.

Guillard, R. R. L. & Hargraves, P. E. (1993). Stichochrysis immobilis is a diatom, not a chrysophyte. *Phycologia,* 32**,** 234-236.

Hagmann, D. F., Goodey, N. M., Mathieu, C., Evans, J., Aronson, M. F. J., Gallagher, F. & Krumins, J. A. (2015). Effect of metal contamination on microbial enzymatic activity in soil. *Soil Biology and Biochemistry,* 91**,** 291-297.

Halim, Y. (1960). Alexandrium minutum, n. gen. n. sp. dinoflagellé provocant des “eaux rouges”. *Vie et Milieu,* 11**,** 102-105.

Hall, M. J., Wharam, S. D., Weston, A., Cardy, D. L. N. & Wilson, W. H. (2002). Use of signal-mediated amplification of RNA technology (SMART) to detect marine cyanophage DNA. *BioTechniques,* 32**,** 604-611.

Hallegraeff, G. M. (1993). A review of harmful algal blooms and their apparent global increase. *Phycologia,* 32**,** 79-99.

Hallegraeff, G. M. (2010). Ocean climate change, phytoplankton community responses, and harmful algal blooms: A formidable predictive challenge. *Journal of Phycology,* 46**,** 220-235.

Han, M., Lee, H., Anderson, D. M. & Kim, B. (2016). Paralytic shellfish toxin production by the dinoflagellate Alexandrium pacificum (Chinhae Bay, Korea) in axenic, nutrient-limited chemostat cultures and nutrient-enriched batch cultures. *Marine Pollution Bulletin,* 104**,** 34-43.

Hansen, G. (2009). *Alexandrium minutum* [Online]. WoRMS. Available: http://www.marinespecies.org/aphia.php?p=image&pic=21984 [Accessed 2020].

Harju, K., Rapinoja, M.-L., Avondet, M.-A., Arnold, W., Schär, M., Burrell, S., Luginbühl, W. & Vanninen, P. (2015). Optimization of Sample Preparation for the Identification and Quantification of Saxitoxin in Proficiency Test Mussel Sample using Liquid Chromatography-Tandem Mass Spectrometry. *Toxins,* 7**,** 4868-4880.

Hatch, A. C., Ray, T., Lintecum, K. & Youngbull, C. (2014). Continuous flow real-time PCR device using multi-channel fluorescence excitation and detection. *Lab on a Chip,* 14**,** 562-568.

Hatfield, R., Bean, T., Turner, A., Lees, D., Lowther, J., Lewis, A. & Baker-Austin, C. (2019). Development of a TaqMan qPCR assay for detection of Alexandrium spp and application to Harmful Algal Bloom monitoring. *Toxicon: X,* 2**,** 100011.

Hawkins, P. R. (2010). *Flow Cytometry of Alexandrium catenella from Elkhorn Slough, California.* MSc, San Jose University.

Heisler, J., Glibert, P. M., Burkholder, J. M., Anderson, D. M., Cochlan, W., Dennison, W. C., Dortch, Q., Gobler, C. J., Heil, C. A., Humphries, E., Lewitus, A., Magnien, R., Marshall, H. G., Sellner, K., Stockwell, D. A., Stoecker, D. K. & Suddleson, M. (2008). Eutrophication and harmful algal blooms: A scientific consensus. *Harmful Algae,* 8**,** 3-13.

Hoagland, P., Jin, D., Beet, A., Kirkpatrick, B., Reich, A., Ullmann, S., Fleming, L. E. & Kirkpatrick, G. (2014). The human health effects of Florida Red Tide (FRT) blooms: An expanded analysis. *Environment International,* 68**,** 144-153.

Hoofnagle, J. H., Nelson, K. E. & Purcell, R. H. (2012). Hepatitis E. *The New England Journal of Medicine,* 367**,** 1237-44.

Ijaz, S. (2018). Hepatitis E Virus in England and Wales. Public Health England: Public Health England.

Iliescu, C., Taylor, H., Avram, M., Miao, J. & Franssila, S. (2012). A practical guide for the fabrication of microfluidic devices using glass and silicon. *Biomicrofluidics,* 6**,** 016505-016505- 16.

Imo. (2004). *International Convention for the Control and Management of Ships' Ballast Water and Sediments (BWM)* [Online]. International Maritime Organization (IMO). Available: http://www.imo.org/en/About/Conventions/ListOfConventions/Pages/International-Convention-for-the-Control-and-Management-of-Ships'-Ballast-Water-and-Sediments-(BWM).aspx [Accessed 17/12/2018 2018].

Ivanova, N. V. & Kuzmina, M. L. (2013). Protocols for dry DNA storage and shipment at room temperature. *Molecular Ecology Resources,* 13**,** 890-8.

Jahanshahi-Anbuhi, S., Pennings, K., Leung, V., Liu, M., Carrasquilla, C., Kannan, B., Li, Y., Pelton, R., Brennan, J. D. & Filipe, C. D. (2014). Pullulan encapsulation of labile biomolecules to give stable bioassay tablets. *Angewandte Chemie International Edition in English,* 53**,** 6155-8.

Jain, N. K. & Roy, I. (2009). Effect of trehalose on protein structure. *Protein Science : A Publication of the Protein Society,* 18**,** 24-36.

Jaksch, K., Eschner, A., Rintelen, T. V. & Haring, E. (2016). DNA analysis of molluscs from a museum wet collection: a comparison of different extraction methods. *BMC research notes,* 9**,** 348-348.

Jeffery, B., Barlow, T., Moizer, K., Paul, S. & Boyle, C. (2004). Amnesic shellfish poison. *Food and Chemical Toxicology,* 42**,** 545-557.

Jha, S. K., Chand, R., Han, D., Jang, Y.-C., Ra, G.-S., Kim, J. S., Nahm, B.-H. & Kim, Y.-S. (2012). An integrated PCR microfluidic chip incorporating aseptic electrochemical cell lysis and capillary electrophoresis amperometric DNA detection for rapid and quantitative genetic analysis. *Lab on a Chip,* 12**,** 4455-4464.

Ji, C., Sun, M., Yu, J., Wang, Y., Zheng, Y., Wang, H. & Niu, R. (2014). Trehalose and Tween 80 Improve the Stability of Marine Lysozyme During Freeze-Drying. *Biotechnology & Biotechnological Equipment,* 23**,** 1351-1354.

Jones, K. L., Drane, D. & Gowans, E. J. (2007). Long-term storage of DNA-free RNA for use in vaccine studies. *BioTechniques,* 43**,** 675-681.

Jothikumar, N., Cromeans, T. L., Robertson, B. H., Meng, X. J. & Hill, V. R. (2006). A broadly reactive one-step real-time RT-PCR assay for rapid and sensitive detection of hepatitis E virus. *Journal of Virological Methods,* 131**,** 65-71.

Kadoya, S., Fujii, K., Izutsu, K.-I., Yonemochi, E., Terada, K., Yomota, C. & Kawanishi, T. (2010). Freeze-drying of proteins with glass-forming oligosaccharide-derived sugar alcohols. *International Journal of Pharmaceutics,* 389**,** 107-113.

Kamar, N., Bendall, R., Legrand-Abravanel, F., Xia, N.-S., Ijaz, S., Izopet, J. & Dalton, H. R. (2012). Hepatitis E. *The Lancet,* 379**,** 2477-2488.

Kamar, N., Dalton, H. R., Abravanel, F. & Izopet, J. (2014). Hepatitis E virus infection. *Clinical Microbiological Reviews,* 27**,** 116-38.

Kasper, J. C. & Friess, W. (2011). The freezing step in lyophilization: Physico-chemical fundamentals, freezing methods and consequences on process performance and quality attributes of biopharmaceuticals. *European Journal of Pharmaceutics and Biopharmaceutics,* 78**,** 248-263.

Kaushik, J. K. & Bhat, R. (2003). Why is trehalose an exceptional protein stabilizer? An analysis of the thermal stability of proteins in the presence of the compatible osmolyte trehalose. *The Journal of Biological Chemistry,* 278**,** 26458-65.

Kellmann, R., Mihali, T. K., Jeon, Y. J., Pickford, R., Pomati, F. & Neilan, B. A. (2008). Biosynthetic Intermediate Analysis and Functional Homology Reveal a Saxitoxin Gene Cluster in Cyanobacteria. *Applied and Environmental Microbiology,* 74**,** 4044-4053.

Kersting, S., Rausch, V., Bier, F. F. & Von Nickisch-Rosenegk, M. (2014a). Multiplex isothermal solid-phase recombinase polymerase amplification for the specific and fast DNA-based detection of three bacterial pathogens. *Microchimica Acta,* 181**,** 1715-1723.

Kersting, S., Rausch, V., Bier, F. F. & Von Nickisch-Rosenegk, M. (2014b). Rapid detection of Plasmodium falciparum with isothermal recombinase polymerase amplification and lateral flow analysis. *Malaria Journal,* 13**,** 99.

Kim, W. J., Managaki, S., Furumai, H. & Nakajima, F. (2009). Diurnal fluctuation of indicator microorganisms and intestinal viruses in combined sewer system. *Water Science and Technology,* 60**,** 2791-2801.

Kirkpatrick, B., Fleming, L. E., Squicciarini, D., Backer, L. C., Clark, R., Abraham, W., Benson, J., Cheng, Y. S., Johnson, D., Pierce, R., Zaias, J., Bossart, G. D. & Baden, D. G. (2004). Literature review of Florida red tide: implications for human health effects. *Harmful Algae,* 3**,** 99-115.

Kudela, R. M., Berdalet, E., Bernard, S., Burford, M., Fernand, L., Lu, S., Roy, S., Usup, G., Tester, P., Magnien, R., Anderson, D., Cembella, A. D., Chinain, M., Hallegraeff, G., Reguera, B., Zingone, A., Enevoldsen, H. & Urban, E. (2015). Harmful Algal Blooms. A scientific summary for policy makers. Paris: IOC/UNESCO.

Kudela, R. M. & Gobler, C. J. (2012). Harmful dinoflagellate blooms caused by Cochlodinium sp.: Global expansion and ecological strategies facilitating bloom formation. *Harmful Algae,* 14**,** 71-86.

Kurekin, A. A., Miller, P. I. & Van Der Woerd, H. J. (2014). Satellite discrimination of Karenia mikimotoi and Phaeocystis harmful algal blooms in European coastal waters: Merged classification of ocean colour data. *Harmful Algae,* 31**,** 163-176.

Labrique, A. B., Kuniholm, M. H. & Nelson, K. E. (2010). Chapter 4 : The Global Impact of Hepatitis E: New Horizons for an Emmerging Virus. *In:* SCHELD, W. M., GRAYSON, M. L. & HUGHES, J. M. (eds.) *Emerging Infections 9.* Washington D.C.: American Society for Microbiology.

Lajeunesse, T. C., Lambert, G., Andersen, R. A., Coffroth, M. A. & Galbraith, D. W. (2005). SYMBIODINIUM (PYRRHOPHYTA) GENOME SIZES (DNA CONTENT) ARE SMALLEST AMONG DINOFLAGELLATES1. *Journal of Phycology,* 41**,** 880-886.

Lamberti, A., Marasso, S. L. & Cocuzza, M. (2014). PDMS membranes with tunable gas permeability for microfluidic applications. *RSC Advances,* 4**,** 61415-61419.

Lamhoujeb, S., Charest, H., Fliss, I., Ngazoa, S. & Jean, J. (2009). Real-time molecular beacon NASBA for rapid and sensitive detection of norovirus GII in clinical samples. *Canadian Journal of Microbiology/Revue Canadienne de Microbiologie,* 55**,** 1375-80.

Larsen, A. C., Dunn, M. R., Hatch, A., Sau, S. P., Youngbull, C. & Chaput, J. C. (2016). A general strategy for expanding polymerase function by droplet microfluidics. *Nature Communications,* 7**,** 11235.

Lauri, A. & Mariani, P. O. (2009). Potentials and limitations of molecular diagnostic methods in food safety. *Genes & Nutrition,* 4**,** 1-12.

Leal-Serrano, G., Ruperez, P. & Leal, J. A. (1980). Acidic polysaccharide from Aureobasidium pullulans. *Transactions of the British Mycological Society,* 75**,** 57-62.

Lee, C.-Y., Chang, C.-L., Wang, Y.-N. & Fu, L.-M. (2011). Microfluidic Mixing: A Review. *International Journal of Molecular Sciences,* 12**,** 3263-3287.

Lee, S. H., Park, S.-M., Kim, B. N., Kwon, O. S., Rho, W.-Y. & Jun, B.-H. (2019). Emerging ultrafast nucleic acid amplification technologies for next-generation molecular diagnostics. *Biosensors and Bioelectronics,* 141**,** 111448.

Lewis, A. M., Coates, L. N., Turner, A. D., Percy, L. & Lewis, J. (2018). A review of the global distribution of Alexandrium minutum (Dinophyceae) and comments on ecology and associated paralytic shellfish toxin profiles, with a focus on Northern Europe. *Journal of Phycology,* 54**,** 581-598.

Lewitus, A. J., Horner, R. A., Caron, D. A., Garcia-Mendoza, E., Hickey, B. M., Hunter, M., Huppert, D. D., Kudela, R. M., Langlois, G. W., Largier, J. L., Lessard, E. J., Ralonde, R., Jack Rensel, J. E., Strutton, P. G., Trainer, V. L. & Tweddle, J. F. (2012). Harmful algal blooms along the North American west coast region: History, trends, causes, and impacts. *Harmful Algae,* 19**,** 133-159.

Lilly, E. L. (2003). *Phylogeny and biogeography of the toxic dinoflagellate Alexandrium.* PhD in Biology/Geology PhD, Woods Hole Oceanographic Institute.

Lilly, E. L., Halanych, K. M. & Anderson, D. M. (2005). Phylogeny, biogeography, and species boundaries within the Alexandrium minutum group. *Harmful Algae,* 4**,** 1004-1020.

Lin, J. & Ganesh, A. (2013). Water quality indicators: bacteria, coliphages, enteric viruses. *International Journal of Environmental Health Research,* 23**,** 484-506.

Liu, D., Daubendiek, S. L., Zillman, M. A., Ryan, K. & Kool, E. T. (1996). Rolling Circle DNA Synthesis: Small Circular Oligonucleotides as Efficient Templates for DNA Polymerases. *Journal of the American Chemical Society,* 118**,** 1587-1594.

Lobato, I. M. & O'sullivan, C. K. (2018). Recombinase polymerase amplification: Basics, applications and recent advances. *TrAC Trends in Analytical Chemistry,* 98**,** 19-35.

Loukas, C.-M. (2016). *Lab-on-a-chip technology for in situ molecular analysis of marine microorganisms.* PhD, University of Southampton.

Luo, G.-C., Yi, T.-T., Jiang, B., Guo, X.-L. & Zhang, G.-Y. (2019). Betaine-assisted recombinase polymerase assay with enhanced specificity. *Analytical Biochemistry,* 575**,** 36-39.

Magiopoulos, I., Mcquillan, J. S., Burd, C. L., Mowlem, M. & Tsaloglou, M. N. (2016). A multi-parametric assessment of decontamination protocols for the subglacial Lake Ellsworth probe. *Journal of Microbiological Methods,* 123**,** 87-93.

Maity, H., O'dell, C., Srivastava, A. & Goldstein, J. (2009). Effects of Arginine on Photostability and Thermal Stability of IgG1 Monoclonal Antibodies. *Current Pharmaceutical Biotechnology,* 10**,** 761-766.

Mancini, R. J., Lee, J. & Maynard, H. D. (2012). Trehalose glycopolymers for stabilization of protein conjugates to environmental stressors. *Journal of the American Chemical Society,* 134**,** 8474-9.

Manen, J.-F., Sinitsyna, O., Aeschbach, L., Markov, A. V. & Sinitsyn, A. (2005). A fully automatable enzymatic method for DNA extraction from plant tissues. *BMC Plant Biology,* 5**,** 23.

Manz, A., Harrison, D. J., Verpoorte, E. M. J., Fettinger, J. C., Paulus, A., Lüdi, H. & Widmer, H. M. (1992). Planar chips technology for miniaturization and integration of separation techniques into monitoring systems. *Journal of Chromatography A,* 593**,** 253-258.

Marras, S. a. E. (2006). Selection of Fluorophore and Quencher Pairs for Fluorescent Nucleic Acid Hybridization Probes. *In:* DIDENKO, V. V. (ed.) *Fluorescent Energy Transfer Nucleic Acid Probes.* 335 ed. New Jersey, US: Humana Press.

Martens, H., Tillmann, U., Harju, K., Dell'aversano, C., Tartaglione, L. & Krock, B. (2017). Toxin Variability Estimations of 68 Alexandrium ostenfeldii (Dinophyceae) Strains from The Netherlands Reveal a Novel Abundant Gymnodimine. *Microorganisms,* 5**,** 29.

Matejtschuk, P. (2007). Lyophilization of Proteins. *In:* DAY, J. G. & STACEY, G. N. (eds.) *Cryopreservation and Freeze-Drying Protocols.* Totowa, NJ: Humana Press.

Matsumura, M. & Matthews, B. W. (1989). Control of Enzyme Activity by an Engineered Disulfide Bond. *Science,* 243**,** 792-794.

Mcdonald, J. C. & Whitesides, G. M. (2002). Poly(dimethylsiloxane) as a material for fabricating microfluidic devices. *Accounts of Chemical Research,* 35**,** 491-499.

Mcginnis, L. K., Zhu, L., Lawitts, J. A., Bhowmick, S., Toner, M. & Biggers, J. D. (2005). Mouse Sperm Desiccated and Stored in Trehalose Medium Without Freezing. *Biology of Reproduction,* 73**,** 627-633.

Mcquillan, J. S. & Robidart, J. C. (2017). Molecular-biological sensing in aquatic environments: recent developments and emerging capabilities. *Current Opinion in Biotechnology,* 45**,** 43-50.

Mcquillan, J. S. & Wilson, M. W. (2019). 'Ready Mixed', improved nucleic acid amplification assays for the detection of Escherichia coli DNA and RNA. *Journal of Microbiological Methods***,** 105721.

Miehls, A. L. J., Mason, D. M., Frank, K. A., Krause, A. E., Peacor, S. D. & Taylor, W. W. (2009). Invasive species impacts on ecosystem structure and function: A comparison of the Bay of Quinte, Canada, and Oneida Lake, USA, before and after zebra mussel invasion. *Ecological Modelling,* 220**,** 3182-3193.

Mok, E., Wee, E., Wang, Y. & Trau, M. (2016). Comprehensive evaluation of molecular enhancers of the isothermal exponential amplification reaction. *Scientific Reports,* 6**,** 37837.

Mokhtari, C., Marchadier, E., Haim-Boukobza, S., Jeblaoui, A., Tesse, S., Savary, J. & Roque-Afonso, A. M. (2013). Comparison of real-time RT-PCR assays for hepatitis E virus RNA detection. *Journal of Clinical Virology,* 58**,** 36-40.

Moore, S. K., Dreyer, S. J., Ekstrom, J. A., Moore, K., Norman, K., Klinger, T., Allison, E. H. & Jardine, S. L. (2020). Harmful algal blooms and coastal communities: Socioeconomic impacts and actions taken to cope with the 2015 U.S. West Coast domoic acid event. *Harmful Algae,* 96**,** 101799.

Mullis, K. B., Faloona, F., Scharf, S., Saiki, R., Horn, G. & Erlich, H. (1986). Specific enzymatic amplification of DNA in vitro: the polymerase chain reaction. *Methods in Enzymology,* 155**,** 335-350.

Murray, S. A., Wiese, M., Stüken, A., Brett, S., Kellmann, R., Hallegraeff, G. & Neilan, B. A. (2011). sxtA-Based Quantitative Molecular Assay To Identify Saxitoxin-Producing Harmful Algal Blooms in Marine Waters. *Applied and Environmental Microbiology,* 77**,** 7050-7057.

Ní Rathaille, A. & Raine, R. (2011). Seasonality in the excystment of Alexandrium minutum and Alexandrium tamarense in Irish coastal waters. *Harmful Algae,* 10**,** 629-635.

Nohe, A., Goffin, A., Tyberghein, L., Lagring, R., De Cauwer, K., Vyverman, W. & Sabbe, K. (2020). Marked changes in diatom and dinoflagellate biomass, composition and seasonality in the Belgian Part of the North Sea between the 1970s and 2000s. *Science of The Total Environment,* 716**,** 136316.

Notomi, T., Okayama, H., Masubuchi, H., Yonekawa, T., Watanabe, K., Amino, N. & Hase, T. (2000). Loop-mediated isothermal amplification of DNA. *Nucleic Acids Research,* 28**,** e63-e63.

O'fagain, C. (2011). Storage and lyophilisation of pure proteins. *Methods in Molecular Biology,* 681**,** 179-202.

Olsson, C., Jansson, H. & Swenson, J. (2016). The Role of Trehalose for the Stabilization of Proteins. *The Journal of Physical Chemistry B,* 120**,** 4723-31.

Orr, R. J. S., Stüken, A., Murray, S. A. & Jakobsen, K. S. (2013). Evolutionary Acquisition and Loss of Saxitoxin Biosynthesis in Dinoflagellates: the Second “Core” Gene, sxtG. *Applied and Environmental Microbiology,* 79**,** 2128-2136.

Pankrantz, T. (2008). Red tide close desalination plants. *Water desalination report,* 44.

Parks, R., Bear, E., Coates, L., Maskrey, B. & Algoet, M. (2020). Annual report on the results of the Biotoxin and Phytoplankton Official Control Monitoring Programmes for England & Wales – 2019. Cefas.

Patterson, S. S., Casper, E. T., Garcia-Rubio, L., Smith, M. C. & Paul, J. H., 3rd (2005). Increased precision of microbial RNA quantification using NASBA with an internal control. *Journal of Microbiological Methods,* 60**,** 343-52.

Peralta, J. P., Ganibay, S. S., Espina, R. M. M., Noble, J. R. N. & Nualla, A. N. (2006). An Investigation into the Algal Bloom Occurance in the Coastal Waters of Barangay Kirayan Norte, Mag-ao, Iloilo, Philippines. *Philippine Agricultural Scientist,* 89**,** 97-100.

Piepenburg, O., Williams, C. H., Stemple, D. L. & Armes, N. A. (2006). DNA Detection Using Recombination Proteins. *PLoS Biology,* 4**,** e204.

Poretsky, R. S., Bano, N., Buchan, A., Lecleir, G., Kleikemper, J., Pickering, M., Pate, W. M., Moran, M. A. & Hollibaugh, J. T. (2005). Analysis of microbial gene transcripts in environmental samples. *Applied Environmental Microbiology,* 71**,** 4121-6.

Preston, C. M., Harris, A., Ryan, J. P., Roman, B., Marin, R., 3rd, Jensen, S., Everlove, C., Birch, J., Dzenitis, J. M., Pargett, D., Adachi, M., Turk, K., Zehr, J. P. & Scholin, C. A. (2011). Underwater application of quantitative PCR on an ocean mooring. *PloS One,* 6**,** e22522-e22522.

Prez, V. E., Gil, P. I., Temprana, C. F., Cuadrado, P. R., Martínez, L. C., Giordano, M. O., Masachessi, G., Isa, M. B., Ré, V. E., Paván, J. V., Nates, S. V. & Barril, P. A. (2015). Quantification of human infection risk caused by rotavirus in surface waters from Córdoba, Argentina. *Science of The Total Environment,* 538**,** 220-229.

Purcell, R. H. & Emerson, S. U. (2008). Hepatitis E: An emerging awareness of an old disease. *Journal of Hepatology,* 48**,** 494-503.

Qian, J., Ferguson, T. M., Shinde, D. N., Ramírez-Borrero, A. J., Hintze, A., Adami, C. & Niemz, A. (2012). Sequence dependence of isothermal DNA amplification via EXPAR. *Nucleic Acids Research,* 40**,** e87-e87.

Ranston, E. R., Webber, D. F. & Larsen, J. (2007). The first description of the potentially toxic dinoflagellate, Alexandrium minutum in Hunts Bay, Kingston Harbour, Jamaica. *Harmful Algae,* 6**,** 29-47.

Reinfelder, J. R. (2011). Carbon Concentrating Mechanisms in Eukaryotic Marine Phytoplankton. *Annual Review of Marine Science,* 3**,** 291-315.

Rey, A., Carney, K. J., Quinones, L. E., Pagenkopp Lohan, K. M., Ruiz, G. M., Basurko, O. C. & Rodríguez-Ezpeleta, N. (2019). Environmental DNA Metabarcoding: A Promising Tool for Ballast Water Monitoring. *Environmental Science & Technology,* 53**,** 11849-11859.

Rezadoost, M. H., Kordrostami, M. & Kumleh, H. H. (2016). An efficient protocol for isolation of inhibitor-free nucleic acids even from recalcitrant plants. *3 Biotech,* 6**,** 61-61.

Rhodes, L., Smith, K. & Moisan, C. (2013). Shifts and stasis in marine HAB monitoring in New Zealand. *Environmental Science and Pollution Research,* 20**,** 6872-6877.

Richlen, M. L., Morton, S. L., Jamali, E. A., Rajan, A. & Anderson, D. M. (2010). The catastrophic 2008–2009 red tide in the Arabian gulf region, with observations on the identification and phylogeny of the fish-killing dinoflagellate Cochlodinium polykrikoides. *Harmful Algae,* 9**,** 163-172.

Robidart, J. C., Church, M. J., Ryan, J. P., Ascani, F., Wilson, S. T., Bombar, D., Marin, R., 3rd, Richards, K. J., Karl, D. M., Scholin, C. A. & Zehr, J. P. (2014). Ecogenomic sensor reveals controls on N2-fixing microorganisms in the North Pacific Ocean. *The ISME Journal,* 8**,** 1175-85.

Rosa, M., Holohan, B. A., Shumway, S. E., Bullard, S. G., Wikfors, G. H., Morton, S. & Getchis, T. (2013). Biofouling ascidians on aquaculture gear as potential vectors of harmful algal introductions. *Harmful Algae,* 23**,** 1-7.

Ryan, J. P., Kudela, R. M., Birch, J. M., Blum, M., Bowers, H. A., Chavez, F. P., Doucette, G. J., Hayashi, K., Marin, R., Mikulski, C. M., Pennington, J. T., Scholin, C. A., Smith, G. J., Woods, A. & Zhang, Y. (2017). Causality of an extreme harmful algal bloom in Monterey Bay, California, during the 2014–2016 northeast Pacific warm anomaly. *Geophysical Research Letters,* 44**,** 5571-5579.

Sakai, K., Trabasso, P., Moretti, M. L., Mikami, Y., Kamei, K. & Gonoi, T. (2014). Identification of Fungal Pathogens by Visible Microarray System in Combination with Isothermal Gene Amplification. *Mycopathologia,* 178**,** 11-26.

Sanseverino, I., Conduto, D., Pozzoli, L., Dobricic, S. & Lettieri, T. (2016). Algal bloom and its economic impact. *JRC Technical Reports.* Italy: European Commision, Joint Research Centre, Institute for Environment and Sustainability.

Santos, M., Costa, P. R., Porteiro, F. M. & Moita, M. T. (2014). First report of a massive bloom of Alexandrium minutum (Dinophyceae) in middle North Atlantic: A coastal lagoon in S. Jorge Island, Azores. *Toxicon,* 90**,** 265-268.

Sato, S., Takata, Y., Kondo, S., Kotoda, A., Hongo, N. & Kodama, M. (2014). Quantitative ELISA Kit for Paralytic Shellfish Toxins Coupled with Sample Pretreatment. *Journal of AOAC International,* 97**,** 339-344.

Schiavo, S., Yang, W. C., Chiu, N. H. L. & Krull, I. S. (2005). Comparison of Fluorometric Detection Methods for Quantitative Polymerase Chain Reaction (PCR). *Journal of Immunoassay and Immunochemistry,* 26**,** 1-12.

Scholin, C., Doucette, G., Jensen, S., Roman, B., Pargett, D., Marin, R., Preston, C., Jones, W., Feldman, J., Everlove, C., Harris, A., Alvarado, N., Massion, E., Birch, J., Greenfield, D., Vrijenhoek, R., Mikulski, C. & Jones, K. (2009). Remote detection of marine microbes, small invertebrates, harmful algae, and biotoxins using the environmental sample processor (ESP). *Oceanography,* 22**,** 158-167.

Scholin, C. A. (2010). What are "ecogenomic sensors?" A review and thoughts for the future. *Ocean Sci.,* 6**,** 51-60.

Schrader, C., Schielke, A., Ellerbroek, L. & Johne, R. (2012). PCR inhibitors – occurrence, properties and removal. *Journal of Applied Microbiology,* 113**,** 1014-1026.

Schuler, F., Trotter, M., Geltman, M., Schwemmer, F., Wadle, S., Dominguez-Garrido, E., Lopez, M., Cervera-Acedo, C., Santibanez, P., Von Stetten, F., Zengerle, R. & Paust, N. (2016). Digital droplet PCR on disk. *Lab on a Chip,* 16**,** 208-216.

Shaw, K. J., Docker, P. T., Yelland, J. V., Dyer, C. E., Greenman, J., Greenway, G. M. & Haswell, S. J. (2010). Rapid PCR amplification using a microfluidic device with integrated microwave heating and air impingement cooling. *Lab on a Chip,* 10**,** 1725-1728.

Sidhu, J. P. S., Ahmed, W., Palmer, A., Smith, K., Hodgers, L. & Toze, S. (2017). Optimization of sampling strategy to determine pathogen removal efficacy of activated sludge treatment plant. *Environmental Science and Pollution Research,* 24**,** 19001-19010.

Singh, R. S., Saini, G. K. & Kennedy, J. F. (2008). Pullulan: Microbial sources, production and applications. *Carbohydrate Polymers,* 73**,** 515-31.

Smayda, T. J. (2006). Harmful Algal Bloom Communities in Scottish Coastal Waters: Relationship to Fish Farming and Regional Comparisons - A Review. *In:* SCOTLAND, N. (ed.). Kingston, RI: University of Rhode Island.

Smayda, T. J. (2007). Reflections on the ballast water dispersal—harmful algal bloom paradigm. *Harmful Algae,* 6**,** 601-622.

Squires, T. M. & Quake, S. R. (2005). Microfluidics: Fluid physics at the nanoliter scale. *Reviews of Modern Physics,* 77**,** 977-1026.

Staley, C., Reckhow, K. H., Lukasik, J. & Harwood, V. J. (2012). Assessment of sources of human pathogens and fecal contamination in a Florida freshwater lake. *Water Research,* 46**,** 5799-5812.

Stüken, A., Riobó, P., Franco, J., Jakobsen, K. S., Guillou, L. & Figueroa, R. I. (2015). Paralytic shellfish toxin content is related to genomic sxtA4 copy number in Alexandrium minutum strains. *Frontiers in Microbiology,* 6.

Sunda, W. G. & Shertzer, K. W. (2014). Positive feedbacks between bottom-up and top-down controls promote the formation and toxicity of ecosystem disruptive algal blooms: A modeling study. *Harmful Algae,* 39**,** 342-356.

Suzuki, H. & Machii, K. (2014). Comparison of toxicity between saxitoxin and decarbamoyl saxitoxin in the mouse bioassay for paralytic shellfish poisoning toxins. *The Journal of veterinary medical science,* 76**,** 1523-1525.

Tamashiro, H., Maskill, W., Emmanuel, J., Fauquex, A., Sato, P. & Heymann, D. (1993). Reducing the cost of HIV antibody testing. *Lancet,* 342**,** 87-90.

Taylor, M., Mcintyre, L., Ritson, M., Stone, J., Bronson, R., Bitzikos, O., Rourke, W., Galanis, E. & Outbreak Investigation, T. (2013). Outbreak of Diarrhetic Shellfish Poisoning associated with mussels, British Columbia, Canada. *Marine Drugs,* 11**,** 1669-76.

Technologies, B. (2015). *How Much is Your qPCR Assay Really Costing You?* [Online]. Biosearch Technologies. Available: http://blog.biosearchtech.com/how-much-is-your-qpcr-assay-really-costing-you#:~:text=To%20demonstrate%20this%2C%20the%20cost,if%20a%20probe%20is%20used. [Accessed 02/11/2020].

Teekamp, N., Tian, Y., Visser, J. C., Olinga, P., Frijlink, H. W., Woerdenbag, H. J. & Hinrichs, W. L. J. (2017). Addition of Pullulan to Trehalose Glasses Improves the Stability of β-Galactosidase at High Moisture Conditions. *Carbohydrate Polymers,* 176**,** 374-380.

Teoh, B.-T., Sam, S.-S., Tan, K.-K., Danlami, M. B., Shu, M.-H., Johari, J., Hooi, P.-S., Brooks, D., Piepenburg, O., Nentwich, O., Wilder-Smith, A., Franco, L., Tenorio, A. & Abubakar, S. (2015). Early Detection of Dengue Virus by Use of Reverse Transcription-Recombinase Polymerase Amplification. *Journal of Clinical Microbiology,* 53**,** 830-837.

Thompson, B. L., Birch, C., Li, J., Duvall, J. A., Le Roux, D., Nelson, D. A., Tsuei, A.-C., Mills, D. L., Krauss, S. T., Root, B. E. & Landers, J. P. (2016). Microfluidic enzymatic DNA extraction on a hybrid polyester-toner-PMMA device. *Analyst,* 141**,** 4667-4675.

Todd, K. (2001). Australian Marine Biotoxin Management Plan for Shellfish Farming. *Cawthorn Report.* Cawthorn Institute.

Touzet, N., Keady, E., Raine, R. & Maher, M. (2009). Evaluation of taxa-specific real-time PCR, whole-cell FISH and morphotaxonomy analyses for the detection and quantification of the toxic microalgae Alexandrium minutum (Dinophyceae), Global Clade ribotype. *FEMS Microbiology Ecology,* 67**,** 329-341.

Trainer, V. L., Bates, S. S., Lundholm, N., Thessen, A. E., Cochlan, W. P., Adams, N. G. & Trick, C. G. (2012). Pseudo-nitzschia physiological ecology, phylogeny, toxicity, monitoring and impacts on ecosystem health. *Harmful Algae,* 14**,** 271-300.

Tsaloglou, M. N., Watson, R. J., Rushworth, C. M., Zhao, Y., Niu, X., Sutton, J. M. & Morgan, H. (2015). Real-time microfluidic recombinase polymerase amplification for the toxin B gene of Clostridium difficile on a SlipChip platform. *Analyst,* 140**,** 258-264.

Twistdx. (2018). *TwistAmp® DNA Amplification Kits Assay Design Manual* [Online]. Maidenhead, UK. Available: https://www.twistdx.co.uk/docs/default-source/RPA-assay-design/twistamp-assay-design-manual-v2-5.pdf?sfvrsn=29 [Accessed 2019].

Unicef (2012). Pneumonia and diarrhoea: Tackling the deadliest diseases for the world's poorest children. New York, NY, US.

Ussler, W., Preston, C., Tavormina, P., Pargett, D., Jensen, S., Roman, B., Marin, R., Shah, S. R., Girguis, P. R., Birch, J. M., Orphan, V. & Scholin, C. (2013). Autonomous Application of Quantitative PCR in the Deep Sea: In Situ Surveys of Aerobic Methanotrophs Using the

Deep-Sea Environmental Sample Processor. *Environmental Science & Technology,* 47**,** 9339-9346.

Usup, G., Pin, L. C., Ahmad, A. & Teen, L. P. (2002). Alexandrium (Dinophyceae) species in Malaysian waters. *Harmful Algae,* 1**,** 265-275.

Vaerman, J. L., Saussoy, P. & Ingargiola, I. (2004). Evaluation of real-time PCR data. *Journal of Biological Regulators and Homeostatic Agents,* 18**,** 212-214.

Van Der Poel, W. H. M. (2014). Food and environmental routes of Hepatitis E virus transmission. *Current Opinion in Virology,* 4**,** 91-96.

Varaljay, V. A., Robidart, J., Preston, C. M., Gifford, S. M., Durham, B. P., Burns, A. S., Ryan, J. P., Marin, R., 3rd, Kiene, R. P., Zehr, J. P., Scholin, C. A. & Moran, M. A. (2015). Single-taxon field measurements of bacterial gene regulation controlling DMSP fate. *The ISME Journal,* 9**,** 1677-86.

Vincent, M., Xu, Y. & Kong, H. (2004). Helicase-dependent isothermal DNA amplification. *EMBO reports,* 5**,** 795-800.

Walker, D. I., Mcquillan, J., Taiwo, M., Parks, R., Stenton, C. A., Morgan, H., Mowlem, M. C. & Lees, D. N. (2017). A highly specific Escherichia coli qPCR and its comparison with existing methods for environmental waters. *Water Research,* 126**,** 101-110.

Walker, G. T., Fraiser, M. S., Schram, J. L., Little, M. C., Nadeau, J. G. & Malinowski, D. P. (1992a). Strand displacement amplification—an isothermal, in vitro DNA amplification technique. *Nucleic Acids Research,* 20**,** 1691-1696.

Walker, G. T., Little, M. C., Nadeau, J. G. & Shank, D. D. (1992b). Isothermal in vitro amplification of DNA by a restriction enzyme/DNA polymerase system. *Proceedings of the National Academy of Sciences of the United States of America,* 89**,** 392-396.

Walsh, J. J., Jolliff, J. K., Darrow, B. P., Lenes, J. M., Milroy, S. P., Remsen, A., Dieterle, D. A., Carder, K. L., Chen, F. R., Vargo, G. A., Weisberg, R. H., Fanning, K. A., Muller-Karger, F. E., Shinn, E., Steidinger, K. A., Heil, C. A., Tomas, C. R., Prospero, J. S., Lee, T. N., Kirkpatrick, G. J., Whitledge, T. E., Stockwell, D. A., Villareal, T. A., Jochens, A. E. & Bontempi, P. S. (2006). Red tides in the Gulf of Mexico: Where, when, and why? *Journal of Geophysical Research,* 111**,** 1-46.

Wang, L., Li, L., Alam, M. J., Geng, Y., Li, Z., Yamasaki, S. & Shi, L. (2008). Loop-mediated isothermal amplification method for rapid detection of the toxic dinoflagellate Alexandrium, which causes algal blooms and poisoning of shellfish. *FEMS Microbiology Letters,* 282**,** 15-21.

Wang, W. (2000). Lyophilization and development of solid protein pharmaceuticals. *International Journal of Pharmaceutics,* 203**,** 1-60.

Watkins, S. M., Reich, A., Fleming, L. E. & Hammond, R. (2008). Neurotoxic shellfish poisoning. *Marine drugs,* 6**,** 431-455.

Webb, J. A. & Bardhan, R. (2014). Emerging advances in nanomedicine with engineered gold nanostructures. *Nanoscale,* 6**,** 2502-2530.

Westh, P. & Ramløv, H. (1991). Trehalose accumulation in the tardigrade Adorybiotus coronifer during anhydrobiosis. *Journal of Experimental Zoology,* 258**,** 303-311.

Whitesides, G. M. (2006). The origins and the future of microfluidics. *Nature,* 442**,** 368-73.

Who (2012). Global costs and benefits of drinking-water supply and sanitation interventions to reach the MDG target and universal coverage. Geneva, Switzerland.

Who. (2019). *Drinking-water* [Online]. WHO. Available: https://www.who.int/news-room/fact-sheets/detail/drinking-water [Accessed].

Who & Unicef (2014). Progress on drinking water and sanitation: 2014 Update. Geneva, Switzerland.

Wiese, M., Murray, S. A., Alvin, A. & Neilan, B. A. (2014). Gene expression and molecular evolution of sxtA4 in a saxitoxin producing dinoflagellate Alexandrium catenella. *Toxicon,* 92**,** 102-112.

Wong, D. C., Purcell, R. H., Sreenivasan, M. A., Prasad, S. R. & Pavri, K. M. (1980). Epidemic and endemic hepatitis in India: evidence for a non-A, non-B hepatitis virus aetology. *The Lancet,* 316**,** 876-879.

Wood, S. A., Biessy, L., Latchford, J. L., Zaiko, A., Von Ammon, U., Audrezet, F., Cristescu, M. E. & Pochon, X. (2020). Release and degradation of environmental DNA and RNA in a marine system. *Science of The Total Environment,* 704**,** 135314.

Woods, J. W. & Burkhardt Lll, W. (2013). 14 - Preventing and controlling viral contamination of shellfish. *In:* COOK, N. (ed.) *Viruses in Food and Water.* Woodhead Publishing.

Xiao, Q., Tong, Q. & Lim, L. T. (2014). Drying process of pullulan edible films forming solutions studied by ATR-FTIR with two-dimensional correlation spectroscopy. *Food Chemistry,* 150**,** 267-73.

Xu, C., Li, L., Jin, W. & Wan, Y. (2014). Recombinase Polymerase Amplification (RPA) of CaMV-35S Promoter and nos Terminator for Rapid Detection of Genetically Modified Crops. *International Journal of Molecular Sciences,* 15**,** 18197-18205.

Xu, N., Huang, B., Hu, Z., Tang, Y., Duan, S. & Zhang, C. (2017). Effects of temperature, salinity, and irradiance on the growth of harmful algal bloom species Phaeocystis globosa Scherffel (Prymnesiophyceae) isolated from the South China Sea. *Chinese Journal of Oceanology and Limnology,* 35**,** 557-565.

Yang, I., Beszteri, S., Tillmann, U., Cembella, A. & John, U. (2011). Growth- and nutrient-dependent gene expression in the toxigenic marine dinoflagellate Alexandrium minutum. *Harmful Algae,* 12**,** 55-69.

Yang, X., Zhou, L., Tan, Y., Shi, X., Zhao, Z., Nie, D., Zhou, C. & Liu, H. (2017). Development and Validation of a Liquid Chromatography-Tandem Mass Spectrometry Method Coupled with Dispersive Solid-Phase Extraction for Simultaneous Quantification of Eight Paralytic Shellfish Poisoning Toxins in Shellfish. *Toxins (Basel),* 9.

Yu, Y., Li, B., Baker, C. A., Zhang, X. & Roper, M. G. (2012). Quantitative Polymerase Chain Reaction Using Infrared Heating on a Microfluidic Chip. *Analytical Chemistry,* 84**,** 2825-2829.

Zhang, F., Shi, Y., Jiang, K., Xu, Z. & Ma, L. (2012). Sensitive and rapid detection of two toxic microalgae Alexandrium by loop-mediated isothermal amplification. *Acta Oceanologica Sinica,* 31**,** 139-146.

Zhong, K. J. Y. & Kain, K. C. (1999). Evaluation of a Colorimetric PCR-Based Assay To Diagnose Plasmodium falciparum Malaria in Travelers. *Journal of Clinical Microbiology,* 37**,** 339-341.

Zhu, B., Furuki, T., Okuda, T. & Sakurai, M. (2007). Natural DNA Mixed with Trehalose Persists in B-Form Double-Stranding Even in the Dry State. *The Journal of Physical Chemistry B,* 111**,** 5542-5544.

Zingone, A. & Oksfeldt Enevoldsen, H. (2000). The diversity of harmful algal blooms: a challenge for science and management. *Ocean & Coastal Management,* 43**,** 725-748.